Phytochemistry of some South African medicinal Rubiaceae and Curtisiaceae species

By

Prince Nqaba Moyo

211543946

A thesis submitted in fulfilment of the academic requirements of the degree of Doctor of Philosophy

College of Agriculture, Engineering and Science

School of Chemistry and Physics

University of KwaZulu-Natal

Pietermaritzburg

Supervisor: Prof. Fanie van Heerden

EXAMINER'S COPY

Declaration 1 Plagiarism

I, ……Prince Nqaba Moyo……., declare that

1. The research reported in this thesis, except where otherwise indicated, is my original research.
2. This thesis has not been submitted for any degree or examination at any other university.
3. This thesis does not contain other persons' data, pictures, graphs or other information, unless specifically acknowledged as being sourced from other persons.
4. This thesis does not contain other persons' writing, unless specifically acknowledged as being sourced from other researchers. Where other written sources have been quoted, then:

a. Their words have been re-written but the general information attributed to them has been referenced

b. Where their exact words have been used, then their writing has been placed in italics and inside quotation marks, and referenced.

5. This thesis does not contain text, graphics or tables copied and pasted from the Internet, unless specifically acknowledged, and the source being detailed in the thesis and in the References sections.

[redacted]

Date: 09 May 2024

Prince N. Moyo

As the candidate's Supervisor I agree to the submission of this thesis.

[redacted]

Prof. F R van Heerden

Date: 09 May 2024

Declaration 2 Publications

Publication 1: Moyo, P.N., Van Heerden, F.R. 2023. An imprecise probability approach-based determination of over-represented southern African plant genera and families used in ethnopharmacology. Journal of Ethnopharmacology 324, 117757

Contributions:

Prince N. Moyo: Conceptualization, Data curation, Formal analysis, Methodology, Writing – original draft, Software, Validation, Visualization.

Fanie R. van Heerden: Formal analysis, Funding acquisition, Project administration, Supervision, Writing – review & editing, Validation.

Publication 2: A review of the phytochemistry of southern African Rubiaceae, In preparation.

Publication 3: Phytochemistry of *Curtisa dentata* (Burm. f.) C.A.Sm. In preparation.

[redacted]

Prince N Moyo

Date: 09 May 2024

[redacted]

Prof F R van Heerden
Supervisor

Date: 09 May 2024

Acknowledgements

I thank my supervisor, Prof. Fanie R. van Heerden, for her support as a teacher and mentor.

I acknowledge the National Research Foundation funding, which made this work possible.

I acknowledge the School of Chemistry and Physics, where these studies were undertaken.

I thank Craig Grimmer, a Technician in the NMR laboratory.

I thank Caryl Janse van Rensburg, a technician at the mass spectrometry laboratory.

I thank Alison Young, Horticulturalist at the School of Life Sciences, for assisting with the identification of plants.

I thank Christina Curry, Principal technician at the Bews Herbarium.

I also thank my wife, Natasha, my parents, Lameck and Sukoluhle, and my sister Dawn for their support throughout my studies.

Abstract

The investigation began by identifying which taxonomic groups from southern Africa are most prominently featured in ethnopharmacological practices. This involved collecting data from ethnopharmacological surveys and performing statistical analyses. Over-represented southern African taxa and the concept of over-represented genera are presented for the first time.

The families and genera with the highest margins of over-representation were found to be Loganiaceae and *Albizia* in southern Africa as a whole and Sapotaceae and *Solanum* in South Africa. The families and genera with the highest margins of over-representation across disease categories are Ebenaceae and *Albizia*, Canellaceae and *Dicoma*, Combretaceae and *Pterocelastrus*, Ebenaceae and *Bersama*, Francoaceae and *Erythrina*, and Aristolochiaceae and *Strychnos* for plants used in the treatment of STIs, febrile and mosquito-vector diseases, microbial infections, pain, skin conditions, and female sexual/reproductive problems, respectively. The Rubiaceae family was found to be one of the 25 most over-represented taxonomic groups in Southern Africa. Plants in the family were targeted for investigation due to the availability of plant material.

The study focused on the phytochemical investigations of three southern African medicinal plants, *Coddia rudis* (E.Mey. ex Harv.) Verdc., *Keetia gueinzii* (Sond.) Bridson and *Curtisia dentata* (Burm.f.) C.A.Sm. The ethnopharmacology and phytochemistry of the Rubiaceae species were first reviewed. The review was intended to be comprehensive, recording and discussing the notable findings of investigations on Rubiaceae species. Hundred and thirteen Rubiaceae species with ethnobotanical applications. Thirty-five species have nutritional applications. Twenty-three out of 34 anti-inflammatory and analgesic species, 17 out of 31 anti-viral and anti-bacterial species, and 13 of 27 Rubiaceae species used for sexual and reproductive problems have not undergone preparative phytochemical analysis. Only 52 southern African Rubiaceae were found to have undergone bioactivity investigations. Two hundred and thirty-three isolated compounds have been reported from 39 Rubiaceae species of southern Africa.

Coddia rudis and *Keetia gueinzii* were selected based on proximal availability in the Pietermaritzburg region. *Curtisia dentata* was chosen due to findings during the review that plants in the Cornales order (of which *C. dentata* is a member) produce iridoid glycosides similarly to the Rubiaceae family members. The study yielded eleven bioactive known

compounds. Gardenoside, geniposidic acid, and astragalin were isolated from *C. rudis* leaves and kaempferitrin was isolated from *K. gueinzi*i leaves. Phlorizin and (-)-epicatechin were isolated from *C. dentata* bark, and loganic acid, secologanoside, geniposide, juglalin, and sweroside were isolated from *C. dentata* leaves.

The study represents the first report of the isolation of these compounds from the species in question. The isolation of phlorizin, a known diuretic with anti-diabetic activities, supports the use of the *C. dentata* bark to treat diabetes in traditional medicine. Furthermore, obtaining juglalin, which has been reported to inhibit the senescence of dermal fibroblast cells, corroborates the application of the plant in the treatment of various skin conditions. The results of the study are consistent with findings reported in literature that show the presence of biologically active iridoid glycosides in Rubiaceae and Cornales species.

Table of Contents

List of Figures

List of schemes

List of Tables

Abbreviations

AChE	Acetylcholinesterase
AIDS	Acquired Immuno Deficiency Syndrome
AO	Angola
BCE	Before Common Era
BChE	Butyrylcholinesterase
BETA.INV	Inverse of the cumulative beta probability density function
BW	Botswana
CE	Common Era
CH_2Cl_2	Dichloromethane
$CHCl_3$	Chloroform
CK	Creatine kinase
COSY	(Homonuclear) Correlation Spectroscopy
COVID	Coronavirus Disease 2019
COX	Cyclooxygenase
DCM	Dichloromethane
DEPT	Distortionless Enhancement by Polarization Transfer
DMAPP	Dimethyl pyrophosphate
DPPH	2,2-diphenyl-1-picrylhydrzyl
EC_{50}	Half maximal effective concentration
EID	Emerging Infectious diseases
ESBL	Extended-spectrum beta-lactamase
EtOAc	Ethyl acetate
EtOH	Ethanol
FLU	Fluoxetine hydrochloride
HDF	Human dermal fibroblast
HIV	Human Immunodeficiency Virus
HMBC	Heteronuclear Multiple Bond Correlation
HSQC	Heteronuclear Single Quantum Coherence
HUVEC	Human umbilical vein endothelial cell
I/R	Ischemia-reperfusion
IC_{50}	Half maximal inhibitory concentration
IDM	Imprecise Dirichlet Model

Inf.	Inferior 95% probability credible interval
J	Jaccard coefficient in Chapter 2, Coupling constant in Chapters 4 and 5
LC_{50}	Lethal concentration 50
LDH	Lactate dehydrogenase
LDL	Low-density lipoprotein
LOX	Lipoxygenase
LS	Lesotho
MAO	Monoamine oxidase
MCD	Methionine-choline deficient
MDA	Malondialdehyde
MDR-TB	Multidrug-resistant tuberculosis
MeOH	Methanol
MIC	Minimum inhibitory concentration
MLC	Minimum lethal concentration
MO	Mozambique
mRNA	Messenger ribonucleic acid
MRSA	Methicillin-resistant *Staphylococcus aureus*
MW	Malawi
NADH	Nicotinamide adenine dinucleotide
NASH	Non-alcoholic steatohepatitis
NM	Namibia
NMR	Nuclear magnetic resonance
NO	Nitric oxide
NOESY	Nuclear Overhauser Effect Spectroscopy
PE	Petroleum ether
POWO	Plants of the world online
RT-PCR	Reverse transcriptase polymerase chain reaction
SANBI	South African National Biodiversity Institute
STI	Sexually transmitted infection
Sup.	Superior 95% probability credible interval
SZ	Eswatini
TCM	Traditional Chinese Medicine
TGI	Total growth inhibition
TNBS	2,4,6-trinitrobenzenesulfonic acid
TNF-α	Tumor necrosis factor

TUNEL	Terminal deoxynucleotidyl transferase dUTP nick end labelling
WFO	World flora online
ZA	South Africa
ZM	Zambia
ZOI	Zone of inhibition
ZW	Zimbabwe

Chapter 1 Introduction and Aim of Investigation

1.1 Background

Phytochemistry involves the isolation and structural analysis of chemicals produced by plants, including studying their biosynthesis and how they interact with and within other species (Wayne, 2019). These compounds are intermediates and products of plant metabolism, and the molecular masses are typically less than 2000 g/mol (Bhattacharya, 2019; Crowley, 2020). Phytochemicals are subdivided into two groups, the first being primary metabolites. This group of compounds forms the most significant share by mass percentage of phytochemicals within a plant and is essential for cell division, reproduction, growth, and development. Primary metabolites generally do not vary in structure from species to species and execute their functions within the cells in which they were synthesised (Crowley, 2020). The compounds that comprise primary metabolites include proteins, carbohydrates, vitamins, nucleic acids, and lipids (Bhattacharya, 2019).

The second group of metabolites, secondary metabolites, is not essential for a cell to survive. However, their utility within a plant lies in their capacity to determine how the plant interacts with its environment (Bhattacharya, 2019). In contrast to primary metabolites, plants use secondary metabolites for communication as signals to attract members of the animal kingdom that facilitate pollination and seed dispersal, defence against herbivores, pathogens, and other competing plants (Wink, 2013). Secondary metabolites may deter herbivores by making the plant tissue indigestible and toxic or attracting predators of herbivores to its vicinity (Jamieson et al., 2017). Defence functions include protection against environmental stressors like drought, ultraviolet light exposure and pollution (Saxena et al., 2013). These compounds also determine plant colours, scents, and how plant tissue tastes (Saxena et al., 2013).

Secondary metabolites may be synthesised in response to an attack on the plant or synthesised prior and stored in the plant cell vacuole, ready to be deployed as and when needed (Wink, 2013). The type of secondary metabolites produced differ by species, with each plant taxa associated with manufacturing a specific class of compounds (Bhattacharya, 2019). Structural variation is higher among secondary metabolites compared to primary metabolites, and these compounds may be found in plants as mixtures of chemically related compounds

(Bhattacharya, 2019). The distribution of secondary metabolites within a single plant differs among plant organs. For example, pigment molecules are located mainly near the surface of tissues (Saxena et al., 2013). The production of secondary metabolites is also affected by climate conditions and the concentration of pollutants (Jamieson et al., 2017). Secondary metabolites confer on plants, biological and pharmacological activities that other species can utilise. Human beings have thus long studied and applied plants for medicinal purposes.

1.2 Ethnopharmacological utilisation of phytochemicals by humans

Various ethnic groups across the globe have used plants as medicaments for millennia. While most of the knowledge was likely lost due to a lack of archiving, the advent of writing in the later course of humankind ensured that some knowledge was stored (Eknoyan, 2016). The Sumerian pharmacopoeia from 5000 years ago forms part of the evidentiary record that suggests an aeonian familiarity of humans with plant medicines (Giannenas et al., 2020). Further corroboration of this fact is found in Mesopotamian cuneiform from 2500 BCE, which suggests that herbal remedies were central to the ancient civilisation's medical system. Around 1000 therapeutic plants alongside various preparations are documented therein (Giannenas et al., 2020).

The *Ebers papyrus* discovered in Egypt dates back to between 1600 and 1500 BCE and comprises about 700 plant formulations (Evans and Evans, 2009; Núñez Sellés, 2019). In the *Ebers papyrus*, the hypnotic and sedative effects of *Papaver somniferum* L., commonly known as the opium poppy, are described (Moosavyzadeh et al., 2018). While it is true that in prehistoric civilisations, religion and medicine were interwoven, attributing disease to displeased gods, demons, witchcraft, and magic, there are indications that rational medicine was also a coexisting system (Biggs, 1969; Retief and Cilliers, 2007; Žuškin et al., 2008). Some letters excavated from sites of ancient Mesopotamia reveal that communicable diseases were somewhat understood. The ill subject was quarantined, and other people were restricted from sharing kitchen utensils, bedding, or a seat or even prevented from entering the patient's room. Some of the letters mentioned the evacuation of towns due to epidemics and the extent of the spread of infections (Biggs, 1969).

Around the 2nd century BCE, the inhabitants of the Indian subcontinent developed their medical system: Ayurveda (Jaiswal and Williams, 2017; Mandal et al., 2015). Some documentation of medicinal uses continued throughout the Middle Ages to the modern historical period. The

Ayurvedic archives provide a wealth of detail, recording the use of around 1550 plant species (Thomas et al., 2020).

Historical Traditional Chinese Medicine (TCM) documents dating back to 2700 BCE list 300 medicinal plants. Between 1368 and 1644 CE, recorded herbal prescriptions number over 60,000. A herbalist by the name of Li Shizhen, who lived between 1518 and 1593 CE, compiled a book with medicinal properties of over 1800 plants, including 365 dried plant materials that were already in use during eras prior (Giannenas et al., 2020). Chinese medicine's philosophy is rooted in the idea that the mind, body and spirit have an equal effect on the body and, therefore, takes a holistic approach to healing (Žuškin et al., 2008). After founding the People's Republic of China in 1949, Chairman Mao Zedong continued to promote TCM and encouraged its integration into Western-style medicine (Zou, 2020).

The renowned physician Hippocrates, acclaimed to be the father of modern medicine, lived from 460 to 377 BCE and compiled over 400 medicinal herbs in his compendium, *Corpus Hippocraticum* (Mandal et al., 2015). Having learned a lot of his medical knowledge from the Egyptians during his many travels, Hippocrates decoupled medicine from superstitions and employed a rational approach to medical treatment by basing treatment on the scientific study of the human body (Parker, 1915; Žuškin et al., 2008).

Another Greek philosopher and natural scientist, Theophrastus, followed. He lived between 371 and 287 BCE. In his writings, Theophrastus referred to over 500 medicinal plants (Butler and Newman, 2008; Mandal et al., 2015). In later years, while travelling with Roman armies, a Greek doctor named Dioscorides, who lived in the 1st century CE, archived the use of 600 medicinal plants and around 900 herbal drugs (Butler and Newman, 2008; Leonti and Verpoorte, 2017). Galen, a physician and pharmacist in Rome, wrote over 30 books that included plant medicines called galenicals (Butler and Newman, 2008). *De Materia Medica* by Dioscorides and *De simplicium medicamentorum facultatibus libri XI,* compiled by Galen, are considered the most influential literature on the spread and use of medicinal plants in the Mediterranean region and Europe up until the 18th century (Leonti and Verpoorte, 2017).

Between the 8th and 10th centuries CE, this Greco-Roman medicinal knowledge, preserved during the Byzantine Empire, was translated into Syriac and then into Arabic (Leonti and Verpoorte, 2017; Russell, 2009). During the 12th century, the Arabic versions, including the Arabic world's additional herbal knowledge, were translated into Latin, thus beginning the

transfer of centuries of wisdom to the Western world (Leonti and Verpoorte, 2017; Russell, 2009).

The indigenous peoples of Sub-Saharan Africa have historically relied on medicinal plants for therapy (Mulholland, 2005). The indigenous custodians of ethnomedicinal knowledge did not store the information in written format to be passed on to posterity. Instead, knowledge was orally shared with subsequent generations, possibly over thousands of years (Light et al., 2005; Van Wyk and Moteetee, 2019). European settlers and missionaries to Africa archived some sub-Saharan African medicinal botanical species in herbaria (Soelberg et al., 2015). References to South African plant species recorded by non-indigenous writers date back to 1685 when Simon van der Stel undertook an ethnobotanical survey of Namaqualand on the west coast of South Africa (Nortje and van Wyk, 2015). William Guybon Atherstone's ethnobotanical observations in Namaqualand between 1854 and 1855 are mentioned in Flora Capensis, one of the most critical pieces of historical ethnopharmacological literature (Nortje and van Wyk, 2015). As can be gathered from this brief historical account, the pre-eminence of plant medicines in times past cannot be gainsaid. The following discussion sets out some ways medicinal plants are still of value to contemporary society.

1.3 Challenges facing southern Africa that are relevant to the current study

Developing countries struggle to provide affordable and accessible medicines to their people. In Africa, there is a reliance on pharmaceutical imports from China and India to meet the health needs of the continent's people (Adekola, 2019). Adekola (2019) pointed out that part of the cause for this is the global intellectual property laws that govern the trade of drugs, which inevitably lead to monopolisation of the supply chain by patent holders. Africa has a high concentration of countries designated as Least Developed Countries by the United Nations and struggles to purchase generic forms of on-patent drugs (Adekola, 2019). For approximately 90% of citizens in developing countries without access to affordable medicines, pharmaceutical requirements become their second largest expenditure after food (Adekola, 2019). The inability to afford the cost of chronic medications increases the chance of dying from a chronic non-communicable disease in Africa by 20% (Adekola, 2019).

Access to medicines by poor demographics is often limited. In South Africa, disparities in access are exacerbated by the inequitable distribution of healthcare facilities, with high-level hospitals concentrated in the more affluent, urbanised provinces of the Western Cape and Gauteng (Harris et al., 2011). In general, Sub-Saharan African countries suffer from a shortage

of pharmaceuticals like essential opioids due to restrictive policies and a diminutive manufacturing capacity (Yao et al., 2023). Additionally, the utility of existing antibiotics is increasingly limited due to growing resistance by microbes. Poor controls on antibiotic use in African countries, including South Africa, the unrestricted use of antibiotics in the agriculture industry, and the use of antibiotics like penicillins for both human and animal diseases likely promote further development of resistance.

South Africa has an increasing problem of pathogenic bacterial resistance to existing drugs. Notable examples include multidrug-resistant tuberculosis (MDR-TB), methicillin-resistant *Staphylococcus aureus* (MRSA) and the extended-spectrum beta-lactamase (ESBL)-producing bacteria (Van den Honert et al., 2018). Plant secondary metabolites are a potential source of drug-lead compounds that can be used as part of the solution to resistance against antibiotics (Newman and Cragg, 2020). Furthermore, there is a reliance on traditional plant medicines for disease treatment in southern Africa. As Mander et al. (2007) point out, 72 per cent of black South Africans use traditional medicines. Therefore, it is in the public health's interest to analyse the ethnological pharmacopoeia and investigate the bioactive phytochemical constituents in medicinal plants. One of the declarations adopted by the 19th International Botanical Conference held in Shenzhen, China, in 2017 was prioritising the valuing, documentation and protection of indigenous, traditional and local knowledge about plants and nature (Van Wyk and Moteetee, 2019). These factors are the impetus behind the current study of southern African medicinal plants.

In this study, we hypothesised that southern African medicinal plants with ethnomedicinal applications contain bioactive phytochemical constituents that can be isolated and identified. As a starting point, we proposed that determining which taxonomic groups are the most significant in southern African ethnopharmacology would streamline the selection of plants for phytochemical investigations. Once a taxonomic group is selected, reviewing previous studies on the group would indicate the potential to obtain biologically active phytochemical constituents from the taxa.

In the next chapter, over-represented medicinal families and genera are analysed. These are taxonomic groups that are most frequently used in southern African ethnopharmacology. The results from this study formed part of the basis for choosing Rubiaceae plant species for phytochemical investigations. The review of Rubiaceae medicinal plants led to the observation that bioactive iridoid glycosides are common constituents of plants in both the Rubiaceae

family and the Cornales order. As a result, three plants were selected for investigation: *Coddia rudis* (E.Mey. ex Harv.) Verdc., *Keetia gueinzii* (Sond.) Bridson, from the Rubiaceae and *Curtisia dentata* (Burm.f.) CA Sm (Curtisiaceae) from the Cornales order.

1.4 Aims and Objectives

The study aimed to investigate the phytochemical constituents of some southern African medicinal plants.

Objectives:

- Determine the most significant medicinal plant taxonomic groups of southern Africa.
- Conduct an in-depth review of a selected ethnopharmacologically significant taxonomic group.
- Select medicinal plant species for phytochemical investigations.
- Isolate and characterise the phytochemical constituents of selected plants.

1.5 Outline of thesis

This thesis aims to report the findings of an investigation into the phytochemistry of selected southern African medicinal plants. Chapter 1 provides a background of phytochemistry and a brief historical account of therapeutic plant science. The importance of phytochemical investigations of ethnopharmacologically significant plants in the context of the challenges faced by southern Africa's public health systems is discussed. Chapter 2 is an analysis of over-represented plants used in southern African ethnopharmacology. The concept of over-representation is defined, and statistical formulae are applied to rank southern African medicinal taxonomic groups. In Chapter 3, Rubiaceae plants of ethnopharmacological significance are reviewed. The Rubiaceae family is chosen partly based on the results in Chapter 2. Chapter 4 is a report and discussion of the findings of an investigation into the phytochemical constituents of two Rubiaceae species, *C. rudis* and *K. guienzii*. The phytochemistry of *Curtisia dentata* is discussed in Chapter 5. Chapter 6 is the conclusion and future lines of inquiry are briefly discussed.

1.6 References

Adekola, T.A., 2019. Public health–oriented intellectual property and trade policies in Africa and the regional mechanism under Trade-Related Aspects of Intellectual Property Rights amendment. Public Health 173, 1-4.

Bhattacharya, A., 2019. High-Temperature Stress and Metabolism of Secondary Metabolites in Plants, in Bhattacharya, A. (Ed.) Effect of High Temperature on Crop Productivity and Metabolism of Macro Molecules. Academic Press, pp. 391-484.

Biggs, R., 1969. Medicine in ancient Mesopotamia. History of Science 8, 94-105.

Butler, M.S., Newman, D.J., 2008. Mother Nature's gifts to diseases of man: the impact of natural products on anti-infective, anticholestemics and anticancer drug discovery, in: Petersen, F., Amstutz, R. (Eds.), Natural Compounds as Drugs Volume I. Springer, Basel, pp. 1-44.

Crowley, T.E., 2020. Chapter 2 - The structure and function of secondary metabolites that are secreted by bacteria, in: Crowley, T.E. (Ed.) Purification and Characterization of Secondary Metabolites. Academic Press, pp. 9-17.

Eknoyan, G., 2016. Beginnings—The Kidney and Nephrology in Ancient Mesopotamian Culture, Seminars in dialysis. Wiley Online Library, pp. 236-246.

Evans, W.C., Evans, D., 2009. Chapter 1 - Plants in medicine: the origins of pharmacognosy, in: Evans, W.C., Evans, D. (Eds.), Trease and Evans' Pharmacognosy (Sixteenth Edition). W.B. Saunders, pp. 3-4.

Giannenas, I., Sidiropoulou, E., Bonos, E., Christaki, E., Florou-Paneri, P., 2020. Chapter 1 - The history of herbs, medicinal and aromatic plants, and their extracts: Past, current situation and future perspectives, in: Florou-Paneri, P., Christaki, E., Giannenas, I. (Eds.), Feed Additives. Academic Press, pp. 1-18.

Harris, B., Goudge, J., Ataguba, J.E., McIntyre, D., Nxumalo, N., Jikwana, S., Chersich, M., 2011. Inequities in access to health care in South Africa. Journal of Public Health Policy 32, S102-S123.

Jaiswal, Y.S., Williams, L.L., 2017. A glimpse of Ayurveda – The forgotten history and principles of Indian traditional medicine. Journal of Traditional and Complementary Medicine 7, 50-53.

Jamieson, M.A., Burkle, L.A., Manson, J.S., Runyon, J.B., Trowbridge, A.M., Zientek, J., 2017. Global change effects on plant–insect interactions: the role of phytochemistry. Current Opinion in Insect Science 23, 70-80.

Leonti, M., Verpoorte, R., 2017. Traditional Mediterranean and European herbal medicines. Journal of Ethnopharmacology 199, 161-167.

Light, M.E., Sparg, S.G., Stafford, G.I., van Staden, J., 2005. Riding the wave: South Africa's contribution to ethnopharmacological research over the last 25 years. Journal of Ethnopharmacology 100, 127-130.

Mandal, S.C., Mandal, V., Das, A.K., 2015. Chapter 2 - History and Background on the Use of Natural Products Obtained from Plants as Therapeutic Agents, in: Mandal, S.C., Mandal, V., Das, A.K. (Eds.), Essentials of Botanical Extraction. Academic Press, Boston, pp. 7-17.

Mander, M., Ntuli, L., Diederichs, N., Mavundla, K., 2007. Economics of the traditional medicine trade in South Africa care delivery. South African Health Review 2007, 189-196.

Moosavyzadeh, A., Ghaffari, F., Mosavat, S.H., Zargaran, A., Mokri, A., Faghihzadeh, S., Naseri, M., 2018. The medieval Persian manuscript of Afyunieh: the first individual treatise on the opium and addiction in history. Journal of Integrative Medicine 16, 77-83.

Mulholland, D.A., 2005. The future of ethnopharmacology: A southern African perspective. Journal of Ethnopharmacology 100, 124-126.

Newman, D.J., Cragg, G.M., 2020. Natural products as sources of new drugs over the nearly four decades from 01/1981 to 09/2019. Journal of Natural Products 83, 770-803.

Nortje, J.M., van Wyk, B.E., 2015. Medicinal plants of the Kamiesberg, Namaqualand, South Africa. Journal of Ethnopharmacology 171, 205-222.

Núñez Sellés, A.J., 2019. Natural Health Products (NHPs)☆, in: Nriagu, J. (Ed.) Encyclopedia of Environmental Health (Second Edition). Elsevier, Oxford, pp. 577-587.

Parker, L.A., 1915. A brief history of materia medica. The American Journal of Nursing 15, 650-653.

Retief, F., Cilliers, L., 2007. Mesopotamian medicine. South African Medical Journal 97, 27-29.

Russell, G.A., 2009. After Galen: late Antiquity and the Islamic world, in: Aminoff, M.J., Boller, F., Swaab, D.F. (Eds.), Handbook of Clinical Neurology. Elsevier, pp. 61-77.

Saxena, M., Saxena, J., Nema, R., Singh, D., Gupta, A., 2013. Phytochemistry of medicinal plants. Journal of Pharmacognosy and Phytochemistry 1, 168-182.

Soelberg, J., Asase, A., Akwetey, G., Jäger, A.K., 2015. Historical versus contemporary medicinal plant uses in Ghana. Journal of Ethnopharmacology 160, 109-132.

Thomas, V., Nair, S.N.V., Ved, D.K., Shankar, D., 2020. Controversial identities of medicinal plants in classical literature of Ayurveda. Journal of Ayurveda and Integrative Medicine, 565-572.

Van den Honert, M., Gouws, P., Hoffman, L., 2018. Importance and implications of antibiotic resistance development in livestock and wildlife farming in South Africa: A review. South African Journal of Animal Science 48, 401-412.

Van Wyk, B.E., Moteetee, N.A., 2019. Ethnobotanical research in sub-Saharan Africa – documenting and analysing indigenous knowledge about medicinal, edible and other useful plants. South African Journal of Botany 122, 1-2.

Wayne, R., 2019. Omic Science: Platforms and Pipelines, in: Wayne, R. (Ed.) Plant Cell Biology (Second Edition). Academic Press, pp. 411-471.

Wink, M., 2013. Evolution of secondary metabolites in legumes (Fabaceae). South African Journal of Botany 89, 164-175.

Yao, J.S., Kibu, O.D., Asahngwa, C., Ngo, N.V., Ngwa, W., Jasmin, H.M., Gobina, R.M., Foretia, D.A., 2023. A scoping review on the availability and utilization of essential opioid analgesics in Sub-Saharan Africa. The American Journal of Surgery 226, 409-421.

Zou, P., 2020. Chinese Medicine, Traditional, in: Kobayashi, A. (Ed.) International Encyclopedia of Human Geography (Second Edition). Elsevier, Oxford, pp. 173-179.

Žuškin, E., Lipozenčić, J., Pucarin-Cvetković, J., Mustajbegović, J., Schachter, N., Mučić-Pučić, B., Neralić-Meniga, I., 2008. Ancient medicine-a review. Acta Dermatovenerologica Croatica 16, 149-157.

Chapter 2 An imprecise probability approach-based determination of over-represented southern African plant genera and families used in ethnopharmacology

2.1 Introduction

Medicinal plant taxonomic groups occur in ethnobotanical pharmacopoeia in different proportions than random chance would allow (Moerman, 1999). This phenomenon implies selectivity in the choice of medicinal plants used in ethnic cultures. Taxonomic groups that occur at higher ratios in pharmacopoeia than in the total flora are said to be over-represented, while those at lower ratios are under-represented (Bennet and Husby, 2008). Analysing the representation of taxa in medicinal flora enhances ethnobotanical understanding and can inform the rationality of phytochemical and bioactivity investigations. Analytical methods have been developed to determine which taxonomic groups are over- or under-represented in medicinal flora. Moerman (1979, 1991) applied a linear regression analytical method, which showed that the residuals associated with plant families used in native American medical ethnobotany are not randomly distributed. Bennet and Husby (2008) introduced an inferential statistical method that applied contingency tables and a goodness of fit test to assess the significance of deviations from the null hypothesis that there is no relationship between family affiliation and proportion of medicinal plants. Weckerle et al. (2011) used a Bayesian theorem-based approach, which took into account the uncertainty associated with the proportion of medicinal plants (θ) in the total flora of Campania (Italy). This method introduces a probability distribution for θ and for θ_j (the fraction of medicinal plants in a taxonomic group j). The imprecise Dirichlet model-based approach used by Weckerle et al. (2012) also considers that the exact values associated with the total flora are unknown. This paper uses this latter method to analyse southern African medicinal flora.

Southern African countries have rich floral diversity and ethnopharmacological traditions. The region under consideration covers the countries of Angola, Botswana, Eswatini, Lesotho, Malawi, Mozambique, Namibia, South Africa, Zambia, and Zimbabwe (Marks, 2023). Analysis of southern African medicinal plants has only been done as part of the broader sub-

Saharan Africa flora (Van Wyk, 2020). Van Wyk observed that families that are prominent in African ethnobotanical medicine are not as prominent in North American medicinal flora. Studies on the over- and under-representation of medicinal taxa have focused on family-level analysis. Analyses at the genus level have not been reported. Given that phytochemical similarities increase down the taxonomic ladder, determining over-represented medicinal genera rather than families may be of more value in selecting plants for further investigation and development of plant-derived medicinal products.

One of the significant unanswered questions is how determining taxonomic families as over-represented taxa translates to the representation of genera within those families. Secondly, are there any differences in over-represented taxa among neighbouring countries of southern Africa? A third question is whether particular disease categories have a preponderant floral taxonomic treatment regime.

Within southern Africa, utilising traditional medicines, particularly those of plant origin, for treating diseases is a wonted practice (Bhuda and Marumo, 2020). Plant preparations are used to treat infectious diseases, cancers, fever, and pain (Cock et al., 2023; Khumalo et al., 2022; Koduru et al., 2007; York et al., 2011). Infertility, problems during childbirth, and some mental diseases are traditionally treated with plant medicines (Kaido et al., 1997; Moteetee and Seleteng Kose, 2016; Stafford et al., 2008). Due to historical and ongoing migration and informal trade, the region has evolved into both an economic and cultural marketplace. Medicinal plants, alongside other goods, are traded across borders. As a result, there is an exchange of traditional medical and cultural practices (Crush et al., 2005; Meke et al., 2017).

The subcontinent suffers from high mortality rates linked to an inordinate incidence of tuberculosis and the human immunodeficiency virus (HIV) (Uren et al., 2017). This block of countries has also met with uneven success in controlling malaria (Raman et al., 2021). The emergence of the novel severe acute respiratory syndrome coronavirus 2 (SARS-CoV-2) and the consequent coronavirus disease 2019 pandemic (COVID-19) has highlighted the vulnerability of Africa to emerging infectious diseases (EIDs) (Nyaruaba et al., 2022). Significant drivers of EIDs, such as dire socio-economic, environmental and ecological factors, and the widespread practice of subsistence animal husbandry are all present in southern Africa (Hanin et al., 2018; Karimuribo et al., 2012). Since 60% of known infections and 75% of EIDs have zoonotic origins, the region is at high risk of infectious disease outbreaks (Elton et al., 2021). Concomitantly, these nations are facing a rise in the prevalence of non-communicable

diseases (Nojilana et al., 2016). Limited access to and affordability of globally produced medicines and the growing threat of antibiotic resistance are all challenges faced by southern Africa (Mercat et al., 2016; Mhlanga and Suleman, 2014; Ooms et al., 2020).

Research on plant-derived natural products has the potential to result in the identification of bioactive drug-lead compounds (Newman and Cragg, 2020). Such research may form part of the solution to southern Africa's disease burden. Plants used in traditional medicine are of particular interest as they have been applied extensively to treating disease over time.

This paper analyses ethnopharmacological data from 43 publications from 10 southern African countries. An Imprecise Dirichlet Model (IDM)-based approach was used to determine over-represented southern African medicinal plant families and genera. The Pearson correlation was applied to gain insight into the relatedness of the flora across the ten countries. Three groups of countries were generated based on the Jaccard coefficients between their total flora. Over-represented taxa in each group were determined. The over-represented taxa of plants used in the treatment of six categories of diseases were also analysed.

2.2 Materials and methods

2.2.1 Data collection and cleaning

Data for the total floral composition used in IDM analyses was obtained from the African plant database (Database, 2022) and the SANBI checklist (Klopper and Winter, 2023). To perform the IDM analysis, species names were updated to the prevailing synonyms on the Plants of the World database (POWO, 2023). Subspecies and variants were not counted separately. As a result, the number of total unique species in each country is less than the number of total taxa.

A list of medicinal plant species from southern Africa was extracted from 43 published surveys and regional medicinal plant-use inventories, as shown in Table 2.1. The surveys were obtained through a general search on Google Scholar, ScienceDirect, Scopus and Web of Science using the phrase, '*X* ethnobotanical plants, medicinal plants survey', where *X* is each of the ten countries in this study. Introduced species were not included in the IDM analyses.

Outdated species synonyms were updated in line with the POWO website. As a consequence of this, the plant families Tiliaceae and Sterculiaceae were merged into Malvaceae, Oliniaceae into Penaeaceae, Hydnoraceae into Aristolochaceae, Alliaceae and Agapanthaceae into Amaryllidaceae, Ruscaceae, Hyacinthaceae, Ptaeroxylaceae and Agavaceae into Asparagaceae, Adiantaceae into Pteridaceae, Asclepiadaceae into Apocynaceae, and

Myrsinaceae into Primulaceae. *Acacia* species were reclassified as *Acacia*, *Senegalia* or *Vachellia*. African species formerly in the *Rhus* genus have been placed in the *Searsia* genus. The *Anemone* genus was reclassified as *Knowltonia*, *Azanza* into *Thespesia*, *Elephantorrhiza* into *Entada*, *Mohria* into *Anemia*, and *Rapanea* into *Myrsine*.

Table 2.1: Sources of medicinal plant data from the ten southern African countries.

Country	Number of reviewed articles	Reference
Angola	4	(Novotna et al., 2020; Pompermaier et al., 2018; Urso et al., 2016; Vahekeni et al., 2020)
Botswana	5	(Dube et al., 2022; Hedberg and Staugard, 1989; Motlhanka and Nthoiwa, 2013; Okatch et al., 2012; Setshogo and Mbereki, 2011)
Eswatini	2	(Amusan, 2009; Amusan et al., 2002)
Lesotho	3	(Mabaleha et al., 2019; Mugomeri et al., 2016; Seleteng Kose et al., 2015)
Malawi	4	(Bundschuh et al., 2011; Meke et al., 2017; Tembo et al., 2021; Williamson, 2005)
Mozambique	3	(Barbosa et al., 2020; Bruschi et al., 2011; Ribeiro et al., 2010)
Namibia	3	(Cheikhyoussef et al., 2011; Chinsembu and Hedimbi, 2010; Chinsembu et al., 2014)
South Africa	12	(Afolayan and Mbaebie, 2010; Arnold and Gulumian, 1984; Grierson and Afolayan, 1999; Hutchings et al., 1996; Koduru et al., 2007; Mahwasane et al., 2013; Masevhe et al., 2015; Mhlongo and Van Wyk, 2019; Mulaudzi et al., 2015; van Wyk et al., 2022; Watt and Breyer-Brandwijk, 1962; York et al., 2011)
Zambia	3	(Chinsembu, K., 2016; Chinsembu, K.C., 2016; Chinsembu et al., 2019)
Zimbabwe	4	(Gelfand et al., 1985; Maroyi, 2011; Ngarivhume et al., 2015; Shopo et al., 2022)

The six disease categories in this analysis are sexually transmitted infections (STIs), non-STI microbial infections, febrile and mosquito vector diseases, pain, skin-related conditions, and maternal/female reproductive and sexual health. The categories were selected based on one of, or a combination of, the high incidence in southern Africa and the high numbers of plant species

used in their treatment. 1484 out of 2168 southern African medicinal plant species are used to treat diseases in these six categories.

2.2.2 Analytical methods

The IDM calculations are based on the paper by Weckerle et al. (2012) and were performed using the inverse of the cumulative beta probability density function (BETA.INV) in Microsoft Excel™ 2016. The formula for the lower limit (inferior or Inf.) of the 95% probability interval is "=(BETA.INV(0.025, *B*, *A*-*B*+4)". The formula for the upper limit (superior or Sup.) of the 95% probability interval is "=BETA.INV(0.975, *B*+4, *A*-*B*)". *A* represents the total number of species in a group, and *B* represents the number of medicinal species in a group. The margin is the difference between the upper limit (Sup.) of the 95% probability interval of total medicinal flora and the lower limit (Inf.) of the probability interval of a taxonomic group's medicinal flora. For example, the margin of Loganiaceae (Appendix A Table S.1) is obtained by subtracting the Sup. value of the total flora (0.076) from the Inf. value of the family (0.218), which gives a margin of 0.142.

Measuring floral relatedness using the Pearson correlation between the number of plants per family has been exemplified by Leonti et al. (2003). In this paper, Pearson correlations between floras were calculated utilising a Python™ program (Python Software Foundation) on the Visual Studio Code™ (Microsoft Corporation) integrated development environment. The source code is supplied in supplementary file.

To determine differences in the over-represented medicinal flora within the southern African region, countries were grouped based on the similarity of their total flora as measured by the Jaccard coefficient. Generated groups are discussed further in section 2.3.3. The Jaccard coefficient measures the similarity between two sets using the quotient of the number of common elements in the set (the intersection) and the total unique elements (the union) of both sets. For 2 sets *A* and *B*, the Jaccard coefficient $J = A \cap B / A \cup B$.

For this study, the lists were considered sufficiently similar if the overall flora *J* between the two countries was close to or above 0.333. The reason for this is that this value constrains the proportion of common elements to ≥ 50% in the smaller of the two sets and ≥ 25% in the larger set while ensuring that the more extensive set is no more than three times the size of the smaller one as shown in Figure 2.1.

Proof:

For two sets *A* and *B*, the number of elements in the intersection $n(A \cap B) = I$ and the number of elements in the union $n(A \cup B) = nA + nB - I$,

$$\text{therefore } J = \frac{I}{nA+nB-I}$$

$$\text{If } J \geq \frac{1}{3} \sim 0.333,$$

$$\text{then } \frac{I}{nA+nB-I} \geq 0.333$$

$$\text{So, } \frac{I}{nA} \geq \frac{0.333}{1.333}\left(1 + \frac{nB}{nA}\right)$$

$$\text{and, } \frac{I}{nA} \geq 0{,}25\left(1 + \frac{nB}{nA}\right)$$

Figure 2.1: Proof that *J* = 1/3 corresponds to at least 50% of common elements in one of the sets**.**

The Jaccard coefficients were calculated using a Python program. The source code is supplied in the supplementary file.

2.3 Results and Discussion

2.3.1 Relatedness of the Southern African total flora

A total of 28426 unique species were retrieved from databases. Pearson correlations between the total species in each country were calculated using data from the African plant database (Database, 2022), and the results are shown in Table 2.2.

Lesotho flora showed relatively low correlations of 0.48, 0.52, 0.57 and 0.58 with Angola, Zambia, Malawi, Mozambique and Zimbabwe, respectively. High correlations of 0.82 (Lesotho and Namibia flora) and 0.86 (Lesotho and South Africa flora) were found. A relatively low correlation of 0.57 exists between South African and Zimbabwean flora. However, there are generally high correlations between most of the countries. Thirty-two of forty-five possible correlations have values of at least 0.70. Except for Lesotho, each country has correlations of 0.6 and higher with at least five countries. The generally high correlations between countries in southern Africa show the relatedness of southern African flora. A total of 2168 medicinal plant species were obtained. The number of indigenous species is 2069. Ninety-nine species are introduced.

Table 1.2: Pearson correlation coefficients (r) between the number of plants per family for each pair of countries.

	BW	SZ	LS	MW	MZ	NM	ZA	ZM	ZW
AO	0.81	0.80	0.48	0.87	0.97	0.68	0.59	0.96	0.92
BW		0.92	0.73	0.73	0.87	0.94	0.75	0.80	0.86
SZ			0.87	0.78	0.88	0.89	0.81	0.80	0.84
LS				0.57	0.58	0.82	0.86	0.52	0.58
MW					0.89	0.62	0.59	0.95	0.95
MZ						0.76	0.65	0.95	0.96
NM							0.86	0.65	0.73
ZA								0.57	0.61
ZM									0.97

p values range between 7.2 exp -106 and 5.5 exp -9

2.3.2 Comparing genus-level over-representation with family-level over-representation

The IDM calculated results for the over-represented families and genera used in southern African ethnopharmacology (Group 1) are shown in Table S.1 and Table S.2 (supplementary appendix A). There are 92 over-represented genera and 42 over-represented families.

In Figure 2.2, the margins of the over-represented families are plotted together with the cumulative margins of over-represented genera. Cumulative margins were obtained by adding the margins of all the over-represented genera belonging to the corresponding family. When family over-representation alone is considered, the Loganiaceae has the highest margin of over-representation (0.142). Fabaceae (0.010), Rubiaceae (0.038), Lamiaceae (0.045), Anacardiaceae (0.101), Malvaceae (0.032) and Boraginaceae (0.008) all have lower margins of over-representation than Loganiaceae. The corresponding cumulative margins of their over-represented genera, however, are all higher than those of Loganiaceae with Fabaceae (0.743), Rubiaceae (0.336), Lamiaceae (0.246), Anacardiaceae (0.168), Malvaceae (0.147) and Boraginaceae (0.177). Nineteen of the 42 over-represented families have margins of over-representation smaller than the cumulative margins of their over-represented genera. Nine over-represented families do not have over-represented genera. Those nine are Annonaceae, Bignoniaceae, Cannabaceae, Caprifoliaceae, Meliaceae, Menispermaceae, Primulaceae, Salvadoraceae and Vitaceae.

Twenty-six of the over-represented genera in Table S.2 belong to families that are not in the over-represented list. Figure 2.3 shows the graph of genera with the 40 highest margins of over-representation and the margins of their corresponding families. The genus *Albizia* has the largest margin of ever-representation (0.156) among genera, even though its corresponding family is only ranked as the 39th over-represented family in Table S.1. *Agapanthus*, *Asparagus*, *Zanthoxylum*, *Ziziphus*, *Gymnanthemum*, *Laggera* and *Cymbopogon* are over-represented, but their corresponding families are under-represented. The margins of over-representation of *Euclea*, *Bersama*, *Searsia*, *Knowltonia*, *Dioscorea*, *Combretum*, and *Diospyros* are out-paced by the margins of over-representation of their families. This is due to the presence of other genera within these families that have high margins of over-representation. In the rest of the taxa in Figure 2.3, the margins of over-represented genera out-pace those of the corresponding families.

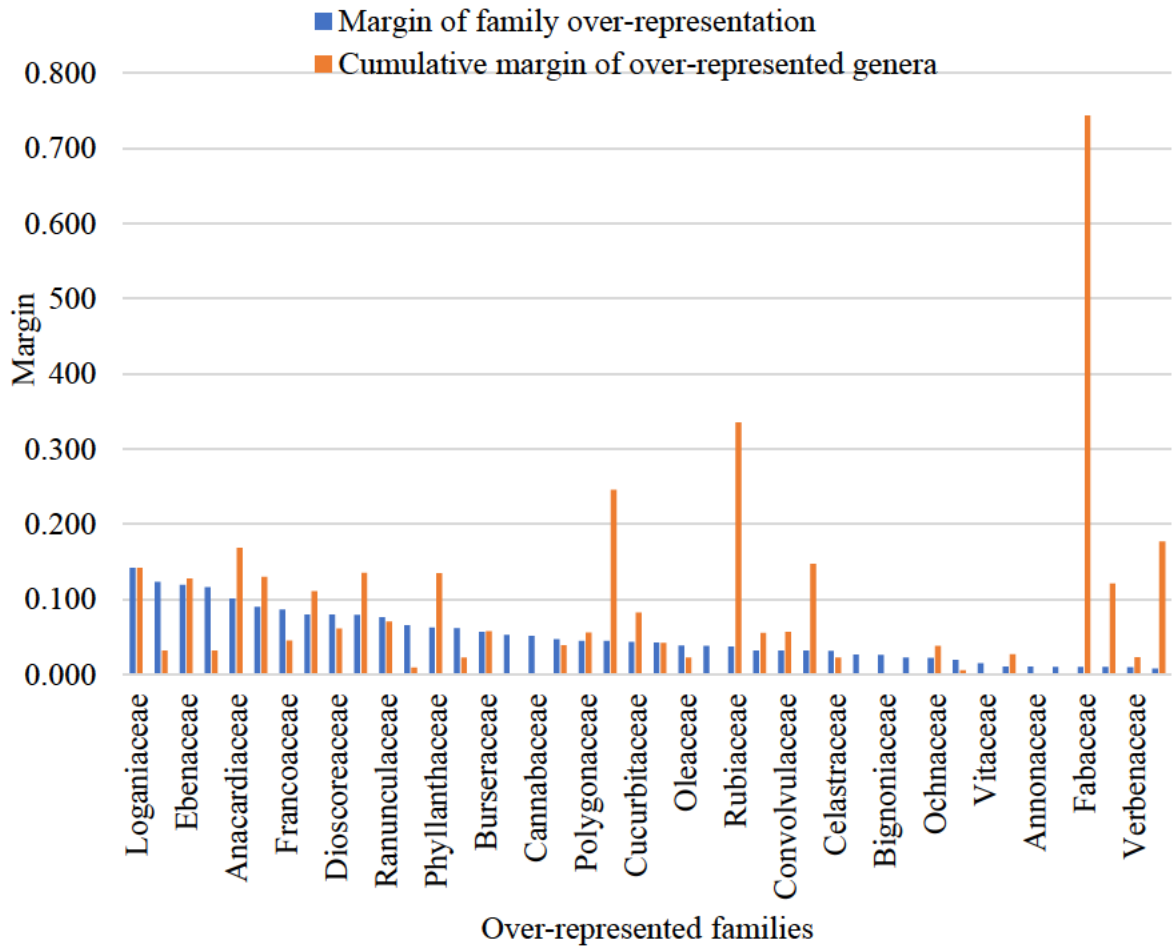

Figure 1.2: Comparison of family-level margins of over-representation with the corresponding cumulative genera margin.

It is clear from this analysis that the determination of medicinal families as over- or under-represented does not necessarily translate to the genera within the family. An analysis considering families only may result in otherwise over-represented genera being disregarded if they belong to under-represented families. Plant natural product researchers cannot rely on over-represented families when selecting plants for bioactive phytochemical screening as these families inevitably include under-represented genera. Analysis at the genus level is more efficient as it delineates between under- and over-represented genera.

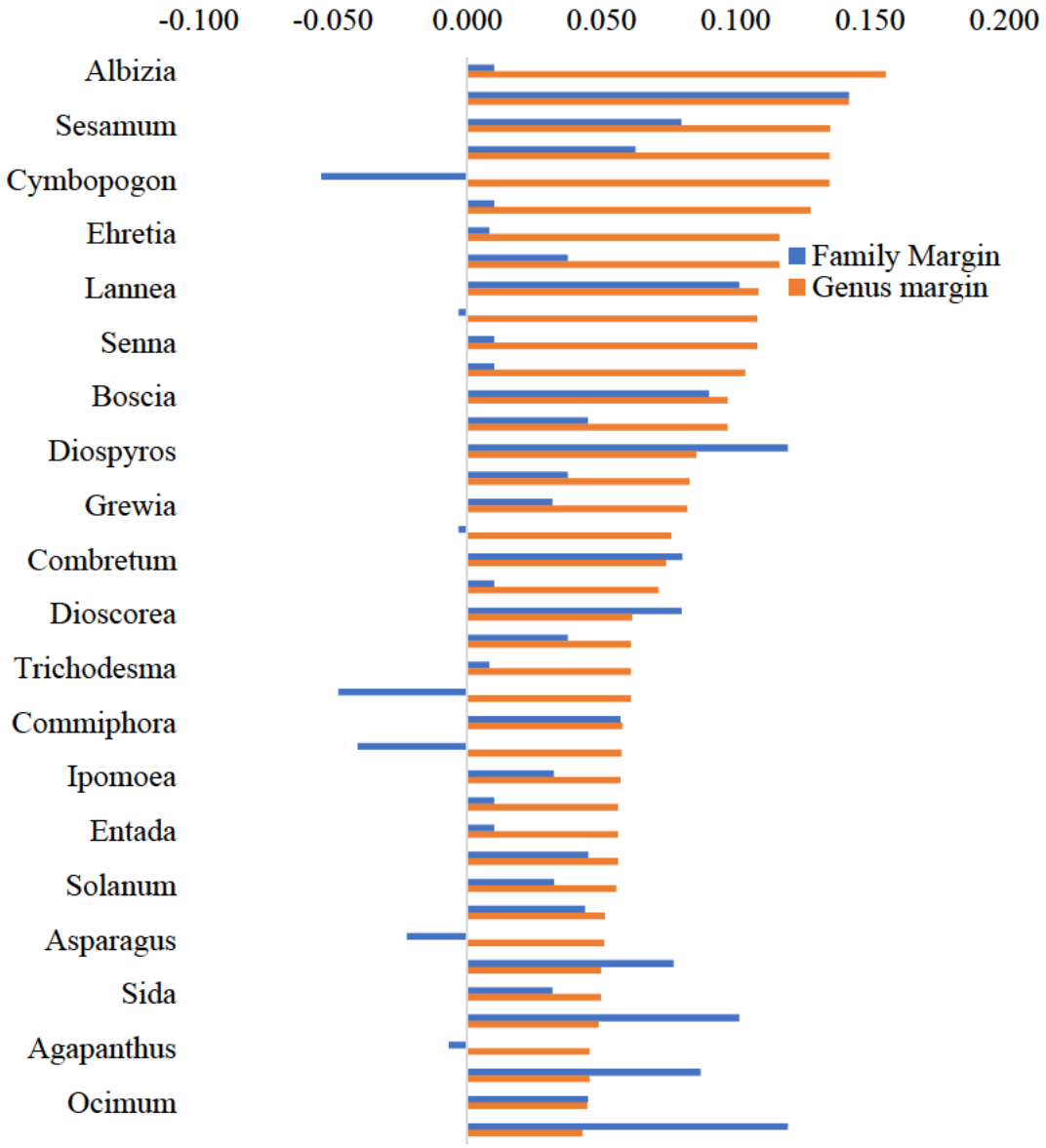

Figure 2.2: Comparison of the margins of over-represented genera with the margins of the corresponding families.

2.3.3 Comparing over-represented taxa among groups of southern African countries

The combination of the ten countries is assigned to group 1. Jaccard coefficients (*J*) between the total number of species in each pair of countries are shown in Table 2.3. The *J* for Botswana and Namibia is 0.363, and no other country shares a *J* of ≥ 0.333 with these two countries. Therefore, Botswana and Namibia are assigned as group 2. Malawi, Mozambique, Zambia and Zimbabwe are designated as group 3. Apart from the *J* for Zambia and Mozambique, which is 0.28, in group 2, all the other *J* values are ≥ 0.333; therefore, both Zambia and Mozambique are included. South Africa is treated separately as group 4 as its *J* values fall outside the constraint of $J \geq 0.333$. Angola, Eswatini and Lesotho are analysed as part of group 1. Figure 2.4 shows the total taxa, total plant species and medicinal plant species for each of the groups 2 to 4 and the countries of Angola, Eswatini and Lesotho.

Table 2.2: Matrix of Jaccard coefficients between total species of southern African countries

	BW	SZ	LS	MW	MZ	NM	ZA	ZM	ZW
AO	0.184	0.113	0.040	0.193	0.195	0.180	0.065	0.295	0.228
BW		0.226	0.095	0.126	0.209	0.363	0.112	0.184	0.290
SZ			0.217	0.153	0.297	0.140	0.157	0.125	0.244
LS				0.066	0.073	0.074	0.125	0.043	0.093
MW					0.333	0.089	0.066	0.380	0.356
MZ						0.142	0.127	0.280	0.416
NM							0.145	0.137	0.195
ZA								0.066	0.119
ZM									0.350

2.3.4 IDM analysis of over-represented taxa in the four groups

Supplementary Tables S.1 to S.8 show the over-represented medicinal genera and families in the four groups. Group 1 has 42 over-represented medicinal plant families. Group 2 has nine over-represented plant families, while groups 3 and 4 have 14 and 37 over-represented families, respectively. There are 44 unique over-represented families across groups 2-4.

Figure 2.5 shows the over-represented families for each of groups 1 to 4. Only four families, Combretaceae, Phyllanthaceae, Ebenaceae and Capparaceae, are over-represented in all four

groups. Bignoniaceae, Salvadoraceae, Peraceae, Clusiaceae and Boraginaceae are over-represented in group 1 (southern Africa) but are not over-represented in any of groups 2 to 4. 37 of the 44 unique over-represented families from groups 2-4 are present in group 1. The seven that are not present in the overall over-represented medicinal families of group 1 are Amaranthaceae, Myrtaceae, Olacaceae, Pteridaceae, Salicaceae, Thymelaeaceae and Urticaceae. The families with the highest margin of over-representation differ for each group: Loganiaceae in group 1, Combretaceae in group 2, Dioscoreaceae in group 3 and Sapotaceae in group 4.

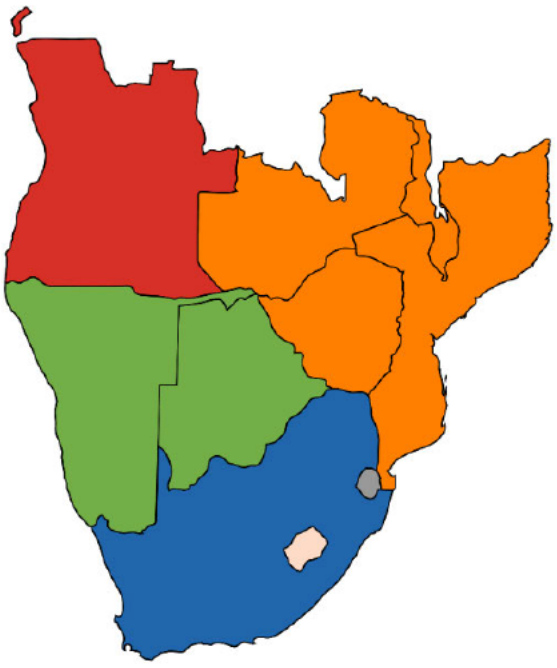

Botswana, Namibia	Taxa	4733
	Species	4483
	Medicinal	366
Malawi, Mozambique, Zambia, Zimbabwe	Taxa	7901
	Species	7775
	Medicinal	735
South Africa	Taxa	23200
	Species	19365
	Medicinal	1268
Angola	Taxa	4294
	Species	4200
	Medicinal	200
Eswatini	Taxa	3005
	Species	2842
	Medicinal	89
Lesotho	Taxa	2482
	Species	2352
	Medicinal	117

Figure 2.3: Map of the floral distribution of southern Africa, highlighting countries grouped by the Jaccard coefficient.

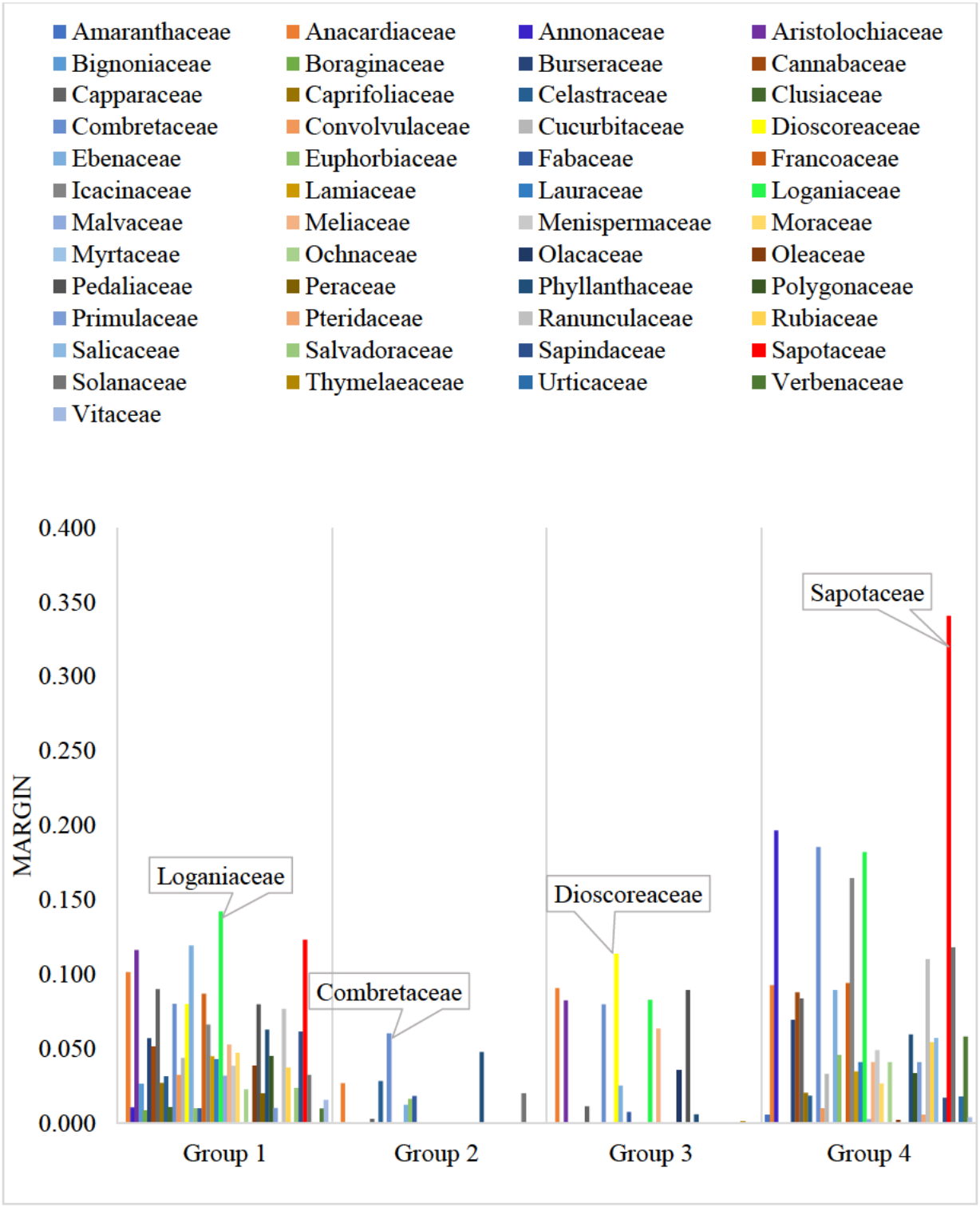

Figure 2.4. Over-represented families by groups of countries.

Figure 2.6 shows the genera with the 20 highest margins of over-representation by group. The number of over-represented genera in groups 1, 2, 3 and 4 is 92, 8, 18 and 61, respectively. There are 72 unique over-represented genera across groups 2 to 4. Only four are over-

represented across all four groups: *Albizia*, *Combretum*, *Grewia* and *Vachellia*. The most over-represented genera in the separate groups differ across the four groups: *Albizia* in group 1, *Vachellia* in group 2, *Senna* in group 3 and *Solanum* in group 4. 57 of the 72 genera from groups 2-4 are present among the 92 genera of group 1.

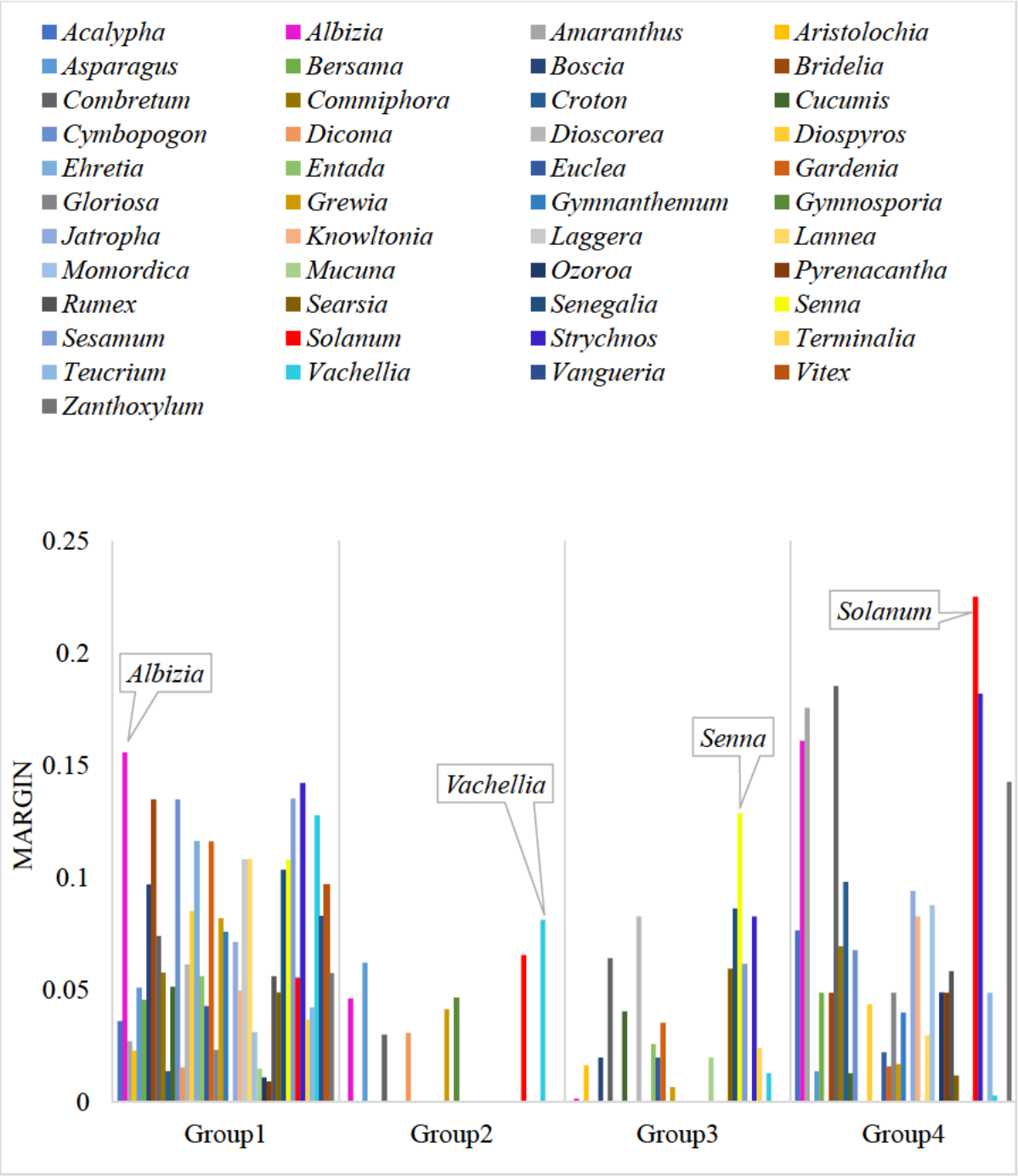

Figure 2.5: Over-represented genera by groups of countries.

Even though the countries share geographical, floral and cultural similarities, over-represented taxa are not uniform across the four groups. These findings imply that the determination of over-representation of taxa across extensive geographical regions may exclude niche taxa. For example, Amaranthaceae is over-represented in group 4 (South Africa) only, and *Gymnosporia* is over-represented only in group 2. *Rubus*, *Eulophia*, *Cissampelos*, *Coleus*, *Cassipourea*, *Dalbergia*, *Thunbergia*, *Hemionitis*, *Convolvulus*, *Dovyalis*, *Melianthus*, *Schistostephium*, *Eucomis*, and *Helichrysum* are over-represented only in group 4.

2.3.5 Comparing over-represented taxa across disease categories

The six disease categories included in the IDM analyses are shown in Table 2.4.

Table 2.3: Disease categories chosen for IDM analysis.

Disease category	Examples	Total number of species used	Number of indigenous species
Sexually transmitted infections (STIs)	Syphilis, gonorrhoea and urinary tract infections	414	388
Febrile and Mosquito vector diseases	Malaria, fever	228	210
Non-STI microbial infections	Tuberculosis, smallpox, colds	560	536
Pain	Headache, arthralgia	596	569
Skin conditions	Boils, burns and wounds	537	515
Female sexual and reproductive health	Prevention of miscarriage, menorrhagia, abortifacients	506	495

Supplementary Tables S.9 to S.20 show the IDM analysis results of over-represented medicinal plant genera and families used for treatment in the six disease categories. The combined number of unique, over-represented families for all six categories is 45. None of the families are over-represented across all six categories. Thirty-six families are over-represented in 3 or fewer categories. Only four families, Anacardiaceae, Ebenaceae, Lamiaceae and Loganiaceae, are over-represented across five disease categories. Figure 2.7 shows the over-represented families in each of the six categories. The families with the highest over-representation margin for STIs, febrile and mosquito vector diseases, non-STI infectious diseases, pain, skin

conditions and female sexual/ reproductive health are Ebenaceae, Canellaceae, Combretaceae, Ebenaceae, Francoaceae, and Aristolochiaceae, respectively.

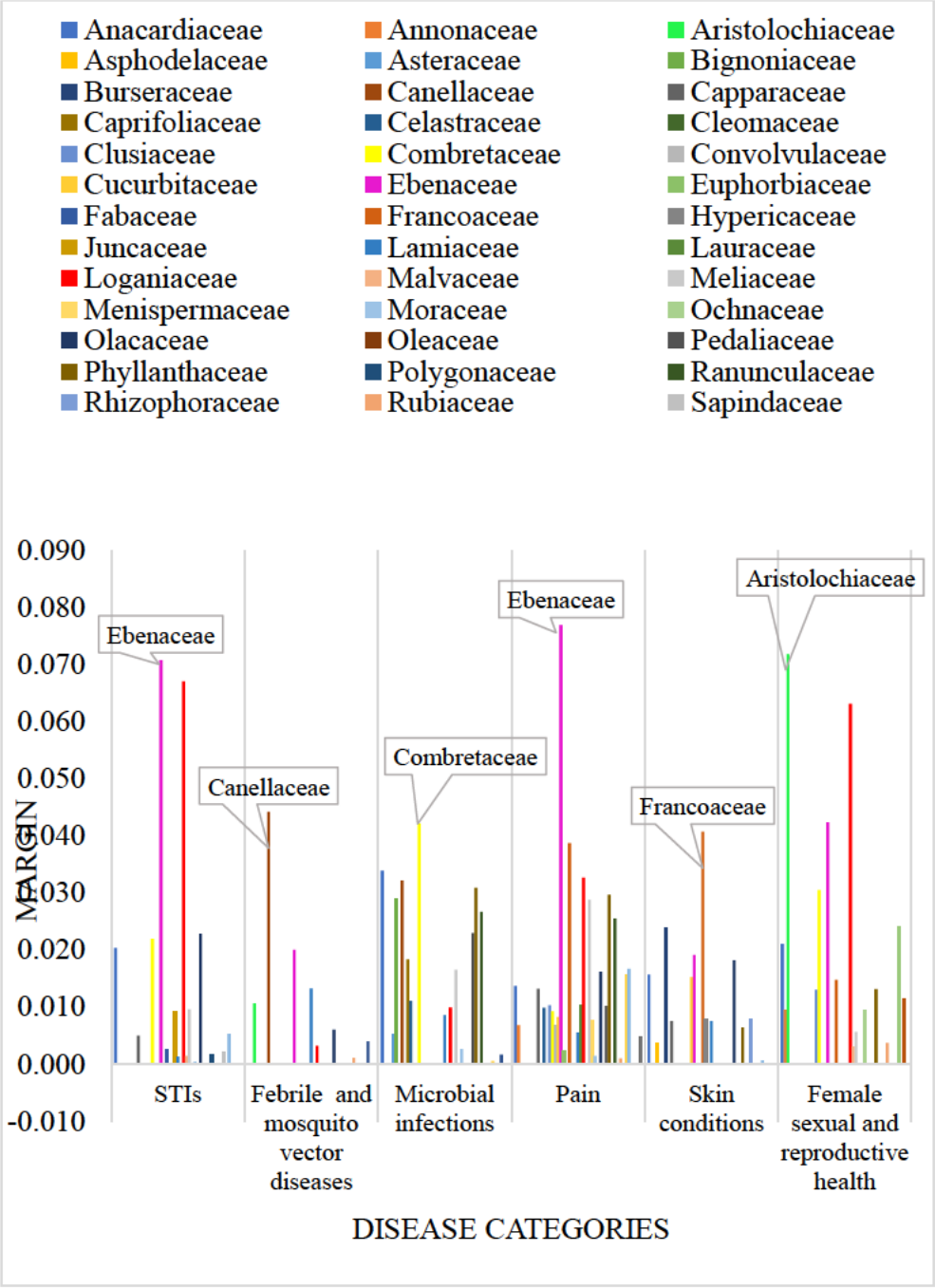

Figure 2.6: Over-represented families of plants used to treat the six disease categories.

There are 135 unique over-represented genera for all six disease categories combined. One hundred five genera are over-represented in three or fewer categories. *Annona* is the only genus that is over-represented across all six disease categories. Seventy-four out of the one hundred

and thirty-five genera are over-represented in only one disease category. Figure 2.8 shows the genera with the 15 highest margins of over-representation per disease category.

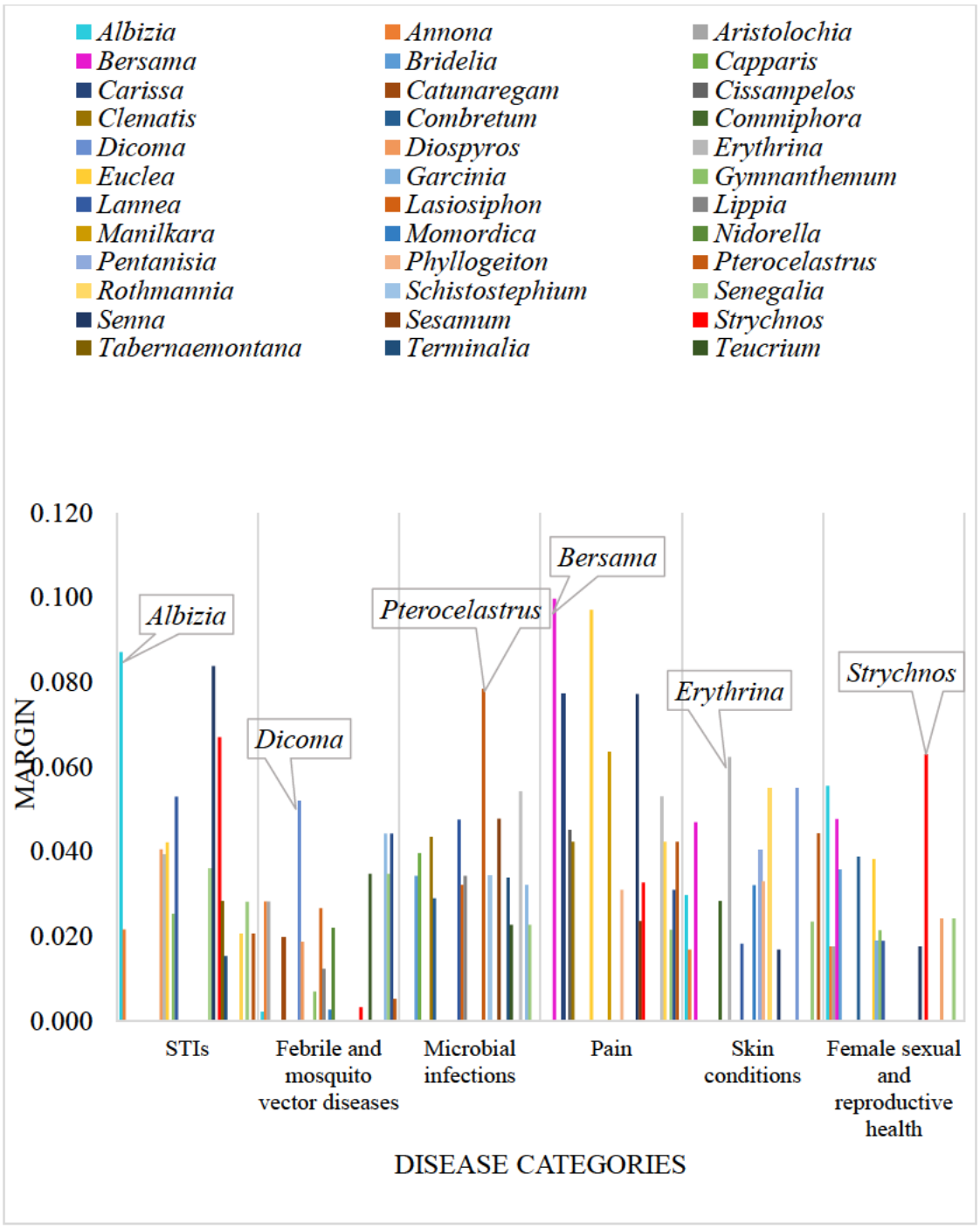

Figure 2.7: Over-represented families of plants used to treat the six disease categories.

The genera with the highest over-representation margin for STI, febrile and mosquito vector diseases, non-STI infectious diseases, pain, skin conditions and female sexual/ reproductive health are *Albizia*, *Dicoma*, *Pterocelastrus*, *Bersama*, *Erythrina* and, *Strychnos*, respectively.

The utility of analysing taxa based on specific disease categories is shown by the fact that some families and genera are under-represented in group 1 (analysis of all southern African medicinal plants) but are over-represented in at least one disease category. The families Olacaceae and Juncaceae are over-represented in the STI disease category but under-represented amongst the total southern African medicinal plants (group 1). Canellaceae, Olacaceae, and Cleomaceae are over-represented in the febrile and mosquito vector disease categories but under-represented in group 1. While Asteraceae and Canellaceae are over-represented in the microbial infectious diseases category, they are under-represented in group 1. Other families that are over-represented among the disease categories but under-represented in group 1 are Olacaceae and Zingiberaceae in the pain category, Olacaceae, Hypericaceae, Rhizophoraceae and Asphodelaceae in the skin conditions category, and Typhaceae in the female sexual/reproductive health category. Fifty-nine genera are under-represented in group 1 but are over-represented in at least one of the six disease categories (Supplementary Table S.21.

2.4 Conclusions

Determining medicinal plant families as over-represented does not necessarily translate to the genera of that family being over-represented. Some over-represented families do not have over-represented genera. In other cases, over-represented genera occur in under-represented families. As a result, using over-represented genera may be a more reliable method than using over-represented families in choosing plant species for further ethnopharmalogical investigations.

Furthermore, the over-representation of medicinal plant genera and families varies among the groups of southern African countries. This variation suggests that determining over-represented taxa using data collated from vast regions across which floral compositions vary may be unreliable. Some niche medicinal taxa may be underestimated if these variations are not considered. This underestimation is also noticed when over-represented taxa for specific disease categories are compared to the over-represented medicinal taxa used for treatment across all disease categories.

Chapter two was published as:

Moyo, P.N., Van Heerden, F.R. 2024. An imprecise probability approach-based determination of over-represented southern African plant genera and families used in ethnopharmacology. Journal of Ethnopharmacology 324, 117757.

2.5 References

Afolayan, A., Mbaebie, B., 2010. Ethnobotanical study of medicinal plants used as anti-obesity remedies in Nkonkobe Municipality of South Africa. Pharmacognosy Journal 2(11), 368-373.

Amusan, O.O., 2009. Some ethnoremedies used for HIV/AIDS and related diseases in Swaziland. The African Journal of Plant Science and Biotechnology 3(1), 20-26.

Amusan, O.O., Dlamini, P.S., Msonthi, J.D., Makhubu, L.P., 2002. Some herbal remedies from Manzini region of Swaziland. Journal of Ethnopharmacology 79(1), 109-112.

Arnold, H.-J., Gulumian, M., 1984. Pharmacopoeia of traditional medicine in Venda. Journal of Ethnopharmacology 12(1), 35-74.

Barbosa, F., Hlashwayo, D., Sevastyanov, V., Chichava, V., Mataveia, A., Boane, E., Cala, A., 2020. Medicinal plants sold for treatment of bacterial and parasitic diseases in humans in Maputo city markets, Mozambique. BMC Complementary Medicine and Therapies 20(1), 1-13.

Bhuda, M.T., Marumo, P., 2020. African traditional medicine and healing in South Africa: Challenges and prospects before and during Covid 19. Ife Centre for Psychological Studies 18(4), 16710-16723.

Bruschi, P., Morganti, M., Mancini, M., Signorini, M.A., 2011. Traditional healers and laypeople: A qualitative and quantitative approach to local knowledge on medicinal plants in Muda (Mozambique). Journal of Ethnopharmacology 138(2), 543-563.

Bundschuh, T.V., Hahn, K., Wittig, R., 2011. The medicinal plants of the woodlands in northern Malawi (Karonga district). Flora et Vegetatio Sudano-Sambesica 14, 3-8.

Cheikhyoussef, A., Shapi, M., Matengu, K., Mu Ashekele, H., 2011. Ethnobotanical study of indigenous knowledge on medicinal plant use by traditional healers in Oshikoto region, Namibia. Journal of ethnobiology and ethnomedicine 7, 1-11.

Chinsembu, K., 2016. Ethnobotanical study of medicinal flora utilised by traditional healers in the management of sexually transmitted infections in Sesheke District, Western Province, Zambia. Revista Brasileira de Farmacognosia 26, 268-274.

Chinsembu, K.C., 2016. Ethnobotanical study of plants used in the management of HIV/AIDS-related diseases in Livingstone, Southern Province, Zambia. Evidence-Based Complementary and Alternative Medicine 2016, 1-14.

Chinsembu, K.C., Hedimbi, M., 2010. An ethnobotanical survey of plants used to manage HIV/AIDS opportunistic infections in Katima Mulilo, Caprivi region, Namibia. Journal of ethnobiology and ethnomedicine 6(1), 1-9.

Chinsembu, K.C., Negumbo, J., Likando, M., Mbangu, A., 2014. An ethnobotanical study of medicinal plants used to treat livestock diseases in Onayena and Katima Mulilo, Namibia. South African Journal of Botany 94, 101-107.

Chinsembu, K.C., Syakalima, M., Semenya, S.S., 2019. Ethnomedicinal plants used by traditional healers in the management of HIV/AIDS opportunistic diseases in Lusaka, Zambia. South African Journal of Botany 122, 369-384.

Cock, I.E., Luwaca, N., Van Vuuren, S.F., 2023. The traditional use of Southern African medicinal plants to alleviate fever and their antipyretic activities. Journal of Ethnopharmacology 303, 115850.

Crush, J., Williams, V., Peberdy, S., 2005. Migration in southern Africa. Policy analysis and research programme of the Global Commission on International Migration.

Database, A.P., 2022. African Plant Database. Conservatoire et Jardin botaniques de la Ville de Genève and South African National Biodiversity Institute, Geneva and Pretoria.

Dube, M., Raphane, B., Sethebe, B., Seputhe, N., Tiroyakgosi, T., Imming, P., Häberli, C., Keiser, J., Arnold, N., Andrae-Marobela, K., 2022. Medicinal plant preparations administered by Botswana traditional health practitioners for treatment of worm infections show anthelmintic activities. Plants 11(21), 2945.

Elton, L., Haider, N., Kock, R., Thomason, M.J., Tembo, J., Arruda, L.B., Ntoumi, F., Zumla, A., McHugh, T.D., And the, P.-I.D.N.E.T.c., 2021. Zoonotic disease preparedness in sub-Saharan African countries. One Health Outlook 3(1), 5.

Gelfand, M., Mavi, S., Drummond, R.B., Ndemera, B., 1985. The traditional medical practitioner in Zimbabwe: His principles of practice and pharmacopoeia. Mambo Press, Gweru, Zimabwe.

Grierson, D.S., Afolayan, A.J., 1999. An ethnobotanical study of plants used for the treatment of wounds in the Eastern Cape, South Africa. Journal of Ethnopharmacology 67(3), 327-332.

Hanin, M.C., Queenan, K., Savic, S., Karimuribo, E., Rüegg, S.R., Häsler, B., 2018. A one health evaluation of the Southern African Centre for Infectious Disease Surveillance. Frontiers in veterinary science 5, 33.

Hedberg, I., Staugard, F., 1989. Traditional Medicine in Botswana. Ipeleng Publishers, Gaborone.

Hutchings, A., Scott, A.H., Lewis, G., Cunningham, A.B., 1996. Zulu Medicinal Plants: An Inventory. University of Natal Press, Pietermaritzburg.

Kaido, T., Veale, D., Havlik, I., Rama, D., 1997. Preliminary screening of plants used in South Africa as traditional herbal remedies during pregnancy and labour. Journal of Ethnopharmacology 55(3), 185-191.

Karimuribo, E.D., Beda, E., Wambura, P., Rweyemamu, M.M., Sayalel, K., Kusiluka, L.J., Short, N., Mboera, L.G., 2012. Towards one health disease surveillance: the Southern African Centre for Infectious Disease Surveillance approach: proceeding. Onderstepoort Journal of Veterinary Research 79(2), 1-7.

Khumalo, G.P., Van Wyk, B.E., Feng, Y., Cock, I.E., 2022. A review of the traditional use of southern African medicinal plants for the treatment of inflammation and inflammatory pain. Journal of Ethnopharmacology 283, 114436.

Klopper, R.R., Winter, P.J.D., 2023. South African National Plant Checklist: yearly release and official documentation. South African National Biodiversity Institute, Pretoria.

Koduru, S., Grierson, D., Afolayan, A., 2007. Ethnobotanical information of medicinal plants used for treatment of cancer in the Eastern Cape Province, South Africa. Current Science, 906-908.

Mabaleha, M.B., Zietsman, P.C., Wilhelm, A., Bonnet, S.L., 2019. Ethnobotanical survey of medicinal plants used to treat mental illnesses in the Berea, Leribe, and Maseru Districts of Lesotho. Natural Product Communications 14(7), 1-13.

Mahwasane, S.T., Middleton, L., Boaduo, N., 2013. An ethnobotanical survey of indigenous knowledge on medicinal plants used by the traditional healers of the Lwamondo area, Limpopo province, South Africa. South African Journal of Botany 88, 69-75.

Maroyi, A., 2011. An ethnobotanical survey of medicinal plants used by the people in Nhema communal area, Zimbabwe. Journal of Ethnopharmacology 136(2), 347-354.

Masevhe, N.A., McGaw, L.J., Eloff, J.N., 2015. The traditional use of plants to manage candidiasis and related infections in Venda, South Africa. Journal of Ethnopharmacology 168, 364-372.

Meke, G.S., Mumba, R.F., Bwanali, R.J., Williams, V.L., 2017. The trade and marketing of traditional medicines in southern and central Malawi. International Journal of Sustainable Development & World Ecology 24(1), 73-87.

Mercat, M., Clermont, O., Massot, M., Ruppe, E., de Garine-Wichatitsky, M., Miguel, E., Valls Fox, H., Cornelis, D., Andremont, A., Denamur, E., 2016. *Escherichia coli* population structure and antibiotic resistance at a buffalo/cattle interface in southern Africa. Applied and Environmental Microbiology 82(5), 1459-1467.

Mhlanga, B.S., Suleman, F., 2014. Price, availability and affordability of medicines. African Journal of Primary Health Care & Family Medicine 6(1), 1-6.

Mhlongo, L.S., Van Wyk, B.E., 2019. Zulu medicinal ethnobotany: new records from the Amandawe area of KwaZulu-Natal, South Africa. South African Journal of Botany 122, 266-290.

Moteetee, A., Seleteng Kose, L., 2016. Medicinal plants used in Lesotho for treatment of reproductive and post reproductive problems. Journal of Ethnopharmacology 194, 827-849.

Motlhanka, D., Nthoiwa, G., 2013. Ethnobotanical survey of medicinal plants of Tswapong North, in eastern Botswana: a case of plants from Mosweu and Seolwane villages. European Journal of Medicinal Plants 3(1), 10-24.

Mugomeri, E., Chatanga, P., Raditladi, T., Makara, M., Tarirai, C., 2016. Ethnobotanical study and conservation status of local medicinal plants: Towards a repository and monograph of herbal medicines in Lesotho. African Journal of Traditional, Complementary and Alternative Medicines 13(1), 143-156.

Mulaudzi, R., Ndhlala, A., Van Staden, J., 2015. Ethnopharmacological evaluation of a traditional herbal remedy used to treat gonorrhoea in Limpopo province, South Africa. South African Journal of Botany 97, 117-122.

Newman, D.J., Cragg, G.M., 2020. Natural products as sources of new drugs over the nearly four decades from 01/1981 to 09/2019. Journal of Natural Products 83(3), 770-803.

Ngarivhume, T., van't Klooster, C.I.E.A., de Jong, J.T.V.M., Van der Westhuizen, J.H., 2015. Medicinal plants used by traditional healers for the treatment of malaria in the Chipinge district in Zimbabwe. Journal of Ethnopharmacology 159, 224-237.

Nojilana, B., Bradshaw, D., Pillay-van Wyk, V., Msemburi, W., Somdyala, N., Joubert, J.D., Groenewald, P., Laubscher, R., Dorrington, R.E., 2016. Persistent burden from non-communicable diseases in South Africa needs strong action. South African Medical Journal 106(5), 436-437.

Novotna, B., Polesny, Z., Pinto-Basto, M.F., Van Damme, P., Pudil, P., Mazancova, J., Duarte, M.C., 2020. Medicinal plants used by 'root doctors', local traditional healers in Bié province, Angola. Journal of Ethnopharmacology 260, 112662.

Nyaruaba, R., Okoye, C.O., Akan, O.D., Mwaliko, C., Ebido, C.C., Ayoola, A., Ayeni, E.A., Odoh, C.K., Abi, M.-E., Adebanjo, O., Oyejobi, G.K., 2022. Socio-economic impacts of emerging infectious diseases in Africa. Infectious Diseases 54(5), 315-324.

Okatch, H., Ngwenya, B., Raletamo, K.M., Andrae-Marobela, K., 2012. Determination of potentially toxic heavy metals in traditionally used medicinal plants for HIV/AIDS opportunistic infections in Ngamiland District in Northern Botswana. Analytica Chimica Acta 730, 42-48.

Ooms, G.I., Kibira, D., Reed, T., Van Den Ham, H.A., Mantel-Teeuwisse, A.K., Buckland-Merrett, G., 2020. Access to sexual and reproductive health commodities in east and southern Africa: a cross-country comparison of availability, affordability and stock-outs in Kenya, Tanzania, Uganda and Zambia. BMC public health 20, 1-14.

Pompermaier, L., Marzocco, S., Adesso, S., Monizi, M., Schwaiger, S., Neinhuis, C., Stuppner, H., Lautenschläger, T., 2018. Medicinal plants of northern Angola and their anti-inflammatory properties. Journal of Ethnopharmacology 216, 26-36.

POWO, 2023. Plants of the World Online. Royal Botanic Gardens, Kew, On the Internet.

Raman, J., Fakudze, P., Sikaala, C.H., Chimumbwa, J., Moonasar, D., 2021. Eliminating malaria from the margins of transmission in southern Africa through the Elimination 8 Initiative. Transactions of the Royal Society of South Africa 76(2), 137-145.

Ribeiro, A., Romeiras, M.M., Tavares, J., Faria, M.T., 2010. Ethnobotanical survey in Canhane village, district of Massingir, Mozambique: medicinal plants and traditional knowledge. Journal of ethnobiology and ethnomedicine 6(1), 1-15.

Seleteng Kose, L., Moteetee, A., Van Vuuren, S., 2015. Ethnobotanical survey of medicinal plants used in the Maseru district of Lesotho. Journal of Ethnopharmacology 170, 184-200.

Setshogo, M.P., Mbereki, C.M., 2011. Floristic diversity and uses of medicinal plants sold by street vendors in Gaborone, Botswana. The African Journal of Plant Science and Biotechnology.

Shopo, B., Mapaya, R.J., Maroyi, A., 2022. Ethnobotanical study of medicinal plants traditionally used in Gokwe South District, Zimbabwe. South African Journal of Botany 149, 29-48.

Stafford, G.I., Pedersen, M.E., van Staden, J., Jäger, A.K., 2008. Review on plants with CNS-effects used in traditional South African medicine against mental diseases. Journal of Ethnopharmacology 119(3), 513-537.

Tembo, N., Lampiao, F., Mwakikunga, A., Chikowe, I., 2021. Ethnobotanical survey of medicinal plants used for cervical cancer management in Zomba District, Malawi. Scientific African 13, e00941.

Uren, C., Möller, M., van Helden, P.D., Henn, B.M., Hoal, E.G., 2017. Population structure and infectious disease risk in southern Africa. Molecular Genetics and Genomics 292(3), 499-509.

Urso, V., Signorini, M.A., Tonini, M., Bruschi, P., 2016. Wild medicinal and food plants used by communities living in Mopane woodlands of southern Angola: Results of an ethnobotanical field investigation. Journal of Ethnopharmacology 177, 126-139.

Vahekeni, N., Neto, P.M., Kayimbo, M.K., Mäser, P., Josenando, T., da Costa, E., Falquet, J., van Eeuwijk, P., 2020. Use of herbal remedies in the management of sleeping sickness in four northern provinces of Angola. Journal of Ethnopharmacology 256, 112382.

Van Wyk, B.-E., 2020. A family-level floristic inventory and analysis of medicinal plants used in Traditional African Medicine. Journal of Ethnopharmacology 249, 112351.

van Wyk, B.E., van Oudtshoorn, B., Gericke, N., 2022. Medicinal Plants of South Africa, Second ed. Briza, Pretoria.

Watt, J.M., Breyer-Brandwijk, M.G., 1962. The medicinal and poisonous plants of southern and eastern Africa, Second ed. E and S Livingstone, Edinburgh.

Williamson, J., 2005. Useful Plants of Malawi, 3rd ed. Montfort Press, Limbe.

York, T., De Wet, H., Van Vuuren, S., 2011. Plants used for treating respiratory infections in rural Maputaland, KwaZulu-Natal, South Africa. Journal of Ethnopharmacology 135(3), 696-710.

Chapter 3 Rubiaceae of southern Africa: A review of the ethnobotany, bioactivity and phytochemistry

3.1 Introduction

Rubiaceae is among the most prominent medicinal plant families in South Africa (Louw et al., 2002). An inventory by Van Wyk (2020) recorded 318 medicinal species of Rubiaceae used in sub-Saharan Africa. This makes the family second only to the Fabaceae in terms of the number of medicinal species per family. It is also among the five most used plant families for treating cardiovascular ailments in sub-Saharan Africa (Odukoya et al., 2022). The ethnopharmacology, bioactivity and phytochemistry of sub-Saharan Rubiaceae have been reviewed in a limited way (Karou et al., 2011). There needs to be a comprehensive published account of the Southern African Rubiaceae species subjected to biological and phytochemical investigations.

Globally, there are 14245 accepted species of Rubiaceae distributed across 610 accepted genera (WFO, 2023). The Rubiaceae is among the largest families in the world, with members distributed in the tropical, subtropical, temperate and cold regions of North America, South America, Europe and Africa (Aro et al., 2015; Conserva and Jesu Costa Ferreira, 2012). According to the African Plant Database (2022), there are at least 572 unique species of Rubiaceae in Southern Africa.

The family boasts a vast evidentiary record of bioactive molecular structural diversity, which may be exploited as templates for the design of drugs (Aro, et al., 2019; Aro et al., 2022). Among these are anthraquinones, flavonoids, coumarins, alkaloids and terpenes (Aro et al., 2016; Conserva and Jesu Costa Ferreira, 2012). It is one of several plant families from which iridoids, monoterpenoids with a cyclopentan[c]pyran system, have been found (Hussain, H. et al., 2019). The family is also one of five from which cyclotides have been isolated. The other families with cyclotides include Violaceae, Fabaceae, Cucurbitaceae, and Solanaceae (Bajpai et al., 2023). Cyclotides are a group of cyclic peptides comprising about 30 amino acid residues with a cystine knot. Three disulfide bridges hold the structure together, making the protein exceptionally stable (Eteme et al., 2023). The bioactivities of cyclotides *Kalata* B1 and B2 isolated from *Oldenlandia affinis* range from anti-HIV antimicrobial to insecticidal activities (Daly et al., 2004; Jennings et al., 2005).

Some Rubiaceae, including species in the genera *Psychotria*, *Pavetta*, *Sericanthe*, *Vangueria* and *Fadogia*, form phytochemically productive symbiotic relationships with the endophytic bacteria of the *Burkholderiaceae* family (Danneels et al., 2023). These endophytes use the plant as a host and participate in plant biological processes without causing harm to the plant itself. These endophytes have been lauded as a potential source of pharmacologically active secondary metabolites (Abdalla et al., 2020). An anthropocidal and insecticidal C_7N aminocyclitol, kirkamide, and an herbicidal cyclitol, streptol glucoside, have been isolated from the bacterial leaf nodules of *Psychoria kirkii*, a Rubiaceae species that is present in Zimbabwe and Zambia (Pinto-Carbó et al., 2018; Pinto-Carbó et al., 2016; Sieber et al., 2015; Van Elst et al., 2013).

Other Rubiaceae phytochemicals are hepatoprotective, inhibit the growth of some pathogenic microbes and parasites, and exhibit anti-oxidant, anti-malarial and anti-inflammatory properties (Aro et al., 2022). Anti-bacterial activity has been reported in at least 48 genera (Aro et al., 2015). As a result, the species in the family have the potential to be a source of new pharmaceutical compounds and lead compounds (Aro et al., 2022).

Another consequence of the Rubiaceae-*Burkholderia* symbiosis is the production of the compound pavettamine (**15**), which is present in the leaves of *Fadogia*, *Pavetta*, *Psychotria* and *Vangueria* (Van Elst et al., 2013). Pavettamine (**15**) is responsible for the livestock cardiotoxic called *gousiekte*. Among plant poison-induced diseases, *gousiekte* is among the top seven maladies resulting in livestock loss in southern Africa (Botha and Penrith, 2008).

3.2 Methodology

A list of indigenous and naturalised southern African Rubiaceae has been compiled with reported ethnobotanical, bioactivity, and phytochemical data (Table 3.1, Table 3.2 and Table 3.3, respectively). Searches were done in academic databases: Google Scholar, Science Direct, Web of Science and Scopus, alongside published inventories and books. The search terms used included southern African medicinal plants, southern African ethnopharmacology, southern African phytochemistry, Rubiaceae, southern African Rubiaceae, Rubiaceae phytochemistry, and Rubiaceae ethnopharmacology. Rubiaceae species that had reported ethnobotanical uses or bioactivities were collated. These were combined with Rubiaceae species obtained from published books and inventories. Each generated plant species was added to the same databases to get reported ethopharmalogical data, bioactivity, and phytochemical information. All species

names were updated in accordance with the accepted synonyms on the Plants of the World online database (POWO, 2023).

3.3 Ethnopharmacology of southern African Rubiaceae

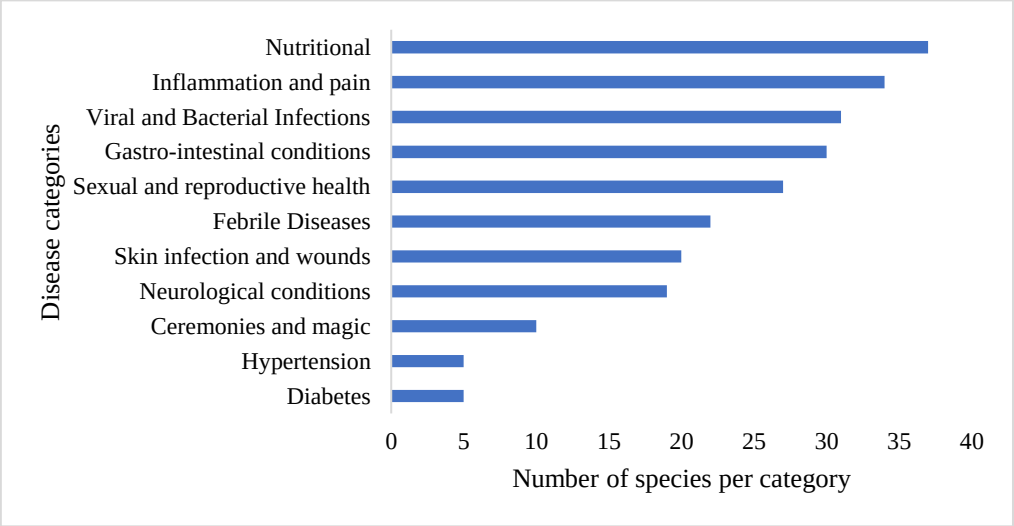

Figure 3.1: Number of Rubiaceae species used for specific disease categories

Figure 3.1 shows ten categories of ethnobotanical use and the number of species utilised in each category. The list was generated from Table 3.1, which summarises the ethnobotanical uses of Rubiaceae plants in southern Africa. One hundred and thirteen species of medicinal and nutritional value were recorded. Thirty-five species have parts that have nutritional applications, and 11 of these belong to the *Vangueria* genus. *Coffea racemosa* is used on a small scale to make coffee beverages. *Fadogia ancylantha* leaves are sold commercially as Makoni tea.

Pharmacological uses fall into nine major categories. There are 34 species grouped in the inflammation and pain category. These treat stomach aches, toothache, headaches, menstrual pain, and swollen body parts. Examples of plants that fall into this category are *Cremaspora triflora* and *Pentanisia prunelloides*. The vernacular Zulu name for *P. prunelloides* is icimamlilo, which means extinguishing a fire, possibly derived from its perceived ability to relieve pain. The number of species that have not been assayed is 18 out of 34 (52%), whilst for 68% (23), there are no reports of compounds isolated from them.

Plants used to treat viral and bacterial conditions account for 31 of the 113 Rubiaceae species. These are applied in treating tuberculosis and other respiratory conditions, as well as STIs like gonorrhoea, colds, and flu. The number of plants in this category that have at least one compound isolated is 14 out of 31, which means 55% of the species have yet to be subjected to preparative phytochemical analysis. Thirty-nine per cent (12) of the species have not been bio-assayed. For *Galium tomentosum*, despite its application in the treatment of urinary tract infections and HIV-related infections, no report of its bioassay and phytochemical investigations have been found. *Leptactina benguelensis*, traditionally applied to treating hemoptysis, coughing, and chest pains, has no reported bioassays or isolated phytochemicals. The leaves and roots of *Pavetta crassipes* are used to treat colds and gonorrhoea infections. However, no reported bioactivity and phytochemical investigations could be obtained. The roots of *Pentodon pentandrus* have applications in treating coughs and pneumonia. The whole plant of *Spermacoce deserti* is used to treat tuberculosis, thrush, skin rash, herpes, and gonorrhoea. No reported bioassay and secondary metabolite investigations were obtained for either species.

Examples of conditions and treatments that fall into the gastrointestinal category include diarrhoea and stomach aches. Plants used as purgatives, aperients and emetics are listed under this category. In total, 29 of the 113 Rubiaceae species fall into this category. *Gardenia cornuta*, *Kohautia angolensis*, *Pavetta lanceolata*, *Psychotria capensis*, *Vangueria dryadum*, and *Vangueria lasiantha* are species used to treat gastrointestinal ailments. Thirteen of the 30 species have had at least one secondary metabolite isolated, and 19 have undergone some form of investigation on bioactivity. This means that for 57% of the species in this category, no reported preparative phytochemical investigations were found, and 37% of the species have yet to be investigated for bioactivities.

Plants in the sexual and reproductive health category are used to treat infertility, amenorrhoea, and dysmenorrhoea and to facilitate child delivery in pregnant women. Some are used as aphrodisiacs. Thirteen out of the 27 species (48%) in this category have undergone neither reported phytochemical nor reported bioactivity investigations. The roots of *Coptosperma littorale* are used in treating amenorrhoea, whilst the leaves are used for menopause. *Galium undulatum* is used as a laxative during pregnancy. The roots of *Pentas purpurea* are used as an aphrodisiac, while those of *Spermacoce quadrisulcata* are used to remedy irregular menstrual cycles. The roots of *Vangueria cyanescens* are used to relieve labour pains and menstrual

bleeding. No reports of bioactivity and phytochemical investigations on these species were found.

The febrile disease category includes plants used to treat malaria and fevers. Twenty-two plants are used in this category. Seven of those plants have yet to undergo bioactivity and phytochemical investigations. These plants are *Agathisanthemum globosum*, *Anthospermum herbaceum*, *Pavetta gardeniifolia*, *Rytigynia umbellulate*, *Spermacoce deserti*, *Spermacoce dibrachiata*, and *Spermacoce natalensis*. Compounds have been isolated in nine of the plants, meaning that 59% have no reported phytochemical investigations. Plants in the skin disease and wounds category are used to treat rashes and pimples and for wound dressing. Twenty plants are used in this category, five of which have no reported phytochemical or bioactivity investigations. These plants include *Anthospermum rigidum*, *Coptosperma neurophyllum*, *Pentanisia angustifolia*, *Pentanisia rubricaulis*, and *Rothmannia whitfieldii*. Of the fifteen for which reported investigations were obtained, only nine have isolated compounds. This implies that phytochemical compounds have yet to be reported for 59% of the species in the category.

Neurological conditions have 19 southern African Rubiaceae species used in their treatment. Conditions in this category include epilepsy, dizziness, and mental breakdowns. Nine species in the category have no reported bioactivity or phytochemical investigations. These are: *Canthium ciliatum*, *Galium capense*, *Galium tomentosum*, *Gardenia resiniflua*, *Multidentia crassa*, *Rubia horrida*, *Spermacoce dibrachiata*, *Vangueria ferruginea*, and *Vangueriopsis lanciflora*. Each of the diabetes and hypertension categories has five species used in their treatment. Two of those plants have no reported bioactivity and phytochemical investigations. Those are *Galium tomentosum* and *Spermacoce natalensis*. Ten plant species are used in ceremonies and for magic purposes.

Table 3.1: Ethnobotanical uses of southern African Rubiaceae

	Species	Ethnobotanical uses	Reference
1	*Afrocanthium burttii* (Bullock) Lantz: BW, ZM	Medicine: Oral candidiasis mouthwash- Unspecified plant parts and preparation	(Chinsembu and Hedimbi, 2010)
2	*Afrocanthium mundianum* (Cham. & Schltdl.) Lantz: SZ, MZ, ZA, ZW	Nutrition: fruit. Medicine: unspecified parts are used to treat gastrointestinal ailments. A tonic made of roots and leaves. Tonsillitis - brewed tuber are applied to treat an unspecified STI disease.	(Arnold and Gulumian, 1984; Mabogo, 1990; Magwede et al., 2019b; Mataha, 2021; Welcome and Van Wyk, 2019).
3	*Agathisanthemum bojeri* Klotzsch subsp. *Bojeri:* AO, MZ, SZ, ZA, ZM, ZW	Medicine: Root decoction used to treat swollen testicles. A decoction of the whole plant is applied to relieve vaginal candidiasis. Roots and leaves are used to treat skin diseases, convulsions, and amenorrhoea. Ring worm infections are treated using an unspecified preparation of flowers. A bulb decoction is taken for the treatment of debility. The smoke of leaves and seeds is inhaled to medicate against respiratory conditions. Leaf juice and a decoction of the roots are orally administered to treat abdominal pain, retained placenta, and worm infections. A leaf infusion is used as a medicament for febrile diseases and prophylactic for communicable diseases. Unspecified leaf, root and flower preparations are used to treat Tooth aches, snake bites, syphilis, sore throat, and diarrhoea.	(Amusan et al., 2005; Chhabra et al., 1991; Lall et al., 2019; Nyagumbo et al., 2022; Tshikalange et al., 2016; Watt and Breyer-Brandwijk, 1962).
4	*Agathisanthemum globosum* (Hochst. ex A. Rich.) Klotzsch: AO, MW, MZ, ZM, ZW	Medicine: Leaf root decoction is administered orally to treat coughs, diarrhoea, and malaria.	(Ngezahayo et al., 2015; Nguta et al., 2011).
5	*Alberta magna* E. Meyer, ZA	Unspecified medicinal applications in KwaZulu Natal	(Drewes et al., 1998).
6	*Anthospermum herbaceum* L.f.: LS, MW, MZ, SZ, ZA, ZM, ZW	Medicine: decoction of twigs taken orally to treat malaria Ceremonial: unspecified parts inserted into incisions on the body of those who have handled a corpse in Lesotho.	(Chhabra and Mahunnah, 1994; Moteetee et al., 2019)
7	*Anthospermum rigidum* Eckl. & Zeyh subsp. *rigidum*: AO, BW, LS, MW, MZ, NM, SZ, ZA, ZM, ZW	Medicine: An unspecified preparation is used to treat lung illnesses, and a leaf infusion is applied to eliminate pubic lice. Root decoction is given to sufferers of menstrual pain, used as a laxative for pregnant women, and to hasten recovery of ill persons. Ceremonial and magic: used to cleanse people who have handled a dead body or sick person, charm to improve marriage prospects and safe journeys.	(Amusan et al., 2007; Moteetee et al., 2019; Moteetee and Seleteng Kose, 2016; Seleteng Kose et al., 2015)
8	*Breonadia salicina* (Vahl) Hepper & J.R.I. Wood: AO, MW, MZ, SZ, ZA, ZM, ZW	Medicine: Bark is used to treat diarrhoea. Pregnant women take unspecified preparations of roots and leaves to hasten child delivery. The sap is orally administered for the treatment of stomach aches.	(Bruschi et al., 2011; Sibandze et al., 2010)

9	*Bridsonia chamaedendrum* (Kuntze) Verstraete & A.E.van Wyk Robyns: SZ, ZA	Nutrition: Fruit	(Welcome and Van Wyk, 2019)
10	*Burchellia bubalina* (L.f.) Sims*:* SZ, ZA	Medicine: Unspecified plant parts used to treat impotence, as a tonic, and as a blood purifier.	(Mhlongo and Van Wyk 2019)
11	*Canthium armatum* (K. Schum.) Lantz: MZ, SZ, ZA	Fruit is consumed as a snack.	(Welcome and Van Wyk, 2019).
12	*Canthium ciliatum* (Klotzsch) Kuntze: SZ, ZA	Nutrition: fruit. Ceremonial and magic: unspecified parts used against abdominal pain caused by witchcraft to prevent disturbance of a recently interred corpse. Roots are used as emetics to induce trances.	(Magwede et al., 2019b). (Corrigan et al., 2011; Sobiecki, 2008). (Moteetee et al., 2019).
13	*Canthium glaucum* Hiern**:** BW, MW, MZ, ZM, ZW	Medicinal: Unspecified preparation of roots and fruit used against malaria.	(Musila et al., 2013; Nguta et al., 2010).
14	*Canthium inerme* (L.f.) Kuntze: MZ, SZ, ZA, ZW	Nutrition: fruit and seed Medicinal: Unspecified plant parts used to boost male virility. A decoction of leaves is used to treat ringworm infection and pimples and to soften and cleanse the skin. Leaves are taken with milk to treat stomach infections. An unspecified preparation of twigs is used against *acne vulgaris*. Ceremonial and magic: infusion of the plant in water is taken orally to exorcise spirits.	(Sobiecki, 2008) (Corrigan et al., 2011; De Wet et al., 2013; Dlova and Ollengo, 2018; Mhlongo and Van Wyk, 2019; Nciki et al., 2016; Otang et al., 2014; Welcome and Van Wyk, 2019)
15	*Canthium spinosum* (Klotzsch exEckl. & Zeyh.) Kuntze: BW, SZ, ZA	Nutrition: Fruit Medicine: Stomach ailments, analgesic and tonic- unspecified plant parts administration, and preparation	(Mhlongo and Van Wyk, 2019) (Welcome and Van Wyk, 2019) (Corrigan et al., 2011)
16	*Catunaregam obovata* (Hochst.) A.E. Gonç.: MZ, SZ, ZA	Medicine: Root infusion is taken to treat pneumonia. The root decoction is applied to treat snake bites, fever, heavy menstruation, nausea, dizziness, tooth aches, melanomas, fever, venereal diseases, tuberculosis, asthma, and to close the fontanelle of infants and as an analgesic. A decoction of stem bark is used to manage epilepsy. An unspecified treatment is used as an aphrodisiac.	(Nyagumbo, Pote et al. 2022). (Cock, I. E. et al., 2023; Sibanda et al., 1989). (Stafford et al., 2008). (Auditeau, Chassagne et al. 2019). (Bruschi et al., 2011).
17	*Catunaregam taylorii* (S. Moore) Bridson: MW, MZ, SZ, ZA, ZM, ZW	Medicine: A decoction of seeds is used to treat kidney disorders. Unspecified preparation of leaves, bark and roots is used against pulmonary and respiratory illnesses. Unspecified parts are used to treat diarrhoea.	(Shopo et al., 2022) (Neuwinger, 2004; Nyagumbo et al., 2022)
18	*Cephalanthus natalensis* Oliv.: LS, MW, MZ, SZ, ZA, ZM	Nutrition: Fruit and flower Medicine: fruits are used against fevers and malaria.	(Cock, I. E. et al., 2023; Ngwenya, 2012) (Welcome and Van Wyk, 2019). (Dlamini and Solomon, 2019)

19	*Coddia rudis* (E. Mey. ex Harv.) Verdc.: SZ, MZ, ZA, ZW	Nutrition: Fruit is consumed. The stem is used as a flavouring and preservative. Medicine: Unspecified parts used as a tonic against impotence, fever, and stomach-related illnesses. A root decoction is used as an aphrodisiac, and an unspecified preparation of leaves is used to de-tick livestock.	(Abdillahi and Van Staden, 2012; Ajao et al., 2019; Asowata-Ayodele et al., 2016; Bruschi et al., 2011; Cock, I. E. et al., 2023; Kambizi, 2014; Mhlongo and Van Wyk, 2019; Welcome and Van Wyk, 2019).
20	*Coffea racemosa* Lour.: MZ, SZ, ZA, ZW	Nutrition: Seeds used for beverage production.	(Welcome and Van Wyk, 2019)
21	*Conostomium natalense* (Hochst.): MZ, ZA, ZW	Medicine: Unspecified parts are used to treat urinary ailments, diarrhoea, and emetics. A root decoction is used to stop bleeding in pregnant women.	(Cock et al., 2021) (Okem et al., 2012). (Mashile, Shalom Pabalelo et al., 2019)
22	*Coptosperma littorale* (Hiern) Degreef: MZ, ZA, ZW	Medicine: Root decoction used to treat chest pains and amenorrhoea. Unspecified preparation of leaves is used to treat menopause.	(Chhabra et al., 1991).
23	*Coptosperma neurophyllum* (S. Moore) Degreef: MW, MZ, ZM, ZW	Medicine: Crushed leaves are applied topically for wound dressing and prevention of maggot infestation.	(Gelfand et al., 1985)
24	*Coptosperma supra-axillare* (Hemsl.) Degreef.: MZ, SZ, ZA, ZW	Nutritional: Fruit (Welcome and Van Wyk, 2019)	(Welcome and Van Wyk, 2019)
25	*Cremaspora triflora* (Thonn.) K. Schum.: AO, MW, MZ, ZM, ZW	Medicinal: Unspecified parts, preparation and administration for pain and inflammation.	(Khumalo et al., 2022; Khumalo et al., 2023).
26	*Crossopteryx febrifuga* (Afzel. ex G. Don) Benth. :AO, BW, MW, MZ, ZA, ZM, ZW	Medicinal: Unspecified parts used to treat urinary schistosomiasis. Unspecified preparation of stem bark and leaves is used to treat malaria. Unspecified plant part used to treat liver conditions. Leaves and roots are taken for epilepsy treatment. A decoction of bark, leaves and roots is taken orally to treat diarrhoea, dysentery, trypanosomiasis and stomach ache. Fruit and bark are used to treat respiratory diseases. Unspecified plant parts are applied topically for wound dressing and pain.	(Ndamba et al., 1994; Ngarivhume et al., 2015) (Atawodi et al., 2015). taken to treat in Tanzania (Auditeau et al., 2019). (Bruschi et al., 2011; Salawu et al., 2009).
27	*Fadogia ancylantha* Schweinf. : MW, MZ, ZM, ZW	Nutrition: Leaves sold commercially as Makoni tea Medicine: Leaf decoctions are taken orally to treat coughing and pneumonia and to facilitate childbirth. The leaf powder is applied to treat skin rashes. A leaf decoction is taken orally and as an enema to treat ringworm infections.	(Ngezahayo et al., 2015; Nyagumbo et al., 2022; Shopo et al., 2022). (Mencherini et al., 2010).
28	*Fadogia homblei* De Wild: AO, MW, MZ, ZA, ZM, ZW	Nutrition: Fruit Toxicological: Leaves cause *gousiekte* (cardio toxicosis) in ruminants.	(Mohammed et al., 2013) (Welcome and Van Wyk, 2019)

29	*Fadogia tetraquetra* K. Krause var. *tetraquetra*: AO, MZ, SZ, ZA, ZM, ZW	Nutrition: Fruit. Medicine: Unspecified medicinal use.	(Magwede et al., 2019b; Welcome and Van Wyk, 2019)
30	*Galium capense* Thunb. *subsp. namaquense* (Eckl. & Zeyh.) Puff: LS, ZA	Medicine: Unspecified parts are used to treat psychological diseases. A root decoction is used for nausea, as a laxative for pregnant women, and to treat stomach ailments.	(Sobiecki, 2008). (Nortje and van Wyk, 2015) (Moteetee and Seleteng Kose, 2016)
31	*Galium mucroniferum* Sond. *var. dregeanum* (Sond.) Puff: ZA	Medicine: Root decoction used to treat sterility in women and toothache relief. Ceremonial and magic: Decoction of unspecified parts is taken by diviners to enable them to fathom instructions from the 'bones.'	(Cock, Ian E. et al., 2023; Moteetee et al., 2019; Sobiecki, 2008)
32	*Galium spurium* L. *subsp. africanum* Verdc.: MW, ZA	Nutrition: Leaves Medicine: Epilepsy- unspecified preparation.	(Welcome and Van Wyk, 2019) (Orhan et al., 2012)
33	*Galium thunbergianum* Eckl. & Zeyh. *var. hirsutum* (Sond.) Verdc.: ZA, ZW	Medicine: Toothache, mouthwash- root decoction used as and to treat. Ceremonial and magic: a root decoction is taken orally to see bones clearly and during initiation.	(Cock, Ian E. et al., 2023). (Moteetee et al., 2019)
34	*Galium tomentosum Thunb.*: NM, ZA	Medicine: Roots are used to induce forgetfulness, treat diabetes, HIV, heartburn, as an emetic and to treat bladder problems. Unspecified parts treat stomach ailments, urinary tract infections, haemorrhoids and headaches. Ceremony and magic: amulet for luck.	(Magwede et al., 2019a). (Aston Philander, 2011; Cock et al., 2021; Odukoya et al., 2022)_ENREF_109. (Nortje and van Wyk, 2015).
35	*Galium undulatum* Puff.: ZA	Medicine: Unspecified parts used to treat reproductive problems. Root decoction is used as a laxative during pregnancy.	(Moteetee et al., 2019; Moteetee and Seleteng Kose, 2016)
36	*Gardenia cornuta* Hemsl.: MZ, SZ, ZA	Nutrition: Fruit consumed during famines Medicine: fruits and roots used as emetics; unspecified plant parts used to treat gastrointestinal ailments. Ceremony and magic: The AmaZulu plant it in the homestead to drive away unwanted spirits.	(Corrigan et al., 2011). (Amusan et al., 2007). (Hutchings, 1989; Welcome and Van Wyk, 2019)
37	*Gardenia resiniflua* Hiern subsp. *resiniflua*: MW, MZ, NM, ZA, ZM, ZW	Medicine: Treatment of convulsions- bark ointment is applied topically to treat convulsions. Root infusion is taken nasally to treat insanity. Leaf and root infusion, ocular administration are used to treat headaches. Root decoction and infusion are used to treat female infertility, epilepsy and dysmenorrhoea. Roots are burnt and applied on incisions on the chest to treat pneumonia and asthma. Bark, fruit and root decoction treat erectile dysfunction and toothache.	(Gelfand et al., 1985; Nyagumbo et al., 2022; Shopo et al., 2022)

38	*Gardenia subacaulis* Stapf and Hutch.: MW, MZ, ZM	Medicine: Traded commercial in Malawi for unspecified medicinal use.	(Meke et al., 2017).
39	*Gardenia ternifolia* Schumach. & Thonn.: AO, BW, MW, MZ, NM, ZA, ZM, ZW	Medicine: burnt roots are applied to incisions on the chest for asthma and pneumonia treatment. Unspecified parts are used in the treatment of insanity, female infertility, menstrual cramps and convulsions. Bark and roots are taken orally to prevent dysentery, stomach ache, tuberculosis, and asthma and to facilitate child delivery.	(Bruschi et al., 2011; Nyagumbo et al., 2022)
40	*Gardenia thunbergia* L.f: MZ, ZA	Medicine: Unspecified parts used to treat malaria. Roots are used to treat leprosy skin lesions, biliousness and problems with the gall bladder. Roots and leaves used to treat syphilis.	(Nethengwe, 2011)
41	*Gardenia volkensii* K. Schum.: AO, BW, MW, MZ, NM, SZ, ZA, ZM, ZW	Nutrition: Fruit consumed as a snack Medicine: Root decoction is used to induce vomiting. The smoke of burning roots is inhaled to treat convulsions. Roots are burnt and applied on incisions on the chest to treat pneumonia and asthma. Root and leaf infusion is applied to the eyes and forehead for headaches. Root infusion is taken nasally for the treatment of madness. Fruit infusion is used as ear drops to relieve pain. Root infusion and decoction are consumed for the treatment of dysmenorrhoea, female infertility and epilepsy. Root infusions are taken orally alongside *Nicotiana tabacum* to treat asthma.	(Amusan et al., 2002; Gelfand et al., 1985; Stafford et al., 2008; Welcome and Van Wyk, 2019)
42	*Guettarda speciosa* L.: MZ, ZA	Medicine: A decoction of flowers is used to treat malaria. Unspecified parts treat inflammatory conditions like fever, coughing and postpartum infection.	(Kaou et al., 2008; Le et al., 2018)
43	*Heinsia crinita* (Afzel.) G. Taylor *subsp. parviflora* (K. Schum. & K. Krause) Verdc.: AO, MW, MZ, ZA, ZM, ZW	Nutrition: Fruit consumed as a snack. Medicine: Root decoctions used in the treatment of parasitic and bacterial infections.	(Barbosa et al., 2020; Welcome and Van Wyk, 2019)
44	*Hexasepalum sarmentosum* (Sw.) Delprete & J.H. Kirkbr.: AO, MZ, ZM, ZW	Medicine: Leaves are crushed in water and applied topically to treat snake bites, skin and rheumatic inflammation. Unspecified plant parts are used to treat ulcers, oedema and pain.	(Akah et al., 1998; Novotna et al., 2020)
45	*Hymenodictyon floribundum* (Hochst. & Steud.) B.L. Rob.	Medicine: Roots are used as an antipyretic for treating malaria.	(Kraft et al., 2003)
46	*Hymenodictyon parvifolium Oliv. subsp. Parvifolium*: MZ, ZA, ZW	Medicine: A decoction of dried bark is used to treat epilepsy. A decoction of roots combined with *Sansevieria conspicua* roots and *Sparagus flagellaris* bark treats bilharziasis. The root is used to alleviate constipation.	(Moshi et al., 2006; Muthee et al., 2011)

47	*Hyperacanthus amoenus* (Sims) Bridson.: MZ, SZ, ZA	Nutrition: Fruit is consumed as a snack and used for making beverages. Medicine: A maceration of the bark is used as veterinary medicine for pain relief and improving appetite in cattle.	(Magwede et al., 2019b; Welcome and Van Wyk, 2019)
48	*Keetia gueinzii* (Sond.) Bridson: AO, MW, MZ, SZ, ZA, ZM, ZW	Nutrition: Fruit consumed as snack. Medicine: Unspecified plant parts used to treat malaria and respiratory illnesses.	(Mailu, 2021; Welcome and Van Wyk, 2019)
49	*Keetia hispida* (Benth.) Bridson: AO	Medicine: A decoction of roots taken orally to treat epilepsy. Leaves are used for respiratory infection treatment.	(Auditeau et al., 2019; Kone et al., 2007)
50	*Keetia zanzibarica* (Klotzsch) Bridson: MW, MZ, ZM	Medicine: A decoction of bark root and leaves treats Cryptococcal meningitis. Roots are used to treat gastrointestinal issues, wounds and malaria.	(Chinsembu and Hedimbi, 2010; Christopher et al., 2023)
51	*Kohautia amatymbica* Eckl. & Zeyh.: LS, MZ, SZ, ZA, ZW	Nutrition: Underground storage organs Medicine: Unspecified plant parts are used as an aperient and to treat female infertility. Ceremony and magic: protective charm for babies in Lesotho	(Moteetee, 2017; Moteetee et al., 2019; Moteetee and Seleteng Kose, 2016; Welcome and Van Wyk, 2019)
52	*Kohautia angolensis* Bremek.: AO, NM	Medicine: Intestinal problems- Unspecified parts.	(Cheikhyoussef et al., 2011)
53	*Kraussia floribunda* Harv.: MZ, SZ, ZA	Nutrition: Fruit	(Welcome and Van Wyk, 2019)
54	*Leptactina benguelensis* (Welw. ex Benth. & Hook. f.) R. D. Good: AO, BW, MW, MZ, ZM, ZW	Medicine: Unspecified parts are used to treat chest pains, cough, hemoptysis, and immobile fetuses.	(Novotna et al., 2020)
55	*Mitragyna stipulosa* (DC.) Kuntze: AO, ZM	Medicine: A decoction of the trunk is used to treat trypanosomiasis. A decoction of the stem is taken orally to treat filariasis.	(Cakupewa et al., 2022; Vahekeni et al., 2020).
56	*Morinda morindoides* (Baker) Milne-Redh.: AO	Leaves are used as anti-inflammation agents in Angola.	(Pompermaier et al., 2018)
57	*Multidentia crassa* (Hiern) Bridson & Verdc.: AO, MW, MZ, ZM, ZW	Medicine: roots are taken orally to treat convulsions, infertility and stomach aches. Leaf infusions are applied topically for an unspecified treatment of pregnant women.	(Augustino et al., 2011; Williamson, 2005).
58	*Mussaenda arcuata* Poir.: AO, MW, MZ, ZM, ZW	Medicine: A brew of the leaves taken orally to treat influenza infections. Unspecified plant parts are used to treat bronchitis. A decoction of whole plant is applied topically to treat boils, scabies, and skin infections.	(Nyagumbo et al., 2022; Suroowan et al., 2019)
59	*Nauclea latifolia* Sm.: AO	Medicine: Unspecified preparation of roots and fruits is used to treat inflammatory conditions. Unspecified parts are used to treat Malaria, epilepsy, diabetes and anxiety.	(Gidado et al., 2005; Ngo Bum et al., 2009; Pompermaier et al., 2018).

60	*Oldenlandia affinis* (Roem. & Schult.) DC. subsp. *fugax* (Vatke) Verdc: AO, BW, MW, MZ, SZ, ZA, ZM, ZW	Medicine: Roots are used to treat hypertension, and a decoction of leaves is used to manage asthma and facilitate labour in pregnant women.	(Balogun and Ashafa, 2019; Gran et al., 2000; Odukoya et al., 2022)
61	*Oldenlandia corymbosa* L.: AO, BW, MW, MZ, SZ, ZA, ZM, ZW	Medicine: Unspecified parts are used to treat necrosis, skin and liver diseases, mouthwash for tooth aches, gastric problems, and bronchitis, detoxification, and as an anthelmintic.	(Archana et al., 2021; Datta and Sen, 1969)
62	*Oldenlandia herbacea* (L.): AO, BW, LS, MW, MZ, NM, SZ, ZA, ZM, ZW	Medicine: Infusion of stem and leaves taken orally to treat diarrhoea. Unspecified parts treat jaundice, rheumatoid arthritis, elephantiasis, asthma and wounds.	(Gelfand et al., 1985; Gunasekaran et al., 2023).
63	*Oxyanthus speciosus* (Andrews) DC.: AO, MW, MZ, SZ, ZA, ZM, ZW	Medicine: unspecified plant parts treat scabies, haemorrhoids and cough. Roots, leaves and stems are used to treat. Snake bites, pulmonary ailments, fever, jaundice, tooth and stomach ache.	(Nyobe et al., 2020; Van Vuuren et al., 2022)
64	*Paederia bojeriana* (A. Rich.) Drake: MW, MZ, ZA, ZM, ZW	Medicine: The leaves are used by the Venda people in Limpopo to treat hypertension.	(Mudau et al., 2020).
65	*Pavetta crassipes* K. Schum.:MW, MZ, ZM	Medicine: Steam of leaves and roots is inhaled to treat colds. An unspecified gonorrhoea-	(Williamson, 2005)
66	*Pavetta edentula* Sond.: MZ, SZ, ZA	Nutrition: Leaves are consumed as snack and vegetable	(Welcome and Van Wyk, 2019)
67	*Pavetta gardeniifolia* A. Rich: AO, BW, MW, MZ, ZA, ZM, ZW	The vapour of leaves and roots is inhaled to treat febrile diseases like malaria.	(Motlhanka and Nthoiwa, 2013).
68	*Pavetta harborii* S. Moore: BW, MZ, NM, ZA	Known as one of the plants that cause *gousiekte* sickness in livestock	(Bode et al., 2010)
69	*Pavetta lanceolata* Eckl.: MZ, SZ, ZA	Unspecified plant parts are used in the treatment of biliousness and to stop vomiting.	(Mhlongo and Van Wyk, 2019; Ndhlovu et al., 2021)
70	*Pavetta revoluta* Hochst.: MZ, ZA	Veterinary: Leaves are used to make an infusion in cold water, administered to livestock to treat gall sickness.	(Masika and Afolayan, 2003)
71	*Pavetta schumanniana* F. Hoffm. ex K. Schum.: AO, BW, MW, MZ, NM, SZ, ZA, ZM, ZW	Nutrition: Sap is considered edible by VhaVenda Medicine: leaf decoction is used to treat chest pains, cough, pneumonia, abdominal pain, diarrhoea, venereal diseases, female infertility and as an aphrodisiac	(Magwede et al., 2019b; Nyagumbo et al., 2022).

72	*Pentanisia angustifolia* (Hochst.) Hochst.: LS, SZ, ZA	Medicine: Root concoction is used to treat sores all over the body.	(Amusan, 2009)
73	*Pentanisia prunelloides* (Klotzsch ex Eckl. & Zeyh.) Walp.: LS, MW, MZ, SZ, ZA, ZM	Medicine: Unspecified leaf, rhizome, and root preparation is used to treat hypertension and diabetes. Unspecified plant parts are used as an analgesic to treat skin sores, stomach problems, inflammation, and burns. Roots are used to treat bladder and kidney ailments. Veterinary: Unspecified plant parts treat conjunctivitis and retained placenta in livestock.	(Cock et al., 2021; Mabona and Van Vuuren, 2013; Masika and Afolayan, 2003; Mhlongo and Van Wyk, 2019; Odukoya et al., 2022)
74	*Pentanisia rubricaulis* (K. Schum.) Kårehed & B. Bremer: AO	Medicine: Fresh leaf poultice applied topically to treat boils.	(Novotna et al., 2020)
75	*Pentas purpurea* Oliv.: AO, MW, MZ, ZM, ZW	Medicine: Root infusion is taken orally to treat dysmenorrhoea and as an aphrodisiac.	(Gelfand et al., 1985)
76	*Pentodon pentandrus* (Schumach. & Thonn.): AO, BW, MW, MZ, NM, SZ, ZA, ZM, ZW	Medicine: An unspecified preparation of roots is used as an emetic, an anthelmintic, and for treating pneumonia and coughing.	(Gakuya et al., 2013; Hutchings et al., 1996)
77	*Psychotria capensis* (Eckl.) Vatke MW, MZ, SZ, ZA, ZM, ZW	Medicine: Unspecified plant parts used as an emetic and treatment of gastric ailments.	(Aro et al., 2022)
78	*Psychotria eminiana (Kuntze) E.M.A. Petit*: AO, MW, MZ, ZM	Medicine: unspecified preparation of roots used as an analgesic during childbirth, breathlessness, and nose bleeds. Unspecified parts are used to treat snake bites.	(Novotna et al., 2020).
79	*Psydrax lividus* (Hiern) Bridson: AO, BW, MW, MZ, NM, ZA, ZM, ZW	Nutrition: Fruit Veterinary applications: unspecified leaf preparation used for infestation by ticks and other parasites.	(Nyahangare et al., 2015; Welcome and Van Wyk, 2019)
80	*Psydrax obovatus (Eckl. & Zeyh.)*: MZ, ZA, ZW	Nutrition: Fruit	(Welcome and Van Wyk, 2019)
81	*Pygmaeothamnus zeyheri* (Sond.) Robyns: AO, BW, NM, ZA, ZM, ZW	Nutrition: Fruit	(Welcome and Van Wyk, 2019).
82	*Richardia brasiliensis* Gomes: *	Medicine: Unspecified plant parts are used in treating diabetes and as an antiemetic. Unspecified parts and preparation topically applied on the mouth or vagina to treat candidal infections.	(Magwede et al., 2019b; Masevhe et al., 2015; Pinto et al., 2008)
83	*Rothmannia capensis* Thunb.: BW, SZ, ZA	Medicine: The sap of the fruit is applied topically to treat wounds. Unspecified parts are used to treat rheumatism. Veterinary applications: The fruit is used as an acaricide on livestock	(Mabona and Van Vuuren, 2013) (Kelmanson et al., 2000; Pavela et al., 2016)
84	*Rothmannia globosa* (Hochst.) Keay: ZA	Nutrition: The fruit is consumed as a snack.	(Welcome and Van Wyk, 2019)

85	*Rothmannia whitfieldii* (Lindl.) Dandy: AO, MW, ZM, ZW	Medicine: The juice of unripe fruit and the root ash are applied topically to treat wounds and eczema.	(Watt and Breyer-Brandwijk, 1962).
86	*Rubia cordifolia L.*: AO, MW, MZ, SZ, ZA, ZM, ZW	Medicine: unspecified parts treat digestive problems, sore throat, and chest pains. A root decoction is used to treat impotence and as an aphrodisiac. Unspecified parts are used to treat amenorrhoea, jaundice, paralysis, and toothache, as well as as a mouth wash. A root and bark decoction are used to medicate uterine problems.	(Abdillahi and Van Staden, 2012; Ajao et al., 2019; Cock, Ian E. et al., 2023; Moteetee et al., 2019; Wang et al., 2023)
87	*Rubia horrida* (Thunb.) Puff*:* BW, LS, NM, SZ, ZA, ZW	Medicine: A leaf decoction is taken to remedy dizziness.	(Setshogo and Mbereki, 2011)
88	*Rubia petiolaris* DC: LS, ZA	Nutrition: Underground storage organs are used as vegetables. Ceremony and Magic: Preparations of the roots are taken orally by initiates to induce dreams. Medicine: Roots and leaves are used to treat tuberculosis, dysentery, and diarrhoea.	(Lawal et al., 2014; Olajuyigbe and Afolayan, 2012) (Sobiecki, 2008; Welcome and Van Wyk, 2019) .
89	*Rytigynia adenodonta* (K. Schum.) Robyns: MW, MZ, ZM	Medicine: Unspecified medicinal use.	(Bundschuh et al., 2011)
90	*Rytigynia monantha (*K. Schum.) Robyns: MW, ZM	Medicine: Unspecified medicinal use.	(Bundschuh et al., 2011)
91	*Rytigynia umbellulata* (Hiern) Robyns: AO, BW, MW, MZ, ZM, ZW	Medicine: Leaf decoction is taken orally to treat malaria and headaches.	(Yetein et al., 2013)
92	*Spermacoce deserti* N.E.Br.: BW, ZA	Medicine: Unspecified preparation of the whole plant treats tuberculosis, thrush, skin rash, herpes, fever, gonorrhoea, and diarrhoea.	(Leteane et al., 2012)
93	*Spermacoce dibrachiata* Oliv.*:* AO, MW, MZ, ZM, ZW	Medicine: The root infusion is taken orally to treat pneumonia, cough, and dizziness and as an aphrodisiac. The smoke of leaves is directed towards the vagina to treat dysmenorrhoea.	(Gelfand et al., 1985).
94	*Spermacoce natalensis* Hochst: MW, MZ, SZ, ZA, ZM, ZW	Medicine: Unspecified leaf, bark and root preparations treat hypertension. An unspecified preparation of roots is used to treat febrile rash.	(Mabona and Van Vuuren, 2013; Odukoya et al., 2022)
95	*Spermacoce quadrisulcata* (Bremek.) Verdc.: AO, BW, MW, NM, ZM	Medicine: A decoction of roots taken orally to treat irregular menstruation.	(Hedberg and Staugard, 1989)
96	*Tarenna pavettoides (Harv.) Sim*: MW, MZ, SZ, ZA, ZM, ZW	Medicine: Leaves are taken to boost appetite. Unspecified parts are used to treat cough and, nose and throat infections.	(Begum et al., 2020; Mugisha et al., 2014).

97	*Tricalysia capensis* (Meisn. ex Hochst.) Sim: SZ, MZ, ZA	Medicine: Unspecified use of roots	(Magwede et al., 2019b)
98	*Tricalysia lanceolata* (Sond.) Burtt Davy: SZ, MZ, ZA	Medicine: Stem and leaves traded commercially for the treatment of unspecified diseases.	(Williams and Balkwill, 2001)
99	*Vangueria apiculata* K. Schum.: MW, MZ, ZM, ZW	Medicine: An unspecified preparation of roots is used as an anthelmintic for roundworms.	(Watt and Breyer-Brandwijk, 1962)
100	*Vangueria cyanescens* Robyns*:* AO, BW, NM, ZM	Nutrition: Fruit Medicine: Underground parts treat labour pain, menstrual bleeding and urinary tract infections.	(Masarirambi et al., 2019; Urso et al., 2016; Welcome and Van Wyk, 2019).
101	*Vangueria dryadum* (S. Moore): MZ, ZA, ZM, ZW	Nutrition: Fruit Medicine: A root decoction used to treat stomach ailments.	(Magwede, 2018; Mataha, 2021; Welcome and Van Wyk, 2019)
102	*Vangueria esculenta* S. Moore: MW, MZ, ZW	Nutrition: fruits	(Magwede et al., 2019b)
103	*Vangueria ferruginea* (Welw.): AO, BW, NM, ZM, ZW	Nutrition: Fruit Medicine: Unspecified parts are used to treat mental illness.	(Shirungu and Cheikhyoussef, 2018; Welcome and Van Wyk, 2019).
104	*Vangueria infausta* Burch.: AO, BW, MW, MZ, NM, SZ, ZA, ZM, ZW	Nutrition: Fruit Medicine: Unspecified preparation of roots, leaf and bark is used to treat diarrhoea and as an analgesic. Unspecified plant parts are used to treat malaria, chest pains, and intestinal roundworm infections, as well as as an aphrodisiac. Unspecified preparation of bark and leaves is used to treat hypertension. Bark, leaves and roots are taken orally to treat stomach aches, cough, asthma, and skin blisters and to facilitate child delivery.	(Ajao et al., 2019; Balogun and Ashafa, 2019; Bruschi et al., 2011; Cock et al., 2018; Corrigan et al., 2011; Maroyi, A., 2018; Mhlongo and Van Wyk, 2019; Welcome and Van Wyk, 2019).
105	*Vangueria lasiantha* (Sond.) Sond.: MZ, ZA	Nutrition: Fruit Medicine: Powdered leaves are used in the treatment of dysentery and diarrhoea. Unspecified plant parts are used as a tonic.	(Corrigan et al., 2011; Mbanjwa, 2020; Mhlongo and Van Wyk, 2019; Welcome and Van Wyk, 2019)
106	*Vangueria latifolia* (Sond.) Sond.:SZ, ZA	Nutrition: Fruit. Toxicology: causes *gousiekte* in livestock.	(Stanton et al., 2013; Welcome and Van Wyk, 2019)
107	*Vangueria macrocalyx* Sond.: MZ, SZ, ZA,	Nutrition: Fruit.	(Welcome and Van Wyk, 2019)
108	*Vangueria madagascariensis* J.F. Gmel.: AO, SZ, MW, MZ, ZA	Nutrition: Fruit. Medicine: unspecified preparations of bark, fruit, leaf and root are used to treat diabetes, diarrhoea, worm infections, stomach-related illnesses, malaria, gonorrhoea and skin infections.	(Maroyi, Alfred, 2018; Mustafa et al., 2019; Suroowan et al., 2019).

109	*Vangueria parvifolia* Sond.: BW, ZA	Nutrition: Fruit	(Welcome and Van Wyk, 2019).
110	*Vangueria pygmaea* Schltr. MW, SZ, ZA, ZM, ZW	Nutrition: Fruit Medicine: Smoke from roots is inhaled to treat convulsions. Toxicology: Causes *gousiekte* in livestock	(Gelfand et al., 1985; Mashile, S. P. et al., 2019; Stanton et al., 2013).
111	*Vangueria thamnus (Robyns) Lantz*: ZA	Toxicology: One of the species that causes *gousiekte*	(Van Elst et al., 2013).
112	*Vangueria vestita* (Robyns) ined: MW, MZ, ZM, ZW	Medicine: A root infusion taken orally to treat stomach pains and worms.	(Watt and Breyer-Brandwijk, 1962).
113	*Vangueriopsis lanciflora* (Hiern) Robyns: AO, BW, MW, MZ, NM, ZA, ZM, ZW	Nutrition: fruit. Medicine: A root decoction is used to treat cough and to promote conception. Unspecified parts are used in the treatment of abdominal, back and neck pain, constipation, swelling on the body, and to dilate the birth canal during birth. The bark powder, root infusion, leaf infusion, and root infusion snuff treat mumps, high myopia, diarrhoea, and mental disorders.	(Fowler, 2002; Masondo et al., 2019; Novotna et al., 2020; Nyagumbo et al., 2022). (Welcome and Van Wyk, 2019)

3.4 Bioactivities of southern African Rubiaceae species

Table 3.2 shows the bioactivities of southern African Rubiaceae that have been studied. Fifty-two southern African Rubiaceae species that have undergone bioactivity investigations were found. The bioactivity investigations ranged from anti-convulsant, anti-diabetic, cell anti-sickling, anti-theileriosis, and serotonin uptake activities to anti-microbial, anti-inflammatory, anti-malarial and anti-cancer activities.

The anti-plasmodium and anti-mosquito activities of 12 Rubiaceae species are recorded in this review. One investigation involved a four-day suppressive test on Swiss albino mice infected with *Plasmodium berghei*. The ethanol extract of *Crossopteryx febrifuga* stem bark had comparable parasitaemia suppression of 71% at 400 mg/kg dosage to 79% observed for chloroquine at 5 mg/kg dosage (Muthaura et al., 2015). Rane's test was conducted with a chloroform fraction of crude methanol extract of *Gardenia ternifolia*. It was found that on day five, the percentage parasitaemia and percentage parasitaemia inhibition observed were 11% and 74%, respectively, for *G. ternifolia* (400 mg/kg) dosed mice, compared to 3% and 93% for chloroquine (10 mg/kg) dosed mice (Aragaw et al., 2020).

Two in vitro studies on *Gardenia thunbergia* and *Vangueria infausta* had notable results. The methanol extracts of *G. thunbergia* leaves inhibited *P. falciparum* (3D7 strain) by more than 80% at 50 μg/mL (Tajuddeen et al., 2022). Dichloromethane extracts of *V. infausta* roots gave an IC_{50} of 1.84 μg/mL against *P. falciparum* (NF54 strain) compared to 0.003 and 0.007 μg/mL by chloroquine and podophyllotoxin, respectively (Bapela et al., 2014). These results indicate that *C. febrifuga* stem bark, *G. ternifolia* leaves, *G. thunbergia* leaves and *V. infausta* roots have anti-malarial therapeutic potential.

Several studies reported the in vitro anti-inflammatory activity of southern African Rubiaceae plants. The plants exert this influence by modulating cytokine levels, cyclooxygenase enzymes, 15-lipoxygenase, nitric oxide production, protein denaturation, and apoptosis. The 15-LOX enzymes synthesise lipoxins from arachidonic acid. Lipoxin A_4 inhibits the production of COX-2, leading to necrosis. The induction of COX-2 upregulates the production of prostaglandin E_2 (PGE_2). PGE_2 prevents necrosis and promotes apoptosis in cells by promoting the repair of the plasma membrane, protecting the mitochondrial membrane from damage and reducing the levels of lipoxin (Behar et al., 2010).

Burchellia bubalina stem and leaf extracts were shown to have an inhibitory effect on COX-1 and COX-2 enzymes. Inhibition of COX-1 was more pronounced at over 90% for petroleum ether and dichloromethane extracts of both stems and leaves at 250 μg/mL. The effect on COX-2 was over 65% for the same extracts. In comparison, in the same study, indomethacin (5 μM) had an inhibitory effect of 74% on COX-1 and 66% on COX-2 (Amoo et al., 2009).

Another study involved four southern African Rubiaceae, namely, *C. spinosum*, *C. rudis*, *C. natalensis*, and *V. lansyantha* at 250 μg/mL. The ethyl acetate extracts of *C. spinosum* and *C. rudis* leaves resulted in COX-2 inhibition greater than 80%. The *C. natalensis* had over 75% inhibitory activity against COX-2. The inhibitory effect of indomethacin (5 μM) in the same study was 75% on COX-2 and 57% on COX-1. The *C. rudis* ethyl acetate extract had the highest inhibitory effect of the Rubiaceae species in the study on COX-1 at over 80% inhibition. The *C. spinosum* ethyl acetate extract also outperformed indomethacin with an inhibitory effect of over 65% on COX-1 (Okem et al., 2012). The ethanol leaf and ethyl acetate root extracts (10 mg/mL) of *P. prunelloides* outperformed indomethacin (20 μM) in the COX-1 inhibition assay. The leaf and root extracts had 88% and 87% inhibition, respectively, compared to 83% by indomethacin (Yff et al., 2002).

The immunomodulatory activity of five southern African Rubiaceae plants, namely *Cephalanthus natalensis*, *Cremaspora trifloral*, *O. speciosus*, *P. lanceolata*, and *P. zombomontana*, has been studied. Their effects on the production of IL-2, IL-4, IL-5, IL-10, IFN-γ, and TNF-α in lipopolysaccharide human promonocytic cells were investigated (Aro, Abimbola O. et al., 2019). The *P. zombomontana* extracts were found to promote the expression of IFN-γ while suppressing IL-5 production. IFN-γ binds to virtually any cell via the IFN-γ receptors found in most cells (Payne, 2017). IFN-γ elicits a host cell's defence mechanisms against viruses and bacteria (Broaddus and Light, 2016; Young and Hodge, 2003). IL-5 regulates eosinophils, which are involved in allergic responses (Ekmekcioglu et al., 2015).

O. speciosus and *C. triflora* decreased the expression of IL-4 AND IL-5, while the two species and *C. natalensis* suppressed the pro-inflammatory cytokine IL-2. *P. zombomontana* and *O. speciosus* increased the expression of IL-10, whereas *C. natalensis*, *C. trifloral* and *P. lanceolata* decreased it. IL-10 is an anti-inflammatory cytokine that can dampen harmful immune responses (Howes et al., 2014). All results mentioned were at a significance level of $p < 0.0001$. This study shows the potential of immunomodulatory phytochemicals that can be

isolated from Rubiaceae species. These compounds could lead to the development of new medicines for inflammatory conditions.

In another investigation, the ability of *Conostomium natalense* extracts to displace citalopram from the serotonin reuptake protein was studied (Nielsen et al., 2004). The results show that the root ethanolic extract inhibited citalopram binding in the assay by 46%. This is significant for the potential discovery and development of anti-depression medicines, as serotonin is one of the neurotransmitters associated with depression. Isolation of the compounds responsible for binding to the serotonin reuptake protein could result in the development of new anti-depression therapies.

Using Emmel's test, an anti-sickling assessment of *Cremaspora triflora* resulted in a 91% sickle cell inhibition rate at 1 mg/mL of extract (Kitambala et al., 2021). The extract was obtained through an alkaloid extraction protocol on the initial methanol whole plant crude extract. Further investigations could lead to the identification and isolation of the active compounds.

Galium spurium (aerial parts ethanol extract) and *Nauclea latifolia* (root bark water extract) have anti-convulsant activity (Ngo Bum et al., 2009; Orhan et al., 2012). In vivo studies involving mice showed that *G. spurium* extracts at 250 mg/kg significantly delay the onset of pentylenetetrazol, picrotoxin and maximal electroshock-induced seizures in Swiss albino mice compared to the control group. None of the *G. spurium*-treated mice died from seizures compared to 100% mortality in the control group. An 80 mg/kg dose of the *N. latifolia* extract significantly increased diazepam-induced sleep. Eighty-three per cent of extract-treated mice did not suffer convulsions after undergoing maximal electric shock. These sets of results demonstrate the potential of these Rubiaceae species for developing anti-convulsant medicines.

Table 3.2: Reported bioactivities of southern African Rubiaceae species

	Species	Biological activity
1	*Afrocanthium mundianum* (Cham. & Schltdl.) Lantz	Bioassay: Enzyme-Linked Immunosorbent Assay Extract: Whole plant water extracts Effect: Positive correlation between extract concentration from 50 µg/mL to 300 µg/mL and interleukin-4 production. Total mRNA detected increased 2-fold at 20 µg/mL and 4-fold at 300 µg/mL. (Samie and Madzie, 2017).
2	*Agathisanthemum bojeri* Klotzsch subsp. *Bojeri*	Bioassay: Antioxidant activity using DPPH radical scavenging activity. Extract: EtOH leaf/stem extracts Effect: IC_{50}±SD = 46.60±3.90 µg/mL (Lall et al., 2019). Bioassay: Antifungal activity against *Candida albicans* by bioautography agar overlay Extract: MeOH extract (unspecified parts) Effect: Zone of inhibition ≥ 10 mm (Runyoro et al., 2006). Bioassay: *P. falciparum* in vitro semi-automated micro-dilution anti-plasmodium assay Extract: Whole plant MeOH extracts Effect: (D6, Chloroquine sensitive strain IC_{50} = 49.8 µg/mL); (W2, Chloroquine resistant strain IC_{50} = 55.9 µg/mL) (Muthaura et al., 2015).
3	*Alberta magna* E. Meyer ZA	Bioassay: *Anopheles arabiensis* repellent activity in vivo. Extract: (**106**) isolated from CH_2Cl_2 leaf extract. Effect: Short-lived mosquito repellent properties on skin patch; 0 mosquitoes settled on skin 3 minutes after application, the same as diethyltoluamide (Drewes et al., 1998).
4	*Anthospermum hispidulum* E. Mey. ex Sond. SZ, ZA	Bioassay: Renal TK10, melanoma UZCC62, and breast cancer MCF7 cell lines Extract: DCM-MeOH extracts of unspecified parts Effect: TGI values between 12.5 and 25 µg/mL (Nthambeleni, 2008).
5	*Breonadia salicina* (Vahl) Hepper & J.R.I. Wood AO, MW, MZ, SZ, ZA, ZM, ZW	Bioassay: Antifungal activity microdilution assay Extract: Acetone, Hexane, Dichloromethane and Methanol Crude leaf extracts Effect: MIC 0.08 mg/mL by all extracts against *Penicillium janthinellum* and hexane extracts against *Fusarium oxysporum* (Mahlo et al., 2010). Bioassay: In vitro antitrypanosomal activity bioassay Extract: EtOH leaf Effect: No motility of *Trypanosoma brucei antitrypanosomally* at 0.5 mg/mL and 30 minutes (Sani et al., 2018).

	Species	Biological activity
		Bioassay: Antioxidant DPPH radical scavenging activity assay Extract: Stem bark MeOH Effect: IC 50 41.7263 ± 7.6401 μg/mL. Bioassay: Antioxidant activity potassium hexacyanoferrate (III) assay Extract: Root MeOH extract Effect: Reducing power, $IC_{0.5}$ 0.1481 ± 0.1441 μg/mL (Tlhapi et al., 2021).
6	*Burchellia bubalina* (L.f.) Sims SZ, ZA	Bioassay: Microdilution antibacterial activity assay Extracts: Bark DCM extracts. Effect: MIC = 0.098 mg/mL for Bark DCM extract against E. coli. MIC =0.39 mg/mL for Stem PE extract against *B. subtilis* and *S. aureus*, Bark PE extract against *E. coli*, Bark DCM and EtOH extracts against *B. subtilis* and *S. aureus*, and Bark EtOH extracts against E. coli and *K. pneumoniae*. MIC = 0.78 mg/mL for Leaf PE and DCM extracts against *B. subtilis*, DCM extract against *K. pneumoniae*, and root DCM extract against *E. coli* and *K. pneumoniae.* Bioassay: Microdilution antifungal activity assay Extracts: Leaf and stem DCM and root petroleum ether extracts Effect: MIC of 0.39, 0.15, and 0.78 mg/mL by stem-DCM, leaf-DCM, and PE-root extracts, respectively, on *C. albicans*. Bioassay: COX-1 and COX-2 Anti-inflammatory activity assay Extracts: PE, DCM, and EtOH extracts of leaves, stems, and roots. Effect: All PE and DCM extracts apart from root-DCM extract had prostaglandin synthesis inhibition ≥ 90% in the COX-1 assay. EtOH leaf and bark extracts had inhibition ≥ 80% on COX-1 assay. Stem PE and DCM extracts and leaf PE extract had prostaglandin inhibition ≥ 90% in the COX-1 assay and ≥ 65% in COX 2 (Amoo et al., 2009). Bioassay: *Plasmodium* viability by parasite lactate dehydrogenase (pLDH) activity assay, in vitro Extracts: Twigs and leaves DCM-MeOH extracts Effect: IC_{50} of 18 μg/mL and 50 μg/mL, respectively, against chloroquine-sensitive strain (D10) of *P. falciparum* (Clarkson et al., 2004).
7	*Canthium glaucum* Hiern BW, MW, MZ, ZM, ZW	Bioassay: In vivo antimalarial activity by a 4-day suppressive antimalarial assay on mice Extract: MeOH-$CHCl_3$ (1:1) extract Effect: The mean parasite (*Plasmodium berghei*) density, mean chemosupression and mice survival rate = Root aqueous dose- 21.68±2.42%; 31.98±7.60%; 20% respectively MeOH: $CHCl_3$ (1:1) dose- 17.92±2.49%; 43.76±7.83%; 20% respectively Chloroquine dosed mice = 4.07±0.81%; 87.23±2.72%; 100%. Bioassay: Toxicity brine shrimp assay Extract: Aqueous and organic root extract

	Species	Biological activity
		Effect: LD_{50}>1000 µg/mL (Musila et al., 2013).
8	*Canthium inerme* (L.f.) Kuntze MZ, SZ, ZA, ZW	Bioassay: Serial dilution antibacterial assay, and Extracts: Hexane, MeOH and Water extract from whole plants Effect: Show no anti-bacterial against *B. subtilis*, *E. coli*, *K. pneumoniae*, *S. aureus* (McGaw et al., 2000). Bioassay: Serial microdilution antimicrobial assay. Extracts: DCM-MeOH extracts of twigs Effect: MIC = 0.25 µg/mL and 30 µg/mL against *Staphylococcus epidermidis* and *Brevibacterium agri*, respectively (Nciki et al., 2016).
9	*Canthium spinosum* (Klotzsch exEckl. & Zeyh.) Kuntze BW, SZ, ZA	Bioassay: Antibacterial and antifungal microdilution assays Extract: EtOAc leaf extracts Effect: MIC 0.78 mg/mL and 0.19 mg/mL against *Enterococcus faecalis* and *C. albicans*, respectively Bioassay: Antibacterial microdilution Extract: The EtOH leaf extracts Effect: MIC = 0.39 mg/mL against assay *S. aureus* Bioassay: Anthelmintic colorimetric assay Extracts: EtOAc, EtOH and water leaf extracts. Effect: MLC values of 0.26, 0.016 and 0.033 mg/mL against *Caenorhabditis elegans* Bioassay: Anti-inflammatory assay Extract: EtOAc and EtOH leaf extracts Effect: Percentage Inhibitory activity of EtOAc >60% and water extracts > 50% against COX-1. The percentage inhibitory activity of EtOH extracts is> 50%, and EtOAc extract is> 80% against COX-2. Bioassay: Genotoxicity *Salmonella* microsome plate incorporation assay. Extract: Leaf EtOAC, EtOH, and H_2O extracts. Effect: Non-mutagenic. There was no increase in the number of revertants, which were not equal to, or greater than, two times that of the negative control among the *Salmonella typhimurium* strains TA98, TA100 and TA1537 (Okem et al., 2012).
10	*Cephalanthus natalensis* Oliv. LS, MW, MZ, SZ, ZA, ZM	Bioassay: Two-fold serial dilution microplate antimycobacterial assay. Extracts: Acetone leaf extracts Effect: MIC±SD (mg/mL) of 0.17±0.19, 0.10±0.08, 0.47±0.39, 0.04±0.08 against *Mycobacterium smegmatis*, *M. aurum*, *M. bovis*, and *M. tuberculosis*, respectively Bioassay: Cytotoxicity MTT assay Extract: Acetone leaf extracts

	Species	Biological activity
		Effect: LC_{50}= 0.138 mg/mL against C3A human liver cells and 0.076 mg/mL against Vero kidney cells (Aro et al., 2015). Bioassay: Anti-mycobacterial synergy with rifampicin Extracts: Acetone leaf extracts Effect: FIC index = 0.08 (Aro et al., 2016). Bioassay: Anti-plasmodium assay Extracts: Bark hexane extracts Effect: MIC = 0.27 µg/mL against *Plasmodium falciparum* (3D7) (Ngwenya, 2012). Bioassay: Immunomodulatory activity using Cytometric Bead Array (CBA) Analysis Extract: Acetone leaf extracts Effect: Reduce the expression of TNF-α, IL-2 and IL-10 cytokines (P< 0.0001) in the Human promonocytic (U937) cell line (Aro. et al., 2019).
11	*Coddia rudis* (E. Mey. ex Harv.) Verdc. SZ, MZ, ZA, ZW	Bioassay: Anti-fungal microdilution assay and Extract: EtOAc leaf extracts Effect: MIC = 0.39 mg/mL against *C. albicans*. Bioassay: Anthelmintic colorimetric assay Extract: EtOH and EtOAc leaf extracts Effect: MLC = 0.008 mg/mL and 0.52 mg/mL, respectively, against *Caenorhabditis elegans* Bioassay: Anti-inflammatory assay Extract: EtOAc and EtOH leaf extracts Effect: Percentage Inhibitory activity of EtOAc extracts > 80% against COX-1 and COX-2. Percentage Inhibitory activity of H_2O extracts > 80% against COX -2 compared to Percentage inhibition by Indomethacin® in COX-1 of 57.15 ± 5.2% and 75.5 ± 4.5% in COX-2, respectively. Bioassay: Genotoxicity *Salmonella* microsome plate incorporation assay. Extract: Leaf EtOAC, EtOH, and H_2O extracts. Effect: Non-mutagenic. There was no increase in the number of revertants, which were not equal to, or greater than, two times that of the negative control among the *Salmonella typhimurium* strains TA98, TA100 and TA1537 (Okem et al., 2012). Bioassay: Antibacterial assay. Extract: Aqueous leaf extracts Effect: MIC = 0.5 mg/mL against *Serratia marcescens* (Kambizi, 2014).

	Species	Biological activity
12	*Conostomium natalense* (Hochst.) Bremek.: MZ, ZA, ZW	Bioassay: Anti-bacterial microdilution assay and Anthelmintic colourimetric assay Extract: EtOAc leaf extract Effect: MIC = 0.09 mg/mL and MLC = 0.270 mg/mL against *Enterococcus faecalis* and *Caenorhabditis elegans*, respectively. Bioassay: Anti-fungal micro-dilution assay Extract: EtOH leaf extracts Effect: MIC = 0.39 mg/mL against *C. albicans* Bioassay: Anti-inflammatory assay Extract: EtOAc leaf extract Effect: Percentage inhibition of prostaglandin synthesis > 70% in COX-2 assay. (Okem et al., 2012). Bioassay: Serotonin reuptake transport protein binding assay, in vitro Extract: Root EtOH extract Effect: 53% [^{3}H]citalopram uptake at 5 mg/mL (Nielsen et al., 2004).
13	*Cremaspora triflora* (Thonn.) K. Schum. AO, MW, MZ, ZM, ZW	Bioassay: Antibacterial activity serial microdilution assay Extracts: Acetone leaf extracts Effect: MIC (mg/mL) = 0.05 ± 0.02, 0.32 ± 0.25, 0.16 and 0.039 against assay *E. coli*, *Salmonella typhimurium*, *Pseudomonas aeruginosa* and *Mycobacterium tuberculosis*, respectively. Bioassay: Cytotoxicity of the against Vero monkey kidney cells was determined by using an MTT assay Extracts: Acetone leaf extracts Effects: LC_{50} = 57.4 ± 2.94 µg/mL, MIC = 0.16 mg/mL, SI = 0.36 (Aro et al., 2019; Elisha, Ishaku Leo et al., 2017). Bioassay: Antimycobacterial assay for a synergistic effect of extract on rifampicin Extract: Acetone leaf extracts Effect: Sum of the fractional inhibitory concentrations against *Mycobacterium aurum* and *M. tuberculosis* ≤ 0.5, indicating a synergistic effect (Aro et al., 2016) Bioassay: Flow Cytometry THP-1 cells apoptosis Extract: Acetone leaf extract Effect: Induce apoptosis at 20, 50, and 100 µg/mL. Bioassay: U397 Immunomodulatory Assay Extract: Acetone extract.

	Species	Biological activity
		Effect: Suppresses expression of cytokine IL-2, stimulates TNF-α production and inhibits TH2, IL-4 and IL-5 cytokines, all at the statistical significance of $P < 0.0001$ (Aro, Abimbola O. et al., 2019). Bioassay: Emmel sickle cell test Extract: Suspected alkaloids in the MeOH extract of whole plant Effect: 1 mg/mL had a sickle cell inhibition rate of 90.66% (Kitambala et al., 2021). Bioassay: Anti-mycobacterial serial microdilution assay Extract: Acetone leaf extracts Effect: MIC values of 0.04, 0.02, and 0.08 mg/mL, respectively, compared to rifampicin (0.06, 0.02 and 0.01) against *Mycobacterium smegmatis*, *M. fortuitum*, and *M. aurum* (Elisha, Ishaku L et al., 2017). Bioassay: Anti-inflammatory NO production inhibition in lipopolysaccharide-activated RAW 264.7 macrophages Extract: Acetone leaf extracts (100 µg/mL) Effect: NO production inhibited by 74.34% with 88.22% macrophage viability (Elisha et al., 2016).
14	*Crossopteryx febrifuga* (Afzel. ex G. Don) Benth. AO, BW, MW, MZ, ZA, ZM, ZW	Bioassay: 4-Day Suppressive Test and Rane's (Curative) Test on *Plasmodium berghei*-infected Swiss albino mice, in vivo Extracts: Ethanol (70%) extracts of Stem-bark Effect: Average parasitaemia suppression at 400 mg/kg during the early infection phase =70.97% compared to 78.805% by chloroquine (Elufioye and Agbedahunsi, 2004). Bioassay: Hepatoprotective effect on CCl_4 intoxicated rats by determining aspartate aminotransferase, alanine aminotransferase and bilirubin levels in Wistar albino rats. Extracts: Leaf MeOH extract Effect: Significant drop ($P<0.05$) in aspartate aminotransferase, bilirubin, and alanine aminotransferase. Also, there was an increase in haemoglobin levels in extract-dosed rats compared to non-dosed rats (Atawodi et al., 2015). Bioassay: Laxative properties of leaf extract in albino rats with loperamide-induced constipation, in vivo. Extracts: Aqueous leaf extracts Effect: Significant ($p< 0.001$) increase in food and water intake, number of faecal pellets, excrement water content and weight of excrement of extract-treated rats compared to non-treated rats Bioassay: Acute toxicity assay in albino mice in vivo Extract: Aqueous leaf extracts Effect: $LD_{50} \geq 3500$ mg/kg (RDG et al., 2023). Extract: MeOH bark extract Effect: Intraperitoneal $LD_{50} \approx 774$ mg/kg (Salawu et al., 2008).

	Species	Biological activity
		Bioassay: Anti-inflammatory activity on albino mice hind paw (raw egg albumin-induced inflammation) Extract: MeOH bark extract Effect: At extract dose of 25 mg/kg volume of oedema after 120 mins = 0.22±0.05 cm^3, at an acetylsalicylic acid dose of 150 mg/kg volume of oedema after 120 mins = 0.34±0.06cm^3 (P< 0.05) (Salawu et al., 2008).
15	*Fadogia ancylantha* Schweinf. MW, MZ, ZM, ZW	Bioassay: Hepatoprotective analysis- Oral glucose tolerance test, insulin tolerance test and liver cell histology of Wistar rats with EtOH-induced liver damage. Extract: Water extracts of Makoni tea Effect: The glucose tolerance curve of EtOH and extract-treated rats was comparable to the control group, while the EtOH-treated group showed an impaired response ($p<0.05$). Normalisation of glucose levels in EtOH + extract-treated rats was faster after insulin-induced hypoglycaemia compared to the EtOH-treated group ($p<0.05$). Fatty liver droplets were present in the EtOH-treated group but absent in the EtOH + extract-treated group (Tiya et al., 2019). Bioassay: Ant-diabetic analysis- Isolated compounds **170**,**171** and **172** inhibitory activities against α-glucosidase and α-amylase Effect: IC_{50} of 160±19 and 180±19 μM respectively; **171** against α-glucosidase and lipase, IC_{50} = 170±25 and 190±25 μM respectively; **172** against lipase, IC_{50} = 200±27 μM (Feng et al., 2015). Bioassay: Anti-diabetic C2C12 muscle and Chang liver cells glucose uptake assay Extract: MeOH/DCM (1:1) leaf extract Effect: Glucose uptake in C2C12 muscle cells improved by 72% compared to the negative control and outperformed metformin by 10%. Bioassay: Antimicrobial activity microdilution method Extract: MeOH/DCM (1:1) leaf extract Effect: MIC values (mg/mL) against S. aureus and E. faecalis = 321. MIC (gentamicin /*E. faecalis*) = 1250. Bioassay: Anti-oxidant activity DPPH assay Extract: Water leaf extract Effect: IC_{50}= 44.3171.42 mg/mL
16	*Fadogia tetraquetra* K. Krause var. *tetraquetra* AO, MZ, SZ, ZA, ZM, ZW	Bioassay: Broth microdilution antibacterial assay and Semliki Forest virus luciferase-based reporter gene assay Extract: Isolated ursolic acid from *n*-hexane Effect: 99.6% inhibition of *S. aureus* at 50μM and 95.4% inhibition of Semliki forest virus at 50μM with IC_{50} of 14.7μM. Cell viability of host human hepatocellular carcinoma (Huh-7) cell line = 86.9 ± 1.4% (Mulholland et al., 2011).
17	*Feretia aeruginescens* Stapf BW, MW, MZ, ZM, ZW	Bioassay: Twofold serial dilution microplate antimycobacterial assay. Extract: Acetone leaf extract Effect: MIC = 0.47±0.22 mg/mL, MIC = 0.31±0.22 mg/mL, MIC = 0.23±0.11 mg/mL, MIC = 0.35±0.11 mg/mL against *Mycobacterium aurum*, *M. Bovis*, *M. smegmatis*, *M. tuberculosis* respectively.

	Species	Biological activity
		Bioassay: Cytotoxicity against C3A liver cells and Vero kidney cells Extract: Acetone leaf extract. Effect: LC_{50} = 0.174 mg/mL, LC_{50} = 0.242 mg/mL, respectively. (Aro et al., 2015)
18	*Galium spurium* L. *subsp. africanum* Verdc. MW, ZA	Bioassay: Anti-convulsant activity against pentylenetetrazol, picrotoxin and maximal electroshock-induced seizures in Swiss albino mice. Extract: Ethanol (80%) extracts of aerial parts. Effect: Dosages of 250 and 500 mg/kg delayed seizure onset in all cases compared to the control groups (at least $p < 0.05$). Mice given 250 and 500 mg/kg extract doses before being administered picrotoxin had a mortality rate of 0% compared to 100% in the control group (Orhan et al., 2012).
19	*Gardenia ternifolia* Schumach. & Thonn. AO, BW, MW, MZ, NM, ZA, ZM, ZW	Bioassay: Acute cytotoxicity test, 4-day suppressive test, and Rane's (Curative) test on *Plasmodium berghei*-infected Swiss albino mice, in vivo Extract: H_2O-MeOH leaf extract of unspecified variety. Effect: No mortality at dosage ≤ 2000 mg/kg; dosages of 100 and 400 mg/kg/day resulted in parasitaemia inhibition of 35.21 and 78.19%, respectively, with a p-value of 0.001, over seven days. (Aragaw et al., 2020). Bioassay: Anti-theileriosis activity on *Theileria lestoquard* infected lymphocytes Extract: Fruit water extract Effect: 60% Macroschizonts killed by 10000 ppm extract ($p<0.05$) (Farah et al., 2012).
20	*Gardenia thunbergia* L.f MZ, ZA	Bioassay: Parasite lactate dehydrogenase (pLDH) Anti-*Plasmodium* assay Extract: Leaf methanol extract Effect: Inhibition of > 80% at 50 µg/mL against *Plasmodium falciparum* strain 3D7 Bioassay: In vitro cytotoxicity assay Extract: Leaf methanol extract Effect: HeLa cell viability > 80% at 50 µg/mL (Tajuddeen et al., 2022). Bioassay: Molluscicidal activity against *Bulinus africanus* Extract: Leaf water extracts Effect: LD 50 = 0.0571 g/L with a 95% confidence interval of 0.0311 and 0.0906 g/L. LD_{90} = 0.196 g/L (Clark and Appleton, 1997).
21	*Gardenia volkensii* K. Schum. AO, BW, MW, MZ, NM, SZ, ZA, ZM, ZW	Bioassay: Genotoxicity assay- micronucleus test on phytohemagglutinin (PHA) stimulated lymphocyte cultures Extract: DCM extracts of twigs and bark Effect: were found to be genotoxic with 12.5 micronuclei per 1000 binucleated human lymphocyte cells compared to 4 micronuclei in the control group at 100 µg/mL extract concentration compared to 4 micronuclei in the control group (p = 0.05) (Verschaeve et al., 2004). Bioassay: lethality against brine shrimps (*Artemia salina*). Extract: MeOH and $CHCl_3$ fruit extracts Effect: LD_{50} = 22.9 ppm and 47.9 ppm, respectively (Juma and Majinda, 2007).

	Species	Biological activity
		Bioassay: Broth microdilution antibacterial activity assay Extract: acetone leaf extracts Effect: MIC of 0.31, 0.31, 0.63 and 0.63 mg/mL against *S. aureus*, *E. coli*, *P. aeruginosa*, and *M. smegmatis*, respectively. Bioassay: Anti-oxidant activity DPPH and Ferric-reducing power assays Extract: Leaf Acetone and MeOH extracts Effect: (MeOH, DPPH), EC_{50}= 376.66 ± 0.81 µg/mL, (Acetone, Fe-reduction), EC_{50}= 123.64 ± 0.41 µg/mL, (Ascorbic acid, DPPH, Fe-reduction), EC_{50}= 20.41 ± 0.92 and 22.67 ± 1.68 µg/mL Bioassay: Anti-inflammatory activity Bovine serum (BSA) and Egg Albumin (EA) Denaturation Inhibition Assay Extracts: Hexane and water leaf extracts Effect: BSA inhibition %= Hex extract, 65%; Diclofenac sodium, 90%. EA inhibition = Water extract, 45%; Diclofenac sodium, 90% (Matotoka et al., 2023).
22	*Guettarda speciosa* L. MZ, ZA	Bioassay: Anti-inflammatory studies against COX-1 Extract: $CHCl_3$ and MeOH leaf extracts 10 µg/mL Effect: Percentage inhibition: $CHCl_3$ and MeOH extracts, COX-1, 60-65%. Indomethacin (4.0 mM), COX-1, >80%, $p< 0.05$. Bioassay: Acute oral toxicity in Sprague-Dawley rats Extracts: MeOH Effect: nontoxic up to 2000 mg/kg Bioassay: Anti- β-amyloid (Aβ) aggregation Thioflavin T (ThT) Assay Extract: and MeOH leaf extracts Effect: $A\beta_{1-42}$ Aggregation Inhibition = 65.78 ± 3.12 % ($CHCl_3$) Bioassay: neuroblastoma SH-SY5 Cell viability assay Extracts: IC_{50}= $CHCl_3$, 8.049 µg/mL; MeOH, 43.44 µg/mL (Tan et al., 2019). Bioassay: Antibacterial activity of Ag nanoparticles formed by extract reduction of $AgNO_3$ against *S. aureus*, *B. subtilis*, *E. coli* Extract: Water leaf extracts Effect: Zone of inhibition = 6, 5, 5 mm, respectively, compared to 7, 7, and 7 mm, respectively, by amoxicillin (Deivanathan and Prakash, 2022). Bioassay: Anti-inflammatory activity in lipopolysaccharide-activated RAW 264.7 macrophages Extract: MeOH extract of unspecified parts Effect: Reduces NO and IL-6 production (Le et al., 2018)

	Species	Biological activity
23	*Heinsia crinita* (Afzel.) G. Taylor *subsp. parviflora* (K. Schum. & K. Krause) Verdc. AO, MW, MZ, ZA, ZM, ZW	Bioassay: Lipid peroxidation, MAO inhibition, Na+/K+-ATPase activity, AChE inhibition, and BChE inhibition assays using male Wistar strain albino rats. Extract: MeOH and aqueous leaf extract. Effect: Fe^{2+} caused a significant increase in MDA content in the rats' brains. Adding the extracts in a dose-dependent manner (0.78–3.5 mg/mL) caused a significant decrease in MDA levels (aqueous extract = 67.9–61.1%; methanol extract = 50.0–79.8%). Inhibition EC_{50} (mg/mL) of aqueous extract against MAO= 4.03 ± 0.07, AChE = 32.11 ± 0.12, BChE = 30.4 ± 0.52. Stimulation EC_{50} (mg/mL) of MeOH extract against Na^{+}/K^{+}-ATPase = 3.33 ± 0.03. Activity stimulated by 13.2% to 44.6% (Oboh et al., 2016).
24	*Hexasepalum sarmentosum* (Sw.) Delprete & J.H. Kirkbr. AO, MZ, ZM, ZW	Bioassay: Chikungunya virus-infected Vero cells neutral red uptake assay Extract: EtOAc leaf and stem extracts Effect: Vero cell viability of ≥ 70% (strong cytopathic effect inhibitory activity) was achieved when extracts were introduced concurrently with the virus inoculum. The virucidal effect was quantified by 5.51-log viral load reduction according to real-time RT-PCR (Chan et al., 2021). Bioassay: Microbial Dehydrogenase Inhibitory Extract: EtOH leaf extract Effect: IC_{50} 275 µg/mL, *Candida spp.* (Iheme et al., 2021)
25	*Hymenodictyon floribundum* (Hochst. & Steud.) B.L. Rob.	Bioassay: Toxicity, carrageenan-induced inflammation model and cytokine modulatory activity in rats in vivo. Extract: Ethanol leaf extracts Effect: LD_{50} > 5000 mg/kg body weighty rats. A 375 mg/kg dose significantly increases IL-6 ($p < 0.05$) compared to the control. Significantly ($p<0.05$) reduced paw oedema at 1500 mg/kg (Danraka et al., 2021). Bioassay: Antimycobacterial activity- *Mycobacterium indicus pranii* and *Mycobacterium madagascariense* broth micro-dilution technique Extract: EtOAc fraction of the stem bark had MIC values of 97 and 197 µg/mL, respectively (Marealle et al., 2023). Bioassay: Trypan blue exclusion anticancer activity in vitro Extract: 80% Ethanol stem bark extract Effect: % Viability A549 cancer cell = 46.31±0.26 (Crude, SI= 2.96), 35.25±0.21(**245**, SI= 3.54**,**), 29.56±0.13(**3**, SI= 3.56), 17.55±0.11 (5-fluorouracil) (Apoptotic) (Moyo et al., 2023)
26	*Hymenodictyon parvifolium Oliv. subsp. Parvifolium* *Yellow Firebush (Aro et al., 2015)* MZ, ZA, ZW	Bioassay: Cytotoxicity and anti-mycobacterial activity (two-fold serial microdilution assay) Extract: Leaf acetone extracts Effect: LC50 of 0.145 and 0.037 mg/mL against C3A liver and Vero kidney cells, respectively. The lowest selectivity index obtained is 0.159 for *Mycobacterium tuberculosis* and Vero cells. The highest SI obtained is 3.919 for *M. tuberculosis* and C3A cells. MIC (mg/mL) 0.47 ± 0.22, 0.19 ± 0.16, 0.35 ± 0.00 and 0.63 ± 0.16 for M. *smegmatis*, *M. aurum*, *M. bovis*, and *M. tuberculosis*, respectively (Aro et al., 2015). Bioassay: Antimicrobial activity disc diffusion method

	Species	Biological activity
		Extract: MeOH stem bark Effect: Bark methanol extract had a diameter of zone of inhibition of 24 mm against *Trichophyton interdigitale* and *Microsporum gypseum* at 800 µg per disc (Kariba, 2002).
27	*Hyperacanthus amoenus* (Sims) Bridson. MZ, SZ, ZA	Bioassay: Antimicrobial activity, serial dilution method Extract: Acetone bark extracts in the presence of polyethylene glycol Effect: MIC of 3.13 mg/mL in the presence of polyethylene glycol against *E. faecalis* and *P. aeruginosa* using the (Mahlo and Chauke, 2013; Mahlo, 2006).
28	*Keetia gueinzii* (Sond.) Bridson Syn. *Canthium gueinzii* Sond. AO, MW, MZ, SZ, ZA, ZM, ZW	Bioassay: Cytotoxicity and anti-mycobacterial activity (twofold serial microdilution assay) Extract: Acetone leaf extracts Effect: MIC (mg/mL) of 0.23±0.11, 0.16, 0.43, and 0.31±0.11 against *Mycobacterium smegmatis*; *M. aurum*; *M. bovis*, and *M. tuberculosis*, respectively, (Aro et al., 2015). Bioassay: Antimicrobial broth dilution method Extract: Acetone root bark extract Effect: MIC= 12.5 mg/mL against *B. cereus*, 12.5 mg/mL against *S. aureus* Bioassay: *Artemia salina* (Brine shrimp) lethality assay Extract: Acetone, MeOH, and water root bark extract Effect: LC_{50} (µg/mL)> $2x10^6$ (Mailu et al., 2021).
29	*Keetia hispida* AO	Bioassay: Antimicrobial diffusion method on agar plates and microdilution in liquid medium. Extract: EtOH leaf extract Effect: IC_{100} of 94 µg/mL against aminoside-resistant strain *E. faecalis* (Kone et al., 2007).
30	*Keetia zanzibarica* MW, MZ, ZM	Bioassay: Antiplasmodial SYBR Green I-based fluorescence Extract: Leaf EtOH extract Effect: Chloroquine sensitive *Plasmodium*: IC_{50} ± SD(µg/mL) = 20.1 ± 0.3. Multi-drug resistant *Plasmodium*: IC50 ± SD(µg/mL) = 14.8 ± 3.5 Bioassay: HepG2 cell line Cytotoxicity assay Extract: EtOH root bark and stem bark Effect: CC_{50} >1000 µg/mL (Christopher et al., 2023).
31	*Kraussia floribunda* Harv. MZ, SZ, ZA	Bioassay: Antimycobacterial twofold serial microdilution assay Extract: Acetone leaf extracts Effect: MIC (mg/mL) of 0.31, 0.23±0.11, 0.19±1.33, and 0.16±0.11 against *Mycobacterium smegmatis*; *M. aurum*; *M. bovis*, and *M. tuberculosis* respectively (Aro et al., 2015).
32	*Mitragyna stipulosa* (DC.) Kuntze	Method: In vivo Anti-inflammatory activity in adult albino Swiss rats Extract: Hydroethanolic leaf extract.

	Species	Biological activity
	AO, ZM	Effect: Orally administered hydroethanolic leaf extracts reduced xylene-induced ear oedema in mice by 53.1% (at 50 mg/kg dosage), 60.4% (at 100 mg/kg) and 73.9% (at 200 mg/kg). Carrageenan-induced paw-oedema was reduced by 63.99%, 49.49% and 87.50% at dosages of 50 mg/kg, 100 mg/kg and 200 mg/kg compared to diclofenac which reduced oedema by 70.8% at a dose of 10 mg/kg. No toxicity up to 5000 mg/kg dose. Results were statistically significant ($p<0.05$) Bioassay: In vitro Anti-oxidant DPPH radical and NO scavenging activities Extracts: 70% EtOH leaf extracts Effect: Extract/ Ascorbic acid/ Gallic acid NO and DPPH radical scavenging = 75-90% (Fageyinbo et al., 2021).
33	*Morinda morindoides* (Baker) Milne-Redh. AO	Bioassay: A SYBR Green-based microfluorometric anti-plasmodium assay and cytotoxicity assay (adult mouse brain cells) Extract: Alcoholic leaf extract Effect: IC_{50} = 66.54 (3D7), 94.38 (Dd2); SI= 7.33 (3D7), 5.17 (Dd2) (Hashim et al., 2021).
34	*Mussaenda arcuata* Poir. AO, MW, MZ, ZM, ZW	Bioassay: Antimycobacterial twofold serial microdilution assay Extract: Acetone leaf extracts Effect: MIC (mg/mL) of 0.08, 0.39±0.33, 1.56±0.16, and 0.31±0.33 against *Mycobacterium smegmatis*; *M. aurum*; *M. bovis*, and *M. tuberculosis* respectively (Aro et al., 2015).
35	*Nauclea latifolia* Sm. AO	Bioassay: Anti-convulsant and sedative activities in adult male mice, *Mus musculus* Swiss, in vivo. Extract: Root bark aqueous extract Effect: Extracts (80 mg/kg) increased the duration of diazepam-induced sleep (50 mg/kg) by 64 minutes. Bark extract protected 83% of mice tested against maximal electroshock-induced convulsions at 160 mg/kg (Ngo Bum et al., 2009). Bioassay: Antidiabetic in vivo tests on white Wistar strain albino rats. Extract: Aqueous leaf extracts Effect: Oral administration of aqueous leaf extracts (200 mg/kg) lowered the blood glucose level in alloxan monohydrate-induced diabetic rats by 19.5% after 1 hr compared to 0.67% by glibenclamide and by 44.5% after 4 hrs compared to 40% by glibenclamide (Gidado et al., 2005).
36	*Oldenlandia affinis* (Roem. & Schult.) DC. subsp. *fugax* (Vatke) Verdc AO, BW, MW, MZ, SZ, ZA, ZM, ZW	Bioassay: Two-stage radial diffusion low salt in vitro bioassay Active agent: A synthetic version of Kalata, the cyclotide first isolated from the plant. Effect: MIC of 0.26 μM against *S. aureus* (Tam et al., 1999). Bioassay: In vitro investigation of uteri contractions of Wistar rats (recorded isotonically), rabbits and humans (recorded isometrically). Active agent: Plant peptide Effect: A dosage of 20 μg/mL of the peptide was required to stimulate contractions in rat, rabbit and human uterine muscle strips (Gran, 1973).
37	*Oldenlandia corymbosa* L. AO, BW, MW, MZ, SZ, ZA, ZM, ZW	Bioassay: Antibacterial activity by disc diffusion method Extract: MeOH root and aerial part extract

	Species	Biological activity
		Effect: Antimicrobial activity measured by zone of inhibition (ZOI): 1 mg MeOH aerial parts extract gave a ZOI of 31 mm against *S. typhi*, 21 mm against *V. cholerae* compared to penicillin ZOI of 35 mm and 16 mm, respectively. 1 mg MeOH root extract gave ZOI of 32 mm against *S. typhi* and 15 mm against *V. cholerae* Bioassay: Anti-oxidant DPPH assay Extracts: MeOH root and aerial part extract Effect: IC_{50}= 0.24 ± 0.005 and 0.49 ± 0.006 mg/mL Bioassay: Cell viability assay by MTT Extract: MeOH aerial part extract Effect: MCF-7 IC_{50}= 0.67 ± 0.18 mg/mL (Archana et al., 2021). Bioassay: Anti-inflammatory in vivo Carrageenan Induced Paw Oedema Test on Swiss albino mice Extract: DCM aerial parts extract Effect: % Oedema inhibition ($p< 0.005$) = Extract (63%, 3hr; 61%, 4hr), Aspirin (97%, 3hr) (Al Bashera et al., 2021)
38	*Oldenlandia herbacea* (L.) AO, BW, LS, MW, MZ, NM, SZ, ZA, ZM, ZW	Bioassay: Antibacterial activity by agar well diffusion. Extract: Whole plant methanol extract Effect: Antimicrobial activity measured by ZOI: (Bacteria; 500 mg MeOH whole plant extract gave a ZOI of 22 mm against *S. aureus* compared to 29 mm by chloramphenicol and 21 mm against *K. pneumonia* compared to 26mm by chloramphenicol (Danlami and Danhalilu, 2015). Bioassay: In vitro antioxidant activity ABTS, H_2O_2, DPPH, and NO assays Extract: Whole plant Effect: MeOH extract resulted in IC_{50} 26.46±0.55 µg/mL in ABTS assay and H_2O_2 assay, EtOAc extract resulted in IC_{50} 42.53±0.03 µg/mL in DPPH assay and 113.83±3.01 µg/mL in NO assay (Singaravelu et al., 2008).
39	*Oxyanthus speciosus* DC. AO, MW, MZ, SZ, ZA, ZM, ZW	Bioassay: Antimycobacterial two-fold serial microdilution assay Extract: Acetone leaf extracts Effect: MIC (mg/mL) of 0.08, 0.06±0.03, 0.12±0.06, and 0.17±0.22 against *Mycobacterium smegmatis*; *M. aurum*; *M. bovis*, and *M. tuberculosis* respectively (Aro et al., 2015) Bioassay: Apoptosis measured using the annexin V-FITC/PI assay on THP-1 cell line and Cytokine Detection via Cytometric Bead Array (CBA) Analysis Extract: Acetone leaf extract Effect: Extracts induce a (65-85%) necrotic effect in the THP-1 cell line at 50 and 100 µg/mL while suppressing the expression of TNF-α, IL-2, IL-4 and IL-5 cytokines and promoting the expression of IL-10 cytokine in the U937 cell line (P-values< 0.001) (Aro, Abimbola O. et al., 2019).
40	*Pavetta lanceolata* Eckl.	Bioassay: Antimycobacterial twofold serial microdilution assay Extract: Acetone leaf extracts

	Species	Biological activity
	MZ, SZ, ZA	Effect: MIC (mg/mL) of 0.12±0.06, 0.10±0.08, 0.17±0.19, and 0.12 against *Mycobacterium smegmatis*; *M. aurum*; *M. bovis*, and *M. tuberculosis* respectively (Aro et al., 2015). Bioassay: 15-Lipoxygenase (15-LOX) inhibition- microplate-based ferric oxidation of xylenol (FOX) orange assay, Cytokine Detection via CBA Analysis, and Apoptosis measured using the annexin V-FITC/PI assay on THP-1 cell line. Extract: Acetone leaf extracts Effect: IC_{50} against 15-LOX 10.85 ± 0.83 µg/mL reduces the expression of IL-10 cytokines in the U-937 cell line ($P< 0.001$), and extracts induce a necrotic effect in the THP-1 cell line at 50 and 100 µg/mL (Aro, Abimbola O. et al., 2019). Hosts *Burkholderia* endophytes (Lemaire et al., 2011).
41	*Pentanisia prunelloides* (Klotzsch ex Eckl. & Zeyh.) Walp. LS, MW, MZ, SZ, ZA, ZM	Bioassay: Anti-inflammatory cyclooxygenase-1 assay Effect: 88% (EtOH) and 87% (EtOAc) inhibition of cyclooxygenase-1, respectively. Extract concentration =10 mg/mL. Indomethacin (83%, 20 µM). Bioassay: Microplate antibacterial method using a serial dilution technique Extract: EtOH leaf and EtOAc root extracts Effect: MLC= 0.2 mg/mL (*S. aureus*, leaf); 0.39 mg/mL (*S. aureus* and *K. pneumoniae*, root). Bioassay: In vitro viral inactivation assay (Influenza-A in vervet monkey kidney cell host) Extract: Leaf and root aqueous extract Effect: Inhibition = 96.2% (root, 125 µg/mL); 83.3% (leaf, 15.62 µg/mL) (Yff et al., 2002). Bioassay: Anti-oxidant Iron Chelation, superoxide anion and hydroxyl radical scavenging assay Extract: Aqueous-ethanol, Hexane root extract Effect: IC_{50} (µg/mL, chelation assay) = 4.24 ± 0.03; Gallic acid (101.7 ± 2.26) IC_{50} (µg/mL, superoxide assay) = 0.33 ± 0.02; Gallic acid (55.50 ± 0.12) IC_{50} (µg/mL, Hydroxyl assay) = 0.51 ± 0.43; Gallic acid (65.70 ± 1.48) Bioassay: Anti-diabetic α-amylase, α-glucosidase, sucrase and maltase inhibitory assay Extract: Hex, EtOH, Water extracts Effect: IC_{50} (µg/mL)= 18.08 ± 0.03 (Hex, α-glucosidase); 19.73 ± 1.53 (EtOH, α-glucosidase); 129.4 ± 5.11 (Acarbose, α-glucosidase); 0.48 ± 0.35 (Hex, α-amylase); 8.82 ± 0.53 (Water, α-amylase); 0.48 ± 0.35 (Hex, α-amylase); 9.87 ± 1.61 (Acarbose, α-amylase) (Makhubu et al., 2019).
42	*Psychotria capensis* (Eckl.) Vatke MW, MZ, SZ, ZA, ZM, ZW	Bioassay: Antimycobacterial twofold serial microdilution assay Extract: Acetone leaf extracts Effect: MIC(mg/mL) of 0.06±0.03, 0.12±0.06, 0.19±0.16, and 0.63±0.39 against *Mycobacterium smegmatis*; *M. aurum*; *M. bovis*, and *M. tuberculosis* respectively (Aro et al., 2015). Bioassay: Anthelmintic activity against *Haemonchus contortus* egg-hatching Extract: Acetone leaf extracts

	Species	Biological activity
		Effect: IC_{50} 160 µg/mL (Hex fraction, SI=) (Aro et al., 2022). Bioassay: Anti-aging Anti-elastase, Anti-collagenase and anti-hyaluronidase assays Extract: Root, stem, leaves, seed-EtOAc and MeOH extracts (200 µg/mL) Effect: % inhibition = 92.84±1.13% (leaf-EtOAc, elastase); Elafin (93.09 ± 4.10, elastase); 78.36 ± 1.50 (seeds-MeOH, collagenase); EDTA (83.75 ± 2.89, collagenase); 52.98 ± 0.66 (leaf-MeOH, hyaluronidase); Sodium aurothiomalate (100 ± 0.01) Bioassay: Anti-oxidant $ABTS^{\bullet+}$ assay Extracts: IC_{50} (µg/mL) = (Root-EtOAc, 9.5 ± 1.06); Trolox (2.84 ± 0.52) (Ndlovu et al., 2013). Bioassay: 15-LOX inhibition- microplate-based ferric oxidation of xylenol (FOX) orange assay, Cytotoxicity Assay using the 3-(4,5-dimethylthiazol)-2,5-diphenyl tetrazolium bromide (MTT) assay, and apoptosis measured using the annexin V-FITC/PI assay on THP-1 cell line. Extract: Acetone leaf extracts Effect: Inhibit 15-LOX (IC_{50}= 5.8±1.94µg/mL), time/dose-dependent induction of apoptosis between 20 and 100 µg/mL of extract was observed in the THP-1 cell line. Extracts were cytotoxic against the U937 cell line (IC_{50}= 25 µg/mL, low cytotoxicity against THP-1 cells (IC_{50}= 761±0.10 mg/mL) (Aro, Abimbola O. et al., 2019).
43	*Psychotria zombamontana* (Kuntze) E.M.A. Petit MW, MZ, ZA, ZM, ZW	Bioassay: a rapid broth microdilution technique with p-iodonitrotetrazolium violet Extract: MeOH extracts of cultures of the isolated endophytic leaf fungi Effect: Symbiotic endophytic fungi *Talaromyces funiculosus* and *Cochliobolus* sp. from leaves show antibacterial activity against *Cryptococcus neoformans* and *Candida albicans* (MIC between 0.625 and 1.25 mg/ mL) (Abdalla et al., 2020). Bioassay: Antimycobacterial twofold serial microdilution assay Extract: Acetone leaf extracts Effect: Acetone leaf extracts have MIC (mg/mL) of 0.04, 008, 0.16, and 0.16 against *Mycobacterium smegmatis*; *M. aurum M. bovis*, and *M. tuberculosis*, respectively (Aro et al., 2015). Bioassay: 15-LOX inhibition- microplate-based ferric oxidation of xylenol (FOX) orange assay and cytotoxicity assay using the 3-(4,5-dimethylthiazol)-2,5-diphenyl tetrazolium bromide (MTT) assay. Extract: Acetone leaf extracts Effect: Immunomodulatory activity by increasing cytokine IFN-γ and IL-10 while decreasing TNF-α levels in the human promonocytic cell line U937 (P< 0.001). Inhibition of 15-LOX occurs with IC_{50} of 4.32±1.10. (Aro, Abimbola O. et al., 2019).
44	*Psydrax lividus* (Hiern) Bridson AO, BW, MW, MZ, NM, ZA, ZM, ZW	Bioassay: Antibacterial- serial microplate dilution method with tetrazolium violet Extract: Acetone extracts from leaves Effect: Show antibacterial activity against *S. aureus*, *E. coli*, *E. feacalis*, and *P. aeruginosa* (MIC = 0.156 mg/mL). Gentamycin MIC = 7.8 E-4, 1.56E-3, 3.9E-4 and 1.56E-3, respectively (Mukandiwa et al., 2012).

	Species	Biological activity
45	*Richardia brasiliensis** Gomes	Bioassay: Antiproliferative activity of cancer cell lines using MTT assay and Annexin PE/7-AAD to detect apoptosis. Extract: Alcoholic extracts of aerial parts. Effect: IC_{50} (µg/mL) and SI against human melanoma (A375) = 344.62 and 2.21, HeLa= 392.40 and 1.94, breast cancer (MCF-7) = 528.58 and 1.44, and human glioblastoma (U87) = 932.30 and 0.81 % Apoptosis = 80% (A375) Bioassay: In vitro cytotoxicity assays (MTT cell viability, DCFH-DA total free radicals, NO levels, DNA quantification) Extract: Alcoholic extracts of aerial parts Effect: No difference between negative control and extract in cell viability, ROS, and NO levels. Extracellular DNA increased at 500 µg/mL. Bioassay: In vivo acute toxicity (Wistar rats) Extract: Alcoholic extracts of aerial parts Effect: No signs of toxicity up to 2000 mg/kg (Dornelles et al., 2022).
46	*Rothmannia capensis* Thunb. BW, SZ, ZA	Bioassay: Disc-diffusion assay. Extracts: Water extracts of stems and roots Effect: Bacteriostatic effect of water stem and root extracts against *Klebsiella pneumoniae* and root water extracts against *E. coli*. (Kelmanson et al., 2000).
47	*Rubia cordifolia L.* AO, MW, MZ, SZ, ZA, ZM, ZW	Test: In vivo anti-diarrheal test on senna leaf-induced diarrhoea in male Swiss albino mice. Extract: Aqueous extracts of aerial parts Effect: Doses of 500 and 1000 mg/kg delayed the onset of diarrhoea in mice ($p< 0.05$ and $p< 0.001$, respectively) Bioassay: Acute oral toxicity test Extract: Aqueous extracts of aerial parts Effect: No signs of toxicity up to 1320 mg/g Bioassay: Anti-inflammatory activity in vivo TNBS-induced colitis Extract: Aqueous extracts of aerial parts Effect: MDA levels reduced at 500 mg/kg compared to TNBS control group ($P< 0.05$); No significant change in MPO levels by extract; Reduction in TNF-α and IL- β ($P< 0.05$) (Gong et al., 2017).
48	*Tarenna pavettoides (Harv.) Sim* MW, MZ, SZ, ZA, ZM, ZW	Bioassay: Anti-plasmodium activity against *P. falciparum* parasites (3D7, chloroquine-sensitive strain) and human embryonic kidney cells (HEK 293) cytotoxicity assays. Extract: Stem bark MeOH and Root bark extract Effect: Stem bark MeOH extracts gave an IC_{50} of 75.70±24.19 µg/mL (3D7) and >400 µg/mL (HEK 293) while the root bark showed IC_{50} of 27.88±18.05 (3D7) against *P. falciparum* (3D7) and 57% (at 400 µg/mL against HEK 293) (Begum et al., 2020).

	Species	Biological activity
49	*Vangueria infausta* AO, BW, MW, MZ, NM, SZ, ZA, ZM, ZW	Bioassay: Antiplasmodium [^{3}H] hypoxanthine incorporation assay using chloroquine-sensitive (NF54) strain and cytotoxicity assay (rat skeletal myoblasts L-6 cells). Extract: DCM-MeOH (1:1) root extracts Effect: IC_{50} of 1.84 µg/mL against *P. falciparum* (NF54) and selectivity index of 24.8 when tested on rat skeletal myoblasts L-6 cells (Bapela et al., 2014). Bioassay: Antimycobacterial twofold serial microdilution assay Extract: Acetone leaf extracts Effect: Acetone leaf extracts have MIC (mg/mL) of 0.63, 0.23±0.11, 0.47±0.44, and 0.63 against *Mycobacterium smegmatis*, *M. aurum*, *M. bovis*, and *M. tuberculosis*, respectively (Aro et al., 2015). Bioassay: Anti-inflammatory activity Extracts: Ripe fruit EtOH extract Effect: % Inhibition of egg albumin denaturation = 79% (200 mg/L, unsaponifiable fraction); 76% (Indomethacin). % NO radical scavenging activity = 83% (800 mg/L, crude); 90% (Indomethacin); 94% (quercetin) (Gwatidzo et al., 2018)
50	*Vangueria lasiantha (Sond.) Sond.* MZ, ZA	Bioassay: Antibacterial microdilution assay and anthelmintic colourimetric assay (free-living Caenorhabditis elegans var. Bristol (N2) nematode larvae viability) Extract: EtOAc leaf extracts Effect: inhibit the growth of *E. faecalis* with MIC of 0.78 mg/mL, anthelmintic activity MLC = 0.065 mg/mL Bioassay: Anti-inflammatory activity COX-1 assay Extracts: Leaf EtOH extracts Effect: Inhibition of prostaglandins= > 60% (EtOH extracts); <60% (Indomethacin) Bioassay: *Salmonella typhimurium* Genotoxicity assay Extracts: EtOAc, EtOH and Water extract Effect: Not mutagenic towards TA98, TA100 and TA1537 strains (Okem et al., 2012).
51	*Vangueria madagascariensis J.F. Gmel.* AO, SZ, MW, MZ, ZA	Bioassay: In vitro α-Glucosidase Assay Extracts: Fresh leaves, unripe and ripe fruits, MeOH and water extracts. Effect: IC_{50} (mg/mL) against α-glucosidase of Leaf water extracts, unripe fruit water extracts, unripe fruit MeOH extract and ripe fruit MeOH extract = 0.61 ± 0.21, 0.50 ± 6.01, 0.36 ± 0.07 and 3.28 ± 0.45 compared to acarbose's 5.03±0.14. Bioassay: DPPH radical scavenging assay Extract: Leaf and unripe fruit MeOH extracts Effect: IC_{50} (µg/mL) = 9.04 ± 0.66 (Leaf), 10.01 ± 0.93 (Unripe fruit) (Ramalingum and Mahomoodally, 2014).

	Species	Biological activity
		Bioassay: Microdilution broth susceptibility assay and Antibiotic potentiating assay Extract: Leaf and fruit MeOH and water extracts Effect: MIC (mg/mL) MeOH leaf extracts = <0.20 against *Enterococcus faecalis*, *Streptococcus* group A, and *Streptococcus* group B. Fruit water extracts MIC (mg/mL) =<0.10 against Streptococcus group A. Combining chloramphenicol with the leaf MeOH extract (1:1) lowered the MIC (µg/mL) from <0.78 to <0.39 against *Klebsiella* spp and 0.39 against MIRSA. Combining Gentamicin (1:1) with leaf MeOH extract lowered MIC from 50 µg/mL to <0.39 µg/mL. The MIC (µg/mL) of ciprofloxacin against *Streptococcus* group B improved from 6.25 to <0.23 when combined with leaf decoctions at 30% antibiotic to 70% extract (Mahomoodally and Dilmohamed, 2016).
52	*Vangueria venosa (Hochst.) Sond.* MZ, SZ, ZA	Bioassay: Molluscicidal, cercaricidal and miracidicidal activity Extracts: Fruit water extracts Effect: Aqueous extracts of fruit had no effect against *Biomphalaria pfeifferi* up to 250 ppm concentration. LC_{100} = 1000 ppm after 90 minutes against *Schistosoma mansoni* cercaria (Sulaiman et al., 1988).

3.5 Phytochemicals isolated from Rubiaceae found in southern Africa

A total of 243 reported compounds have been isolated from 39 Rubiaceae plants that are found in southern Africa. The compound classes include alkaloids, coumarins, flavonoids, iridoids, lignans, nitriles, steroids, and other compounds that were not classed. A list of isolated compounds is shown in Table 3.3. The different classes of compounds are discussed in more detail in the following sections.

Table 3.3: Compounds isolated from southern African Rubiaceae

Species	Compounds isolated
Afrocanthium gilfillanii (N.E.Br.) Lantz BW, SZ, ZA	**127** (L) (Nahrstedt et al., 1995)
Alberta magna E. Meyer, ZA	Compounds: **104, 105, 106, 205**(L) (Drewes et al., 1998; Horn, 1996)
Anthospermum hispidulum E. Mey. ex Sond. SZ, ZA	Compounds 1**56**, **3 (U)** (Nthambeleni, 2008)
Breonadia salicina (Vahl) Hepper & J.R.I. Wood AO, MW, MZ, SZ, ZA, ZM, ZW	Compounds: **156**(L), **4**, **160**, **204**, **205**, **5**, **6**, **76**, **157**, **220**, **161**, **224**, **221** (SB). (Mahlo and Eloff, 2014; Nvau et al., 2019; Tlhapi et al., 2021).
Burchellia bubalina (L.f.) Sims SZ, ZA	Compounds: **107**, **108** (L) (Drewes et al., 1999)
Catunaregam obovata (Hochst.) A.E. Gonç. MZ, SZ, ZA	Compounds: **3**, **7**, **8** (RB) (Sibanda et al., 1989)
Cephalanthus natalensis Oliv. LS, MW, MZ, SZ, ZA, ZM	Compound(s): **222**(L) (Ngwenya, 2012)
Crossopteryx febrifuga (Afzel. ex G. Don) Benth. AO, BW, MW, MZ, ZA, ZM, ZW	**162**, **163** (R), **167** (RB)**, 158, 159, 164, 109, 110, 165, 166, 205, 206, 111, 195, 196**(SB) (Aristide et al., 2021; Babady et al., 1991; Chouna et al., 2015; Gariboldi et al., 1990; Kayangar et al., 2019; Tomás-Barberán and Hostettmann, 1988)
Fadogia ancylantha Schweinf. MW, MZ, ZM, ZW	**168**, **169**, **170**,**81**, **77**, **78**, **171**, **79** (L) (Mencherini et al., 2010)
Fadogia homblei De Wild AO, MW, MZ, ZA, ZM, ZW	**156** (L), **3 (**L/S**)**, **204**, **205**, **157** (F/L/S), **165**(L), **87**(F), **88**(L), **172** (F/L/S), **173**, **174** (F), **213** (S), **15** (U) (Bode et al., 2010; Fourie et al., 1995; Mohammed et al., 2013).
Fadogia tetraquetra K. Krause var. *tetraquetra* AO, MZ, SZ, ZA, ZM, ZW	**156**, **204**, **205**, **165**, **175**, **176** (L) (Mulholland et al., 2011)
Galium spurium L. *subsp. africanum* Verdc. MW, ZA	**80**, **82**, **83**, **84**, **85**, **86**, **128**, **112**, **219**(A) (Yang et al., 2011)
Gardenia ternifolia Schumach. & Thonn. AO, BW, MW, MZ, NM, ZA, ZM, ZW	**204**, **205**, **100**, **101**, **102**, **96** (L) (Awas et al., 2016).
Gardenia thunbergia L.f MZ, ZA	**3**, **204**, **205**, **157**,**81**, **177**,**225**, **227** (L) (Tajuddeen et al., 2022).
Gardenia volkensii K. Schum. AO, BW, MW, MZ, NM, SZ, ZA, ZM, ZW	**165** (S), **178**, **113**, **129**, **130**, **36** (F/S) (Juma and Majinda, 2007; Kinuthia et al., 2012)

Guettarda speciosa L. MZ, ZA	**228**, **226**, **114**, **115** (L), **230**, **207**, **47**, **16**, **17**, **116**, **231**(RB)**, 229**, **233** (L) (Cai et al., 2011; Muangrom et al., 2021)
Heinsia crinita (Afzel.) G. Taylor *subsp. parviflora* (K. Schum. & K. Krause) Verdc. AO, MW, MZ, ZA, ZM, ZW	**118**, **119, 120** (SB) (Tshisekedi Tshibangu et al., 2017)
Hymenodictyon floribundum (Hochst. & Steud.) B.L. Rob.	**3**, **12**, **13**, **39**,**121**,**179**, **234, 243** (SB) (Borges et al., 2010; Marealle et al., 2023).
Kraussia floribunda Harv. MZ, SZ, ZA	**205**, **216**, **82**, **87**, **213**, **117**, **91** (L/S) (Mohammed et al., 2012)
Mitragyna stipulosa (DC.) Kuntze AO, ZM	**156**, **3**, **204**, **205**, **165**, **206**, **114**, **122**, **123, 55, 242, 10, 197, 64** (F), **180, 181, 182,** (SB) (Fatima et al., 2002; Ndoumbe et al., 2023)
Morinda morindoides (Baker) Milne-Redh. AO	**140** – **155, 66**, **67**, **86**, **94, 95**, **238** L (Hashim et al., 2021; Hashim et al., 2022)
Nauclea latifolia Sm. Syn. *Sarcocephalus latifolius* (Sm.) E.A. Bruce AO	**18-23**, **33**, **34**, **37**, **38**, **41-54**, **56-61**, **24-32, 183-188**, **217, 189** (R, SB, W) (Agomuoh et al., 2013; Ata et al., 2009; Boucherle et al., 2016; Kakuguchi et al., 2009; Kezetas Bankeu et al., 2019; Ngnokam et al., 2003; Shigemori et al., 2003)
*Oldenlandia affinis (*Roem. & Schult.) DC. subsp. *fugax* (Vatke) Verdc AO, BW, MW, MZ, SZ, ZA, ZM, ZW	**198** – **203** (U) (Craik et al., 1999; Gran et al., 2008; Pelegrini et al., 2007; Plan et al., 2010)
Oldenlandia corymbosa L. AO, BW, MW, MZ, SZ, ZA, ZM, ZW	**112**, **131-137**, **124** (W), **138, 139, 215** (W) (Noiarsa et al., 2008; Otsuka et al., 1991)
Oldenlandia herbacea (L.) AO, BW, LS, MW, MZ, NM, SZ, ZA, ZM, ZW	**208**, **223** (W) (Singaravelu et al., 2008)
Oxyanthus pyriformis (Hochst.) Skeels MZ, ZA	**209-211** (L, S, Fr, Fl) (Rockenbach et al., 1992)
Oxyanthus speciosus DC. AO, MW, MZ, SZ, ZA, ZM, ZW	**35**, **65, 172, 189, 239**, **232, 190-192, 212** (L, S,R,Fl) (Aro, A. O. et al., 2019; Nahrstedt et al., 1995; Nyobe et al., 2020; Rockenbach et al., 1992)
Pavetta harborii S. Moore BW, MZ, NM, ZA	**15** (U) (Bode et al., 2010; Fourie et al., 1995)
Pavetta lanceolata Eckl. MZ, SZ, ZA	**40** (A) (Jordaan and Joynt, 1968).
Pavetta schumanniana F. Hoffm. ex K. Schum.	**15** (U). (Bode et al., 2010; Fourie et al., 1995)
Pentanisia prunelloides (Klotzsch ex Eckl. & Zeyh.) Walp. LS, MW, MZ, SZ, ZA, ZM	**193** (R), **221** (R) (Makhubu, 2017; Yff et al., 2002).
Psychotria punctata (Syn. *Psychotria kirkii*) MW, MZ, ZM, ZW	**62**, **254** (L) (Sieber et al., 2015).
Psydrax lividus (Hiern) Bridson AO, BW, MW, MZ, NM, ZA, ZM, ZW	**209**, **240**, **241** (L) (Nahrstedt et al., 1995; Rockenbach et al., 1992)
*Richardia brasiliensis** Gomes	**3, 93**, **156**, **204**, **205**, **165**, **235**, **181** (U), (Matias et al., 2018; Pinto et al., 2008; Poonkodi, 2016)
Rothmannia globosa (Hochst.) Keay ZA	**107**, **108**, **125**, **126**, **129**, **131**, **134**, (Fr) (Jensen, 1983)
Rubia cordifolia L. AO, MW, MZ, SZ, ZA, ZM, ZW	**3**, **9**, **11**, **63, 156**, **205**, **221**, **165, 249-253** (R)**, 81**, **82**, **84**, **87**, **244-248**, **89**, **90, 97-99, 214, 217-219, 194, 238, 91, 236, 92, 237** (A) (He et al., 2021; Wang et al., 2023; Zhang et al., 2024)

Vangueria infausta AO, BW, MW, MZ, NM, SZ, ZA, ZM, ZW	**103** (L) (Mbukwa et al., 2007)
Vangueria pygmaea Schltr. MW, SZ, ZA, ZM, ZW	**15** (U) (Bode et al., 2010; Fourie et al., 1995; Van Elst et al., 2013)
Vangueria thamnus (Robyns) Lantz, ZA	**15** (U) (Verstraete et al., 2011)

3.5.1 Coumarins

The number of coumarins that were retrieved from the searches is 11. Coumarins are heterocyclic compounds with a benzo-α-pyrone structure (Sethna and Shah, 1945). Coumarins distinguish themselves from benzo-γ-pyrone compounds by having the carbonyl group in position 2 instead of 4, as illustrated by compounds **1** and **2** in Figure 3.2.

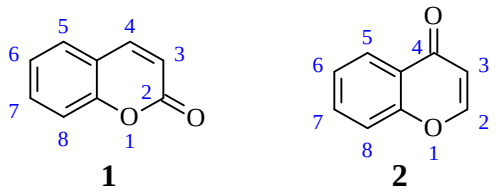

Figure 3.2: Structures of benzo-α-pyron (**1**) and benzo-γ-pyrone (**2**)

The first coumarin was isolated from tonka beans (*Dipteryx odorata*) in 1820. Since then, various plant species have been shown to produce this class of compounds, and progress has been made in developing synthetic versions (Sethna and Shah, 1945).

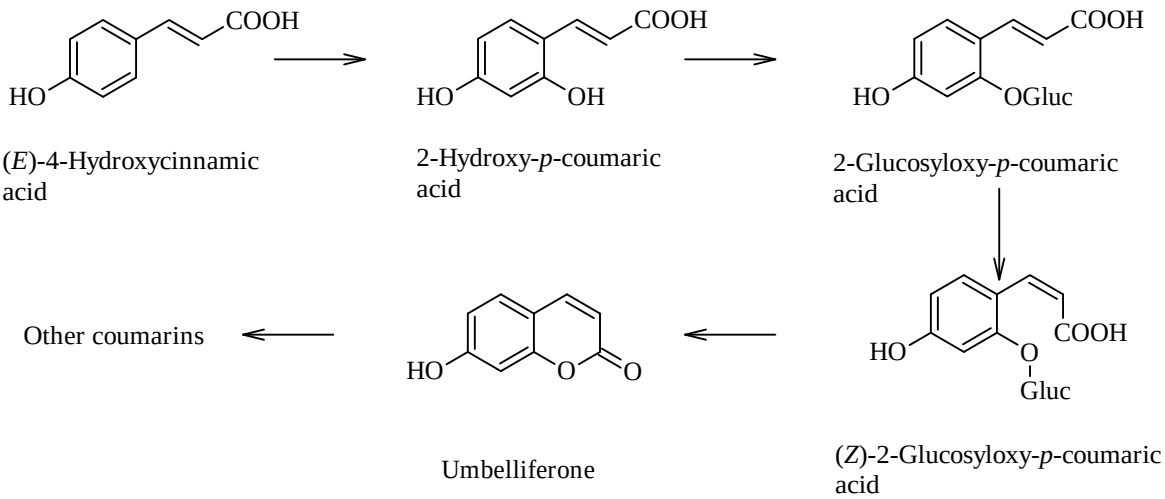

Scheme 3.1: A general coumarin biosynthetic pathway

Coumarins isolated from plants are diversified, with some occurring as phenols, phenol ethers, phenol esters, phenol glycosides and coumarinolignoids (Murray, 1989). Most plant coumarins

that have been isolated are oxygenated at position 7, as is the case with umbelliferone (**5**). The biosynthetic route for the formation of umbelliferone begins with *p*-coumaric acid, as shown in Scheme 3.1 (Sarker and Nahar, 2017). An enzyme oxidises 4-hydroxycinnamic acid, producing 2-hydroxy-*p*-coumaric acid and glucosylates the product. Isomerisation then forms (*Z*)-2-glucosyloxy-*p*-coumaric acid, from which umbelliferone is formed by ring closure (Sarker and Nahar, 2017).

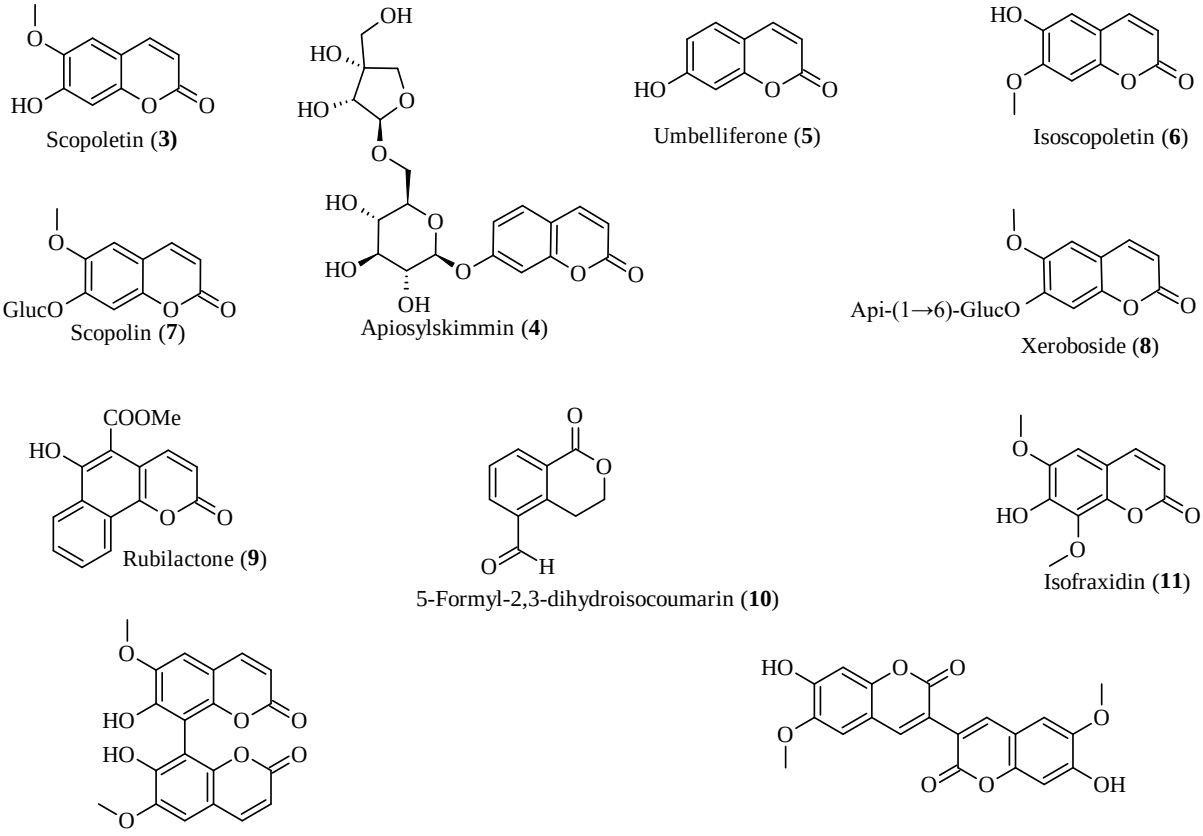

Figure 3.3: Coumarins isolated from Rubiaceae found in southern Africa

The biological activities of coumarins range from anti-oxidant activity, anti-diabetes, anti-inflammatory, antihypertensive, and antimicrobial (Hussain, M.I. et al., 2019). Isofraxidin (**11**) has demonstrated anti-diabetic properties in vivo studies on mice, 1,2-benzopyrone is effective against oedema, and esculetin has been shown to inhibit lipoxygenase and cyclooxygenase (Hoult and Payá, 1996; Hussain, M.I. et al., 2019; Kostova et al., 2011; Sarker and Nahar, 2017). Coumarins isolated from southern African Rubiaceae are collated in Figure 3.3. The plants from which they have been isolated and the references are shown in Table 3.3.

3.5.2 Alkaloids

Alkaloids are generally defined as nitrogen-containing natural products. Alkaloids are usually formed from amino acids. The number of alkaloids that have been identified is about 12 000, making up 12-15% of known natural products (Rosales et al., 2020). Alkaloids are classified based on their structure. Classes of alkaloids include piperidine, pyrrolidine, pyrrole, pyridine, quinolone, isoquinoline, indole, quinolizidine, pyrrolizidine, tropane, benzylisoquinoline, purine, β-carboline, indoline and quinolizidine alkaloids (Rosales et al., 2020).

The literature search yielded 54 alkaloids isolated from Rubiaceae plants in southern Africa. Forty-three are indole alkaloids, two are iridoid alkaloids, and two are glutamic acid-based alkaloids. Indole alkaloids are derived from tryptophan (**14**). Their basic structure is a fusion of a benzene ring and a five-sided pyrrole ring. The bioactivities of indole alkaloids range from anti-HIV, antioxidant, and anti-inflammatory activities. Some indole alkaloids have analgesic properties (Singh and Singh, 2018). Piperazine-, cyclitol-, pyrrolidine-, pyridine-, and triterpene-based alkaloids each have one representative (Boucherle et al., 2016; Nyobe et al., 2020; Sieber et al., 2015). The other two alkaloids are the polyamine pavettamine (**15**) (Bode et al., 2010; Fourie et al., 1995) and the lactonic enamino ketone gentiocrucine (**55**) (Ndoumbe et al., 2023).

The alkaloids isolated from southern African Rubiaceae are shown in Figures 3.4a and 3.4b. The plants from which they have been isolated together with the references are shown in Table 3.3.

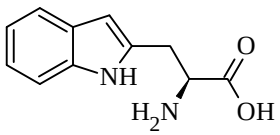

Figure **3.4**: Structure of tryptophan (**14**)

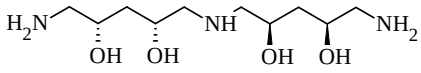

Pavettamine (**15**)

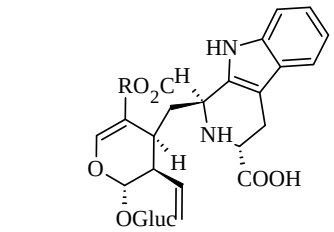

R = H, 5α-Carboxystrictosidinic acid (**16**)
R = CH_3, 5α-Carboxystrictosidine (**17**)

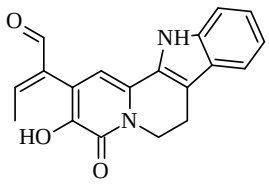

Latifoliaindole A (**24**)

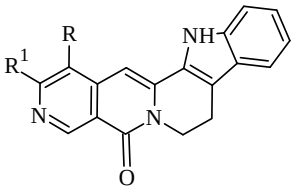

R=R[1]= H, Nauclefine (**18**)
R= $COCH_3$, R[1]= H, Naucletine (**19**)
R= $CHCH_2$, R[1]= H, Angustine (**20**)
R= (*S*)-$CH(OH)CH_3$, R[1]= H, Angustoline (**21**)
R= H, R[1]= CH_3, Angustidine (**22**)
R= (*S*)-$CH(OEt)CH_3$, R[1]= H, 19-*O*-Ethylangustoline (**23**)

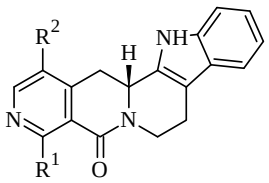

R[1]= H, R[2]= CH_3, Latifoliamide D (**26**)
R[1]= $COCH_3$, R[2]= $CH(OH)CH_3$,
Latifoliamide E (**27**)

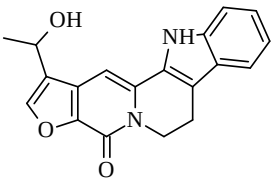

Latifoliaindole B (**25**)

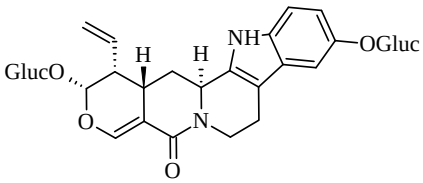

10-β-Glucosyloxyvincoside lactam (**28**)

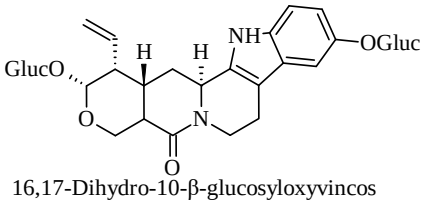

16,17-Dihydro-10-β-glucosyloxyvincos
ide lactam (**29**)

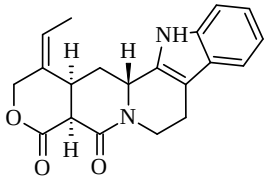

Pobeguinine (**31**)

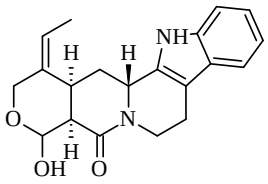

Naucleofficine D (**32**)

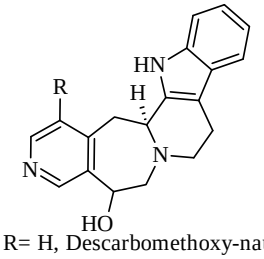

R= H, Descarbomethoxy-nauclechine (**33**)
R= CO_2CH_3, Nauclechine (**34**)

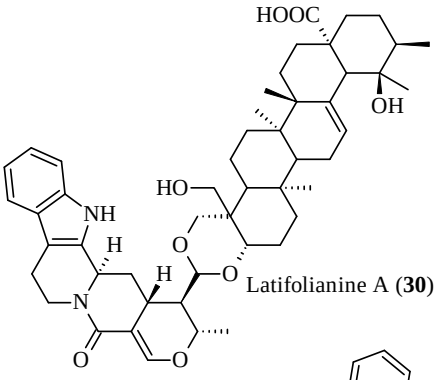

Latifolianine A (**30**)

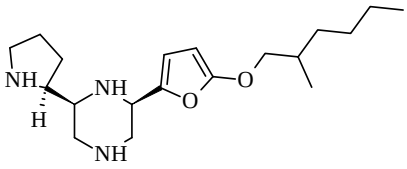

2-(7'-Methylhexyloxy)furan-
5'-yl)-6-(pyrrolidin7-yl)piperazine)(**35**)

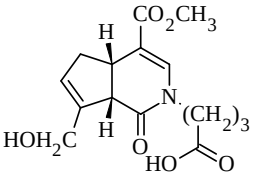

4-(2*N*-Gardenamide)*n*-butanoic acid (**36**)

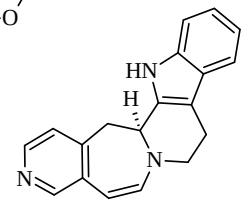

Naufoline (**37**)

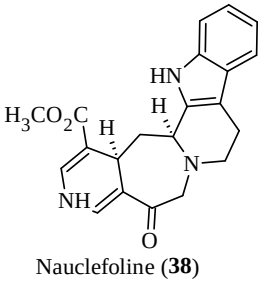

Nauclefoline (**38**)

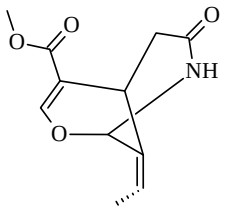

Floribundane A (**39**)

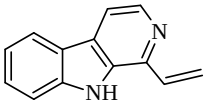

Pavettine (**40**)

Figure 3.4a: Structures of alkaloids isolated from southern African Rubiaceae

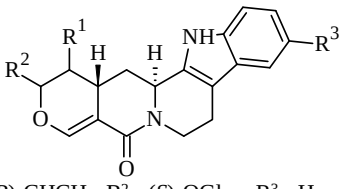

R^1= (*R*)-$CHCH_2$, R^2= (*S*)-OGluc, R^3= H, Strictosamide (**41**)
R^1= (*S*)-CHO, R^2= (*R*)-CH_3, R^3= H, Naucleidinal (**42**)
R^1= (*S*)-CHO, R^2= (*S*)-CH_3, R^3= H, 19-epi-Naucleidinal (**43**)
R^1= (*R*)-$CHCH_2$, R^2= (*S*)-OCH_3, R^3= H, 21-*O*-Methylstrictosamide aglycone (**44**)
R^1= (*R*)-$CHCH_2$, R^2= (*S*)-OCH_2CH_3, R^3= H, 21-*O*-Ethylstrictosamide aglycone (**45**)
R^1= (*R*)-$CHCH_2$, R^2= (*S*)-OGluc, R^3= OH, 10-Hydroxystrictosamide (**46**)

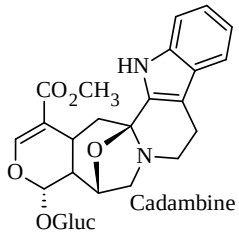

Cadambine (**47**)

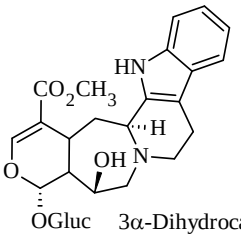

3α-Dihydrocadambine (**48**)

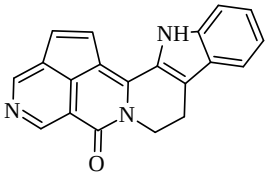

Naulafine (**49**)

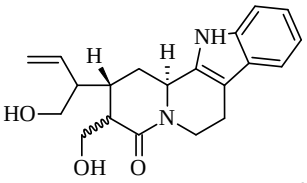

Naucleamide A (*R*) (**50**)
Naucleamide B (*S*) (**51**)

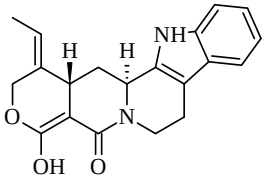

Naucleamide C (**52**)

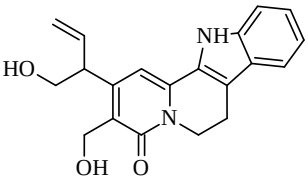

Naucleamide D (**53**)

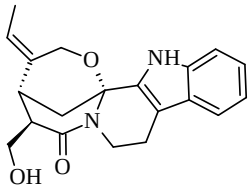

Naucleamide E (**54**)

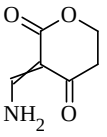

Gentiocrucine E/Z isomers (**55**)

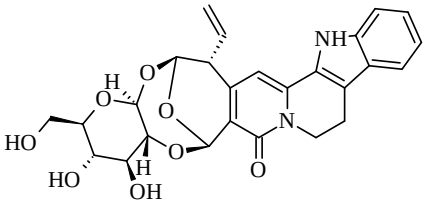

Naucleamide F (**56**)

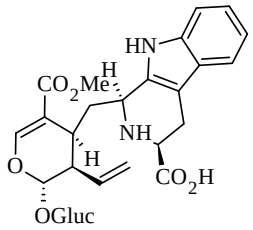

Tetrahydrodesoxycordifoline (**57**)

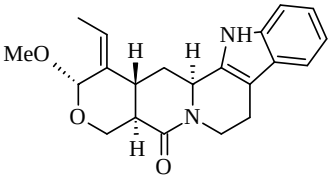

Nauclefolinine (**58**)

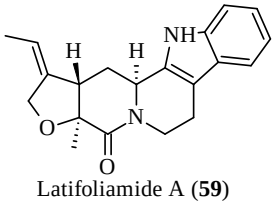

Latifoliamide A (**59**)

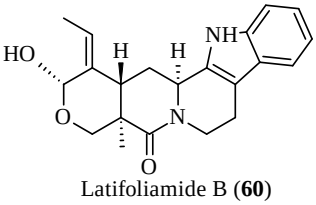

Latifoliamide B (**60**)

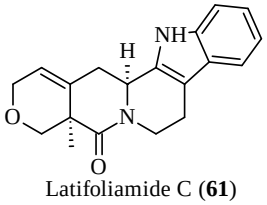

Latifoliamide C (**61**)

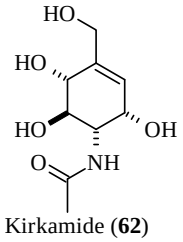

Kirkamide (**62**)

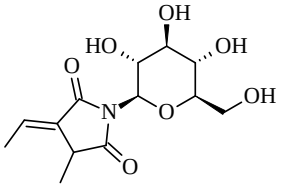

(E)-3-Ethylidene-4-methylpyrrolidine-2,5-dione *N*-β-D-glucopyranoside (**63**)

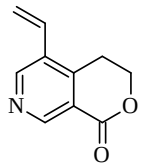

Gentianine (**64**)

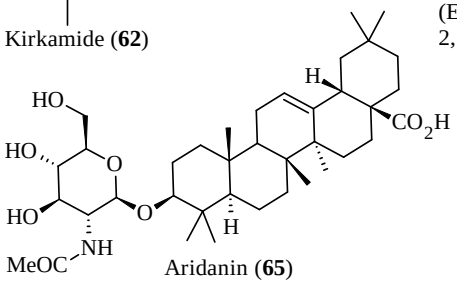

Aridanin (**65**)

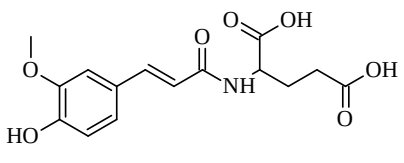

N-[4′-Hydroxy-3′-methoxy-(E)-cinnamoyl]-L-glutamic acid (**66**)

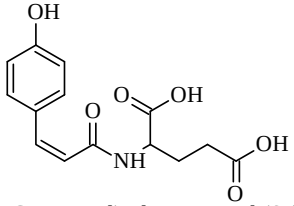

(Z)-*N*-(p-Coumaroyl)-glutamic acid (**67**)

Figure 3.4b: More alkaloids isolated from southern African Rubiaceae

3.5.3 Flavonoids

Flavonoids are phenolic natural compounds consisting of at least two phenyls linked via a six-membered ring or a two- or three-carbon chain. The basic structure of a flavonoid comprises three six-membered rings, A, B and C (Panche et al., 2016). The C ring is open in chalcones, as shown in Figure 3.5. Some basic types of flavonoids are shown in Figure 3.5.

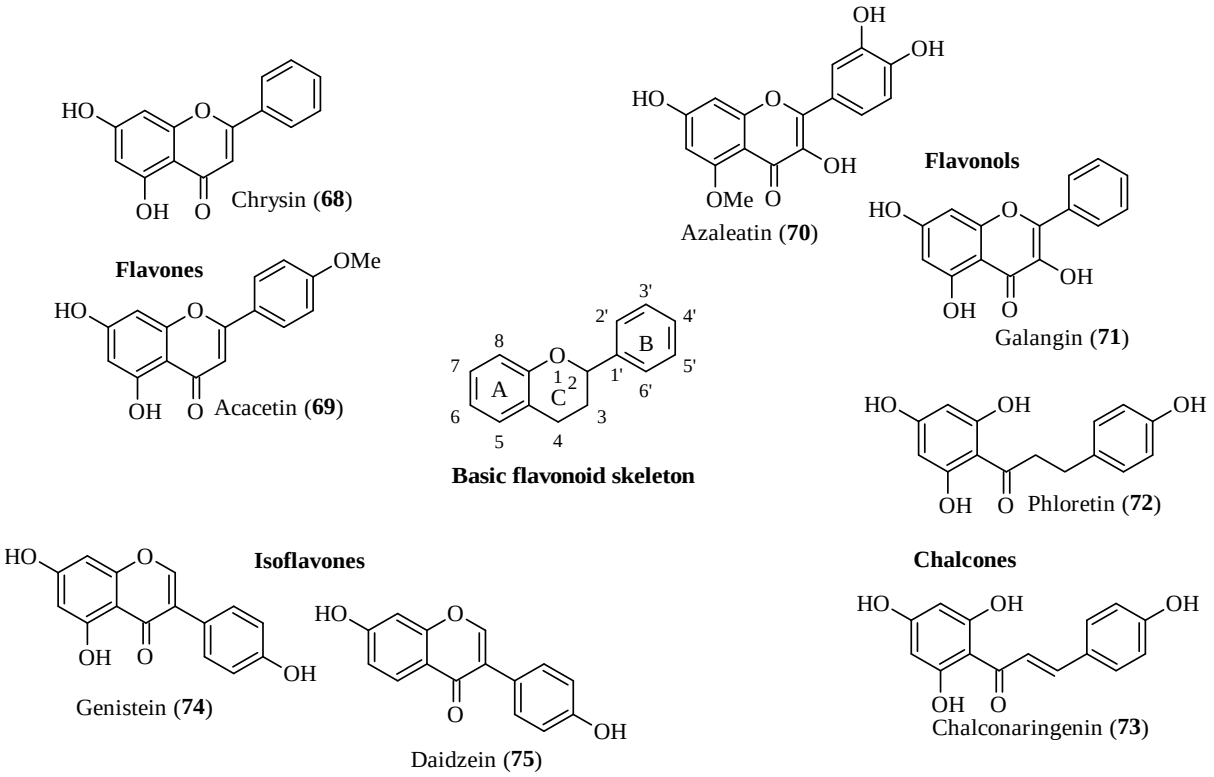

Figure 3.5. Basic structure of flavonoids

The biosynthesis of flavonoids occurs through the phenylpropanoid pathway utilising phenylalanine from the shikimate pathway. (Liu et al., 2021). Phenylalanine to *p*-coumaroyl-CoA via the action of three enzymes in the phenylpropanoid pathway. These enzymes are phenylalanine ammonia lyase, cinnamic acid 4-hydroxylase, and 4-coumarate: CoA ligase (Liu et al., 2021). *p*-Coumaroyl-CoA reacts with three equivalents of malonyl-CoA in the presence of chalcone synthase, producing naringenin chalcone. The biosynthesis of most flavonoids begins from the chalcone (Liu et al., 2021). The bioactivities of flavonoids include the inhibition of acetylcholinesterase by quercetin (**82**), rutin (**80**), and kaempferol 3-O-β-D-galactoside. This activity is essential in treating conditions like Alzheimer's disease, where an increase in acetylcholine levels improves symptoms (Panche et al., 2016). Thirty-one flavonoids isolated from southern Africa Rubiaceae are shown in Figure 3.6. The plants from which they have been isolated and the references are shown in Table 3.3.

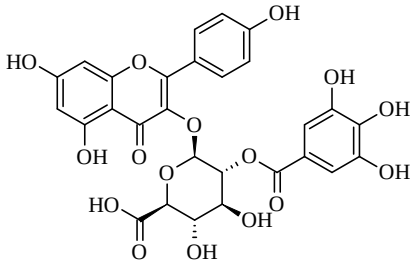

Kaemferol 3-*O*-(2″-*O*-galloyl)-glucuronide (**76**)

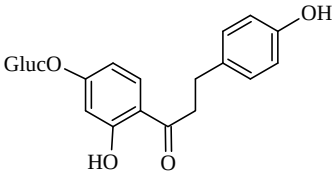

Confusoside (**77**)

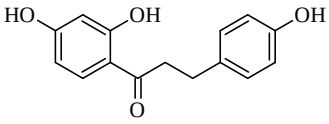

Davidigenin (**78**)

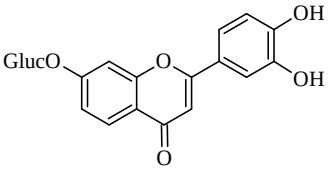

7-*O*-*β*-D-Glucopyranosyl-7,3′,4′-trihydroxyflavone (**79**)

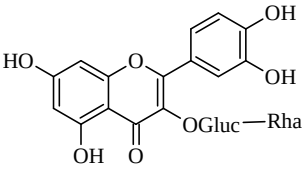

Rutin (**80**)

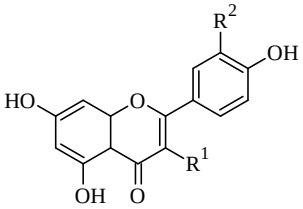

R^1 = OGluc R^2 = OH, Isoquercetin (**81**)

R^1 = OH, R^2 = OH, Quercetin (**82**)

R^1 = ORha, R^2 = H, Kaemferol 3-*O*-L-rhamnopyranoside (**83**)

R^1 =OGluc, R^2 = OMe, Isorhamnetin 3-*O*-glucopyranoside (**84**)

R^1 = ORha, R^2 =OH, Quercetin 3-*O*-L-rhamnopyranoside (**85**)

R^1 = ORutinose, R^2 = H (**86**)

R^1 = H, R^2 = OH, Luteolin (**87**)

R^1 = OGal, R^2 = OH, Hyperoside (**88**)

R^1 = OGluc, R^2 = H, Astragalin (**89**)

R^1= R^2= H, Apigenin (**90**)

R^1= OH, R^2= H, Kaemferol (**91**)

R^1= OH, R^2= OMe, Isorhamnetin (**92**)

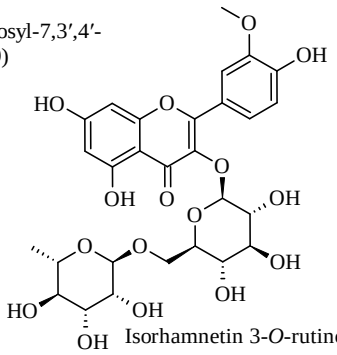

Isorhamnetin 3-*O*-rutinoside (**93**)

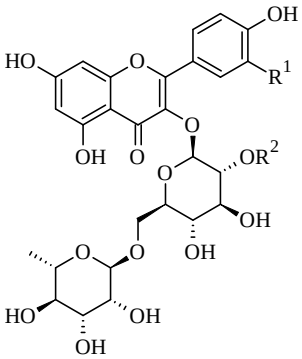

R^1=OH, R^2= Gluc, Quercetin 3-O-β-D-glucopyranosyl-(1→2)-[α-L-rhamnopyranosyl-(1→6)-β-D-glucopyranoside] (**94**)

R^1=H, R^2= Gluc, Kaempferol 3-O-β-D-glucopyranosyl- (1 → 2)-[α-L-rhamnopyranosyl-(1→6)]-β-D-glucopyranoside (**95**)

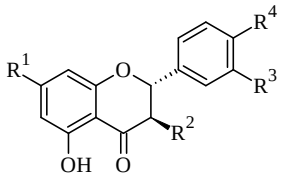

R^1= OMe, R^2= R^3= H, R^4= OH, 5,4′-Dihydroxy-7-methoxyflavanone (**96**)

R^1=R^4= OH, R^2= R^3= H, Naringenin (**97**)

R^1= R^2= R^3= R^4= OH, Taxifolin (**98**)

R^1=R^2= R^3= OH, R^4= OMe, Dihydroquercetin-4'-methyl ether (**99**)

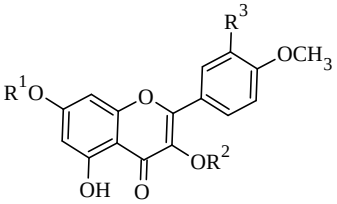

R^1 = CH_3 R^2 = H, R^3= OH, 3,5,3′-Trihydroxy-7,4′-dimethoxyflavone (**100**)

R^1 = H, R^2 = CH_3, R^3= OH, 5,7-Dihydroxy-3,4′-dimethoxyflavone (**101**)

R^1=R^2=R^3=H, 5,7-Trihydroxy-4'-methoxyflavone (**102**)

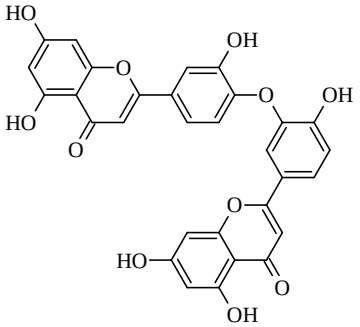

5,7,3',5'',7'',4'''-Hexahydroxy (4'-*O*-3''')-biflavone (**103**)

Figure 3.6. Flavonoids isolated from southern African Rubiaceae plants

3.5.4 Iridoids

Fifty-four iridoids were found to have been isolated from Rubiaceae plants found in southern Africa. Iridoids are monoterpenes whose structure is based on an iridane skeleton. They usually occur as a fused cyclopentane pyran ring system, as shown in Figure 3.7. Iridoids also occur in nature as secoiridoids in which the C7-C8 bond of the pentane ring is cleaved.

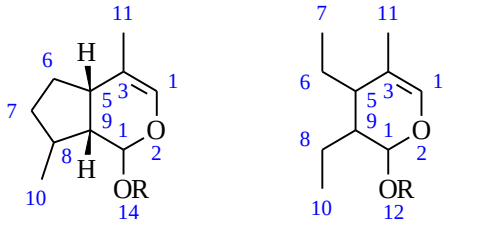

Iridoid skeleton Secoiridoid skeleton

Figure 3.7: The basic skeleton of iridoids

Studies on the biosynthetic pathway for manufacturing iridoids have been conducted on *Catharanthus roseus*. The following describes the published pathway for the production of loganic acid. Dimethylallyl pyrophosphate (DMAPP) reacts with isopentenyl pyrophosphate (IPP) in the presence of geranyl diphosphate synthase to produce geranyl diphosphate. Geraniol is formed from geranyl diphosphate through the action of geraniol synthase (Kouda and Yakushiji, 2020). This product is hydroxylated by geraniol-8-oxidase to form 8-hydroxygeraniol. An oxidation step is catalysed by geraniol-8-oxidase oxidoreductase forming 8-oxogeranial. Iridoid synthase generates an enol or enolate from 8-oxogeranial. The mechanism of the cyclisation of the pyran ring is thought to occur either via a Michael addition or Diels-Alder reaction (Kouda and Yakushiji, 2020). This step results in the formation of nepetalactone in equilibrium with iridodials. Nepetalactol is the basic unit from which loganic acid is formed via three enzymatic steps involving iridoid oxidase, 7-deoxyloganetic acid glucosyl transferase, and 7-deoxyloganic acid hydroxylase. To form secologanin, the carboxylic acid group is esterified by loganic acid *O*-methyl transferase. This step is followed by bond cleavage at position C-7 to form secologanin in the presence of secologanin synthase (Kouda and Yakushiji, 2020). A summarised biosynthetic pathway is presented in Scheme 3.2.

Iridoid bioactivities are varied. Investigation on an iridoid (oldenlandoside) isolated from *Oldenlandia diffusa* Roxb. revealed that the compound has antioxidant properties towards low-density lipoproteins (LDL) (Kim et al., 2005). Oxidised LDLs are thought to be proatherogenic

(Maiolino et al., 2013). Kim et al. (2005) suggests that oldenlandoside may have therapeutic potential for treating atherosclerosis.

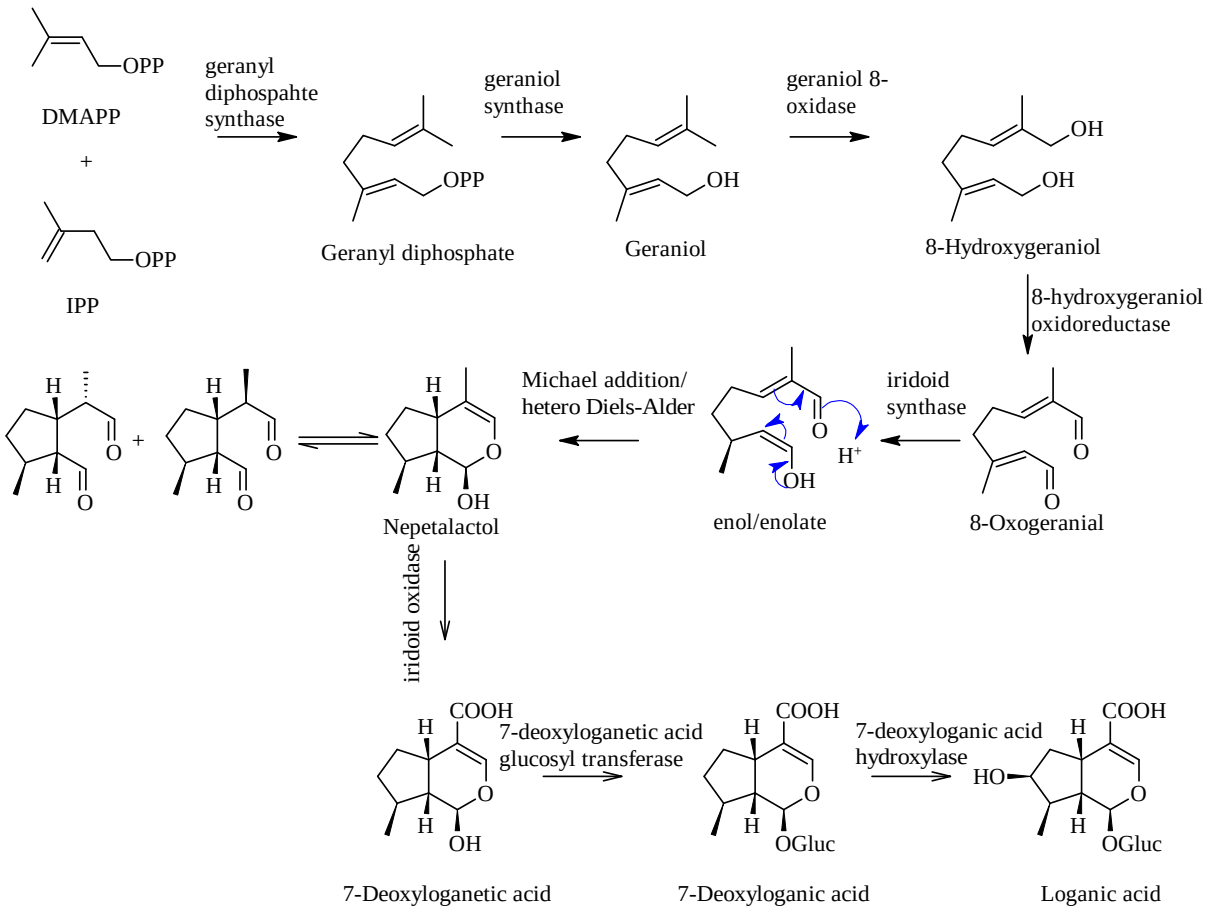

Scheme 3.2: The iridoid biosynthetic pathway for loganic acid (Kouda and Yakushiji, 2020)

The bioactivities of iridoids that have been reported include neuroprotective and hepatoprotective effects (Wang et al., 2020). Some iridoids can lower hyperglycaemia and hyperlipidaemia. These properties could be used in the development of medicines for diabetes and cardiovascular conditions (Wang et al., 2020). The iridoids isolated from southern African Rubiaceae are shown in Figures 3.8a and 3.8b. The plants from which they have been isolated and references are shown in Table 3.3.

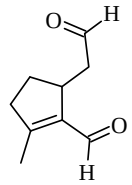

Rotundial (**104**)

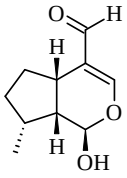

Boschnarol (**105**)

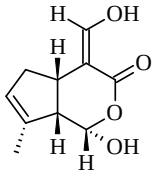

Amagnalactone (**106**)

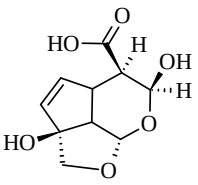

β-Gardiol (**107**)

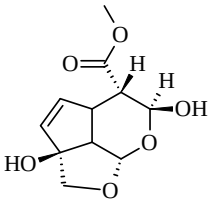

α-Gardiol (**108**)

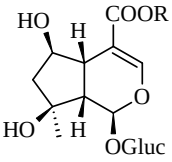

R=H, Shanzhiside (**109**)
R= CH_3, Shanzhiside methyl ester (**110**)

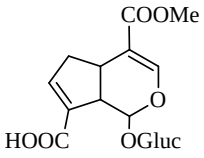

11-Methylixoside (**111**)

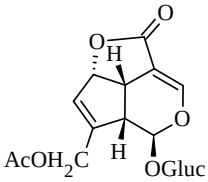

Asperuloside (**112**)

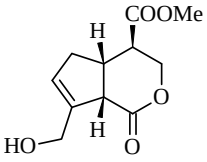

10-Hydroxy-1-oxo-7-iriden-11-oic acid methyl ester (**113**)

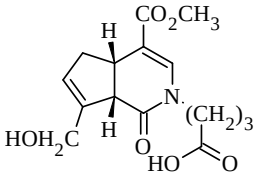

4-(2*N*-Gardenamide)*n*-butanoic acid (**36**)

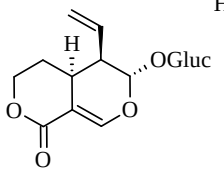

Sweroside (**114**)

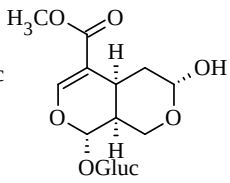

Morroniside (**115**)

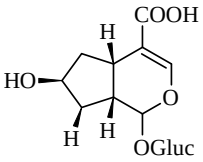

Loganic acid (**116**)

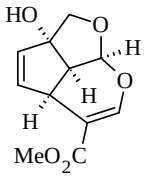

Garjasmine (**117**)

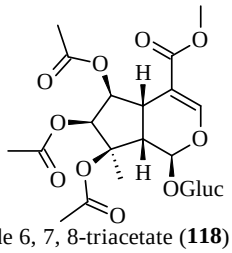

Lamalbide 6, 7, 8-triacetate (**118**)

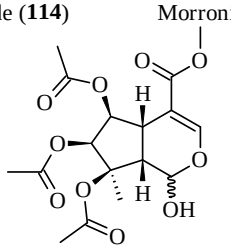

OH-1β, Lamiridosin A triacetate (**119**)
OH-1α, Lamiridosin B triacetate (**120**)

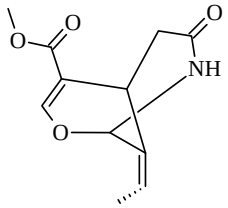

Floribundane A (**39**)

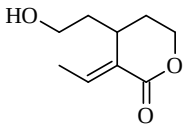

Floribundane B (**121**)

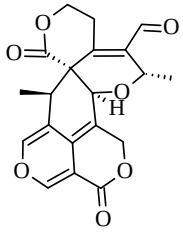

Mitragynoid (**122**)

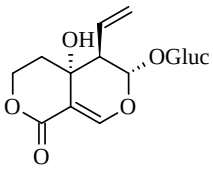

Swertiamarin (**123**)

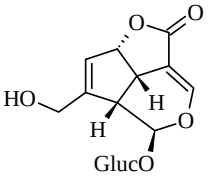

Deacetyl asperuloside (**124**)

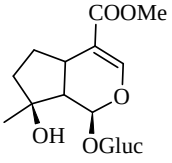

Mussaenoside (**125**)

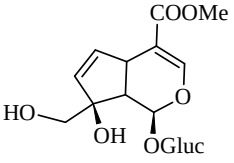

Gardenoside (**126**)

R=R^1=R^2=R^3=H, R^4= OGluc, Geniposidic acid (**127**)

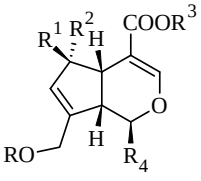

R=Ac, R^1=R^2=H, R^3=Me, R^4= OGluc, Asperulosidic acid methyl ester (**128**)
R=R^1=R^2=H, R^3=Me, R^4= OH, Genipin (**129**)
R=R^1=R^2=H, R^3=Me, R^4=O-gentibiose, Genipin gentibioside (**130**)
R= R^1= R^2= H, R^3= Me, R^4= OGluc, Geniposide (**131**)
R= R^1= H, R^2= OH, R^3= Me, R^4= OGluc, 6α-Hydroxygeniposide (**132**)
R= Ac, R^1= R^3= H, R^2= OH, R^4= OGluc, Asperulosidic acid (**133**)
R= R^2= H, R^1= OH, R^3= Me, R^4= OGluc, Scandoside methyl ester (**134**)
R= Benzoyl, R^1= OH, R^2= H, R^3= Me, R^4= OGluc, 10-O-Benzoylscandoside methyl ester (**135**)
R= *p*-benzoyl, R^1= OH, R^2= H, R^3= Me, R^4= OGluc, 10-O-*p*-Hydroxybenzoylscandoside methyl ester (**136**)
R= R^1= R^3= H, R^2= OH, R^4= OGluc, Deacetylasperulosidic acid (**137**)
R=Benzoyl, R^1=H, R^2= OH, R^3= Me, 10-*O*-Benzoyl deacetylapserulosidic acid methyl ester (**138**)
R= trans/cis Coumaroyl, R^1= OH, R^2= H, R^3= Me, 10-*O*-*p*-*trans*, *cis*-Coumaroyl scandoside methyl ester (**139**)

Figure 3.8a: Iridoids isolated from southern African Rubiaceae species

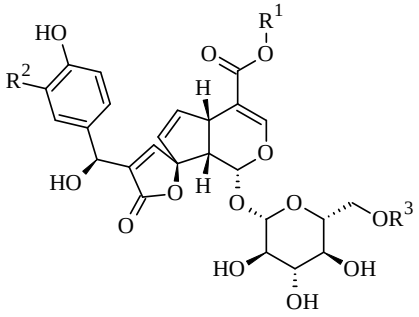

R^1=R^2=H, R^3=$COCH_3$, Acetylgaertneric acid (**140**)
R^1=CH_3, R^2=H, R^3=$COCH_3$, Acetylgaertneroside (**141**)
R^1=CH_3, R^2=H, R^3=H, Gaertneroside (**142**)
R^1=CH_3, R^2=OCH_3, R^3=H, Methoxygaertneroside (**143**)

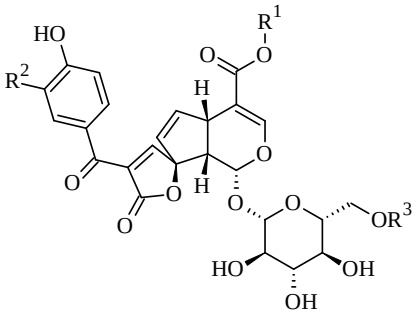

R^1=CH_3, R^2=H, R^3= $COCH_3$, Acetyldehydrogaertneroside (**144**)
R^1=CH_3, R^2=H, R^3= H, Dehydrogaertneroside (**145**)
R^1=CH_3, R^2=OCH_3, R^3= H, Dehydromethoxygaertneroside (**146**)
R^1=H, R^2=H, R^3= H, Dehydrogaertneric acid (**147**)

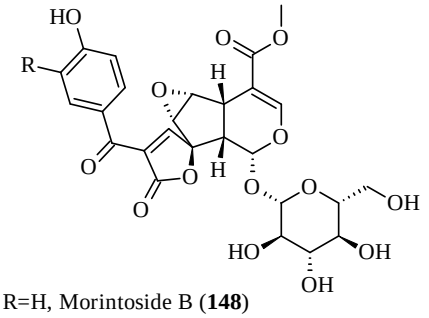

R=H, Morintoside B (**148**)
R= OCH_3, Dehydroepoxymethoxygaertneroside (**149**)

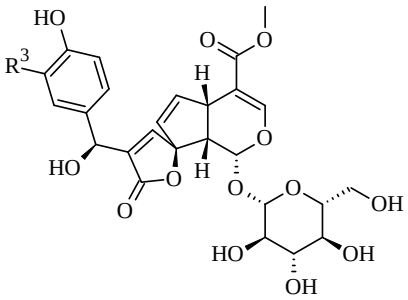

R=H, Epoxygaertneroside (**150**)
R=OCH_3, Epoxymethoxygaertneroside (**151**)

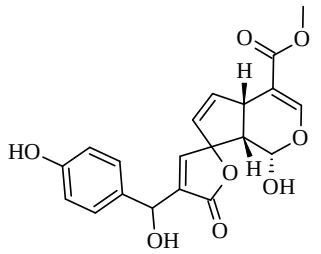

Deglucosyl gaertneroside (**152**)

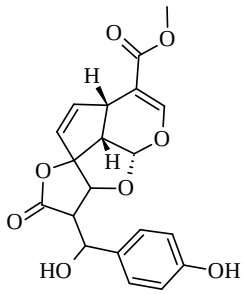

Morindoidin (**153**)

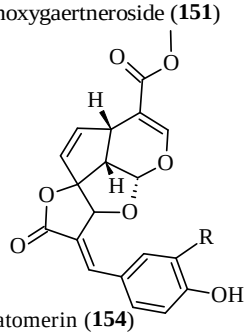

R=H, Prismatomerin (**154**)
R=OCH_3, Molucidin (**155**)

Figure 3.8b: Iridoids isolated from southern African Rubiaceae species

3.5.5 Triterpenes

Triterpenes are formed from the mevalonic acid pathway-derived isopentenyl diphosphate (IPP). A condensation reaction between IPP and dimethylallyl diphosphate in the presence of farnesyl pyrophosphate synthase forms farnesyl pyrophosphate (FPP) (Dhar et al., 2013). A two-step process involving the enzyme squalene synthase condenses two FPP units to form presqualene diphosphate (PSPP). In the second step, PSPP is reduced using NADPH to form squalene (Santana-Molina et al., 2020). Squalene is oxidised to 2,3-oxidosqualene by the enzyme squalene monooxygenase (Chua et al., 2020). This product is then cyclised by oxidosqualene cyclase (OSC) (Sawai and Saito, 2011).

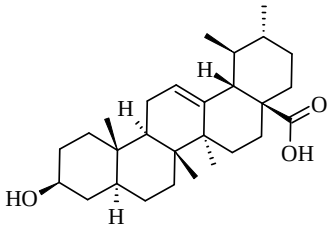

Ursolic acid (**156**)

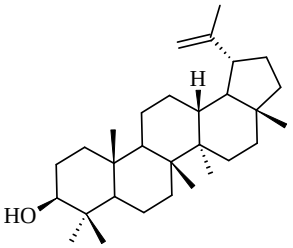

Lupeol (**157**)

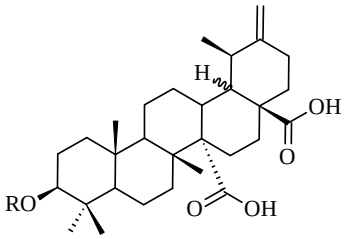

R= H; Epimers: 3β-urs-12,20(30)-diene-27,28-dioic acid, and its epimer at position 18 (**158**).
R= Glc, Glycosides of **158** (**159**)

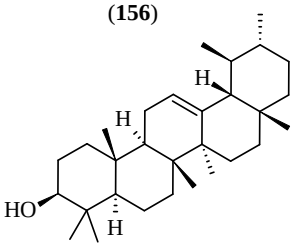

α-Amyrin (**160**)

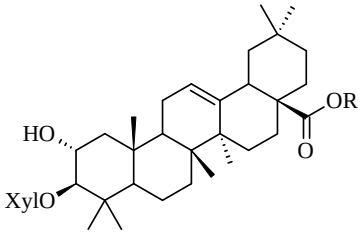

R= Gluc-(2→1)-Rha, Bodinioside Q (**161**)

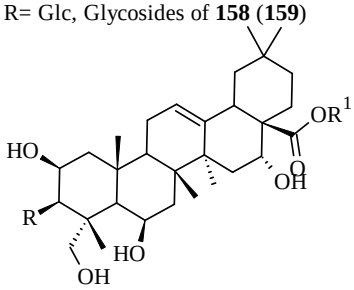

R= OGluc, R^1= Ara-(2→1)-Rha-(4→1)-Xyl-(3→1)-Rha (**162**)
R=OGluc-(3→1)-Api, R^1= Ara-(2→1)-Rha-(4→1)-Xyl-(3→1)-Rha (**163**)

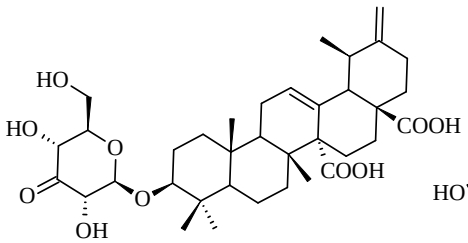

3-O-β–D-3-Oxo-glucopyranosyl-ursa-12 ,20(30)-diene-27,28-dioic acid (**164**)

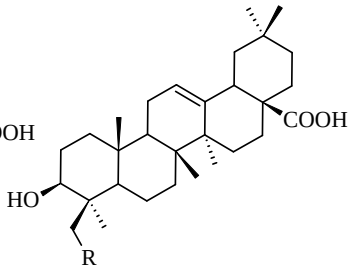

R=H, Oleanolic acid (**165**)
R=OH, Hederagenin (**166**)

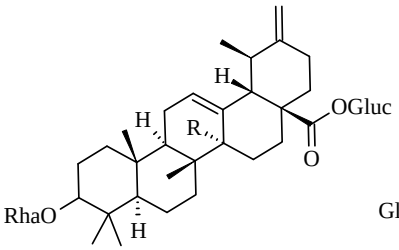

R=COOH (**167**)

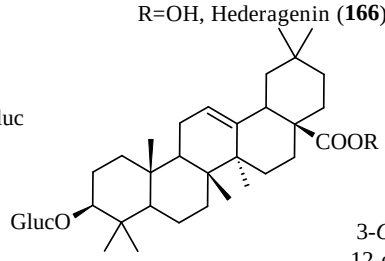

R= Gluc-(2→1)-Rha (**168**)
R= Gluc-(2→1)-Api (**169**)
R= Gluc-(2→1)-Gluc (**170**)

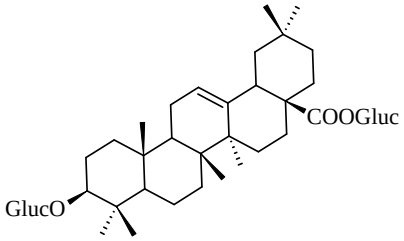

3-*O*-*β*-D-Glucopyranosyl-3*β*-hydroxyolean-12-en-28-oic acid 28-*O*-*β*-D-glucopyranoside (**171**)

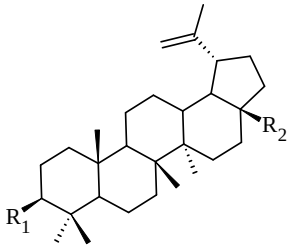

R_1= OH, R_2= COOH, Betulinic acid (**172**)
R_1= $CH_3(CH_2)_9H_2COO$, R_2= CHO, 3β-Dodecanoyllup-20(29)-en-28-al (**173**)
R_1= $CH_3(CH_2)_{13}H_2COO$, R_2= CH_3, Lup-20(29)-en-3β-ylhexadecanoate (**174**)

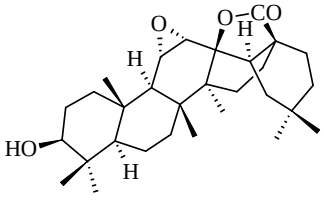

3β-Hydroxy-11α,12α-epoxyoleanan-28,13β-olide (**175**)

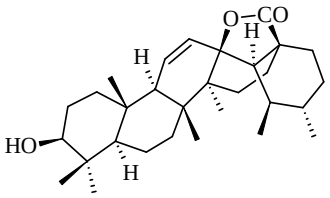

3β-Hydroxyurs-11-en-28,13β-olide (**176**)

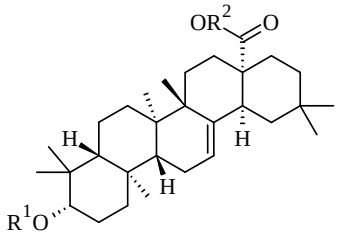

R^1 = Rha-(1→2)-Gluc, R^2 = Gluc (**177**)

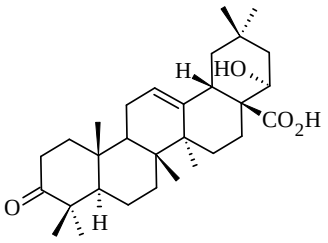

22α-Hydroxyoleanonic acid (**178**)

Figure 3.9a: Triterpenes isolated from southern African Rubiaceae species

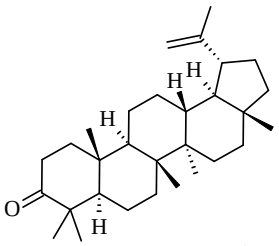

Lupenone (**179**)

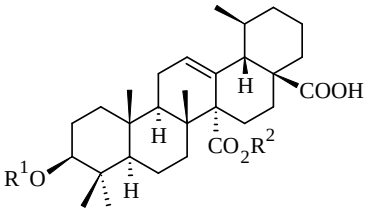

R^1 = H, R^2 = H, Quinovic acid (**180**)
R^1 = Gluc, R^2 = H, Quinovic acid 3-*O*-[-D-glucopyranoside] (**181**)
R^1 = Gluc, R^2 = Gluc, Quinovic acid 3-*O*-[-D-quinovopyranoside]-27-*O*-[-D-glucopyranosyl] ester (**182**)

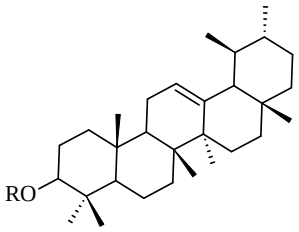

R= α-Rhamnose, Quinovic acid-3-*O*-β-rhamnosylpyranoside (**183**)
R= β-Fucose, Quinovic acid 3-*O*-β-fucosylpyranoside (**184**)

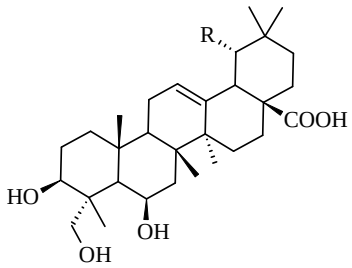

R= H, 3β,6β,19α,23-Tetrahydroxyolean-12-en-28-oic acid (**185**)
R= OH, 3β,6β,19α,23-Tetrahydroxyolean-12-en-28-oic acid (**186**)

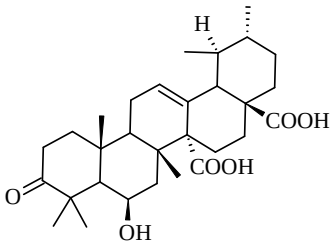

Quafrinoic acid (**187**)

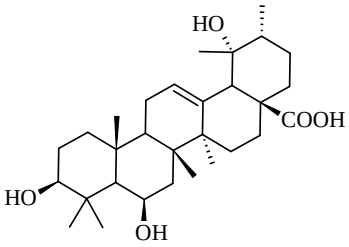

Pomolic acid (**188**)

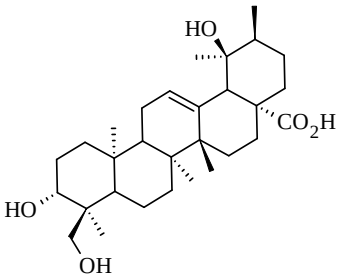

Rotundic acid (**189**)

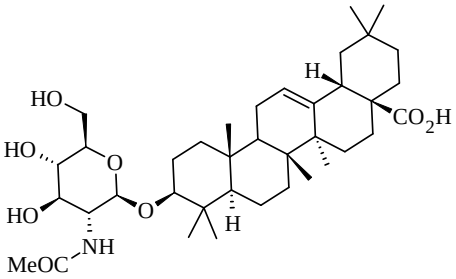

Aridanin (**190**)

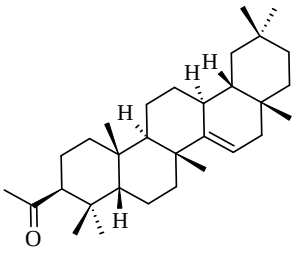

R= Ac, Taraxeryl acetate (**191**)

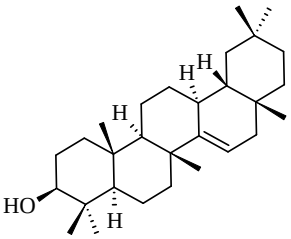

R= OH, Taraxerol (**192**)

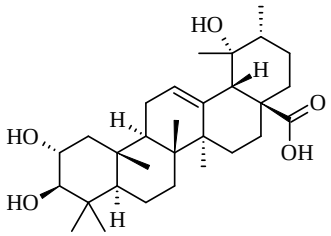

Tormentic acid (**193**)

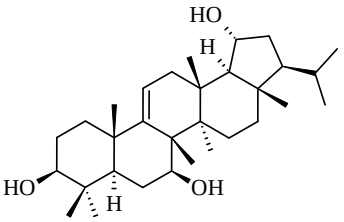

Rubiarbonol B (**194**)

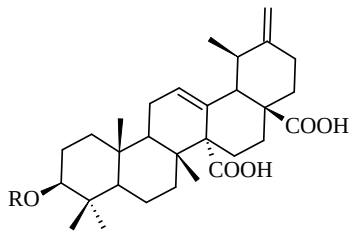

R= H, Ursa-12,20(30)-diene-27,28-dioic acid (**195**)
R= Gluc, 3β-D-Glucopyranosyl-ursa12,20(30)-diene-27,28-dioic acid (**196**)

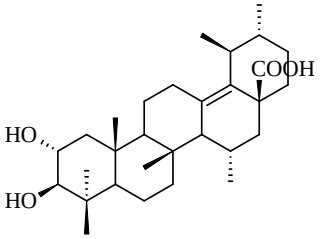

Corosolic acid (**197**)

Figure 3.9b: Triterpenes isolated from southern African Rubiaceae species

The action of enzymes results in the production of triterpenes. For example, oxidosqualene is converted to β-amyrin by β-amyrin synthase (Kushiro et al., 1998).

The reported bioactivities of triterpenes include their ability to act as immunomodulators, anti-microbial, anti-HIV, anti-tumour, anti-inflammatory and anti-oxidant agents. Other pharmacological properties of triterpenoids are hepatoprotective and antiatherosclerotic (Renda et al., 2022). The triterpenoid oleanolic acid (**165**) has been shown to stimulate the proliferation of T-cells, while ursolic acid (**156**) and betulinic acid (**172**) inhibit the process. These effects show the potential of this class of compounds to act as immunomodulators (Renda et al., 2022). In vivo studies on rats and mice involving lupeol (**157**) have shown its capacity to act as an anti-inflammatory agent. While lupeol (**157**) did not show analgesic activity, it was able to reduce carrageenin-induced oedema. At a dosage of 100 mg/kg, the anti-inflammatory activity of lupeol (**157**) in a chronic arthritic model was comparable to the activity of acetylsalicylic acid (Patocka, 2003). Investigations on the anti-tumour effects of betulinic acid (**172**) suggest that it is active against melanoma and neuroblastoma cells (Patocka, 2003). The terpenoids isolated from southern African Rubiaceae are shown in Figures 3.9a and 3.9b. The plants from which they have been isolated, together with references, are shown in Table 3.3.

3.5.6 Cyclotides

Cyclotides are a class of macrocyclic proteins consisting of 28 to 37 amino acids. The amino acid chain forms a cyclised head-to-tail backbone. Six cysteine residues provide disulphide bridges that keep the cyclic cystine knot (CCK) motif described by (Craik et al., 1999). The CCK motif of cyclotides makes them exceptionally stable (Daly et al., 2009). Research into cyclotides has grown since the discovery of the first known cyclotide from extracts of Congolese *Oldenlandia affinis* in 1970. The decoctions had been used to facilitate child birth in pregnant women. The uterotonic agent was shown to be a peptide that was then named Kalata B1. Between 1997 and 1999 a series of experiments described methods for the production of synthetic cyclotides. More cyclotides have been isolated from other plants including plants in the families of the Violaceae, Fabaceae, Cucurbitaceae, and Solanaceae as mentioned earlier. Additionally, the known pharmacoactivities of cyclotide have expanded.

Investigations conducted at the United States Cancer Institute involved screening *Chassalia parvifolia* (Rubiaceae) extracts for anti-viral activities led to the isolation of two circular peptides (Gustafson et al., 1994). These cyclotides exhibited concentration dependant

cytoprotective activity parallel to a decrease in the HIV p24 antigen. In another study involving another Rubiaceae plant, *Psychotria longipes*, an isolated cyclotide inhibited the binding of neurotensin to HT-29 tumour cell lines (Witherup et al., 1994). This activity is significant for potential anti-cancer therapies because of the role of neurotensin in promoting cancer progression (Christou et al., 2020; Takahashi et al., 2021).

This review found six cyclotides that have all been isolated from *Oldenlandia affinis*. Their amino acid sequences are shown in Table 3.4.

Table 3.4: Cyclotides isolated from *Oldenlandia affinis*

	Loop 1	Loop 2	Loop 3	Loop 4	Loop 5	Loop 6
Kalata B1 (**198**)	CGET	CVGGT	CNT--PG	CT	C-SWPV	CTRNG-LPV
Kalata B2 (**199**)	CGET	CGGGT	CNT--PG	CS	C-TWPI	CTRDG-LPV
Kalata B3 (**200**)	CGET	CFGGT	CNT--PG	CT	CDPWPI	CTRDG-LPT
Kalata B4 (**201**)	CGET	CVGGT	CNT--PG	CT	C-SWPV	CTRDG-LPV
Kalata B5 (**202**)	CGES	CVYIP	CISGVIG	CS	CTD-KV	CYLNG-TP-
Kalata S (**203**)	CGET	CVGGT	CNT--PG	CS	C-SWPV	CTRNG-LPV

3.5.7 Other classes of compounds

Four phytosterols, four cyanogenic glycosides, and seven lignans are among the compounds isolated from Rubiaceae plants found in southern Africa. 31 Compounds, including five anthraquinones, were not placed in their unique classes. Figure 3.10 shows the phytosterols isolated from southern African Rubiaceae. The plants from which they have been isolated, together with references, are shown in Table 3.3.

In vitro studies have shown that the phytosterol stigmasterol has immunomodulatory activities and inhibits cytokines and other inflammatory indices associated with osteoarthritis (Gabay et al., 2010). Other studies have demonstrated stigmasterol's anti-microbial, anti-cancer, and neuroprotective effects (Bakrim et al., 2022). Some steroidal saponins have been shown to inhibit PEG_2, COX-2, and macrophages and modulate TNF-α and IL-6 (Passos et al., 2022).

Asteroidal saponin whose anti-inflammatory potential has been investigated is 25(*R, S*)-ruscogenin-1-O- [β-D-glucopyranosyl- (1→2)] [β-D-xylopyranosyl-(1→3)]-β-D fucopyranoside, known as DT-13. It has been found in *Ophiopogon japonicus* and *Liriope muscari*. Tests on mice with TNF-α induced vascular endothelial inflammation show that DT-13 reduces the levels of pro-inflammatory cytokines IL-8 and MCP-1 (Passos et al., 2022).

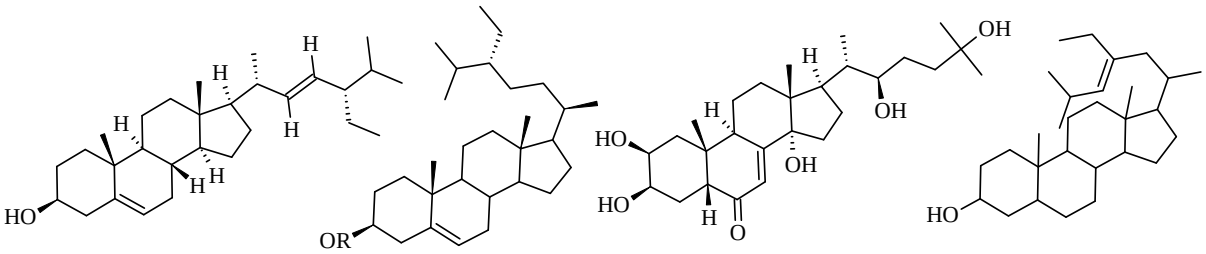

Stigmasterol (**204**)

R=H, β-Sitosterol (**205**)
R=Gluc, β–Sitosterol-3-*O*-β–D-glucopyranoside (**206**)

Ecdysone (**207**)

23-Ethyl-cholest-23-en-3-ol (**208**)

Figure 3.10: Phytosterols isolated from southern African Rubiaceae

The bioregulatory potential of cyanogenic glycosides has been examined in some studies (MichalcovÃ et al., 2016). The anti-inflammatory potential of amygdalin has been demonstrated by its inhibitory activity on Cyclooxygenase enzymes (Figurová et al., 2021). The lignan syringaresinol has been shown to promote apoptosis of the human leukaemia (HL-60) cell line (Park et al., 2008). Anthraquinone derivatives have pharmacological activities that include anti-cancer, anti-microbial, anti-inflammatory and neuroprotective properties (Malik and Müller, 2016). Figures 3.11 and 3.12 show cyanogenic compounds and lignans, respectively, that have been isolated from southern African Rubiaceae. The plants from which they have been isolated, together with references, are shown in Table 3.3.

Other isolated and reported compounds are placed in the Appendix.

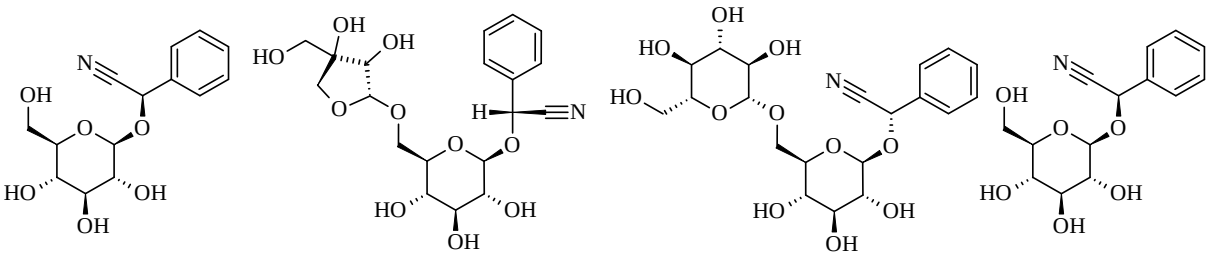

Prunasin (**209**) Oxyanthin (**210**) Amygdalin (**211**) Holocalin (**212**)

Figure 3.11: Cyanogenic glycosides isolated from southern African Rubiaceae species

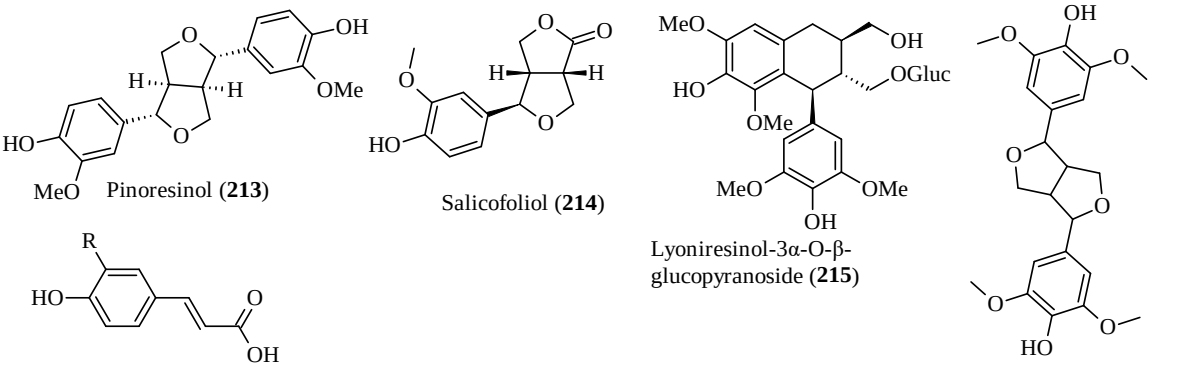

Figure 3.12: Lignans isolated from southern African Rubiaceae

3.6 Conclusion

Southern African Rubiaceae have numerous recorded ethnopharmacological uses, bioactivities and pharmacologically active compounds. The family can provide researchers with alternative therapies for various diseases. Research on the family is still less than ideal as some known medicinal plants have not been bio-assayed, and some biologically active extracts still need to undergo phytochemical identification.

3.7 References

Abdalla, M.A., Aro, A.O., Gado, D., Passari, A.K., Mishra, V.K., Singh, B.P., McGaw, L.J., 2020. Isolation of endophytic fungi from South African plants, and screening for their antimicrobial and extracellular enzymatic activities and presence of type I polyketide synthases. South African Journal of Botany 134, 336-342.

Abdillahi, H.S., Van Staden, J., 2012. South African plants and male reproductive healthcare: Conception and contraception. Journal of Ethnopharmacology 143, 475-480.

African Plant Database. Conservatoire et Jardin botaniques de la Ville de Genève and South African National Biodiversity Institute, Geneva and Pretoria

Agomuoh, A.A., Ata, A., Udenigwe, C.C., Aluko, R.E., Irenus, I., 2013. Novel indole alkaloids from *Nauclea latifolia* and their renin-inhibitory activities. Chemistry & Biodiversity 10, 401-410.

Ajao, A.A., Sibiya, N.P., Moteetee, A.N., 2019. Sexual prowess from nature: A systematic review of medicinal plants used as aphrodisiacs and sexual dysfunction in sub-Saharan Africa. South African Journal of Botany 122, 342-359.

Akah, P.A., Orisakwe, O.E., Gamaniel, K.S., Shittu, A., 1998. Evaluation of Nigerian traditional medicines: II. effects of some Nigerian folk remedies on peptic ulcer. Journal of Ethnopharmacology 62, 123-127.

Al Bashera, M., Mosaddik, A., El-Saber Batiha, G., Alqarni, M., Islam, M.A., Zouganelis, G.D., Alexiou, A., Zahan, R., 2021. In Vivo and In Vitro Evaluation of Preventive Activity of Inflammation and Free Radical Scavenging Potential of Plant Extracts from *Oldenlandia corymbosa* L. Applied Sciences 11, 9073.

Amoo, S.O., Ndhlala, A.R., Finnie, J.F., Van Staden, J., 2009. Antibacterial, antifungal and anti-inflammatory properties of *Burchellia bubalina*. South African Journal of Botany 75, 60-63.

Amusan, O.O., 2009. Some ethnoremedies used for HIV/AIDS and related diseases in Swaziland. The African Journal of Plant Science and Biotechnology 3, 20-26.

Amusan, O.O., Dlamini, P.S., Msonthi, J.D., Makhubu, L.P., 2002. Some herbal remedies from Manzini region of Swaziland. Journal of Ethnopharmacology 79, 109-112.

Amusan, O.O., Sukati, N.A., Dlamini, P.S., Sibandze, F.G., 2007. Some Swazi phytomedicines and their constituents. African Journal of Biotechnology 6, 267-272.

Amusan, O.O., Sukati, N.A., Shongwe, M.S., 2005. Some phytomedicines from Shiselweni region of Swaziland. Journal of Natural Remedies 5, 19-25.

Aragaw, T.J., Afework, D.T., Getahun, K.A., 2020. Antimalarial activities of hydromethanolic crude extract and chloroform fraction of *Gardenia ternifolia* leaves in *Plasmodium berghei* infected mice. Evidence-Based Complementary and Alternative Medicine 2020, 1-11.

Archana, V., Thomas, N.N., Lakshmi, S., Rauf, A.A., Edwin, B.T., 2021. Pharmaceutical properties of *Oldenlandia corymbosa* Linn. Materials Today: Proceedings 41, 698-702.

Aristide, B., Paul, S., Favier, L., Hauchard, D., Guegan, J., Neol, N., 2021. Chemical constituents of *Crossopteryx febrifuga* (Afzel ex G. Don) Benth (Rubiaceae), their phytotoxicity and antioxidant activities. Natural Products Chemistry and Research 9, 1-9.

Arnold, H.-J., Gulumian, M., 1984. Pharmacopoeia of traditional medicine in Venda. Journal of Ethnopharmacology 12, 35-74.

Aro, A.O., Dzoyem, J.P., Awouafack, M.D., Selepe, M.A., Eloff, J.N., McGaw, L.J., 2019. Fractions and isolated compounds from *Oxyanthus speciosus* subsp. *stenocarpus* (Rubiaceae) have promising antimycobacterial and intracellular activity. BMC complementary and alternative medicine 19, 1-11.

Aro, A.O., Dzoyem, J.P., Eloff, J.N., McGaw, L.J., 2016. Extracts of six Rubiaceae species combined with rifampicin have good in vitro synergistic antimycobacterial activity and good anti-inflammatory and antioxidant activities. BMC complementary and alternative medicine 16, 1-8.

Aro, A.O., Dzoyem, J.P., Goddard, A., Fonteh, P., Kayoka-Kabongo, P.N., McGaw, L.J., 2019. In vitro Antimycobacterial, Apoptosis-Inducing Potential, and Immunomodulatory Activity of Some Rubiaceae Species. FRONTIERS IN PHARMACOLOGY 10, 185.

Aro, A.O., Dzoyem, J.P., Hlokwe, T.M., Madoroba, E., Eloff, J.N., McGaw, L.J., 2015. Some South African Rubiaceae tree leaf extracts have antimycobacterial activity against pathogenic and non-pathogenic mycobacterium species. Phytotherapy Research 29, 1004-1010.

Aro, A.O., Famuyide, I.M., Oyagbemi, A.A., Kabongo-Kayoka, P.N., McGaw, L.J., 2022. In vitro potential of the acetone leaf extract and fractions of *Psychotria capensis* (Eckl.) Vatke (Rubiaceae) to combat co-infection of tuberculosis and helminthiasis. FRONTIERS IN PHARMACOLOGY 12, 744137.

Asowata-Ayodele, A.M., Afolayan, A.J., Otunola, G.A., 2016. Ethnobotanical survey of culinary herbs and spices used in the traditional medicinal system of Nkonkobe Municipality, Eastern Cape, South Africa. South African Journal of Botany 104, 69-75.

Aston Philander, L., 2011. An ethnobotany of Western Cape Rasta bush medicine. Journal of Ethnopharmacology 138, 578-594.

Ata, A., Udenigwe, C.C., Matochko, W., Holloway, P., Eze, M.O., Uzoegwu, P.N., 2009. Chemical constituents of *Nauclea latifolia* and their anti-GST and anti-fungal activities. Natural Product Communications 4, 1185-1188.

Atawodi, S.E.-O., Yusufu, S., Onoja, E., Idakwo, P., Olubodun, M., Yaya, H., Muhammad, S.D., 2015. Antioxidant status, organ integrity and lipid profile of carbon tetrachloride intoxicated rats following pre-treatment with methanolic extract of *Crossopteryx febrifuga* Benth leaf. Annual Research & Review in Biology, 501-511.

Auditeau, E., Chassagne, F., Bourdy, G., Bounlu, M., Jost, J., Luna, J., Ratsimbazafy, V., Preux, P.-M., Boumediene, F., 2019. Herbal medicine for epilepsy seizures in Asia, Africa and Latin America: A systematic review. Journal of Ethnopharmacology 234, 119-153.

Augustino, S., Hall, J.B., Makonda, F.B., Ishengoma, R.C., 2011. Medicinal resources of the Miombo woodlands of Urumwa, Tanzania: Plants and its uses. Journal of Medicinal Plants Research 5, 6352-6372.

Awas, E., Omosa, L., Midiwo, J., Ndakala, A., Mwanik, J., 2016. Antioxidant activities of flavonoid aglycones from Kenyan *Gardenia ternifolia* Schum and Thonn. Journal of Pharmacy and Biological Sciences 11, 136-141.

Babady, B., Ngalamulume, T., Kilonda, A., Toppet, S., Compernolle, F., Hoornaert, G., 1991. An ursadienedioic acid glycoside from *Crossopteryx febrifuga*. Phytochemistry 30, 3069-3072.

Bajpai, A., Jackson, M.A., Huang, Y.-H., Yap, K., Du, Q., Chau, T.C.-Y., Craik, D.J., Gilding, E.K., 2023. Nematicidal activity of cyclotides: toxicity against *Caenorhabditis elegans*. Journal of Natural Products 86, 1222-1229.

Bakrim, S., Benkhaira, N., Bourais, I., Benali, T., Lee, L.-H., El Omari, N., Sheikh, R.A., Goh, K.W., Ming, L.C., Bouyahya, A., 2022. Health benefits and pharmacological properties of stigmasterol. Antioxidants 11, 1912.

Balogun, F.O., Ashafa, A.O.T., 2019. A review of plants used in South African traditional medicine for the management and treatment of hypertension. Planta medica 85, 312-334.

Bapela, M.J., Meyer, J.J.M., Kaiser, M., 2014. In vitro antiplasmodial screening of ethnopharmacologically selected South African plant species used for the treatment of malaria. Journal of Ethnopharmacology 156, 370-373.

Barbosa, F., Hlashwayo, D., Sevastyanov, V., Chichava, V., Mataveia, A., Boane, E., Cala, A., 2020. Medicinal plants sold for treatment of bacterial and parasitic diseases in humans in Maputo city markets, Mozambique. BMC Complementary Medicine and Therapies 20, 1-13.

Begum, S., Munissi, J.J., Buriyo, A.S., Makangara, J.J., Lucantoni, L., Avery, V.M., Erdelyi, M., Nyandoro, S.S., 2020. Antiplasmodial, antimicrobial and cytotoxic activities of extracts from selected medicinal plants growing in Tanzania. Journal of Biologically Active Products from Nature 10, 165-176.

Behar, S.M., Divangahi, M., Remold, H.G., 2010. Evasion of innate immunity by *Mycobacterium tuberculosis*: is death an exit strategy? Nature Reviews Microbiology 8, 668-674.

Bode, M.L., Gates, P.J., Gebretnsae, S.Y., Vleggaar, R., 2010. Structure elucidation and stereoselective total synthesis of pavettamine, the causal agent of gousiekte. Tetrahedron 66, 2026-2036.

Borges, C.M., Diakanawma, C., de Mendonça, D.I., 2010. Iridoids from *Hymenodictyon floribundum*. Journal of the Brazilian Chemical Society 21, 1121-1125.

Botha, C.J., Penrith, M.L., 2008. Poisonous plants of veterinary and human importance in southern Africa. Journal of Ethnopharmacology 119, 549-558.

Boucherle, B., Haudecoeur, R., Queiroz, E.F., De Waard, M., Wolfender, J.-L., Robins, R.J., Boumendjel, A., 2016. *Nauclea latifolia*: biological activity and alkaloid phytochemistry of a west African tree. Natural Product Reports 33, 1034-1043.

Broaddus, V.C., Light, R.W., 2016. 79 - Pleural Effusion, in: Broaddus, V.C., Mason, R.J., Ernst, J.D., King, T.E., Lazarus, S.C., Murray, J.F., Nadel, J.A., Slutsky, A.S., Gotway, M.B. (Eds.), Murray and Nadel's Textbook of Respiratory Medicine (Sixth Edition). W.B. Saunders, Philadelphia, pp. 1396-1424.e1310.

Bruschi, P., Morganti, M., Mancini, M., Signorini, M.A., 2011. Traditional healers and laypeople: A qualitative and quantitative approach to local knowledge on medicinal plants in Muda (Mozambique). Journal of Ethnopharmacology 138, 543-563.

Bundschuh, T.V., Hahn, K., Wittig, R., 2011. The medicinal plants of the woodlands in northern Malawi (Karonga district). Flora et Vegetatio Sudano-Sambesica 14, 3-8.

Cai, W.-H., Matsunami, K., Otsuka, H., Shinzato, T., Takeda, Y., 2011. A glycerol α-d-glucuronide and a megastigmane glycoside from the leaves of *Guettarda speciosa* L. Journal of Natural Medicines 65, 364-369.

Cakupewa, M.F., Mukeba, F.B., Mulonda, A.B., Mokoso, J., Idrissa, A., 2022. Antibacterial activities of 13 medicinal plants used against infectious and parasitic diseases in Kinshasa and its surroundings, DR Congo. International Journal of Biological and Pharmaceutical Sciences Archive 3, 039-047.

Chan, S.M., Khoo, K.S., Sekaran, S.D., Sit, N.W., 2021. Mode-dependent antiviral activity of medicinal plant extracts against the mosquito-borne chikungunya virus. Plants 10, 1658.

Cheikhyoussef, A., Shapi, M., Matengu, K., Mu Ashekele, H., 2011. Ethnobotanical study of indigenous knowledge on medicinal plant use by traditional healers in Oshikoto region, Namibia. Journal of ethnobiology and ethnomedicine 7, 1-11.

Chhabra, S.C., Mahunnah, R., 1994. Plants used in traditional medicine by Hayas of the Kagera region, Tanzania. Economic Botany, 121-129.

Chhabra, S.C., Mahunnah, R.L.A., Mshiu, E.N., 1991. Plants used in traditional medicine in eastern Tanzania. V. Angiosperms (Passifloraceae to Sapindaceae). Journal of Ethnopharmacology 33, 143-157.

Chinsembu, K.C., Hedimbi, M., 2010. An ethnobotanical survey of plants used to manage HIV/AIDS opportunistic infections in Katima Mulilo, Caprivi region, Namibia. Journal of ethnobiology and ethnomedicine 6, 1-9.

Chouna, J.R., Tamokou, J.-d.-D., Nkeng-Efouet-Alango, P., Lenta, B.N., Sewald, N., 2015. Antimicrobial triterpenes from the stem bark of *Crossopteryx febrifuga*. Zeitschrift für Naturforschung C 70, 169-173.

Christopher, R., Msonga, A., Hoppe, H.C., Boyom, F.F., 2023. Ethanol extracts from selected Tanzanian Medicinal Plants selectively inhibit *Plasmodium falciparum* growth in vitro. Tanzania Journal of Science 49, 41-47.

Christou, N., Blondy, S., David, V., Verdier, M., Lalloué, F., Jauberteau, M.-O., Mathonnet, M., Perraud, A., 2020. Neurotensin pathway in digestive cancers and clinical applications: an overview. Cell Death & Disease 11, 1027.

Chua, N.K., Coates, H.W., Brown, A.J., 2020. Squalene monooxygenase: a journey to the heart of cholesterol synthesis. Progress in Lipid Research 79, 101033.

Clark, T.E., Appleton, C.C., 1997. The molluscicidal activity of *Apodytes dimidiata* E. Meyer ex Arn (Icacinaceae), *Gardenia thunbergia* L.f. (Rubiaceae) and *Warburgia salutaris* (Bertol. F.) Chiov. (Cannelaceae), three South African plants. Journal of Ethnopharmacology 56, 15-30.

Clarkson, C., Maharaj, V.J., Crouch, N.R., Grace, O.M., Pillay, P., Matsabisa, M.G., Bhagwandin, N., Smith, P.J., Folb, P.I., 2004. In vitro antiplasmodial activity of medicinal plants native to or naturalised in South Africa. Journal of Ethnopharmacology 92, 177-191.

Cock, I., Mavuso, N., Van Vuuren, S., 2021. A review of plant-based therapies for the treatment of urinary tract infections in traditional Southern African Medicine. Evidence-Based Complementary and Alternative Medicine 2021.

Cock, I.E., Luwaca, N., Van Vuuren, S.F., 2023. The traditional use of southern African medicinal plants to alleviate fever and their antipyretic activities. Journal of Ethnopharmacology 303, 115850.

Cock, I.E., Ndlovu, N.A., Van Vuuren, S.F., 2023. The traditional use of southern African medicinal plants to treat oral pathogens, and studies into their relevant antimicrobial properties. South African Journal of Botany 153, 258-279.

Cock, I.E., Selesho, M.I., Van Vuuren, S.F., 2018. A review of the traditional use of southern African medicinal plants for the treatment of selected parasite infections affecting humans. Journal of Ethnopharmacology 220, 250-264.

Conserva, L.M., Jesu Costa Ferreira, J., 2012. Borreria and Spermacoce species (Rubiaceae): A review of their ethnomedicinal properties, chemical constituents, and biological activities. Pharmacognosy reviews 6, 46.

Corrigan, B.M., Van Wyk, B.E., Geldenhuys, C.J., Jardine, J.M., 2011. Ethnobotanical plant uses in the KwaNibela Peninsula, St Lucia, South Africa. South African Journal of Botany 77, 346-359.

Craik, D.J., Daly, N.L., Bond, T., Waine, C., 1999. Plant cyclotides: a unique family of cyclic and knotted proteins that defines the cyclic cystine knot structural motif. Journal of Molecular Biology 294, 1327-1336.

Daly, N.L., Gustafson, K.R., Craik, D.J., 2004. The role of the cyclic peptide backbone in the anti-HIV activity of the cyclotide kalata B1. Federation of European Biochemical Societies Letters 574, 69-72.

Daly, N.L., Rosengren, K.J., Craik, D.J., 2009. Discovery, structure and biological activities of cyclotides. Advanced Drug Delivery Reviews 61, 918-930.

Danlami, U., Danhalilu, R.L., 2015. Antibacterial, proximate and antioxidant studies of *Oldenlandia Herbacea* extract. Journal of Pharmaceutical and Biological Sciences 3, 61.

Danneels, B., Blignaut, M., Marti, G., Sieber, S., Vandamme, P., Meyer, M., Carlier, A., 2023. Cyclitol metabolism is a central feature of Burkholderia leaf symbionts. Environmental Microbiology 25, 454-472.

Danraka, R., Salaudeen, M., Maje, I., I. Ejiofor, J., 2021. Anti-inflamatory activity of ethanol leaf extract of *Hymenodictyon Floribundum* (Hochst. & Steud) BL Rob in rats: Impact of inflammatory biomarkers. The Federation of American Societies for Experimental Biology Journal 35, 373.

.

Datta, P., Sen, A., 1969. Pharmacognosy of *Oldenlandia corymbosa* Linn. Quarterly Journal of Crude Drug Research 9, 1365-1371.

De Wet, H., Nciki, S., van Vuuren, S.F., 2013. Medicinal plants used for the treatment of various skin disorders by a rural community in northern Maputaland, South Africa. Journal of ethnobiology and ethnomedicine 9, 1-10.

Deivanathan, S.K., Prakash, J.T.J., 2022. Green synthesis of silver nanoparticles using aqueous leaf extract of *Guettarda Speciosa* and its antimicrobial and anti-oxidative properties. Chemical Data Collections 38, 100831.

Dhar, M.K., Koul, A., Kaul, S., 2013. Farnesyl pyrophosphate synthase: a key enzyme in isoprenoid biosynthetic pathway and potential molecular target for drug development. New Biotechnology 30, 114-123.

Dlamini, N.P., Solomon, W.K., 2019. Optimization of blending ratios of jam from swazi indigenous fruits tincozi (*Syzygium cordatum*), tineyi (*Phyllogeiton zeyheri*) and umfomfo (*Cephalanthus natalensis* oliv.) using mixture design. Cogent Food and Agriculture 5, 1684864.

Dlova, N.C., Ollengo, M.A., 2018. Traditional and ethnobotanical dermatology practices in Africa. Clinics in Dermatology 36, 353-362.

Dornelles, R.C., Guex, C.G., de Lima, R., Nogueira-Librelotto, D.R., Casoti, R., Engelmann, A.M., Emanuelli Mello, C.B., Brandt de Souza, J., Melazzo de Andrade, C., Machado, A.K., Pillat, M.M., Manfron, M.P., de Freitas Bauermann, L., 2022. *Richardia brasiliensis* Gomes: phytochemical characterization, antiproliferative capacity and in vitro and in vivo toxicity. Regulatory Toxicology and Pharmacology 133, 105221.

Drewes, S.E., Horn, M.M., Connolly, J.D., Bredenkamp, B., 1998. Enolic iridolactone and other iridoids from *Alberta magna*. Phytochemistry 47, 991-996.

Drewes, S.E., Horn, M.M., Munro, O.Q., Ramesar, N., Ochse, M., Bringmann, G., Peters, K., Peters, E.-M., 1999. Stereostructure, conformation and reactivity of β- and α-gardiol from *Burchellia bubalina*. Phytochemistry 50, 387-394.

Ekmekcioglu, S., Kurzrock, R., Grimm, E.A., 2015. 57 - Hematopoietic Growth Factors and Cytokines, in: Mendelsohn, J., Gray, J.W., Howley, P.M., Israel, M.A., Thompson, C.B. (Eds.), The Molecular Basis of Cancer (Fourth Edition). W.B. Saunders, Philadelphia, pp. 789-808.e784.

Elisha, I.L., Botha, F.S., Madikizela, B., McGaw, L.J., Eloff, J.N., 2017. Acetone leaf extracts of some South African trees with high activity against *Escherichia coli* also have good antimycobacterial activity and selectivity index. BMC complementary and alternative medicine 17, 1-5.

Elisha, I.L., Botha, F.S., McGaw, L.J., Eloff, J.N., 2017. The antibacterial activity of extracts of nine plant species with good activity against *Escherichia coli* against five other bacteria and cytotoxicity of extracts. BMC complementary and alternative medicine 17, 1-10.

Elisha, I.L., Dzoyem, J.-P., McGaw, L.J., Botha, F.S., Eloff, J.N., 2016. The anti-arthritic, anti-inflammatory, antioxidant activity and relationships with total phenolics and total flavonoids of nine South African plants used traditionally to treat arthritis. BMC complementary and alternative medicine 16, 307.

Elufioye, T.O., Agbedahunsi, J.M., 2004. Antimalarial activities of *Tithonia diversifolia* (Asteraceae) and *Crossopteryx febrifuga* (Rubiaceae) on mice in vivo. Journal of Ethnopharmacology 93, 167-171.

Eteme, O.N., Zondegoumba, E.N., Tadayozzi, Y.S., Serafim, J.A., Leite, W.Q., Severino, M.d.F.G., Vicente, E.F., 2023. Methods for extraction, isolation and sequencing of cyclotides and others cyclic peptides with anti-helminthic activities: An overview. Parasitology International 98, 102808.

Fageyinbo, M., Oduniyi, O., Nwatu, C., Rotimi, K., 2021. Anti-inflammatory effect of hydroethanol leaf extract of *Mitragyna stipulosa*. University of Lagos Journal of Basic Medical Sciences 5, 9.

Farah, H.M., El Amin, T.H., Khalid, H.S., Hassan, S.M., El Hussein, A.R.M., 2012. In vitro activity of the aqueous extract of *Gardenia ternifolia* fruits against *Theileria lestoquardi*. Journal of Medicinal Plants Research 6, 5447-5451.

Fatima, N., Tapondjou, L.A., Lontsi, D., Sondengam, B., Atta-Ur-Rahman, Choudhary, M.I., 2002. Quinovic acid glycosides from *Mitragyna stipulosa*-first examples of natural inhibitors of snake venom phosphodiesterase I. Natural Product Letters 16, 389-393.

Feng, Z.L., Wu, S.P., Li, W.H., Guo, T.T., Liu, Q.C., 2015. Concise synthesis and antidiabetic effect of three natural triterpenoid saponins isolated from *Fadogia ancylantha* (Makoni tea). Helvetica Chimica Acta 98, 1254-1266.

Figurová, D., Tokárová, K., Greifová, H., Knížatová, N., Kolesárová, A., Lukáč, N., 2021. Inflammation, it's regulation and antiphlogistic effect of the cyanogenic glycoside amygdalin. Molecules 26, 5972.

Fourie, N., Erasmus, G., Schultz, R.A., Prozesky, L., 1995. Isolation of the toxin responsible for *gousiekte*, a plant-induced cardiomyopathy of ruminants in southern Africa. Onderstepoort Journal of Veterinary Research 62, 77-87.

Fowler, D.G., 2002. Traditional ila plant remedies from Zambia. Kirkia 18, 35-48.

Gabay, O., Sanchez, C., Salvat, C., Chevy, F., Breton, M., Nourissat, G., Wolf, C., Jacques, C., Berenbaum, F., 2010. Stigmasterol: a phytosterol with potential anti-osteoarthritic properties. Osteoarthritis and Cartilage 18, 106-116.

Gakuya, D.W., Itonga, S.M., Mbaria, J.M., Muthee, J.K., Musau, J.K., 2013. Ethnobotanical survey of biopesticides and other medicinal plants traditionally used in Meru central district of Kenya. Journal of Ethnopharmacology 145, 547-553.

Gariboldi, P., Verotta, L., Gabetta, B., 1990. Saponins from *Crossopteryx febrifuga*. Phytochemistry 29, 2629-2635.

Gelfand, M., Mavi, S., Drummond, R.B., Ndemera, B., 1985. The traditional medical practitioner in Zimbabwe: His principles of practice and pharmacopoeia. Mambo Press, Gweru, Zimabwe.

Gidado, A., Ameh, D., Atawodi, S., 2005. Effect of *Nauclea latifolia* leaves aqueous extracts on blood glucose levels of normal and alloxan-induced diabetic rats. African Journal of Biotechnology 4, 91-93.

Gong, X.-P., Sun, Y.-Y., Chen, W., Guo, X., Guan, J.-K., Li, D.-Y., Du, G., 2017. Anti-diarrheal and anti-inflammatory activities of aqueous extract of the aerial part of *Rubia cordifolia*. BMC complementary and alternative medicine 17, 20.

Gran, L., 1973. On the effect of a polypeptide isolated from "Kalata-Kalata"(*Oldenlandia affinis* DC) on the oestrogen dominated uterus. Acta Pharmacologica et Toxicologica 33, 400-408.

Gran, L., Sandberg, F., Sletten, K., 2000. *Oldenlandia affinis* (R&S) DC: A plant containing uteroactive peptides used in African traditional medicine. Journal of Ethnopharmacology 70, 197-203.

Gran, L., Sletten, K., Skjeldal, L., 2008. Cyclic peptides from *Oldenlandia affinis* DC. Molecular and biological properties. Chemistry & Biodiversity 5, 2014-2022.

Gunasekaran, S., Nayagam, A.A.J., Natarajan, R., 2023. Acute toxicity studies of aqueous and ethanol extracts of *Oldenlandia herbacea* Roxb. in albino rats. Journal of Stress Physiology & Biochemistry 19, 67-76.

Gustafson, K.R., Sowder, R.C., II, Henderson, L.E., Parsons, I.C., Kashman, Y., Cardellina, J.H., II, McMahon, J.B., Buckheit, R.W., Jr., Pannell, L.K., Boyd, M.R., 1994. Circulins A and B. Novel human immunodeficiency virus (HIV)-inhibitory macrocyclic peptides from the tropical tree *Chassalia parvifolia*. Journal of the American Chemical Society 116, 9337-9338.

Gwatidzo, L., Chowe, L., Musekiwa, C., Mukaratirwa-Muchanyereyi, N., 2018. In vitro anti-inflammatory activity of *Vangueria infausta*: An edible wild fruit from Zimbabwe. African Journal of Pharmacy and Pharmacology 12, 168-175.

Hashim, Y., Toume, K., Mizukami, S., Ge, Y.-W., Taniguchi, M., Teklemichael, A.A., Huy, N.T., Bodi, J.M., Hirayama, K., Komatsu, K., 2021. Phenylpropanoid conjugated iridoids with anti-malarial activity from the leaves of *Morinda morindoides*. Journal of Natural Medicines 75, 915-925.

Hashim, Y., Toume, K., Mizukami, S., Kitami, T., Taniguchi, M., Teklemichael, A.A., Tayama, Y., Huy, N.T., Lami, J.N., Bodi, J.M., 2022. Phenylpropanoid-conjugated iridoid glucosides from leaves of *Morinda morindoides*. Journal of Natural Medicines 76, 281-290.

He, D.-B., Bai, X., Ma, Y.-H., Qin, H.-J., Wu, Y.-B., Lv, D.-J., Mei, R.-Q., 2021. One new nucleoside and three furanpentanone derivatives from the aerial part of *Rubia cordifolia* L. Phytochemistry Letters 41, 125-128.

Hedberg, I., Staugard, F., 1989. Traditional Medicine in Botswana. Ipeleng Publishers, Gaborone.

Horn, M.M., 1996. Muthi compounds from indigenous Lauraceae and Rubiaceae species, Master of Science University of KwaZulu Natal, Pietermaritzburg.

Hoult, J., Payá, M., 1996. Pharmacological and biochemical actions of simple coumarins: natural products with therapeutic potential. General Pharmacology: The Vascular System 27, 713-722.

Howes, A., Gabryšová, L., O'Garra, A., 2014. Role of IL-10 and the IL-10 receptor in immune responses, Reference Module in Biomedical Sciences. Elsevier.

Hussain, H., Green, I.R., Saleem, M., Raza, M.L., Nazir, M., 2019. Therapeutic Potential of Iridoid Derivatives: Patent Review. Inventions 4, 15.

Hussain, M.I., Syed, Q.A., Khattak, M.N.K., Hafez, B., Reigosa, M.J., El-Keblawy, A., 2019. Natural product coumarins: biological and pharmacological perspectives. Biologia 74, 863-888.

Hutchings, A., 1989. A survey and analysis of traditional medicinal plants as used by the Zulu; Xhosa and Sotho. Bothalia 19, 112-123.

Hutchings, A., Scott, A.H., Lewis, G., Cunningham, A.B., 1996. Zulu Medicinal Plants: An Inventory. University of Natal Press, Pietermaritzburg.

Iheme, C.I., Ukairo, D.I., Oguoma, O.I., Nwaogu, L.A., Ezirim, A.U., Nzebude, C.P., Ezerioha, C.C., 2021. GC-MS Profile of *Diodella sarmentosa* (SW) Bacigalupo El Cabral ex Borhidi ethanol leaf extract and its total dehydrogenase inhibitory potential. arXiv.

Jennings, C.V., Rosengren, K.J., Daly, N.L., Plan, M., Stevens, J., Scanlon, M.J., Waine, C., Norman, D.G., Anderson, M.A., Craik, D.J., 2005. Isolation, solution structure, and insecticidal activity of kalata B2, a circular protein with a twist: do Möbius strips exist in nature? Biochemistry 44, 851-860.

Jensen, S.R., 1983. Iridoids in *Rothmannia globosa*. Phytochemistry 22, 1761-1765.

Jordaan, A., Du Plessis, LM**, Joynt, V., 1968. The structure and synthesis of pavettine, an alkaloid from *Pavetta lanceolata* Eckl.(Rubiaceae). South African Journal of Chemistry 21, 22-25.

Juma, B.F., Majinda, R.R., 2007. Constituents of *Gardenia volkensii*: their brine shrimp lethality and DPPH radical scavenging properties. Natural Product Research 21, 121-125.

Kakuguchi, Y., Ishiyama, H., Kubota, T., Kobayashi, J.i., 2009. Naucleamide F, a new monoterpene indole alkaloid from *Nauclea latifolia*. Heterocycles 79, 765-771.

Kambizi, L., 2014. Indigenous plants for ethnoveterinary uses in the Pondoland, South Africa, XXIX International Horticultural Congress on Horticulture: Sustaining Lives, Livelihoods and Landscapes (IHC2014): V World 1125. pp. 309-314.

Kaou, A.M., Mahiou-Leddet, V., Hutter, S., Aïnouddine, S., Hassani, S., Yahaya, I., Azas, N., Ollivier, E., 2008. Antimalarial activity of crude extracts from nine African medicinal plants. Journal of Ethnopharmacology 116, 74-83.

Kariba, R.M., 2002. Antimicrobial activity of *Hymenodictyon parvifolium*. Fitoterapia 73, 523-525.

Karou, S.D., Tchacondo, T., Ilboudo, D.P., Simpore, J., 2011. Sub-Saharan Rubiaceae: a review of their traditional uses, phytochemistry and biological activities. Pakistan Journal of Biological Sciences 14, 149-169.

Kayangar, M., Nono, R.N., Kühlborn, J., Tchuenguem, R., Ponou, B.K., Jenett-Siems, K., Teponno, R.B., Dzoyem, J.P., Opatz, T., Melzig, M.F., 2019. A new ursane-type triterpene oxoglucopyranoside from *Crossopteryx febrifuga*. Zeitschrift für Naturforschung C 74, 289-293.

Kelmanson, J.E., Jäger, A.K., van Staden, J., 2000. Zulu medicinal plants with antibacterial activity. Journal of Ethnopharmacology 69, 241-246.

Kezetas Bankeu, J.J., Kenou Kagho, D.U., Fotsing Fongang, Y.S.p., Kouipou Toghueo, R.M., Mba'ning, B.M.r., Tchouya Feuya, G.R., Boyom Fekam, F., Tchouankeu, J.C., Ngouela, S.r.A., Sewald, N., 2019. Constituents from *Nauclea latifolia* with anti-*Haemophilus influenzae* type b inhibitory activities. Journal of Natural Products 82, 2580-2585.

Khumalo, G.P., Van Wyk, B.E., Feng, Y., Cock, I.E., 2022. A review of the traditional use of southern African medicinal plants for the treatment of inflammation and inflammatory pain. Journal of Ethnopharmacology 283, 114436.

Khumalo, G.P., Van Wyk, B.E., Feng, Y., Cock, I.E., 2023. Toxicity and phytochemical properties of southern African medicinal plants used traditionally to treat pain and inflammatory ailments. South African Journal of Botany 160, 102-122.

Kim, D.-H., Lee, H.-J., Oh, Y.-J., Kim, M.-J., Kim, S.-H., Jeong, T.-S., Baek, N.-I., 2005. Iridoid glycosides isolated from *Oldenlandia diffusa* inhibit LDL-oxidation. Archives of Pharmacal Research 28, 1156-1160.

Kinuthia, E.W., Langat, M.K., Mwangi, E.M., Cheplogoi, P.K., 2012. Constituents of Kenyan *Gardenia volkensii*. Natural Product Communications 7, 13-14.

Kitambala, M.M., Mutombo, E.K., Niyibizi, B.N., Kamulete, G.S., Kalubandika, G.M., Muidikija, J.M., wa Ilunga, E.N., Kalunga, R.M., Kalonji, S.M., Non, W.M., 2021. The in vitro antisickling effect of purified alkaloids of *Cremaspora triflora* (Thonn.) K. Schum.(Rubiaceae) and *Macaranga schweinfurthii* Pax.(Euphorbiaceae). World Journal of Advanced Research and Reviews 9, 129-137.

Kone, W.M., Atindehou, K.K., Kacou-N, A., Dosso, M., 2007. Evaluation of 17 medicinal plants from Northern Côte d'Ivoire for their in vitro activity against *Streptococcus pneumoniae*. African Journal of Traditional, Complementary and Alternative Medicines 4, 17-22.

Kostova, I., Bhatia, S., Grigorov, P., Balkansky, S., S Parmar, V., K Prasad, A., Saso, L., 2011. Coumarins as antioxidants. Current Medicinal Chemistry 18, 3929-3951.

Kouda, R., Yakushiji, F., 2020. Recent advances in Iridoid chemistry: biosynthesis and chemical synthesis. Chemistry–An Asian Journal 15, 3771-3783.

Kraft, C., Jenett-Siems, K., Siems, K., Jakupovic, J., Mavi, S., Bienzle, U., Eich, E., 2003. In vitro antiplasmodial evaluation of medicinal plants from Zimbabwe. Phytotherapy Research 17, 123-128.

Kushiro, T., Shibuya, M., Ebizuka, Y., 1998. Beta-amyrin synthase--cloning of oxidosqualene cyclase that catalyzes the formation of the most popular triterpene among higher plants. European Journal of Biochemistry 256, 238-244.

Lall, N., Van Staden, A.B., Rademan, S., Lambrechts, I., De Canha, M.N., Mahore, J., Winterboer, S., Twilley, D., 2019. Antityrosinase and anti-acne potential of plants traditionally used in the Jongilanga community in Mpumalanga. South African Journal of Botany 126, 241-249.

Lawal, I., Grierson, D., Afolayan, A., 2014. Phytotherapeutic information on plants used for the treatment of tuberculosis in Eastern Cape Province, South Africa. Evidence-Based Complementary and Alternative Medicine 2014, 735423.

Le, H.T.T., Cho, Y.C., Cho, S., 2018. Methanol extract of *Guettarda speciosa* Linn. inhibits the production of inflammatory mediators through the inactivation of Syk and JNK in macrophages Corrigendum International Journal of Molecular Medicine 41, 1783-1791.

Lemaire, B., Vandamme, P., Merckx, V., Smets, E., Dessein, S., 2011. Bacterial leaf symbiosis in angiosperms: host specificity without co-speciation. PLoS One 6, e24430.

Leteane, M.M., Ngwenya, B.N., Muzila, M., Namushe, A., Mwinga, J., Musonda, R., Moyo, S., Mengestu, Y.B., Abegaz, B.M., Andrae-Marobela, K., 2012. Old plants newly discovered: *Cassia sieberiana* D.C. and *Cassia abbreviata* Oliv. Oliv. root extracts inhibit in vitro HIV-1c replication in peripheral blood mononuclear cells (PBMCs) by different modes of action. Journal of Ethnopharmacology 141, 48-56.

Liu, W., Feng, Y., Yu, S., Fan, Z., Li, X., Li, J., Yin, H., 2021. The flavonoid biosynthesis network in plants. International Journal of Molecular Sciences 22, 12824.

Louw, C.A.M., Regnier, T.J.C., Korsten, L., 2002. Medicinal bulbous plants of South Africa and their traditional relevance in the control of infectious diseases. Journal of Ethnopharmacology 82, 147-154.

Mabogo, D.E.N., 1990. The ethnobotany of the VhaVenda, Magister Scientiae, University of Pretoria, Pretoria.

Mabona, U., Van Vuuren, S.F., 2013. Southern African medicinal plants used to treat skin diseases. South African Journal of Botany 87, 175-193.

Magwede, K., 2018. A quantitative survey of traditional plant use of the Vhavenḓa, Limpopo Province, South Africa, Doctor of Philosophy, University of Johannesburg (South Africa), Johannesburg.

Magwede, K., Ramovha, L.I., Mabogo, Ḓ.E.N., van Wyk, A.E., van Wyk, B.E., 2019a. Traditional uses of the remarkable root bark hairs of *Lannea schweinfurthii* var. *stuhlmannii* (Anacardiaceae) by the Vhavenḓa, South Africa. South African Journal of Botany 122, 529-534.

Magwede, K., van Wyk, B.E., van Wyk, A.E., 2019b. An inventory of Vhavenḓa useful plants. South African Journal of Botany 122, 57-89.

Mahlo, S., Chauke, H., 2013. Antibacterial activity of selected medicinal plants used in ethnoveterinary medicine. Journal of Medicinal Plants Research 7, 2777-2782.

Mahlo, S.M., 2006. Antibacterial activity of selected plants used in ethnoveterinary medicine, Master of Science, University of Limpopo (Turfloop Campus).

Mahlo, S.M., Eloff, J.N., 2014. Acetone leaf extracts of *Breonadia salicina* (Rubiaceae) and ursolic acid protect oranges against infection by Penicillium species. South African Journal of Botany 93, 48-53.

Mahlo, S.M., McGaw, L.J., Eloff, J.N., 2010. Antifungal activity of leaf extracts from South African trees against plant pathogens. Crop Protection 29, 1529-1533.

Mahomoodally, M.F., Dilmohamed, S., 2016. Antibacterial and antibiotic potentiating activity of *Vangueria madagascariensis* leaves and ripe fruit pericarp against human pathogenic clinical bacterial isolates. Journal of Traditional and complementary Medicine 6, 399-403.

Mailu, J.K., 2021. Ethnopharmacological and toxicological study of medicinal plants used against respiratory infections in Kisumu East sub-county, Master of Science, University of Nairobi, Nairobi.

Mailu, J.K., Nguta, J.M., Mbaria, J.M., Okumu, M.O., 2021. Qualitative and quantitative phytochemical composition, antimicrobial activity, and brine shrimp cytotoxicity of different solvent extracts of *Acanthus polystachyus*, *Keetia gueinzii*, and *Rhynchosia elegans*. Future Journal of Pharmaceutical Sciences 7, 1-11.

Maiolino, G., Rossitto, G., Caielli, P., Bisogni, V., Rossi, G.P., Calò, L.A., 2013. The role of oxidized low-density lipoproteins in atherosclerosis: The myths and the facts. Mediators of Inflammation 2013, 714653.

Makhubu, F., 2017. Isolation of bioactive compounds and in vitro studies on *Pentanisia prunelloides* (Klotzsch ex Eckl. & Zeyh.) Walp. used in the eastern Free State for the management of diabetes mellitus, Master of Science, University of the Free State Qwaqwa.

Makhubu, F.N., Ashafa, A.O.T., Fouché, G., Balogun, F.O., 2019. Phytochemical screening, free radical mitigation and antidiabetic potentials of *Pentanisia prunelloides* (Klotzsch ex Eckl. & Zeyh.) Walp. root extracts. Journal of Food and Nutrition Research 7, 391-401.

Malik, E.M., Müller, C.E., 2016. Anthraquinones as pharmacological tools and drugs. Medicinal Research Reviews 36, 705-748.

Marealle, A.I., Moyo, A.A., Machumi, F., Qwarse, M., Chenyambuga, Y.M., Heydenreich, M., Moshi, M., 2023. Antimycobacterial activity of scopoletin from ethanolic extract of *Hymenodictyon floribundum* (Hochst. & Steud.) B.L.Rob. stem bark. Scientific African 21, e01778.

Maroyi, A., 2018. Nutraceutical and ethnopharmacological properties of *Vangueria infausta* subsp *infausta*. Molecules 23, 1-19.

Maroyi, A., 2018. *Vangueria madagascariensis* fruit tree: nutritional, phytochemical, pharmacological, and primary health care applications as herbal medicine. Scientifica 2018, 4596450.

Masarirambi, M., Zwane, P., Surana, N., Kunene, E., Moyo, S., Mabuza, L., Makhanya, B., 2019. Indigenous dye plants of the Kingdom of Eswatini, traditional uses and new prospects. Advancement in Medicinal Plant Research 7, 8-14.

Masevhe, N.A., McGaw, L.J., Eloff, J.N., 2015. The traditional use of plants to manage candidiasis and related infections in Venda, South Africa. Journal of Ethnopharmacology 168, 364-372.

Mashile, S.P., Tshisikhawe, M.P., Masevhe, N.A., 2019. Indigenous fruit plants species of the Mapulana of Ehlanzeni district in Mpumalanga province, South Africa. South African Journal of Botany 122, 180-183.

Mashile, S.P., Tshisikhawe, M.P., Masevhe, N.A., 2019. Medicinal plants used in the treatment of maternal health-related problems by the Mapulana of Ehlanzeni District, Mpumalanga province, South Africa. Journal of Applied Pharmaceutical Science 9, 021-029.

Masika, P., Afolayan, A., 2003. An ethnobotanical study of plants used for the treatment of livestock diseases in the Eastern Cape Province, South Africa. Pharmaceutical Biology 41, 16-21.

Masondo, N.A., Stafford, G.I., Aremu, A.O., Makunga, N.P., 2019. Acetylcholinesterase inhibitors from southern African plants: An overview of ethnobotanical, pharmacological potential and phytochemical research including and beyond Alzheimer's disease treatment. South African Journal of Botany 120, 39-64.

Mataha, L., 2021. Medicinal Ethnobotany of the Modjadji Area of the Limpopo Province, South Africa, Master of Science, University of Johannesburg (South Africa), Johannesburg.

Matias, R., Canale, F.S., Corrêa, B.O., Bono, J.A.M., de Oliveira, A.K.M., Dourado, D.M., Roel, A.R., Rivero-Wendt, C.L.G., Pedrino, D.R., 2018. Chemical constituents and antifungal potential of the *Richardia brasiliensis* (Gomes) ethanolic extract. Tropical and Subtropical Agroecosystems 21, 457-465.

Matotoka, M.M., Mashabela, G.T., Masoko, P., 2023. Phytochemical content, antibacterial activity, and antioxidant, anti-inflammatory, and cytotoxic effects of traditional medicinal plants against respiratory tract bacterial pathogens. Evidence-Based Complementary and Alternative Medicine 2023, 1243438.

Mbanjwa, S.G., 2020. A Quantitative Ethnobotanical Survey of the Ixopo Area of KwaZulu-Natal, South Africa, Master of Science, University of Johannesburg (South Africa), Ann Arbor.

Mbukwa, E., Chacha, M., Majinda, R.R., 2007. Phytochemical constituents of *Vangueria infausta*: their radical scavenging and antimicrobial activities. Arkivoc 9, 104-112.

McGaw, L.J., Jäger, A.K., van Staden, J., 2000. Antibacterial, anthelmintic and anti-amoebic activity in South African medicinal plants. Journal of Ethnopharmacology 72, 247-263.

Meke, G.S., Mumba, R.F., Bwanali, R.J., Williams, V.L., 2017. The trade and marketing of traditional medicines in southern and central Malawi. International Journal of Sustainable Development & World Ecology 24, 73-87.

Mencherini, T., Picerno, P., Del Gaudio, P., Festa, M., Capasso, A., Aquino, R., 2010. Saponins and polyphenols from *Fadogia ancylantha* (Makoni tea). Journal of Natural Products 73, 247-251.

Mhlongo, L.S., Van Wyk, B.E., 2019. Zulu medicinal ethnobotany: new records from the Amandawe area of KwaZulu-Natal, South Africa. South African Journal of Botany 122, 266-290.

MichalcovÃ, K., HalenÃ, M., KolesÃ, A., 2016. Cyanogenic glycosides as a potential bioregulator. Journal of Microbiology, Biotechnology and Food Sciences 6, 743-746.

Mohammed, A.M., Coombes, P.H., Crouch, N.R., Mulholland, D.A., 2012. Garjasmine unequivocally isolated from the Rubiaceae. Biochemical Systematics and Ecology 44, 109-111.

Mohammed, A.M., Coombes, P.H., Crouch, N.R., Mulholland, D.A., 2013. Chemical constituents from *Fadogia homblei* de wild (Rubiaceae). International Letters of Chemistry, Physics and Astronomy 9, 116-124.

Moshi, M.J., Mbwambo, Z., Nondo, R.S., Masimbaa, P., Kamuhabwa, A., Kapingu, M.C., Thomas, P., Richard, M., 2006. Evaluation of ethnomedical claims and brine shrimp toxicity of some plants used in Tanzania as traditional medicines. African Journal of Traditional, Complementary and Alternative Medicines 3, 48-58.

Moteetee, A., 2017. A review of plants used for magic by Basotho people in comparison with other cultural groups in Southern Africa. Indian Journal of Traditional Knowledge 16, 229-234.

Moteetee, A., Moffett, R.O., Seleteng-Kose, L., 2019. A review of the ethnobotany of the Basotho of Lesotho and the Free State Province of South Africa (South Sotho). South African Journal of Botany 122, 21-56.

Moteetee, A., Seleteng Kose, L., 2016. Medicinal plants used in Lesotho for treatment of reproductive and post reproductive problems. Journal of Ethnopharmacology 194, 827-849.

Motlhanka, D., Nthoiwa, G., 2013. Ethnobotanical survey of medicinal plants of Tswapong North, in Eastern Botswana: a case of plants from Mosweu and Seolwane villages. European Journal of Medicinal Plants 3, 10-24.

Moyo, A.A., Jagadhane, K.S., Bhosale, S.R., Shinde, S.B., Marealle, A.I., Shimpale, V.B., Anbhule, P.V., 2023. Anticancer and apoptotic effects of *Hymenodictyon floribundum* (Hochst. & Steud.) BL Rob. stem bark hydroethanolic extract. Chemistry Africa, 1-16.

Muangrom, W., Bacher, M., Berger, A., Valant-Vetschera, K., Vajrodaya, S., Schinnerl, J., 2021. A novel tryptophan-derived alkaloid and other constituents from *Guettarda speciosa* (Rubiaceae: Cinchonoideae–Guettardeae). Biochemical Systematics and Ecology 95, 104239.

Mudau, G., Odeyemi, S., Dewar, J., 2020. Vhavenda herbal remedies as sources of antihypertensive drugs: Ethnobotanical and ethnopharmacological studies. Oxidative Medicine and Cellular Longevity 2020, 6636766.

Mugisha, M.K., Asiimwe, S., Namutebi, A., Borg-Karlson, A.-K., Kakudidi, E.K., 2014. Ethnobotanical study of indigenous knowledge on medicinal and nutritious plants used to manage opportunistic infections associated with HIV/AIDS in western Uganda. Journal of Ethnopharmacology 155, 194-202.

Mukandiwa, L., Naidoo, V., Eloff, J.N., 2012. In vitro antibacterial activity of seven plants used traditionally to treat wound myiasis in animals in southern Africa. Journal of Medicinal Plants Research 6, 4379-4388.

Mulholland, D.A., Mohammed, A.M., Coombes, P.H., Haque, S., Pohjala, L.L., Tammela, P.S., Crouch, N.R., 2011. Triterpenoid acids and lactones from the leaves of *Fadogia tetraquetra* var. *tetraquetra* (Rubiaceae). Natural Product Communications 6, 1573-1576.

Murray, R., 1989. Coumarins. Natural Product Reports 6, 591-624.

Musila, M.F., Dossaji, S.F., Nguta, J.M., Lukhoba, C.W., Munyao, J.M., 2013. In vivo antimalarial activity, toxicity and phytochemical screening of selected antimalarial plants. Journal of Ethnopharmacology 146, 557-561.

Mustafa, S.E., Mohamed, R.A., Mariod, A.A., 2019. *Vangueria madagascariensis*: Phytochemical constituents, bioactive compounds, traditional and medicinal uses, in: Mariod, A.A. (Ed.) Wild Fruits: Composition, Nutritional Value and Products. Springer Cham, pp. 157-164.

Muthaura, C.N., Keriko, J.M., Mutai, C., Yenesew, A., Gathirwa, J.W., Irungu, B.N., Nyangacha, R., Mungai, G.M., Derese, S., 2015. Antiplasmodial potential of traditional antimalarial phytotherapy remedies used by the Kwale community of the Kenyan Coast. Journal of Ethnopharmacology 170, 148-157.

Muthee, J.K., Gakuya, D.W., Mbaria, J.M., Kareru, P.G., Mulei, C.M., Njonge, F.K., 2011. Ethnobotanical study of anthelmintic and other medicinal plants traditionally used in Loitoktok district of Kenya. Journal of Ethnopharmacology 135, 15-21.

Nahrstedt, A., Rockenbach, J., Wray, V., 1995. Phenylpropanoid glycosides, a furanone glucoside and geniposidic acid from members of the Rubiaceae. Phytochemistry 39, 375-378.

Nciki, S., Vuuren, S., van Eyk, A., de Wet, H., 2016. Plants used to treat skin diseases in northern Maputaland, South Africa: antimicrobial activity and in vitro permeability studies. Pharmaceutical Biology 54, 2420-2436.

Ndamba, J., Nyazema, N., Makaza, N., Anderson, C., Kaondera, K., 1994. Traditional herbal remedies used for the treatment of urinary schistosomiasis in Zimbabwe. Journal of Ethnopharmacology 42, 125-132.

Ndhlovu, P.T., Omotayo, A.O., Otang-Mbeng, W., Aremu, A.O., 2021. Ethnobotanical review of plants used for the management and treatment of childhood diseases and well-being in South Africa. South African Journal of Botany 137, 197-215.

Ndlovu, G., Fouche, G., Tselanyane, M., Cordier, W., Steenkamp, V., 2013. In vitro determination of the anti-aging potential of four southern African medicinal plants. BMC complementary and alternative medicine 13, 304.

Ndoumbe, C.M.M., Nono, R.N., Zeutsop, J.F., Bitchagno, G.T.M., Lenta, B.N., Nkeng-Efouet-Alango, P., Sewald, N., Chouna, J.R., 2023. Iridoid and irido-alkaloids from the fruits of *Mitragyna stipulosa*, and the plausible biosynthetic route to the new ring formation. Biochemical Systematics and Ecology 111, 104732.

Nethengwe, M.F., 2011. Antiplasmodial/antipyretic activity of some Zulu medicinal plants, Master of Science, University of Zululand.

Neuwinger, H.D., 2004. Plants used for poison fishing in tropical Africa. Toxicon 44, 417-430.

Ngarivhume, T., van't Klooster, C.I.E.A., de Jong, J.T.V.M., Van der Westhuizen, J.H., 2015. Medicinal plants used by traditional healers for the treatment of malaria in the Chipinge district in Zimbabwe. Journal of Ethnopharmacology 159, 224-237.

Ngezahayo, J., Havyarimana, F., Hari, L., Stévigny, C., Duez, P., 2015. Medicinal plants used by Burundian traditional healers for the treatment of microbial diseases. Journal of Ethnopharmacology 173, 338-351.

Ngnokam, D., Ayafor, J., Connolly, J., Nuzillard, J., 2003. Nauclefolinine: a new alkaloid from the roots of *Nauclea latifolia*. Bulletin of the Chemical Society of Ethiopia 17, 173-176.

Ngo Bum, E., Taiwe, G.S., Moto, F.C.O., Ngoupaye, G.T., Nkantchoua, G.C.N., Pelanken, M.M., Rakotonirina, S.V., Rakotonirina, A., 2009. Anticonvulsant, anxiolytic, and sedative properties of the roots of *Nauclea latifolia* Smith in mice. Epilepsy & Behavior 15, 434-440.

Nguta, J.M., Mbaria, J.M., Gakuya, D.W., Gathumbi, P.K., Kiama, S.G., 2010. Antimalarial herbal remedies of Msambweni, Kenya. Journal of Ethnopharmacology 128, 424-432.

Nguta, J.M., Mbaria, J.M., Gathumbi, P.K., Gakuya, D., Kabasa, J.D., Kiama, S.G., 2011. Ethnodiagnostic skills of the Digo community for malaria: A lead to traditional bioprospecting. FRONTIERS IN PHARMACOLOGY 2, 30.

Ngwenya, N.M., 2012. Biological and Phytochemical Screening of Major Compounds in *Cephalanthus natalensis*, Master of Science, University of Johannesburg (South Africa), Ann Arbor.

Nielsen, N.D., Sandager, M., Stafford, G.I., van Staden, J., Jäger, A.K., 2004. Screening of indigenous plants from South Africa for affinity to the serotonin reuptake transport protein. Journal of Ethnopharmacology 94, 159-163.

Noiarsa, P., Ruchirawat, S., Otsuka, H., Kanchanapoom, T., 2008. Chemical constituents from *Oldenlandia corymbosa* L. of Thai origin. Journal of Natural Medicines 62, 249-250.

Nortje, J.M., van Wyk, B.E., 2015. Medicinal plants of the Kamiesberg, Namaqualand, South Africa. Journal of Ethnopharmacology 171, 205-222.

Novotna, B., Polesny, Z., Pinto-Basto, M.F., Van Damme, P., Pudil, P., Mazancova, J., Duarte, M.C., 2020. Medicinal plants used by 'root doctors', local traditional healers in Bié province, Angola. Journal of Ethnopharmacology 260, 112662.

Nthambeleni, R., 2008. Isolation and characterization of cytotoxic compounds from *Anthospermum hispidulum* and *Eriocephalus tenuifolius*, Master of Science, University of KwaZulu Natal, Pietermaritzburg.

Nvau, B.J., Sami, B., Ajibade, O.S., Gray, I.A., Igoli, J.O., 2019. Adicardin and other coumarins from *Breonadia salicina* (Vahl) Hepper. Tropical Journal of Natural Product Research 3, 298-301.

Nyagumbo, E., Pote, W., Shopo, B., Nyirenda, T., Chagonda, I., Mapaya, R.J., Maunganidze, F., Mavengere, W.N., Mawere, C., Mutasa, I., Kademeteme, E., Maroyi, A., Taderera, T., Bhebhe, M., 2022. Medicinal plants used for the management of respiratory diseases in Zimbabwe: Review and perspectives potential management of COVID-19. Physics and Chemistry of the Earth, Parts A/B/C 128, 103232.

Nyahangare, E.T., Mvumi, B.M., Mutibvu, T., 2015. Ethnoveterinary plants and practices used for ecto-parasite control in semi-arid smallholder farming areas of Zimbabwe. Journal of ethnobiology and ethnomedicine 11, 1-16.

Nyobe, J.C.N., Bikélé, D.M., Fodouop, M.B., Mpondo, E.M., Ndom, J.C., 2020. A new pyrrolidinyl-piperazine alkaloid derivative from *Oxyanthus speciosus* DC.(Rubiaceae). Trends in Phytochemical Research 4, 109-116.

Oboh, G., Nwanna, E.E., Oyeleye, S.I., Olasehinde, T.A., Ogunsuyi, O.B., Boligon, A.A., 2016. In vitro neuroprotective potentials of aqueous and methanol extracts from *Heinsia crinita* leaves. Food Science and Human Wellness 5, 95-102.

Odukoya, J.O., Odukoya, J.O., Mmutlane, E.M., Ndinteh, D.T., 2022. Ethnopharmacological study of medicinal plants used for the treatment of cardiovascular diseases and their associated risk factors in sub-Saharan Africa. Plants 11, 1387.

Okem, A., Finnie, J.F., Van Staden, J., 2012. Pharmacological, genotoxic and phytochemical properties of selected South African medicinal plants used in treating stomach-related ailments. Journal of Ethnopharmacology 139, 712-720.

Olajuyigbe, O., Afolayan, A., 2012. Ethnobotanical survey of medicinal plants used in the treatment of gastrointestinal disorders in the Eastern Cape Province, South Africa. Journal of Medicinal Plants Research 6, 3415-3424.

Orhan, N., Orhan, D.D., Aslan, M., Şüküroğlu, M., Orhan, I.E., 2012. UPLC–TOF-MS analysis of *Galium spurium* towards its neuroprotective and anticonvulsant activities. Journal of Ethnopharmacology 141, 220-227.

Otang, W.M., Grierson, D.S., Afolayan, A.J., 2014. A survey of plants responsible for causing irritant contact dermatitis in the Amathole district, eastern cape, South Africa. Journal of Ethnopharmacology 157, 274-284.

Otsuka, H., Yoshimura, K., YAMASAKI, K., CANTORIA, M.C., 1991. Isolation of 10-O-acyl iridoid glucosides from a Philippine medicinal plant, *Oldenlandia corymbosa* L.(Rubiaceae). Chemical and Pharmaceutical Bulletin 39, 2049-2052.

Panche, A.N., Diwan, A.D., Chandra, S.R., 2016. Flavonoids: an overview. Journal of Nutritional Science 5, e47.

Park, B.-Y., Oh, S.-R., Ahn, K.-S., Kwon, O.-K., Lee, H.-K., 2008. (–)-Syringaresinol inhibits proliferation of human promyelocytic HL-60 leukemia cells via G1 arrest and apoptosis. International Immunopharmacology 8, 967-973.

Passos, F.R.S., Araújo-Filho, H.G., Monteiro, B.S., Shanmugam, S., Araújo, A.A.d.S., Almeida, J.R.G.d.S., Thangaraj, P., Júnior, L.J.Q., Quintans, J.d.S.S., 2022. Anti-inflammatory and modulatory effects of steroidal saponins and sapogenins on cytokines: A review of pre-clinical research. Phytomedicine 96, 153842.

Patocka, J., 2003. Biologically active pentacyclic triterpenes and their current medicine signification. Journal of Applied Biomedicine 1, 7-12.

Pavela, R., Canale, A., Mehlhorn, H., Benelli, G., 2016. Application of ethnobotanical repellents and acaricides in prevention, control and management of livestock ticks: A review. Research in Veterinary Science 109, 1-9.

Payne, S., 2017. Chapter 6 - Immunity and Resistance to Viruses, in: Payne, S. (Ed.) Viruses. Academic Press, pp. 61-71.

Pelegrini, P.B., Quirino, B.F., Franco, O.L., 2007. Plant cyclotides: An unusual class of defense compounds. Peptides 28, 1475-1481.

Pinto-Carbó, M., Gademann, K., Eberl, L., Carlier, A., 2018. Leaf nodule symbiosis: function and transmission of obligate bacterial endophytes. Current Opinion in Plant Biology 44, 23-31.

Pinto-Carbó, M., Sieber, S., Dessein, S., Wicker, T., Verstraete, B., Gademann, K., Eberl, L., Carlier, A., 2016. Evidence of horizontal gene transfer between obligate leaf nodule symbionts. The ISME Journal 10, 2092-2105.

Pinto, D.S., Tomaz, A.C.d.A., Tavares, J.F., Tenório-Souza, F.H., Dias, C.d.S., Braz-Filho, R., da-Cunha, E.V., 2008. Secondary metabolites isolated from *Richardia brasiliensis* Gomes (Rubiaceae). Revista Brasileira de Farmacognosia 18, 367-372.

Plan, M.R., Rosengren, K.J., Sando, L., Daly, N.L., Craik, D.J., 2010. Structural and biochemical characteristics of the cyclotide kalata B5 from *Oldenlandia affinis*. Peptide Science 94, 647-658.

Pompermaier, L., Marzocco, S., Adesso, S., Monizi, M., Schwaiger, S., Neinhuis, C., Stuppner, H., Lautenschläger, T., 2018. Medicinal plants of northern Angola and their anti-inflammatory properties. Journal of Ethnopharmacology 216, 26-36.

Poonkodi, K., 2016. Phytoconstituents from *Richardia scabra* L. and its biological activities. Asian Journal of Pharmaceutical and Clinical Research 9, 168-171.

POWO, 2023. Plants of the World Online. Royal Botanic Gardens, Kew, On the Internet.

Ramalingum, N., Mahomoodally, M.F., 2014. Biologic propensities and phytochemical profile of *Vangueria madagascariensis* JF Gmelin (Rubiaceae): an underutilized native medicinal food plant from Africa. BioMed Research International 2014, 681073.

RDG, E.I., AW, E.O., Abena, A., 2023. Acute toxicity and laxative effect of the aqueous extract of the leaves *Crossopteryx febrifuga* (Benth) in rats. African Journal of Pharmacy and Pharmacology 17, 10-16.

Renda, G., Gökkaya, İ., Şöhretoğlu, D., 2022. Immunomodulatory properties of triterpenes. Phytochemistry Reviews 21, 537-563.

Rockenbach, J., Nahrstedt, A., Wray, V., 1992. Cyanogenic glycosides from PS *Psydrax* and *Oxyanthus* species[a/t]. Phytochemistry 31, 567-570.

Rosales, P.F., Bordin, G.S., Gower, A.E., Moura, S., 2020. Indole alkaloids: 2012 until now, highlighting the new chemical structures and biological activities. Fitoterapia 143, 104558.

Runyoro, D.K., Matee, M.I., Ngassapa, O.D., Joseph, C.C., Mbwambo, Z.H., 2006. Screening of Tanzanian medicinal plants for anti-Candida activity. BMC complementary and alternative medicine 6, 1-10.

Salawu, O., Chindo, B., Tijani, A., Adzu, B., 2008. Analgesic, anti-inflammatory, antipyretic and antiplasmodial effects of the methanolic extract of *Crossopteryx febrifuga*. Journal of Medicinal Plant Research 2, 213-218.

Salawu, O., Chindo, B., Tijani, A., Obidike, I., Salawu, T., Akingbasote, A.J., 2009. Acute and sub-acute toxicological evaluation of the methanolic stem bark extract of *Crossopteryx febrifuga* in rats. African Journal of Pharmacy and Pharmacology 3, 621-626.

Samie, A., Madzie, N., 2017. Effects of *Combretum hereroense* and *Canthium mundianum* water extracts on production and expression of interleukin-4. African Journal of Traditional, Complementary and Alternative Medicines 14, 302-309.

Sani, A., Zakariyya, U.A., Mahe, A., Singh, D., Jain, M., Hassan, F., 2018. In vitro antitrypanosomal activity of *Breonadia salicina* on *Trypanasoma brucei brucei*. Internation Journal of Pharma Sciences and Research 9, 975-9492.

Santana-Molina, C., Rivas-Marin, E., Rojas, A.M., Devos, D.P., 2020. Origin and evolution of polycyclic triterpene synthesis. Molecular Biology and Evolution 37, 1925-1941.

Sarker, S.D., Nahar, L., 2017. Progress in the chemistry of naturally occurring coumarins. Progress in the Chemistry of Organic Natural Products 106, 241-304.

Sawai, S., Saito, K., 2011. Triterpenoid biosynthesis and engineering in plants. Frontiers in Plant Science 2, 25.

Seleteng Kose, L., Moteetee, A., Van Vuuren, S., 2015. Ethnobotanical survey of medicinal plants used in the Maseru district of Lesotho. Journal of Ethnopharmacology 170, 184-200.

Sethna, S.M., Shah, N.M., 1945. The chemistry of coumarins. Chemical Reviews 36, 1-62.

Setshogo, M.P., Mbereki, C.M., 2011. Floristic diversity and uses of medicinal plants sold by street vendors in Gaborone, Botswana. The African Journal of Plant Science and Biotechnology 5, 69-74.

Shigemori, H., Kagata, T., Ishiyama, H., Morah, F., Ohsaki, A., Kobayashi, J.i., 2003. Naucleamides A—E, New monoterpene indole alkaloids from *Nauclea latifolia*. Chemical and Pharmaceutical Bulletin 51, 58-61.

Shirungu, M.M., Cheikhyoussef, A., 2018. Therapeutic powers of medicinal plants used by traditional healers in Kavango, Namibia, for mental illness. Anthropology Southern Africa 41, 127-135.

Shopo, B., Mapaya, R.J., Maroyi, A., 2022. Ethnobotanical study of medicinal plants traditionally used in Gokwe South District, Zimbabwe. South African Journal of Botany 149, 29-48.

Sibanda, S., Ndengu, B., Multari, G., Pompi, V., Galeffi, C., 1989. A coumarin glucoside from *Xeromphis obovata*. Phytochemistry 28, 1550-1552.

Sibandze, G.F., van Zyl, R.L., van Vuuren, S.F., 2010. The anti-diarrhoeal properties of Breonadia salicina, *Syzygium cordatum* and *Ozoroa sphaerocarpa* when used in combination in Swazi traditional medicine. Journal of Ethnopharmacology 132, 506-511.

Sieber, S., Carlier, A., Neuburger, M., Grabenweger, G., Eberl, L., Gademann, K., 2015. Isolation and total synthesis of kirkamide, an aminocyclitol from an obligate leaf nodule symbiont. Angewandte Chemie 127, 8079-8081.

Singaravelu, P., Shrishailappa, B., Subban, R., 2008. In vitro antioxidant activity of *Oldenlandia herbacea* and isolation of 9, 9-dimethyl hexacosane and 23-ethyl-cholest-23-en-3 β-ol. Natural Product Research 22, 1510-1515.

Singh, T.P., Singh, O.M., 2018. Recent progress in biological activities of indole and indole alkaloids. Mini Reviews in Medicinal Chemistry 18, 9-25.

Sobiecki, J., 2008. A review of plants used in divination in southern Africa and their psychoactive effects. Southern African Humanities 20, 333-351.

Stafford, G.I., Pedersen, M.E., van Staden, J., Jäger, A.K., 2008. Review on plants with CNS-effects used in traditional South African medicine against mental diseases. Journal of Ethnopharmacology 119, 513-537.

Stanton, S., Meyer, J.J.M., Van der Merwe, C.F., 2013. An evaluation of the endophytic colonies present in pathogenic and non-pathogenic Vanguerieae using electron microscopy. South African Journal of Botany 86, 41-45.

Sulaiman, S.M., Bashir, A.K., Mohamed, A.M., 1988. Effects of certain Sudanese plant extracts on egg-hatching, miracidia and cercariae of *Schistosoma mansoni*. International Journal of Crude Drug Research 26, 17-21.

Suroowan, S., Pynee, K.B., Mahomoodally, M.F., 2019. A comprehensive review of ethnopharmacologically important medicinal plant species from Mauritius. South African Journal of Botany 122, 189-213.

Tajuddeen, N., Swart, T., Hoppe, H.C., van Heerden, F.R., 2022. Phytochemical and antiplasmodial investigation of *Gardenia thunbergia* L. f. leaves. Natural Product Research 36, 4052-4060.

Takahashi, K., Ehata, S., Miyauchi, K., Morishita, Y., Miyazawa, K., Miyazono, K., 2021. Neurotensin receptor 1 signaling promotes pancreatic cancer progression. Molecular Oncology 15, 151-166.

Tam, J.P., Lu, Y.-A., Yang, J.-L., Chiu, K.-W., 1999. An unusual structural motif of antimicrobial peptides containing end-to-end macrocycle and cystine-knot disulfides. Proceedings of the National Academy of Sciences 96, 8913-8918.

Tan, M.A., Lagamayo, M.W.D., Alejandro, G.J.D., An, S.S.A., 2019. Anti-amyloidogenic and cyclooxygenase inhibitory activity of *Guettarda speciosa*. Molecules 24, 4112.

Tiya, S.Y., Sewani-Rusike, C.R., Taderera, T., 2019. Hepatoprotective effects of *Fadogia ancylantha* (Makoni Tea) on ethanol-induced liver damage in Wistar rats. Journal of Biologically Active Products from Nature 9, 352-363.

Tlhapi, D.B., Ramaite, I.D., Anokwuru, C.P., 2021. Metabolomic profiling and antioxidant activities of *Breonadia salicina* using 1H-NMR and UPLC-QTOF-MS analysis. Molecules 26, 6707.

Tomás-Barberán, F.A., Hostettmann, K., 1988. A cytotoxic triterpenoid and flavonoids from *Crossopteryx febrifuga*. Planta medica 54, 266-267.

Tshikalange, T.E., Mophuting, B.C., Mahore, J., Winterboer, S., Lall, N., 2016. An ethnobotanical study of medicinal plants used in villages under Jongilanga tribal council, Mpumalanga, South Africa. African Journal of Traditional, Complementary and Alternative Medicines 13, 83-89.

Tshisekedi Tshibangu, P., Mutwale Kapepula, P., Kabongo Kapinga, M.J., Tujibikila Mukuta, A., Kalenda, D.T., Tchinda, A.T., Mouithys-Mickalad, A.A., Jansen, O., Cieckiewicz, E., Tits, M., Angenot, L., Frédérich, M., 2017. Antiplasmodial activity of *Heinsia crinita* (Rubiaceae) and identification of new iridoids. Journal of Ethnopharmacology 196, 261-266.

Urso, V., Signorini, M.A., Tonini, M., Bruschi, P., 2016. Wild medicinal and food plants used by communities living in Mopane woodlands of southern Angola: Results of an ethnobotanical field investigation. Journal of Ethnopharmacology 177, 126-139.

Vahekeni, N., Neto, P.M., Kayimbo, M.K., Mäser, P., Josenando, T., da Costa, E., Falquet, J., van Eeuwijk, P., 2020. Use of herbal remedies in the management of sleeping sickness in four northern provinces of Angola. Journal of Ethnopharmacology 256, 112382.

Van Elst, D., Nuyens, S., Van Wyk, B., Verstraete, B., Dessein, S., Prinsen, E., 2013. Distribution of the cardiotoxin pavettamine in the coffee family (Rubiaceae) and its significance for gousiekte, a fatal poisoning of ruminants. Plant physiology and biochemistry 67, 15-19.

Van Vuuren, S.F., Motlhatlego, K.E., Netshia, V., 2022. Traditionally used polyherbals in a southern African therapeutic context. Journal of Ethnopharmacology 288, 114977.

Van Wyk, B.E., 2020. A family-level floristic inventory and analysis of medicinal plants used in Traditional African Medicine. Journal of Ethnopharmacology 249, 112351.

Verschaeve, L., Kestens, V., Taylor, J.L.S., Elgorashi, E.E., Maes, A., Van Puyvelde, L., De Kimpe, N., Van Staden, J., 2004. Investigation of the antimutagenic effects of selected South African medicinal plant extracts. Toxicology in Vitro 18, 29-35.

Verstraete, B., Van Elst, D., Steyn, H., Van Wyk, B., Lemaire, B., Smets, E., Dessein, S., 2011. Endophytic bacteria in toxic South African plants: identification, phylogeny and possible involvement in gousiekte. PLoS One 6, e19265.

Wang, C., Gong, X., Bo, A., Zhang, L., Zhang, M., Zang, E., Zhang, C., Li, M., 2020. Iridoids: research advances in their phytochemistry, biological activities, and pharmacokinetics. Molecules 25, 287.

Wang, P., Wang, J., El-Demerdash, F.M., Wei, J., 2023. Coagulant compounds in *Rubia cordifolia* L. Journal of Future Foods 3, 220-224.

Watt, J.M., Breyer-Brandwijk, M.G., 1962. The medicinal and poisonous plants of southern and eastern Africa, Second ed. E and S Livingstone, Edinburgh.

Welcome, A.K., Van Wyk, B.E., 2019. An inventory and analysis of the food plants of southern Africa. South African Journal of Botany 122, 136-179.

WFO, 2023. World Flora Online. On the internet.

Williams, V., Balkwill, K., 2001. A lexicon of plants traded in the Witwatersrand *umuthi* shops, South Africa. Bothalia 31, 71 - 98.

Williamson, J., 2005. Useful Plants of Malawi, 3rd ed. Montfort Press, Limbe.

Witherup, K.M., Bogusky, M.J., Anderson, P.S., Ramjit, H., Ransom, R.W., Wood, T., Sardana, M., 1994. Cyclopsychotride A, a Biologically Active, 31-Residue Cyclic Peptide Isolated from *Psychotria longipes*. Journal of Natural Products 57, 1619-1625.

Yang, S., Park, S., Ahn, D., Yang, J.H., Kim, D.K., 2011. Antioxidative constituents of the aerial parts of *Galium spurium*. The Korean Society of Applied Pharmacology 19, 336-341.

Yetein, M.H., Houessou, L.G., Lougbégnon, T.O., Teka, O., Tente, B., 2013. Ethnobotanical study of medicinal plants used for the treatment of malaria in plateau of Allada, Benin (West Africa). Journal of Ethnopharmacology 146, 154-163.

Yff, B.T.S., Lindsey, K.L., Taylor, M.B., Erasmus, D.G., Jäger, A.K., 2002. The pharmacological screening of *Pentanisia prunelloides* and the isolation of the antibacterial compound palmitic acid. Journal of Ethnopharmacology 79, 101-107.

Young, H.A., Hodge, D.L., 2003. Interferon-γ, in: Henry, H.L., Norman, A.W. (Eds.), Encyclopedia of Hormones. Academic Press, New York, pp. 391-397.

Zhang, H., Fang, W.-T., Li, Y., Kong, Q.-H., Fang, C.-W., Luo, H., Liu, S.-J., 2024. Chemical constituents from the aerial parts of *Rubia cordifolia* L. with their NO inhibitory activity. Natural Product Research 38, 711-718.

Chapter 4 Phytochemical investigation of *Coddia rudis* (E.Mey. ex Harv.) Verdc. and *Keetia gueinzii* (Sond.) Bridson

4.1 Introduction

As shown in Chapters 2 and 3, many Rubiaceae species are used in ethnopharmacology, and many bioactive compounds have been isolated from this family. However, the phytochemistry of many species in this family has yet to be investigated. In a previous study, the chemical compositions of *Burchellia bubalina* (L.f.) Sims and *Psychotria capensis* (Eckl.) Vatke have been investigated (Moyo, 2018). The current study examined two further South African species, *Coddia rudis* (E.Mey. ex Harv.) Verdc. and *Keetia gueinzii* (Sond.) Bridson, are described.

Coddia rudis is a multi-stemmed shrub classified under the Rubiaceae. The standard English name is small bone apple, whilst the isiZulu name is umDondwane (Sepheka, 2012). The plant is aromatic and evergreen and can grow up to three metres tall. According to Ajao et al. (2019), a decoction of ground roots is taken orally as an aphrodisiac. The plant forms part of the typical browse for Nguni goats. One study found that *C. rudis* extracts did not show antibacterial activity against gram-negative and gram-positive bacteria (Okem et al., 2012). However, the ethyl acetate extract exhibited a minimum inhibitory concentration (MIC) of 0.39 mg/mL against the fungus *Candida albicans*. Aqueous extracts of *C. rudis* were shown to have anti-inflammatory properties based on a reasonably good inhibitory effect on the enzymes cyclooxygenase 1 and 2 (Okem et al., 2012).

The leaf extracts of *C. rudis* exhibited anthelmintic properties against *Caenorhabditis elegans.* The results gave a minimum lethal concentration of 0.52 mg/mL for the ethyl acetate extract and 0.008 mg/mL for the ethanol extract. According to a study by Okem et al. (2012), *C. rudis* leaf extracts contain a high level of flavonoids and gallotannins. Okem et al. (2012) assert that these flavonoids in high concentrations could explain the anti-inflammatory effects of the *C. rudis* extracts (Okem et al., 2012). In a study performed in the Eastern Cape province of South Africa, Kambizi (2014) found that *C. rudis* was one of the area's two most used plants for ethno-veterinary purposes. No compounds isolated from this species have been reported.

Keetia gueinzii is a climbing tree or shrub that can grow up to 25 meters in height (POWO, 2023). Other characteristics include dark-brown stems, branchlets at right angles, globose-shaped fruit, and an oblong-lanceolate to ovate leaf shape (Tilney and Van Wyk, 2009). Ethnobotanical uses of the plant include the consumption of the fruit. Unspecified plant parts are used in Kenya to treat malaria (Njoroge and Bussmann, 2006). The powdered root bark is inhaled to treat respiratory conditions like asthma, coughing, pneumonia, and allergies (Mailu et al., 2020). Acetone extracts of root bark resulted in a MIC of 12.5 mg/mL against the gram-positive bacteria *Bacillus cereus* and *Staphylococcus aureus* while showing no toxicity towards *Artemia salina* (Mailu et al., 2021). Acetone leaf extracts had moderate activity (MIC = 0.1-0.625 mg/mL) against *Mycobacteria smegmatis*, *M. aurum*, *M. bovis*, and *M. tuberculosis* (Aro et al., 2015). No published studies have reported the identification of compounds from *K. gueinzii*.

The phytochemical investigations of *C. rudis* and *K. gueinzii* are described below.

4.2 Materials and Methods

4.2.1 General experimental procedures

Nuclear magnetic resonance (NMR) spectra were obtained on Bruker AVANCE III spectrometers (400 or 500 MHz for ^{1}H and 100 or 125 MHz for ^{13}C) using a 5 mm BBOZ probe. The NMR solvent used was deuterated methanol (CD_3OD), obtained from Merck. The spectra were referenced to residual solvent peaks, δ_H 3.31 and δ_C 49.03 for CD_3OD. The silica used in column chromatography was Merck Millipore 0.040-0.063 mm silica gel 60 (230-400 mesh). Analytical and preparative thin-layer chromatography (TLC) was performed on pre-coated TLC silica gel 60 F_{254} (Merck) plates. Centrifugal thin-layer chromatography was performed on a model 7924 Harrison Research Chromatotron®, using circular Chromatotron™ plates coated with silica gel containing gypsum binding agent (Merck 7749). Solvents used, i.e. ethanol (EtOH), methanol (MeOH), ethyl acetate (EtOAc), dichloromethane (DCM) and hexane (Hex), were HPLC or analytical grade and were purchased from Merck. HRMS experiments were performed on a TOF Quadrupole Waters Synapt XS with an Acquity Premier UPLC, and data were analysed using the Masslynx 4.2 software. Samples for UPLC and mass spectrometry (MS) were prepared by filtration through 1 mL Phenomex Strata C8 solid-phase cartridges. The solvents used were HPLC-grade Merck products. A Bellingham and Stanley ADP440+ polarimeter was used to determine the specific rotations of compounds.

4.2.2 Plant collection

Aerial parts of *C. rudis* were obtained from The Indigenous Nursery at the SANBI KwaZulu-Natal National Botanical Garden. Andrew James, the owner of the nursery, identified the plant. A voucher specimen was prepared and deposited after being identified at the John Bews Herbarium, UKZN, South Africa. The voucher number is NU0094995. The plants were air-dried at room temperature for two weeks. Dry plant material was ground in a milling machine. The total mass of dry, ground plant material was 540 g. The material was treated as described below.

Aerial parts of *K. gueinzii* were harvested in Ashburton along the regional road R103 at coordinates -29.6739058, 30.4574798, at the Gwahumbe nature reserve. Ms Alison Young, the chief horticulturist at the botanical garden of the School of Life Sciences, UKZN, Pietermaritzburg, identified the plant. A voucher specimen was prepared and deposited after being identified at the John Bews Herbarium, UKZN, South Africa. The voucher number is NU0094992. Plant material was dried in open air at room temperature in a drying facility for two weeks. The dry plant material was ground in a mill. The mass of the ground plant material was 430 g.

4.2.3 Preliminary search for alkaloids

The first step was to perform preliminary alkaloid and cyclotide extractions according to standard protocols. To perform the alkaloid extraction, 10 g of dry, crushed bark and leaves (separately) were wetted with 15 mL of ammonium hydroxide to basify the material. The material was then macerated in 300 mL of EtOAc. After filtration, the EtOAc extract was dried under a vacuum. The dry residue was dissolved in water and acidified with 0.05 M sulfuric acid. Liquid-liquid extraction was performed with petroleum ether. The aqueous bottom layer was collected and basified with ammonium hydroxide. The solution was then extracted with chloroform. The bottom organic layer was collected and washed three times with water, dried over anhydrous sodium sulfate, and evaporated to dryness. Analytical thin-layer chromatography was performed on the residue, and visualisation was done with Dragendorff's reagent. Deep orange spots did not develop, indicating the absence of alkaloids in both plants.

4.2.4 Preliminary search for cyclotides

This method was adapted from Craik et al. (2012):

1. Macerate overnight with MeOH-DCM (1:1).

2. Filter to separate the extract from the plant material
3. Pour the extract into a separating funnel, add 5 mL of water, shake, and allow it to separate.
4. Collect the top aqueous layer and dry it under a vacuum
5. Load the aqueous layer onto a C18 flash column and elute with solvent A (0.05% 2,2,2-trifluoroacetic acid (TFA) (v/v)) mixed with increasing concentrations (25%, 50%, 75%, 100% (v/v)) of solvent B (90% acetonitrile (v/v), 0.045% TFA (v/v)). Concentrate individual fractions on a rotary evaporator and freeze dry for purification.
6. Perform analytical reverse-phase high-performance liquid chromatography (RP-HPLC), dissolve individual samples acquired during step 5 in 100% solvent A. Load dissolved samples onto a C18 column and elute with a linear gradient from 0% to 80% solvent B. Analyse via MS to detect a peak in the *m/z* region of 2.5–4 kDa.

No cyclotides were detected in the two plants.

4.2.5 Extraction of C. rudis and fractionation of crude extract

The ground aerial parts of *C. rudis* (540 g) were extracted with 2.5 L of MeOH. Extraction was repeated twice more with the same solvent, and then the plant material was extracted with EtOH-H_2O (9:1) using the same volumes. The combined extracts of each plant were dried under vacuum, yielding a mass of 39 g for *C. rudis*. The *C. rudis* crude extract was named pnm_fvh_cr.

Pnm_fvh_cr (39 g) was separated by vacuum liquid column chromatography (VLC) using DCM, followed by DCM-MeOH (1:1), and finally 100% MeOH. This fraction yielded fractions pnm_fvh_CR_A-G. Pnm_fvh_CR_F and G, 2 g and 4 g, respectively, were combined based on analytical TLC profiles and further separated by column chromatography to yield 53 fractions by using a gradient elution with EtOAc-MeOH (0-100% MeOH). Fractions 17 - 19 and 27 - 31 were combined based on similar analytical TLC profiles. For simplicity, the fractions were renamed pnm_fvh_CR_fg 6 (202 mg) and pnm_fvh_CR_fg_7 (195 mg).

Pnm_fvh_CR_fg_6 was fractionated using centrifugal thin-layer chromatography with solvent system Hex-EtOAc-MeOH (2:6:2), resulting in 6 fractions, pnm_fvh_CR_fg_6a-f. Fractions c and d were combined (61 mg) based on similar analytical TLC profiles. The sample was purified using preparative thin-layer chromatography with solvent system Hex-Acetone-

MeOH (4:4:2), yielding 21 mg of pnm_fvh_cr_cmpnd_2a, gardenoside (**126**) and 17 mg of pnm_fvh_cr_d_cmpnd_hb, astragalin (**89**).

Fraction pnm_fvh_CR_fg_7 was separated by column chromatography with a gradient solvent system EtOAc-MeOH (1:1) to 100% MeOH. Fifteen fractions were collected. Based on the TLC profiles, fractions 9 to 12 were combined (65 mg). The combined fractions were purified using preparative TLC, yielding 18 mg pnm_fvh_cr_cmpnd_3c, geniposidic acid (**127**).

4.2.6 Physical and spectroscopic data of compounds 89, 126 and 127:

Gardenoside (**126**)

Light yellow amorphous solid (21 mg)

Specific rotation $[\alpha]_D^{27}$ -103.4° (*c* = 0.22, MeOH).

^{1}H NMR spectroscopy: Table 4.1, Figure S2.3

^{13}C NMR spectroscopy: Table 4.1, Figure S2.5

UV spectroscopy: λ_{max} 236 nm (see Figure S2.2)

HR-ESI-(+)-MS: Observed 427.1231, calculated for $C_{17}H_{24}O_{11}Na$ 427.1216 (See Figure S2.1).

Geniposidic acid (**127**)

Light-yellow needles (18 mg).

Specific rotation $[\alpha]_D^{26}$ + 22.3° (*c* = 0.11, MeOH).

^{1}H NMR spectroscopy: Table 4.2, Figure S3.3.

^{13}C NMR spectroscopy: Table 4.2, Figure S3.5.

UV spectroscopy: λ_{max} 232 nm, (see Figure S3.2).

HR-ESI-(-)-MS: *m/z* 373.1131 (calc. for $C_{16}H_{21}O_{10}$ 373.1135). (Figure S3.1).

Astragalin (**89**)

Yellow amorphous solid (17 mg).

Specific rotation $[\alpha]_D^{26}$ + 21.1° (*c* = 0.17, MeOH).

^{1}H NMR spectroscopy: Figure S4.3, Table 4.3.

^{13}C NMR spectroscopy: Figure S4.5, Table 4.3.

UV spectroscopy: λ_{max} 266, 238 nm (see Figure S4.2).

HR-ESI-(-)-MS: *m/z* 447.0917 (calc. for $C_{21}H_{19}O_{11}$ 447.0927), see Figure S4.1.

4.2.7 Extraction of K. gueinzii and fractionation of crude extract

The ground aerial parts of *K. gueinzii* (430 g) were extracted with 6 L MeOH. Extraction was repeated twice with the same solvent and then the plant material was extracted with EtOH-H_2O (9:1) using the same volumes. The combined extracts were dried under vacuum, yielding a mass of 197 g for *K. gueinzii crude* extract. The *K. gueinzii* crude was labelled pnm_fvh_kg_AB.

Pnm_fvh_kg_AB (197 g) was separated by vacuum liquid column chromatography (VLC) using DCM, followed by DCM-MeOH (1:1) and finally 100% MeOH. This fraction yielded fractions pnm_fvh_kg_AB_1-9. Fraction pnm_fvh_kg_AB_7 (3 g) was subjected to column chromatography with solvent system DCM-MeOH (8:2) and yielded 27 mg of the compound pnm_fvh_kg_cmpnd _1, kaempferitrin (**255**).

4.2.8 Physical and spectroscopic data of compound 255:

Kaempferitrin (**255**)

Yellow amorphous solid (27 mg).

Specific rotation $[\alpha]_D^{31}$ -198.3° (*c* = 0.23, MeOH).

^{1}H NMR spectroscopy: Table 4.4, Figure S5.3.

^{13}C NMR spectroscopy: Table 4.4, Figure S5.5.

UV spectroscopy: λ_{max} 265, 346 nm (See Figure S5.2).

HR-ESI-(+)-MS: *m/z* of 579.1736, Calc. for $C_{27}H_{31}O_{14}$ 579.1714 (See Figure S5.1).

4.3 Results and Discussion

4.3.1 Structural elucidation of gardenoside (126) isolated from C. rudis

Compound **126** was isolated as a yellowish amorphous solid. The molecular formula ($C_{17}H_{24}O_{11}$) was determined by HR-ESI-(+)-MS, which showed an $[M+Na]^+$ ion with *m/z* 427.1231 (calculated for $C_{17}H_{24}O_{11}Na$ 427.1216), indicating six degrees of unsaturation. The mass spectrum is shown in Figure S2.3 in Appendix C. The UV-Vis spectrum (Figure S2.2) showed absorbances at λ_{max} 236 nm. The chemical structure is shown in Figure 4.2.

The ^{13}C NMR and DEPT-135 spectra (Figure S2.5 and S2.6, respectively) showed 17 carbon resonances, one methyl, two methylene, eleven methine and three non-protonated carbon atoms. Four methine carbons resonated at δ_C 71.6, 74.7, 78.0 and 78.4. The two methylene carbons had chemical shifts of δ_C 62.8 and 66.9. These chemical shifts suggested that the carbons were attached to electron-withdrawing atoms. The low-field resonances suggest that the electron-withdrawing atoms were oxygen atoms and that a sugar moiety was present in the molecule.

The chemical shifts of two methine carbons at δ_C 94.4 and 99.7 are characteristic of carbons bound to two oxygen atoms in an acetal moiety. The HSQC spectrum (Figure S2.7) showed that the two carbons are bound to protons that resonate at δ_H 5.79 (1H, d, J = 2.6 Hz) and 4.65 (1H, d, J = 7.9 Hz). Previous studies have shown that some Rubiaceae species produce iridoid glycosides (Moyo, 2018). Similar signal patterns with chemical shifts of δ_H 7.39, 5.79 and 4.65 in the ^1H NMR spectrum (Figure S2.3) are commonly observed in iridoid glycosides as a result of the presence of an enolic proton at C-3, acetal proton at C-1, and the anomeric proton of a β-glucoside, respectively. Therefore, the structure proposed here, *i.e.* an iridoid glycoside, agrees with the phytochemistry of Rubiaceae. The skeleton and numbering of an iridoid is shown in Figure 4.1.

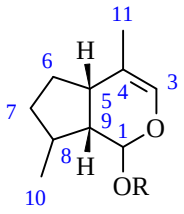

Figure 4.1. Skeleton of iridoids

In the COSY spectrum (Figure S2.4), H-1 correlated with a proton resonating at δ_H 2.62. This proton was assigned as H-9, which also correlated with a proton at δ_H 3.72 (H-5). Two signals were observed at δ_H 5.74 and 6.16. These chemical shifts are characteristic of vinylic protons. The two resonances correlated with each other and had a coupling constant of 5.8 Hz. This signified that there is a *cis*-relationship between the two protons. The signal at δ_H 6.16 showed a COSY correlation to H-5 and was assigned as H-6, whereas the resonance at δ_H 5.74 was assigned to H-7. The doublet of doublets of the vinylic protons was previously observed as the H-6 and H-7 protons of gardenoside isolated from *Burchellia bubalina* (Moyo, 2018). This led to the assignment of the compound isolated for *C. rudis* as gardenoside (**126**) (Figure 4.2).

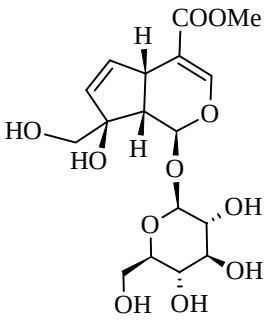

Figure 4.2: Structure of gardenoside (**126**)

Two methylene carbons observed in the DEPT spectrum (Figure S2.6) had typical alkoxy chemical shifts of δ_C 66.9 and 62.8. An HMBC correlation (Figure S2.8) between C-9 and one of the protons of the CH_2 correlating with δ_C 66.9 led to the tentative assignment of this signal as C-10. The two methylene protons had a coupling constant of J = 11.4 Hz, confirming a *geminal* coupling and the absence of a proton on the neighbouring carbon. Therefore, C-8 was proposed to be attached to a hydroxy group and C-10.

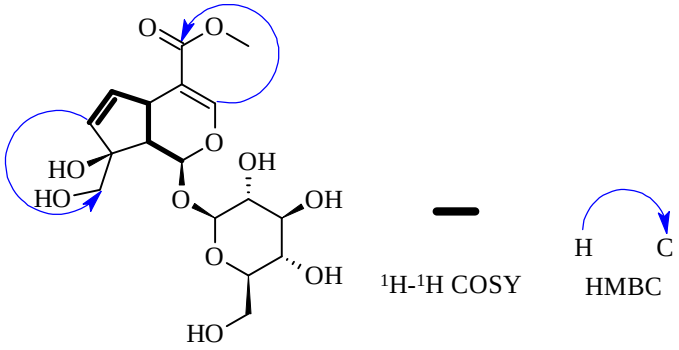

Figure 4.3: COSY and HMBC correlations observed for gardenoside (**126**)

A non-protonated carbon (δ_C 86.3) was detected by comparing the ^{13}C NMR and DEPT spectra. The signal was assigned to C-8, based on the HMBC correlation between this carbon and H-5

(Figure 4.3). A methyl signal at δ_H 3.70 is characteristic of a methyl ester. The HSQC correlation aligned this proton with a carbon resonating at δ_C 52.4. Iridoids typically have a methyl ester or carboxylic group attached to the C-4 carbon. The COSY and HMBC correlations observed for gardenoside (**126**) are shown in Figure 4.3. The NMR data were consistent with the data for gardenoside reported in the literature, (Farid et al., 2002; Ishiguro et al., 1983), as shown in Table 4.1. This is the first known report of the isolation of gardenoside from *C. rudis*.

Table 4.1: Experimental (in CD_3OD, referenced to δ_H 3.31 and δ_C 49.03) and literature NMR (in CD_3OD) chemical shift values of gardenoside (**126**)

Position	Type	Experimental values (100 and 400 MHz for δ_C and δ_H, respectively)		Literature values (Farid et al., 2002; Ishiguro et al., 1983)	
		δ_C	δ_H	δ_C	δ_H
1	sp^3, O-CH-O	94.4	5.79 (1H, d, *J* = 2.6 Hz)	93.9	5.82 (d, *J* = 2.7 Hz)
3	sp^2, CH	152.0	7.39 (1H, d, *J* = 1.4 Hz)	151.6	7.36 (d, *J* = 1.7 Hz)
4	sp^2, C	111.6		111.1	
5	sp^3, CH	38.9	3.72 (1H, m)	38.4	3.36 (m)
6	sp^2, CH	135.7	6.16 (1H, dd, *J* = 5.8, 2.8 Hz)	135.8	6.16 (dd, J = 6.0, 2.7 Hz)
7	sp^2, CH	135.9	5.74 (1H, dd, *J* = 5.8, 1.7 Hz)	135.7	5.37 (dd, J = 6.0, 1.9 Hz)
8	sp^3, C-O	86.3		85.8	
9	sp^3, CH	51.7	2.62 (1H, dd, *J* = 8.6, 2.6 Hz)	51.9	2.61 (dd)
10b	sp^3, CH_2-O	66.9	3.64, (1H, d, *J* = 11.4 Hz)	66.6	3.65 (1H, d, *J* = 11.5 Hz)
10a			3.52 (1H, d, *J* = 11.4 Hz)		3.55 (1H, d, *J* = 11.5 Hz)
11	sp^2, C=O	168.9		168.5	
12	sp^3, OCH_3	52.4	3.70 (s)	52.3	3.60 (s)
1'	sp^3, O-CH-O	99.7	4.65 (1H, d, *J* = 7.9 Hz)	99.9	4.66 (d)
2'	sp^3, CH-O	74.7	3.18 (1H, dd, *J* = 9.0, 8.0 Hz)	74.2	3.18 (t)
3'	sp^3, CH-O	71.6	3.28 (Obscured by solvent peak)	77.5	3.37 (t)
4'	sp^3, CH-O	78.4	3.31 (1H, m)	71.1	3.26 (t)
5'	sp^3, CH-O	78.0	3.36 (1H, m)	77.9	
6' a	sp^3, CH_2-O	62.8	3.89 (1H, dd, *J* = 11.9, 2.0 Hz)	62.3	3.88 & 3.66 (m)
6' b			3.68 (1H, dd, *J* = 16.2, 11.9 Hz)		

4.3.2 Structural elucidation of geniposidic acid (127) isolated from C. rudis

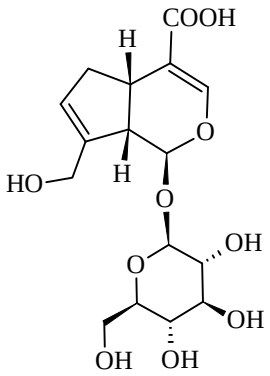

Figure 4.4: Structure of geniposidic acid (**127**)

Compound **127** was isolated as light-yellow needles. HR-ESI(-)-MS (Figure S3.1) confirmed the molecular formula, ($C_{16}H_{22}O_{10}$). An $[M-H]^-$ ion with *m/z* of 373.1131 (calculated for $C_{16}H_{21}O_{10}$, 373.1135) was observed, indicating six degrees of unsaturation. The UV-Vis spectrum (Figure S3.2) showed absorbances at λ_{max} 232 nm. The chemical structure is shown in Figure 4.4.

The ^{1}H NMR spectrum (Figure S3.3) shows some impurities resulting from gardenoside (**126**). The typical iridoid protons, that is, the enolic H-3 proton, H-1 and H-1' acetal protons were observed at δ_H 7.27, 5.08 and 4.73 in the ^{1}H NMR spectrum. The β-glucose anomeric proton was identified based on its chemical shift δ_H 4.73 and coupling constant of a doublet as J = 7.9 Hz. With these observations in mind, the compound was tentatively proposed to be an iridoid glucoside. A signal at δ_H 5.79 is characteristic of a vinylic proton. Protons H-9 and H-5 were determined by COSY correlations (Figure S3.4). A signal at δ_H 2.69 has a COSY correlation with H-1. These characteristics are typical of the H-9 proton. A COSY correlation between H-9 and a signal at δ_H 3.25 can be observed. The signal was assigned as H-5.

The DEPT spectrum (Figure S3.6) shows the compound has three methylene carbon atoms with signals at δ_C 40.0, 61.6 and 62.6. The first methylene was assigned as C-6 based on the COSY correlation of one of its protons with H-5. The vinylic proton has a COSY correlation with the C-6 proton, and, as a result, δ_H 5.79 was assigned to H-7. This implies that a double bond exists between C-7 and C-8.

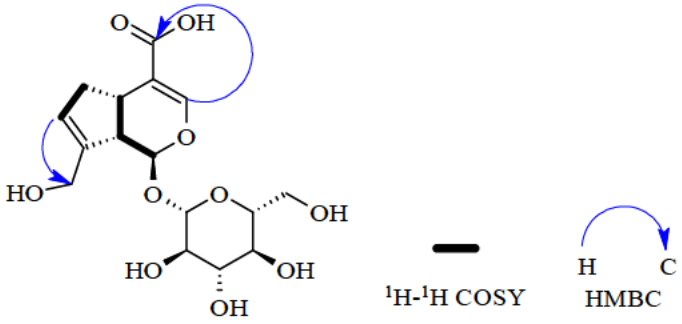

Figure 4.5: COSY and HMBC correlations oberved for geniposidic acid (**127**)

Table 4.2: Experimental (in CD_3OD, referenced to δ_H 3.31 and δ_C 49.03) and literature (in CD_3OD) NMR chemical shift values of geniposidic acid (**127**)

Position	Type	Experimental values (100 and 400 MHz for δ_C and δ_H, respectively)		Literature values in (Liang et al., 2014)	
		δ_C	δ_H	δ_C	δ_H
1	sp^3 O-CH-O	97.9	5.08 (1H, d, J = 7.7 Hz)	98.1	5.13 (1H, d, J = 5.7 Hz)
3	sp^2, CH	149.2	7.27 (1H, d, J = 0.7 Hz)	152.7	7.42 (1H, s)
4	sp^2, C	118.0		113.4	
5	sp^3, CH	37.6	3.25 (1H, m)	36.9	3.08 (1H, m)
6b	sp^3, CH_2	40.0	2.09 (1H, dddd, J = 2.2, 2.2, 7.7, 16.2 Hz)	40.1	2.14 (1H, m)
6a			2.86 (1H, dd, J = 16.2, 8.4 Hz)		2.92 (1H, m)
7	sp^2, CH	128.5	5.79 (1H, s)	128.5	5.84 (1H, s)
8	sp^2, C	144.8		145.0	
9	sp^3, CH	47.4	2.69 (1H, dd, J = 7.7 Hz)	47.3	2.92 (1H, m)
10b	sp^3, CH_2-O	61.6	4.32 (1H, d, J = 14.5 Hz)	61.6	4.37 (1H, d, J = 14.4 Hz)
10a			4.19 (1H, dd, J = 14.5, 1.7 Hz)		4.24 (1H, d, J = 14.0 Hz)
11	sp^2, C=O	175.3		172.0	
1'	sp^3 O-CH-O	100.2	4.73 (1H, d, J = 7.9 Hz)	100.3	4.24 (1H, d, J = 7.2 Hz)
2'	sp^3, CH-O	74.9	3.24 (1H, m)	75.0	3.28 (1H, m)
3'	sp^3, CH-O	77.8	3.41 (1H, m)	77.9	3.46 (1H, m)
4'	sp^3, CH-O	71.5	3.32 (1H, m)	71.6	3.29 (1H, m)
5'	sp^3, CH-O	78.2	3.29 (1H, m)	78.3	3.29 (1H, m)
6'b	sp^3, CH_2-O	62.6	3.68 (1H, m)	62.7	3.63 (1H, m)
6'a			3.85 (1H, m)		3.89 (1H, m

The second methylene carbon was determined to be C-10, based on the HMBC correlation (Figure S3.8) with H-7. Furthermore, the methylene is located downfield compared to C-6, which suggests that C-10 is bound to an electronegative atom. A hydroxy group was therefore attached at C-10. The third methylene carbon was assigned as C-6' of the glucose. The ^{13}C

NMR spectrum shows the typical carbonyl carbon chemical shift at δ_C 175.3. An HMBC correlation (Figure S3.9) between this carbon and H-3 suggests that the carbonyl is attached to C-4. The lack of a methyl signal in the region δ_H 3-4 led to the conclusion that the carbonyl is part of a carboxylic acid moiety rather than an alkyl ester group, both of which are common in iridoids. The structure of the compound was assigned as geniposidic acid (**127**). The chemical shift values of the isolated compound were compared to literature values (Liang et al., 2014), and there was a reasonable agreement, as shown in Table 4.2. The COSY and HMBC correlations are shown in Figure 4.5.

This is the first report of the isolation of geniposidic acid from *C. rudis*.

4.3.3 Structural elucidation of astragalin (89) isolate from C. rudis

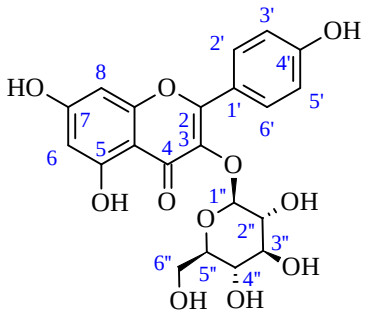

Figure 4.6: Structure of astragalin (**89**)

The compound was isolated as a light brown amorphous solid. The molecular formula, $C_{21}H_{20}O_{11}$, was confirmed by HR-ESI-(-)-MS (Figure S4.1), which showed an $[M-H]^-$ ion with *m/z* of 447.0917 (calculated for $C_{21}H_{19}O_{11}$ 447.0927). The UV-Vis spectrum (Figure S4.2) showed absorbances at λ_{max} 266 and 238 nm. The chemical structure is shown in Figure 4.6.

The ^{1}H NMR spectrum (Figure S4.3) shows a pair of doublets at δ_H 8.04 and 6.90 with a mutual coupling constant of J = 8.9 Hz, each integrating for two protons. These signals are typical of *ortho*-coupled protons on a *para*-substituted benzene (Figure 4.7). Two more doublet signals at δ_H 6.38 and 6.19, with a shared coupled constant of 1.6 Hz, each integrating for one proton, were observed. These observations suggest that the protons are *meta*-coupled on a benzene ring in a mono-substituted phloroglucinol-like structure (Figure 4.7). This arrangement is characteristic of some flavonoids.

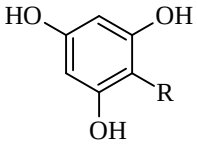

256

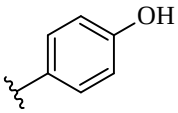

257

Figure 4.7: Structure of a monosubstituted phloroglucinol (**256**) and a *para*-substituted phenol (**257**)

Table 4.3: Experimental (in CD_3OD, referenced to δ_H 3.31 and δ_C 49.03) and literature (in DMSO-d_6) NMR chemical shift values of astragalin (**89**)

Position	Type	Experimental values (100 and 400 MHz for δ_C, and δ_H, respectively)		Literature values (Deng et al., 2009)	
		δ_C	δ_H	δ_C	δ_H
2	sp^2, C	159.1		156.9	
3	sp^2, C-O	135.4		133.7	
4	sp^2, C=O	179.3		178.0	
5	sp^2, C-O	162.8		161.7	
6	sp^2, CH	100.5	6.19 (1H, d, *J* = 1.6 Hz)	99.2	6.21 (1H, d, *J* = 1.6 Hz)
7	sp^2, C-O	167.4		164.6	
8	sp^2, CH	95.2	6.38 (1H, bs)	94.1	6.44 (1H, d, *J* = 1.6 Hz)
9	sp^2, C-O	158.6		156.8	
10	sp^2, C	105.3		104.5	
1'	sp^2, C	122.8		121.4	
2', 6'	sp^2, CH	132.3	8.04 (2H, d, *J* = 8.9 Hz)	131.4	8.05 (2H, d, *J* = 8.8 Hz
3', 5'	sp^2, CH	116.2	6.90 (2H, d, *J* = 8.9 Hz)	115.6	6.90 (2H, d, *J* = 8.8 Hz)
4'	sp^2, C-O	161.5		160.4	
1''	sp^3, O-CH-O	104.3	5.17 (1H, d, *J* = 7.3 Hz)	101.4	5.47 (1H, d, *J* = 7.6 Hz)
2''	sp^3, CH-O	75.7	3.35 (m)	74.7	*
3''	sp^3, CH-O	77.9	3.43 (m)	76.9	*
4''	sp^3, CH-O	71.3	3.33 (m)	70.4	*
5''	sp^3, CH-O	78.3	3.20 (1H, ddd, *J* = 9.6, 5.3, 2.4 Hz)	78.0	*
6''a	sp^3, CH_2-O	62.6	3.53	61.4	*
6''b			3.68		*

*HNMR chemical shifts not provided in Deng et al., 2009

The ^{13}C NMR spectrum (Figure S4.5) showed five signals at δ_C 95.2, 100.5, 105.3, 116.2 and 132.3. These signals are typical of sp^2 signals on an aromatic ring. Five more signals at δ_C 158.6, 159.1, 161.5, 162.8, and 167.4 were observed. These signals are typical of aromatic carbons bound to electronegative atoms, likely oxygen. A carbonyl chemical shift at δ_C 179.3 was also observed. The HSQC spectrum (Figure S4.6) indicates that the protons δ_H 8.04 and 6.90 are bonded to carbons resonating at δ_C 132.3 and 116.2, respectively. Based on the HSQC correlations (Figure S4.6), the protons at δ_H 6.38 and 6.19 are attached to carbons resonating

at δ_C 95.2 and 100.5, respectively. The chemical shifts and coupling constants of the proton signals at δ_H 8.04 and 6.90 are consistent with *ortho*-coupled protons on ring B of a kaempferol-type flavonoid. Building on this assumption of a flavonoid, the signals at δ_H 6.38 and 6.19 were assigned as the protons in positions H-6 and H-8 of the A ring.

The ^{13}C NMR spectrum showed the presence of five signals with chemical shifts between δ_C 60 and δ_C 80 ppm. The chemical shifts are characteristic of the oxygen-bound carbons of a glycoside. The doublet proton NMR signal at δ_H 5.17 with a coupling constant of J = 7.3 Hz occurs at the anomeric position of glucosides. An HMBC correlation (Figure S4.7) between C-3 of the flavonoid and the anomeric proton indicates that the sugar is attached at the C-3 position. Therefore, the structure of the compound was proposed to be kaempferol 3-*O*-glucoside (astragalin) (**89**) (Figure 4.6). The NMR chemical shifts were found to agree with literature values (Deng et al., 2009), as shown in Table 4.3.

This is the first known report of the isolation of astragalin from *C. rudis*.

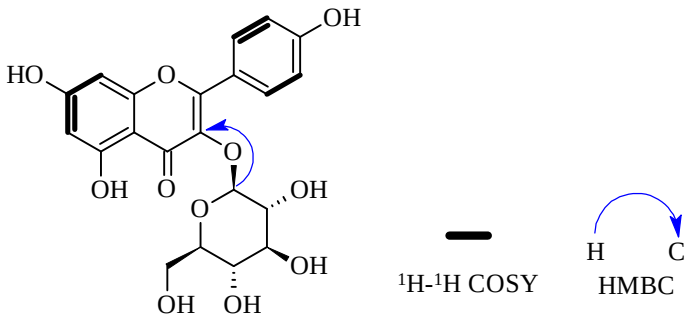

Figure 4.8: COSY and HMBC correlations oberved for astragalin (**89**)

4.3.4 Structural elucidation of kaempferitrin (255) isolated from Keetia gueinzii

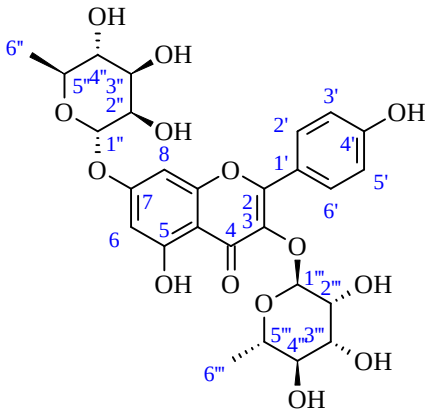

Figure 4.9: Structure of kaempferitrin (**255**)

Compound **255** was isolated from *K. gueinzii* as a yellow amorphous solid. The molecular formula ($C_{27}H_{30}O_{14}$) was determined by HR-ESI-(+)-MS (Figure S5.1), which showed an $[M+H]^+$ ion with *m/z* of 579.1736 (calculated for $C_{27}H_{31}O_{14}$, 579.1714), indicating 12 degrees of unsaturation. The UV-Vis spectrum (Figure S5.2) showed absorbances at λ_{max} 265 and 346 nm. The structure of the compound is shown in Figure 4.9.

The ^{1}H NMR spectrum (Figure S5.3) signals at δ 7.75 (2H, d, *J* = 8.7 Hz) and δ 6.86 (2H, d, *J* = 8.7 Hz) were observed. The signals suggest the presence of a *para*-substituted phenyl group, with two pairs of *ortho*-coupled chemically equivalent protons. Two more signals further upfield at δ 6.69 (1H, d, *J* = 1.9 Hz) and δ 6.44 (1H, d, *J* = 1.9 Hz) corresponded to two *meta*-coupling protons in a tetra-substituted benzene ring. This arrangement resembles a kaempferol derivative. The presence of two methine signals at δ_C 99.5 and 103.2 in the DEPT NMR spectrum (Figure S5.5) suggested the existence of two acetal moieties in the compound. Eight methine sp^3 carbons with chemical shifts at δ_C 70-75 indicated that the carbons are bonded to electronegative atoms. The high number of these methine carbons pointed to a kaempferol di-glycoside in which two sugar moieties are attached to the molecule. Two methyl signals at δ_C 17.4 and 17.8 were observed in the DEPT spectrum. The proton NMR spectrum showed the two methyls at δ 0.96 (3H, d, *J* = 6.2 Hz) and δ 1.26 (3H, d, *J* = 6.2 Hz). In the HSQC spectrum (Figure S5.6), the acetal carbons correlate with the typical anomeric proton chemical shifts at δ 5.56 (1H, s) and δ 5.37 (1H, s).

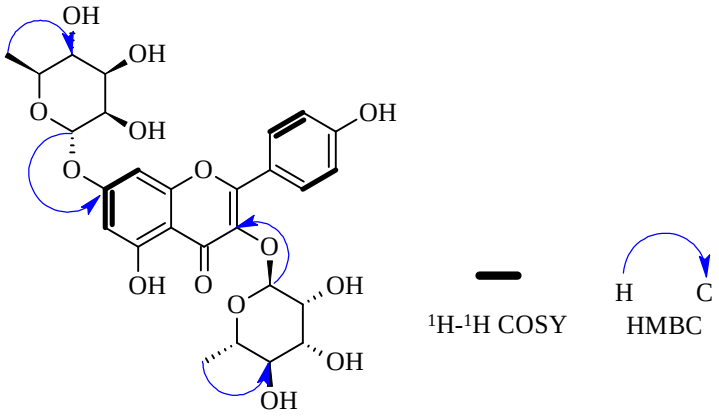

Figure 4.10: COSY and HMBC correlations observed for kaempferitrin (**255**)

Table 4.4: Experimental (in CD_3OD, referenced to δ_H 3.31 and δ_C 49.03) and literature (in CD_3OD) NMR chemical shift values of kaempferitrin (**255**)

Position	Type	Experimental values (100 and 400 MHz for δ_C, and δ_H, respectively)		Literature values (Liang et al., 2011; Valente et al., 2009)	
		δ_C	δ_H	δ_C	δ_H
2	sp^2, C	160.1		158.4	
3	sp^2, C-O	135.1		134.5	
4	sp^2, C=O	179.5		178.4	
5	sp^2, C-O	162.9		161.6	
6	sp^2, CH	100.2	6.44 (1H, d, *J* = 1.9 Hz)	98.5	6.46 (1H, d, *J* = 1.9 Hz)
7	sp^2, C-O	163.0		162.2	
8	sp^2, CH	95.3	6.69 (1H, d, *J* = 1.9 Hz)	94.2	6.80 (1H, d, *J* = 1.9 Hz)
9	sp^2, C-O	157.8		156.7	
10	sp^2, C	106.9		105.8	
1'	sp^2, C	119.8		120.7	
2', 6'	sp^2, CH	131.7	7.75 (2H, d, *J* = 8.7 Hz)	130.6	7.80 (2H, d, *J* = 8.8 Hz)
3', 5'	sp^2, CH	117.6	6.86 (2H, d, *J* = 8.7 Hz)	115.2	6.93 (2H, d, *J* = 8.8 Hz)
4'	sp^2, C-O	165.4		160.4	
1"	sp^3, O-CHO	103.2	5.37 (1H, bs)	101.9	5.30 (1H, d, *J* = 1.6 Hz)
2"	sp^3, O-CH	71.7	4.23 (1H, dd, *J* = 1.5, 3.3 Hz)	70.0	3.99 (1H, dd, *J* =1.6 and 3.2 Hz)
3"	sp^3, O-CH	71.9	3.77 (1H, dd, *J* = 3.2, 9.4 Hz)	70.3	3.47 (1H, dd, *J* = 3.2 and 8.8 Hz)
4"	sp^3, O-CH	73.0	3.33 m	71.1	3.15 (1H, t, *J* = 8.8 Hz)
5"	sp^3, O-CH	71.8	3.48 m	70.7	3.13 m
6"	sp^3, CH_3	17.4	0.96 (3H, d, *J* = 6.3 Hz)	17.5	0.81 (3H, d, *J* = 5.6 Hz)
1'"	sp^3, CH-O O	99.5	5.56 bs	98.4	5.56 (1H, d, *J* = 1.6 Hz)
2'"	sp^3, CH-O	71.4	4.04 bs	69.8	3.84 (1H, dd, *J* = 1.6 and 3.4 Hz)
3'"	sp^3, CH-O	71.8	3.85 (1H, dd, *J* = 3.3, 9.3 Hz)	70.2	3.64 (dd, *J* = 3.4 and 9.2 Hz)
4'"	sp^3, CH-O	73.3	3.49 m	71.6	3.31 (1H, t, *J* = 9.2 Hz)
5'"	sp^3, CH-O	73.6	3.67 m	70.0	3.43 m
6'"	sp^3, CH_3-	17.8	1.26 (3H, d, *J* = 6.2 Hz)	17.9	1.13 (3H, d, *J* = 6.4 Hz)
Non-hydrogenated carbon chemical shifts were estimated from HMBC correlations.					

HMBC correlations (Figure S5.7) were observed between the methyl proton at δ_H 0.96 and δ_C 71.8, and the methyl proton at δ_H 1.26 and δ_C 73.6. The methyl protons also exhibited COSY correlations (Figure S5.4) with protons resonating at δ_H 3.48 and 3.67, respectively. The HSQC spectrum shows that those protons are connected to methines resonating at δ_C 71.8 and 73.6, respectively. The chemical shifts are typical of sp^3 CH-OH carbons of a sugar. The methyl group were thus assigned to be part of the two sugars on the molecule. It was proposed that the sugars were both α-L-rhamnose due to the characteristic coupling constant of the anomeric protons. HMBC correlations between the anomeric protons and C-3 and 7 of kaempferol led to the proposal that the compound was kaempferol-3,7-*O*-α-L-dirhamnoside (kaempferitrin). The experimental NMR were compared with the literature values (Liang et al., 2011; Valente et al., 2009), as shown in Table 4.4 and confirmed to be kaempferitrin. The phytochemistry of *K. gueinzii* has not been previously reported, and this is the first report of the isolation of kaempferitrin from the species.

4.4 Significance of Findings

4.4.1 Gardenoside (126)

The anti-inflammatory effects of gardenoside (**126**) have been widely investigated. In one study, the in-vitro and in-vivo investigations aimed to determine how gardenoside influences the inflammation cascade in an osteoarthritis-induced environment (Xia et al., 2023). In the in vitro study, chondrocyte cells were obtained from male Sprague-Dawley rats and were treated with interleukin-1 beta (IL-1β). Chondrocyte cells make up cartilage and maintain the extracellular matrix. These cells are not vascularised or innervated and, as a result, are susceptible to degeneration, such as when arthritis occurs (Archer and Francis-West, 2003). IL-β is a critical factor in promoting chronic inflammatory conditions, including neurodegenerative conditions (Rong et al., 2020). IL-β also simulates the onset of osteoarthritis by promoting the production of catabolic agents that degrade the cartilage while at the same time inhibiting the production of collagen, leading to the degradation of cartilage (Xia et al., 2023). Agents that block the action of IL-1β ameliorate inflammation, including some monoclonal antibodies shown in clinical trials to attenuate rheumatoid arthritis (Alten et al., 2008; Rong et al., 2020). In their study, Xia et al. (2023) found that injecting IL-β treated chondrocytes with gardenoside (**126**) led to a significant reduction in the production of COX-2, iNOS, IL-6 and nitric oxide synthase, which are promoted by IL-β. The in vivo investigations

involved cutting the rat's right knee joint anterior cruciate ligament and treating the animals with gardenoside. The rats that did not receive treatment had reduced levels of proteoglycan and cells on the joint surface, indicating degradation. However, the gardenoside-treated group showed reduced cartilage matrix degradation (Xia et al., 2023). These results demonstrate the potential of gardenoside as a treatment for inflammatory conditions such as osteoarthritis.

In another study, the therapeutic effects of gardenoside on sciatica were investigated in an in vivo study that involved surgically constricting the sciatic nerve of male Sprague Dawley rats just enough to avoid blocking the flow of epineural blood (Austin et al., 2012; Yu et al., 2018). This model simulates sciatica in mammals. Sciatica may be described as pain radiating from the buttock region to the lower leg via the sciatic nerve path. The principal common cause of sciatica is the rupture of vertebral disc material through the annulus, leading to the compression of the sciatic nerve (Ropper and Zafonte, 2015). While there is no effective treatment for sciatica, it is one of the leading causes of neuropathic pain (Yu et al., 2018). In their study, Yu et al. (2018) measured the levels of iNOS, IL-1β, and TNF-α and the mRNA expression of P2X3 and P2X7 purinoceptors. P2X receptors are the binding sites, though adenosine triphosphate (ATP) acts as a neurotransmitter, inducing sensations such as pain (Nakatsuka and Gu, 2006). Yu et al. (2018) found that gardenoside-administered sciatic nerve-constricted rats had significantly lower levels of iNOS, IL-1β, and TNF-α ($p< 0.05$) compared to the non-treated sciatic nerve-constricted rats. Furthermore, treatment with gardenoside decreased the mRNA expression of P2X receptors compared to the non-treated group.

Another in vitro study investigated the effect of gardenoside on free fatty acid-induced steatosis in a human liver cancer cell line (HepG) (Liang et al., 2015). Steatosis is a significant event in the development of non-alcoholic fatty liver disease and is followed by hepatic injury, inflammation, and oxidative stress (Liang et al., 2015). Gardenoside was assayed for cytotoxicity and was toxic to HepG2 above 30 μM. The study was carried out using 10 and 20 μM concentrations. To induce steatosis, the cells were treated with oleic and palmitic acid over 24 hours. The triglyceride (TG) levels were measured, and it was found that gardenoside significantly lowered the TG levels by 36% and 46% at a gardenoside concentration of 10 and 20 μM, respectively. Additionally, the study showed that gardenoside reduced the levels of inflammatory cytokines TNF-α and IL-β by 51% and 46%, respectively. This is significant as it shows that gardenoside affects both stages of non-alcoholic liver disease progression.

4.4.2 Geniposidic acid (127)

An in vivo study using APP/PS1 mice as test subjects investigated the effect of geniposidic acid on amyloid-β deposition and cognitive performance (Zhou et al., 2020). APP/PS1 mice are the transgenic model for Alzheimer's disease (AD), expressing the human amyloid precursor protein and the mutant human presenilin 1. These proteins are involved in the development of AD. C57BL/6J (non-AD mice were used as a control group. Three tests were employed to investigate cognitive abilities, two of which were passive avoidance protocols. These tests assess the ability of mice to memorise events. The assay is ideal as an AD model because memory loss is one of the effects of AD.

The first test involved the use of the Morris water maze test. In this test, animals are trained to swim to a platform in a pool of water. Eventually, the platform is submerged, and the water is made opaque. The mice would have to use memory to find the platform, and the time it takes to find the platform is the escape latency. The first of the passive avoidance tests involved a step-through test where mice were placed in a box with two compartments, one dark and the other lit. The floor of the dark compartment had an electricity-conducting grid. When mice followed their propensity for dark spaces, they received an electric shock and had to escape. The other passive avoidance test included using a container with two electricity conducting bars and a wooden platform. Mice were allowed to explore the container, but once they stepped on the bars, they received an electric shock and had to step on the platform to escape. Both passive avoidance tests measured the latency period between the time at which the electric shock was administered and when the mice escaped (Zhou et al., 2020).

The Morris water maze test results showed that treating AD mice with geniposidic acid significantly reduced the escape latency period compared to the non-treated group. Both passive avoidance tests showed lower latency for the non-treated group than the geniposidic acid-treated group. The Morris water maze test results indicate a potential for geniposidic acid to improve spatial learning and cognitive capacity. These results from the passive avoidance tests demonstrate the potential for geniposidic acid to limit the effects of short-term memory loss (Zhou et al., 2020).

After 90 days of treatments, the mice were sacrificed, and their brains were analysed for histopathological and histochemical differences. To observe changes in the brain morphology, haematoxylin and eosin (H and E) staining was conducted. Zhou et al. (2020) observed that the pyramidal cells in the C57BL/6J control exhibited normal histological features with regular

arrangements of neurons. The non-treated APP/PS1 mice showed that the hippocampus and cortex had vacuolated nuclei and irregular neuronal arrangements. The geniposidic acid-treated mice showed improved neuronal function and reduced vacuolated nuclei compared to the non-treated group (Zhou et al., 2020). Proteins associated with amyloid deposition were analysed by incubating brain slices with mouse anti-β-amyloid primary antibodies. Observation with a microscope showed that while the control group showed no significant signs of amyloid-β deposits, the non-treated mice had extensive deposits of amyloid-β in the hippocampus and cortex. The regions with amyloid-β plaques in geniposidic acid-treated mice brains were significantly less than those of the non-treated mice (Zhou et al., 2020). The results of these experiments show that geniposidic acid has the potential to reduce the brain alterations that are associated with Alzheimer's disease.

Another study looked at the potential anti-atherosclerotic activity of geniposidic acid (Gao et al., 2015). The in vivo investigation involved the use of rabbits as test subjects. The rabbits were grouped into three main groups based on feed over twelve weeks. The normal group was given a basal diet, the first model group (control group) was fed a high-cholesterol diet, and the geniposidic acid group was fed a high-cholesterol diet in combination with geniposidic acid at different concentrations (80, 160, and 240 mg/kg). The rabbits were killed, and a segment of the aorta was surgically removed. The aorta segment was examined to determine differences in the aortic plaque area, intimal/medial thickness, and foam cell number.

The high-cholesterol diet rabbit aortas were observed to have white plaque covering the arterial wall, and the intima was lesioned. Furthermore, it was observed that a significant accumulation of foam cells had occurred, adding to the thickening of the aortic intima. Examination of the aorta segments from the geniposidic acid sub-groups (160 and 240 mg/kg) revealed a significant reduction in plaque thickness and foam cell accumulation and a smoother aortic intima. Additionally, cell cultures that were performed during the study showed that geniposidic acid promotes the proliferation of human umbilical vein endothelial cells (HUVEC) while inhibiting the proliferation of the human umbilical artery smooth cells (HUASC) (Gao et al., 2015). HUASCs promote atherosclerotic plaque formation. The results show the potential effectiveness of geniposidic acid in preventing damage to blood vessels and restoring the vessel structure damaged due to atherosclerosis.

4.4.3 Astragalin (89)

A study explored the anti-candidal potential of astragalin (Ivanov et al., 2020). Parameters that were investigated include the MIC of astragalin against *Candida albicans*, the antibiofilm activity, interference with the ERG11 gene and lanosterol 14–α demethylase (CYP51) enzyme, and its effect on CDR1 expression. The ERG11 gene encodes CYP51 enzyme. The enzyme influences membrane permeability by demethylating lanosterol to form ergosterol (Zhang et al., 2019). Azole drugs target the enzyme, preventing this from happening. Ergosterol is an essential component of fungal membranes and is crucial for survival (Jordá and Puig, 2020).

Using serial dilution and 24 hours of incubation, Ivanov et al. (2020) determined the MIC and MFC to be 0.075±0.002 and 0.15±0.01 mg/mL, respectively, for four strains of *C. albicans*. They also measured the MIC of astragalin and amphotericin B in the presence and absence of exogenous ergosterol. They found that the MIC of amphotericin B was tripled in the presence of ergosterol, whereas that of astragalin had no significant change. The study also investigated the difference in the UV-visible spectral response of free CYP51 enzyme compared to the response of the enzyme in the presence of astragalin. The spectral response did not show any differences. These two experiments show that astragalin does not interfere with the ergosterol biosynthetic pathway as a mode of action. This is important as it shows the potential of astragalin to inhibit fungi that have developed resistance towards azole-based compounds. Additionally, the study revealed that astragalin reduces the expression of the fungal CDR1 gene that encodes efflux pumps. The efflux pumps contribute to drug resistance by removing drugs from fungal cells (Kumar and Jha, 2017).

Qu et al. (2016) studied the potential of astragalin to ameliorate myocardial injury. The in vivo investigation used adult male Sprague-Dawley rats separated into five groups. After killing, the hearts of the rats were removed and treated according to the group parameters. The control group's hearts perfused throughout 90 minutes; the ischemia group was subjected to zero-flow ischemia followed by reperfusion. Ischemia refers to restricting blood flow to organs, whereas reperfusion is restoring blood flow. Three astragalin groups were treated with K-H buffer solution containing concentrations of astragalin 5, 10 and 20 μmol/L followed by ischemia and reperfusion. The results showed that the astragalin-treated hearts restored functionality significantly more than the ischemia group, measured by the left ventricular developed pressure and coronary flow (Qu et al., 2016).

The study also revealed that the levels of lactate dehydrogenase (LDH) and creatine kinase (CK) were significantly lower in the astragalin-treated groups compared to the ischemia group. This is significant as elevated LDH and CK levels are indicators of myocardial infarction. H and E stain showed that heart muscles, oedema, necrosis, fractures, and degeneration were absent in the control group. The ischemia group exhibited all these conditions. However, the astragalin-treated group showed a significant damage reduction compared to the ischemia group (Qu et al., 2016). These results point to the potential cardioprotective properties of astragalin.

4.4.4 Kaempferitrin (255)

Alonso-Castro et al. (2012) found that kaempferitrin is the principal active constituent of an antitumour active extract of *Justicia spicigera*. *J. spicigera* is used in Mexico for the treatment of cervical cancer. Alonso-Castro et al. (2013) investigated the cytotoxicity of kaempferitrin towards HeLa cells. The investigation included in vitro and in vivo components. The in vitro experiments included the use of the MTT assay to evaluate cytotoxicity, the terminal deoxynucleotidyl transferase dUTP nick end labelling (TUNEL assay) to determine the ability of kaempferitrin to induce apoptosis, detection of reactive oxygen species (ROS), using flow cytometry and cell cycle analysis. The in vivo component involved the subcutaneous injection of HeLa cells into the back of NU/NU mice. The mice were then dosed with kaempferitrin followed by examining the chemo-preventative and anti-tumour capacity of the compound. Kaempferitrin had an IC_{50} of 45±2.6 μM against HeLa cells compared to 2.3±0.1 and 0.1±0.001 μM for cisplatin and paclitaxel, respectively. Against non-tumour HaCaT, kaempferitrin had an IC_{50} of 177±7.9 μM, compared to 8.9±1.1 and 0.5±0.1 μM for cisplatin and paclitaxel, respectively.

The TUNEL test showed that HeLa cells treated with 45 μM kaempferitrin exhibited significant chromatin condensation and DNA fragmentation, indicating apoptosis. Treatment of HeLa cells with kaempferitrin also increased levels of cyclin-dependent kinase inhibitor proteins p16 and p21 while reducing Cyclin D1. Kinases are critical in cancer development as they can mutate and cause cell anomalies that lead to cancerous growths (Cicenas et al., 2018). Cyclin D1 upregulation is linked to the progression of cancer (Chen and Li, 2022). While the apoptosis inhibiting protein kinase B (Akt) levels were not influenced by kaempferitrin treatment of HeLa cells, production of the other anti-apoptotic protein, B-cell lymphoma 2 protein, was reduced.

The apoptosis-promoting tumour protein P53, p53 upregulated modulator of apoptosis protein, and Bcl-2-associated death promoter protein were upregulated after kaempferitrin treatment. The chemo-preventative effects of kaempferitrin were impressive at 87% and 97% inhibition of tumour growth at 10 and 25 mg/kg, respectively, in mice treated four hours after tumour implantation. Cisplatin and paclitaxel inhibited growth by 99% and 98% at a dose of 1 mg/kg. These results support the anti-cancer potential of kaempferitrin.

4.5 Conclusion

The isolation of known pharmacologically active compounds from *C. rudis* and *K. gueinzii* supports using plant species for medicinal purposes. The isolated compounds' anti-inflammatory, neuroprotective and anti-cancer activities are consistent with the findings of the literature, which show that other Rubiaceae plants exhibit these activities, as discussed in Chapter 3. However, more investigations need to be carried out to understand how the bioactivities of the compounds influence the disease conditions for which the plants are traditionally applied. For instance, the aphrodisiac properties of *C. rudis* need to be investigated in a controlled laboratory environment, and the active agent must be identified. In future studies, bioassay-guided fractionation of *K. gueinzii* extracts could be performed to identify the active compounds with antimalarial and antimicrobial activities reported in the literature.

4.6 References

Ajao, A.A., Sibiya, N.P., Moteetee, A.N., 2019. Sexual prowess from nature: A systematic review of medicinal plants used as aphrodisiacs and sexual dysfunction in sub-Saharan Africa. South African Journal of Botany 122, 342-359.

Alonso-Castro, A.J., Ortiz-Sánchez, E., Domínguez, F., Arana-Argáez, V., del Carmen Juárez-Vázquez, M., Chávez, M., Carranza-Álvarez, C., Gaspar-Ramírez, O., Espinosa-Reyes, G., López-Toledo, G., 2012. Antitumor and immunomodulatory effects of *Justicia spicigera* Schltdl (Acanthaceae). Journal of Ethnopharmacology 141(3), 888-894.

Alonso-Castro, A.J., Ortiz-Sánchez, E., García-Regalado, A., Ruiz, G., Núñez-Martínez, J.M., González-Sánchez, I., Quintanar-Jurado, V., Morales-Sánchez, E., Dominguez, F., López-Toledo, G., Cerbón, M.A., García-Carrancá, A., 2013. Kaempferitrin induces apoptosis via intrinsic pathway in HeLa cells and exerts antitumor effects. Journal of Ethnopharmacology 145(2), 476-489.

Alten, R., Gram, H., Joosten, L.A., Berg, W.B.v.d., Sieper, J., Wassenberg, S., Burmester, G., van Riel, P., Diaz-Lorente, M., Bruin, G.J.M., Woodworth, T.G., Rordorf, C., Batard, Y., Wright, A.M., Jung, T., 2008. The human anti-IL-1β monoclonal antibody ACZ885 is effective in joint inflammation models in mice

and in a proof-of-concept study in patients with rheumatoid arthritis. Arthritis Research & Therapy 10(3), R67.

Archer, C.W., Francis-West, P., 2003. The chondrocyte. The International Journal of Biochemistry & Cell Biology 35(4), 401-404.

Aro, A.O., Dzoyem, J.P., Hlokwe, T.M., Madoroba, E., Eloff, J.N., McGaw, L.J., 2015. Some South African Rubiaceae tree leaf extracts have antimycobacterial activity against pathogenic and non-pathogenic *Mycobacterium* species. Phytotherapy Research 29(7), 1004-1010.

Austin, P.J., Wu, A., Moalem-Taylor, G., 2012. Chronic constriction of the sciatic nerve and pain hypersensitivity testing in rats. Journal of Visualized Experiments(61), e3393.

Chen, S., Li, L., 2022. Degradation strategy of cyclin D1 in cancer cells and the potential clinical application. Frontiers in Oncology 12, 949688.

Cicenas, J., Zalyte, E., Bairoch, A., Gaudet, P., 2018. Kinases and cancer. Cancers (Basel) 10(3), 63.

Craik, D.J., Henriques, S.T., Mylne, J.S., Wang, C.K., 2012. Chapter Three - Cyclotide Isolation and Characterization, in: Hopwood, D.A. (Ed.) Methods in Enzymology. Academic Press, pp. 37-62.

Deng, S., Deng, Z., Fan, Y., Peng, Y., Li, J., Xiong, D., Liu, R., 2009. Isolation and purification of three flavonoid glycosides from the leaves of *Nelumbo nucifera* (Lotus) by high-speed counter-current chromatography. Journal of Chromatography B 877(24), 2487-2492.

Farid, H.A., Kunert, O., Haslinger, E., Seger, C., 2002. Isolation and structure elucidation of iridoide and coumarin derivatives from *Xeromphis nilotica* (Rubiaceae). Monatshefte Für Chemie/Chemical Monthly 133, 1453-1458.

Gao, Y., Chen, Z.-y., Liang, X., Xie, C., Chen, Y.-f., 2015. Anti-atherosclerotic effect of geniposidic acid in a rabbit model and related cellular mechanisms. Pharmaceutical Biology 53(2), 280-285.

Ishiguro, K., Yamaki, M., Takagi, S., 1983. Studies on iridoid-related compounds, II. The structure and antimicrobial activity of aglucones of galioside and gardenoside. Journal of Natural Products 46(4), 532-536.

Ivanov, M., Kannan, A., Stojkovic, D., Glamoclija, J., Grdadolnik, S.G., Sanglard, D., Sokovic, M., 2020. Revealing the astragalin mode of anticandidal action. Experimental and Clinical Sciences Journal 19, 1436.

Jordá, T., Puig, S., 2020. Regulation of ergosterol biosynthesis in *Saccharomyces cerevisiae*. Genes (Basel) 11(7), 795.

Kambizi, L., 2014. Indigenous plants for ethnoveterinary uses in the Pondoland, South Africa, XXIX International Horticultural Congress on Horticulture: Sustaining Lives, Livelihoods and Landscapes (IHC2014): V World 1125. pp. 309-314.

Kumar, A., Jha, A., 2017. Chapter 5 - Multidrug resistance and transporters, in: Kumar, A., Jha, A. (Eds.), Anticandidal Agents. Academic Press, pp. 49-54.

Liang, H., Zhang, L., Wang, H., Tang, J., Yang, J., Wu, C., Chen, S., 2015. Inhibitory effect of gardenoside on free fatty acid-induced steatosis in HepG2 hepatocytes. International Journal of Molecular Sciences 16(11), 27749-27756.

Liang, Y., Wei, L., Zhu, Z., Pan, Y., Wang, H., Liu, P., 2011. Isolation and purification of kaempferol-3,7-O-α-L-dirhamnopyranoside from *Siraitia grosvenori* leaves by high-speed counter-current chromatography and its free radical scavenging activity. Separation Science and Technology 46(9), 1528-1533.

Liang, Z., Yang, M., Xu, X., Xie, Z., Huang, J., Li, X., Yang, D., 2014. Isolation and purification of geniposide, crocin-1, and geniposidic acid from the fruit of *Gardenia jasminoides* Ellis by high-speed counter-current chromatography. Separation Science and Technology 49(9), 1427-1433.

Mailu, J.K., Nguta, J.M., Mbaria, J.M., Okumu, M.O., 2020. Medicinal plants used in managing diseases of the respiratory system among the Luo community: an appraisal of Kisumu East Sub-County, Kenya. Chinese Medicine 15(1), 95.

Mailu, J.K., Nguta, J.M., Mbaria, J.M., Okumu, M.O., 2021. Qualitative and quantitative phytochemical composition, antimicrobial activity, and brine shrimp cytotoxicity of different solvent extracts of *Acanthus polystachyus*, *Keetia gueinzii*, and *Rhynchosia elegans*. Future Journal of Pharmaceutical Sciences 7, 195.

Moyo, P.N., 2018. Phytochemistry of some Rubiaceae plants, Master of Science Dissertation, University of KwaZulu-Natal, Pietermaritzburg.

Nakatsuka, T., Gu, J.G., 2006. P2X purinoceptors and sensory transmission. Pflügers Archiv 452(5), 598-607.

Njoroge, G.N., Bussmann, R.W., 2006. Diversity and utilization of antimalarial ethnophytotherapeutic remedies among the Kikuyus (Central Kenya). Journal of Ethnobiology and Ethnomedicine 2(1), 8.

Okem, A., Finnie, J., Van Staden, J., 2012. Pharmacological, genotoxic and phytochemical properties of selected South African medicinal plants used in treating stomach-related ailments. Journal of Ethnopharmacology 139(3), 712-720.

POWO, 2023. Plants of the World Online. Royal Botanic Gardens, Kew, On the Internet.

Qu, D., Han, J., Ren, H., Yang, W., Zhang, X., Zheng, Q., Wang, D., 2016. Cardioprotective effects of astragalin against myocardial ischemia/reperfusion injury in isolated rat heart. Oxidative Medicine and Cellular Longevity 2016, 8194690.

Rong, H., He, X., Wang, L., Bai, M., Jin, T., Wang, Y., Yang, W., He, Y., Yuan, D., 2020. Association between IL1B polymorphisms and the risk of rheumatoid arthritis. International Immunopharmacology 83, 106401.

Ropper, A.H., Zafonte, R.D., 2015. Sciatica. New England Journal of Medicine 372(13), 1240-1248.

Sepheka, W.K., 2012. *Coddia rudis* (E.Mey. ex Harv.) Verdc. http://pza.sanbi.org/*coddia-rudis*. (Accessed 18-06 2021).

Tilney, P.M., Van Wyk, A., 2009. Taxonomy of the genus *Keetia* (Rubiaceae-subfam. Ixoroideae-tribe Vanguerieae) in southern Africa, with notes on bacterial symbiosis as well as the structure of colleters and the 'stylar head'complex. Bothalia 39(2), 165-175.

Valente, L.M., Bizarri, C.H., Liechocki, S., Barboza, R.S., Paixão, D.d., Almeida, M.B.S., Benevides, P.J., Magalhães, A., Siani, A.C., 2009. Kaempferitrin from *Uncaria guianensis* (Rubiaceae) and its potential as a chemical marker for the species. Journal of the Brazilian Chemical Society 20, 1041-1045.

Xia, T., Zhao, R., He, S., Wang, L., Fu, X., Zhao, Y., Qiao, S., An, J., 2023. Gardenoside ameliorates inflammation and inhibits ECM degradation in IL-1β-treated rat chondrocytes via suppressing NF-κB signaling pathways. Biochemical and Biophysical Research Communications 640, 164-172.

Yu, M., Su, B., Zhang, X., 2018. Gardenoside suppresses the pain in rats model of chronic constriction injury by regulating the P2X3 and P2X7 receptors. Journal of Receptors and Signal Transduction 38(3), 198-203.

Zhang, J., Li, L., Lv, Q., Yan, L., Wang, Y., Jiang, Y., 2019. The fungal CYP51s: their functions, structures, related drug resistance, and inhibitors. Frontiers in Microbiology 10, 691.

Zhou, Z., Hou, J., Mo, Y., Ren, M., Yang, G., Qu, Z., Hu, Y., 2020. Geniposidic acid ameliorates spatial learning and memory deficits and alleviates neuroinflammation via inhibiting HMGB-1 and downregulating TLR4/2 signaling pathway in APP/PS1 mice. European Journal of Pharmacology 869, 172857.

Chapter 5 Phytochemical investigation of *Curtisia dentata* (Burm.f.) C.A.Sm.

5.1 Introduction

Curtisia dentata (Burm.f.) C.A.Sm., the solitary representative of the genus *Curtisia* and the family Curtisiaceae, is native to South Africa and Zimbabwe (Manchester et al., 2007). The local names for the plants include assegaai (Afrikaans), usirayi (isiXhosa), umlahleni (isiZulu) and musangwe (chiVenda) (Doughari et al., 2012). The Angiosperm Phylogeny Group III places the Curtisiaceae in the order of the Cornales. Other families in this order include the more prominent families of Cornaceae, Hydrangeaceae, and Loasaceae. The smaller families are the Grubbiaceae and Hydrostachyaceae (Berry, 2013). Seven other southern African species belong to the Cornales order, namely *Kissenia capensis* Endl., *Grubbia rosmarinifolia* P. J. Bergius, *Grubbia tomentosa* (Thunb.) Harms, *Grubbia rourkei* Carlquist, *Hydrostachys insignis* Mildbr. & Reimers, *Hydrostachys polymorpha* Klotzsch, and *Hydrostachys triaxialis* Engl. & Gilg (POWO, 2023). *C. dentata* is a protected species in South Africa as its populations are diminishing (Bih et al., 2023).

The bark of *C. dentata* is sold as an herbal medicine across South Africa (Maroyi, 2019). A decoction of the bark is used in the Eastern Cape to treat diabetes, stomach ailments, hypertension, pimples and other skin-related conditions and for weight loss (Afolayan and Mbaebie, 2010; Grierson and Afolayan, 1999; Raletsena et al., 2023). The bark is also used to treat stomach ailments like diarrhoea and as an aphrodisiac (Hutchings et al., 1996). A decoction of *C. dentata* and *Rapanea melanophloeos* barks is administered to treat cowdriosis, an infectious fatal tickborne disease that affects ruminants (Dold and Cocks, 2001). Other ethnopharmacological applications of *C. dentata* include the use of decoctions of leaves, bark and roots to treat cancer (Koduru et al., 2007).

Phytochemical investigations on *C. dentata* have resulted in the isolation of lupeol (**159**), betulinic acid (**174**), 2α-hydroxyursolic acid and ursolic acid (**158**) from the leaves (Shai et al., 2008). Other phytochemicals that have been isolated include betulinaldehyde, stigmasterol (**204**), β-sitosterol (**205**), *n*-tetracosanol and *n*-hexadecanoic acid from the stem bark (Van Wyk, 2020). Isoeugenol has been detected in the Hex extracts, and a seasonal variation in secondary metabolite concentration has been observed in the bark (van Wyk and Prinsloo,

2021). Bioactive iridoid glycosides have been isolated from members of the Cornaceae (Hao et al., 2023), Hydrangeacea (Gousiadou et al., 2016), and Loasaceae (Rodríguez et al., 2002).

Dichloromethane, acetone and MeOH leaf extracts of *C. dentata* had MIC values of 0.11, 0.21 and 0.50 mg/mL, respectively, against *Candida albicans* with selectivity indices less than 1 for the DCM and acetone extracts (Shai et al., 2008). The methanolic extract of the bark was shown to reduce the concentration of the mycotoxin aflatoxin B1 (AFB_1) in a detoxification assay by 71.1% compared to 57.8% in the control (AFB_1 + MeOH) after 48 hours (Kalemba et al., 2024). The ethnopharmacology, phytochemistry, and bioactivities of *C. dentata* have been reviewed in depth, including its antibacterial, anthelminthic, anti-inflammatory, antioxidant, cytotoxicity and glucose utilization activities (Maroyi, 2019; Raletsena et al., 2023).

5.2 Materials and Methods

5.2.1 General experimental procedures

Nuclear magnetic resonance (NMR) spectra were obtained on Bruker AVANCE III spectrometers (400 or 500 MHz for ^{1}H and 100 or 125 MHz for ^{13}C) using a 5 mm BBOZ probe. The NMR solvent used was deuterated methanol (CD_3OD), obtained from Merck. The spectra were referenced to residual solvent peaks, δ_H 3.31 and δ_C 49.03 for CD_3OD. The silica used in column chromatography was Merck Millipore 0.040-0.063 mm silica gel 60 (230-400 mesh). Analytical and preparative thin-layer chromatography (TLC) was performed on pre-coated TLC silica gel 60 F_{254} (Merck) plates. Centrifugal thin-layer chromatography was performed on a model 7924 Harrison Research Chromatotron®, using circular Chromatotron™ plates coated with silica gel containing gypsum binding agent (Merck 7749). Solvents used, i.e. ethanol (EtOH), methanol (MeOH), ethyl acetate (EtOAc), dichloromethane (DCM) and hexane (Hex), were HPLC or analytical grade and were purchased from Merck. HRMS experiments were performed on a TOF Quadrupole Waters Synapt XS with an Acquity Premier UPLC, and data were analysed using the Masslynx 4.2 software. Samples for UPLC and mass spectrometry (MS) were prepared by filtration through 1 mL Phenomex Strata C8 solid-phase cartridges. The solvents used were HPLC-grade Merck products. A Bellingham and Stanley ADP440+ polarimeter was used in optical rotation experiments.

5.2.2 Plant collection

The bark and aerial parts of *C. dentata* were collected from the University of KwaZulu-Natal (UKZN) Life Science Botanical Garden on the Pietermaritzburg campus. A voucher specimen

was prepared and deposited after being identified at the Bews Herbarium, UKZN, South Africa. The voucher number is NU0094993. Leaves and bark were air-dried at room temperature and ground separately in a mill.

5.2.3 Preliminary search for alkaloids

The first step was to perform preliminary alkaloid and cyclotide extractions according to standard protocols. To perform the alkaloid extraction, 10 g of dry, crushed bark and leaves (separately) were wetted with 15 mL of ammonium hydroxide to basify the material. The material was then macerated in 300 mL EtOAc. After filtration, the EtOAc extract was dried under a vacuum. The dry residue was dissolved in water and acidified with 0.05 M sulfuric acid. Liquid-liquid extraction was performed with petroleum ether. The aqueous bottom layer was collected and basified with ammonium hydroxide. The solution was then extracted with chloroform. The bottom organic layer was collected and washed three times with water, dried over anhydrous sodium sulfate, and evaporated to dryness. Analytical thin-layer chromatography was performed on the residue, and visualisation was done with Dragendorff's reagent. No deep orange spots were observed, indicating the absence of alkaloids.

5.2.4 Preliminary search for cyclotides

This method was adapted from Craik et al. (2012).

1. Macerate overnight with MeOH-DCM (1:1).
2. Filter to separate the extract from the plant material.
3. Pour the extract into a separating funnel and add 5 mL of water, shake, and allow it to separate.
4. Collect the top aqueous layer and dry it under vacuum.
5. Load the aqueous layer onto a C18 flash column and elute with solvent A (0.05% 2,2,2-trifluoroacetic acid (TFA) (v/v)) mixed with increasing concentrations (25%, 50%, 75%, 100% (v/v)) of solvent B (90% acetonitrile (v/v), 0.045% TFA (v/v)). Concentrate individual fractions on a rotary evaporator and freeze dry for purification.
6. Perform analytical reverse-phase high-performance liquid chromatography (RP-HPLC), dissolve individual samples acquired during step 5 in 100% solvent A. Load dissolved samples onto a C18 column and elute with a linear gradient from 0% to 80%

solvent B. Analyse by mass spectrometry to detect a peak in the *m/z* region of 2.5–4 kDa.

The search for cyclotides in the extracts did not yield any isolated compounds.

5.2.5 Extraction of C. dentata and fractionation of crude extracts

Two hundred and thirty grams of ground bark and 760 g of ground aerial parts were macerated overnight in 2.5 L and 6 L of MeOH, respectively. Maceration was repeated twice with the same solvent, and then the plant material was extracted with EtOH-H_2O (9:1). The extracts were combined and dried under vacuum, yielding masses of 19 g of pnm_fvh_curtd_bark_crude from the bark and 65 g of pnm_fvh_curtd_leaves_crude from the aerial parts.

The bark extract was fractionated in a vacuum liquid chromatography column, and four fractions were obtained (a-d). Elution with Hex-DCM (1:1) yielded pnm_fvh_curtd_bark_a (3.11 g). The DCM-EtOAc (1:1) fraction yielded pnm_fvh_curtd_bark_b (4.97 g)). Elution with 100% EtOAc and MeOH each yielded pnm_fvh_curtd_bark_c (5.09 g) and pnm_fvh_curtd_bark_d (5.21 g), respectively. Fraction pnm_fvh_curtd_bark_c (5.09 g) was separated by column chromatography using gradient elution $CHCl_3$-MeOH, 0% - 100% MeOH. Sixteen fractions were generated. Fraction pnm_fvh_curtd_bark_c_7 (160 mg) was stored and combined with leaf extract fractions with comparable TLC profiles.

Fraction d was separated in a chromatography column using gradient elution with $CHCl_3$-MeOH, 0% - 100% MeOH. This resulted in 6 fractions pnm_fvh_curtd_bark_d 1-6 with the following masses (mg): 650, 730, 903, 818, 712 and 619, respectively. Fractions d_3 and d_4 were combined based on similarity of TLC profiles. Further column chromatography fractionation was performed with solvent systems Hex-$CHCl_3$-MeOH (2:7:1), (0:9:1), (2:6:2) and (0:8:2), consecutively. This yielded 37 mg of pnm_fvh_curtd_bark_compnd_1 (**258**) and 30 mg of pnm_fvh_curtd_bark_cmpnd_2 (**259**)

The crude leaf extract was fractionated by VLC to give four fractions (A-D). DCM-EtOAc (1:1) yielded pnm_fvh_curtd_leaves_a (18.3 g). Elution with EtOAc (100%), EtOAc-MeOH (1:1) and MeOH each yielded pnm_fvh_curtd_leaves_b (15.1 g), pnm_fvh_curtd_leaves_c (13.6 g) and pnm_fvh_curtd_leaves_d (14.4 g), respectively.

Fraction pnm_fvh_curtd_leaves_c (13.6 g) was separated by column chromatography using gradient elution DCM-EtOAc, 50% - 100% EtOAc, and EtOAc-MeOH, 0 - 100% MeOH. This

yielded 26 fractions pnm_fvh_curtd_leaves_C_1-26. Based on similar analytical TLC profiles, fractions 13-15 (322 mg) were combined with fraction pnm_fvh_curtd_bark_c_7 (160 mg) from the bark. They formed a fraction named pnm_fvh_curtd_bark_leaves.

Fraction pnm_fvh_curtd_bark_leaves (480 mg) was separated using gradient elution EtOAc-MeOH, 0% - 100% MeOH. Twenty-eight fractions were generated. Fractions 21 to 26 were combined (55 mg) and purified by preparative TLC using solvent systems Hex-Acetone-MeOH (5:4:1) followed by 2:7:1 composition, yielding 14 mg of pnm_fvh_curtd_bark_leaves_iridoid_2 (**118**).

Fractions pnm_fvh_curtd_leaves_c_19 to 24 (150 mg) were combined and separated by preparative TLC using solvent systems Hex-Acetone-MeOH (5:4:1) followed by 2:7:1. This resulted in the isolation of 9 mg of pnm_fvh_curtd_u34b (**263**) and 12 mg pnm_fvh_curtd_leaves_ce51D (**133**).

Fraction pnm_fvh_curtd_leaves_d (14.4 g) was separated by gradient elution $CHCl_3$-MeOH, 0% - 100% MeOH in a chromatography column. This produced 27 fractions. Fractions 13 to 19 were combined into one sample, pnm_fvh_curtd_etohh2o_567 c6d4 (51 mg), and fractions 20 to 25 were combined into pnm_fvh_curtd_leaves_c4c5_b1 (66 mg). These two fractions were each separated by preparative TLC using solvent systems Hex-Acetone-MeOH (5:4:1), 2:7:1, and 0:9:1. This fractionation produced compounds pnm_fvh_curtd_etohh2o_567_c6d4_456_f_56 (**116**) with a mass of 3 mg and pnm_fvh_curtd_leaves_c4c5_b1_k (**262**) with a mass of 25 mg. Part of compound **116** was lost due to a broken vial.

5.2.6 Physical and spectroscopic data of isolated compounds

Phlorizin (**259**)

Yellow powder (30 mg)

Specific rotation $[\alpha]_D^{27}$ -56.17 (*c* = 0.11, MeOH).

^{1}H NMR spectroscopy: See Table 5.1, Fig S6.4.

^{13}C NMR spectroscopy: See Table 5.1, Figure S6.6.

UV spectroscopy: λ_{max} 222 and 286 nm (see Figure S6.2).

IR spectroscopy: IR ν_{max}, (see Figure S6.3) MeOH (cm^{-1}) 3347, 2931, 1604, 1552.

HR-ESI-(+)-MS: *m/z* of 459.1288 (calculated for $C_{21}H_{24}O_{10}Na$ 459.1267). See S6.1.

(+)-catechin (**258**)

Brown powder (37 mg)

Specific rotation, $[\alpha]_D^{25}$ +23.2° (*c* = 0.08, MeOH).

^{1}H NMR spectroscopy: See Table 5.2, Figure S7.4.

^{13}C NMR spectroscopy: See Table 5.2, Figure S7.6.

UV spectroscopy: λ_{max} 279 nm (see Figure S7.2)

IR spectroscopy: IR ν_{max}, MeOH (cm^{-1}) 3223, 2938, 1614, 1460 (see Figure S7.3).

HR-ESI-(+)-MS: *m/z* of 291.0883 (calculated for $C_{15}H_{15}O_6$ 291.0869). See S7.1.

Loganic acid (**116**)

Yellow amorphous solid (14 mg)

Specific rotation, $[\alpha]_D^{23}$ -86.2° (*c* = 0.21, MeOH).

^{1}H NMR spectroscopy: See Table 5.3, Figure S8.3.

DEPT-135 NMR spectroscopy: See Table 5.3, Figure S8.5.

UV spectroscopy: λ_{max} 230 nm (see Figure S8.2)

HR-ESI-(+)-MS: *m/z* of 399.1282 (calculated for $C_{16}H_{24}O_{10}Na$ 399.1267). See S8.1.

Geniposide (**131**)

Yellow amorphic solid (12 mg)

Specific rotation $[\alpha]_D^{27}$ -15.91 (*c* = 0.15, MeOH).

^{1}H NMR spectroscopy: See Table 5.4, Figure S9.3.

DEPT-135 NMR spectroscopy: See Table 5.4, Figure S9.5.

UV spectroscopy: λ_{max} 240 nm (see Figure S9.2).

HR-ESI-(+)-MS: *m/z* 411.1279 (calculated for $C_{17}H_{24}O_{10}Na$ 411.1267). See S9.1.

Secologanoside (**260**)

Yellow viscous substance (25 mg)

Specific rotation, $[\alpha]_D^{25}$ -104.3° (*c* = 0.08, MeOH).

^{1}H NMR spectroscopy: See Table 5.5, Figure S10.4.

DEPT-135 NMR spectroscopy: See Table 5.5, Figure S10.6.

UV spectroscopy: λ_{max} 233 nm (see Figure S10.2).

IR spectroscopy: IR ν_{max}, MeOH (cm^{-1}) 3311, 2918, 1636, 1604 (see Figure S10.3).

HR-ESI-(+)-MS: *m/z* of 413.1079 (calculated for $C_{16}H_{22}O_{11}Na$ 413.1060). See S10.1.

Juglalin (**262**)

Yellow amorphous solid (9 mg)

Specific rotation, $[\alpha]_D^{25}$ -46.3° (*c* = 0.05, MeOH).

^{1}H NMR spectroscopy: See Table 5.6, Figure S11.3.

DEPT-135 NMR spectroscopy: See Table 5.6, Figure S11.5.

UV spectroscopy: λ_{max} 266, 349 nm (see Figure S11.2).

HR-ESI-(+)-MS: *m/z* of 441.0819 (calculated for $C_{20}H_{18}O_{10}Na$ 441.0798). See S11.1.

Sweroside (**114**)

Yellow amorphous solid (3 mg)

Specific rotation, $[\alpha]_D^{25}$ 130.2° (*c* = 0.03, MeOH).

^{1}H NMR spectroscopy: See Table 5.7, Figure S12.3.

UV spectroscopy: λ_{max} 242 nm (see Figure S12.2).

HR-ESI-(+)-MS: *m/z* of 381.1177 (calculated for $C_{16}H_{22}O_9Na$ 381.1162), See S12.1

5.3 Results and Discussion

5.3.1 Structural elucidation of phlorizin (259) C. dentata bark

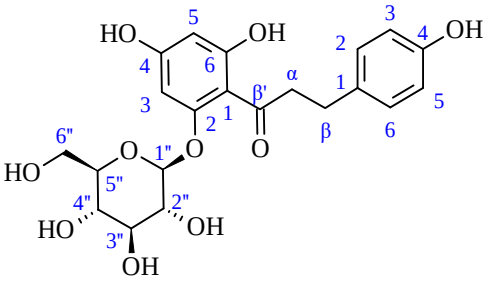

Figure 5.1: Structure of phlorizin (**259**)

The compound was obtained as a yellowish powder. The observed specific rotation was $[\alpha]_D^{27}$-56.17 (*c* = 0.11, MeOH). The molecular weight was determined by HR-ESI-MS (Figure S6.1), which showed an $[M+Na]^+$ ion at an *m/z* of 459.1288 (calculated for $C_{21}H_{24}O_{10}Na$ 459.1267), indicating 10 degrees of unsaturation. In the IR spectrum (Figure S6.3), absorption bands at ν_{max}, MeOH (cm^{-1}) 3347, 2931, 1604, and 1552 were observed, indicating the presence of OH, CH, C=O, and double bonds, respectively. The UV-Vis spectrum (Figure S6.2) showed absorbances at λ_{max} 222 and 286 nm, consistent with a benzoyl moiety. The chemical structure is shown in Figure 5.1.

In the ^{1}H NMR spectrum (Figure S6.4), signals at δ 7.07 (2H, d, *J* = 8.5 Hz) and δ 6.71 (2H, d, *J* = 8.5 Hz) were observed. The size of the coupling constant suggests the presence of a *para*-substituted phenol (**257**) with two *ortho*-coupling pairs of chemically equivalent methine protons (Figure 5.2). Two up-field signals occur at δ 6.18 (1H, d, *J* = 2.1 Hz) and δ 5.96 (1H, d, *J* = 2.1 Hz). The size of the coupling constants is typical of *meta*-coupling protons in tetrasubstituted benzene rings with a substituted phloroglucinol-like structure such as phloroglucinaldehyde (**261**). The presence of the signal at δ_H 5.06 is typical of the anomeric proton of a glucoside.

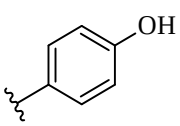

para-substituted phenol **(257)**

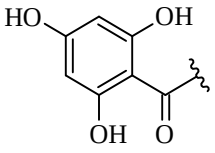

phloroglucinaldehyde (**261**)

Figure 5.2: Structure of phloroglucinaldehyde and a para-substituted phenol

The ^{1}H NMR showed two CH_2 signals at δ_H 2.88 and 3.43 (2H, t, J = 7.3 Hz). A COSY correlation (Figure S6.5) between the two CH_2 signals and a COSY correlation between the downfield *ortho*-coupled protons and the up-field methylene signal were observed. This suggested the presence of a -CH_2-CH_2- bridging link between the phloroglucinaldehyde and the *para*-substituted phenol. The structure was proposed to be a chalcone akin to phloretin (**72**) (See flavonoid, Chapter 3).

Twenty-one carbons were observed in the ^{13}C (Figure S6.6), DEPT-135 (Figure S6.7) and HSQC (Figure S6.8) NMR spectra: two sp^3 methylene carbons (δ_C 31.0 and 46.8), one oxygen bound sp^3 methylene carbon (δ_C 62.4 ppm), four methine oxygen bound sp^3 carbons (δ_C 70.9-78.4), one acetal methine (δ_C 101.9), twelve sp^2 hybridised carbons (δ_C 96.1-167.5), six of which were methines and the other six were hydrogen free sp^2 carbons. Four of the non-protonated sp^2 carbons are shifted downfield, likely due to being directly bound to an electronegative atom. One sp^2 carbonyl carbon (>200 ppm) was observed.

An HMBC (Figure S6.9) correlation between the carbonyl carbon and the up-field methylene protons of the -CH_2-CH_2- bridging link was also observed. The HMBC showed a correlation between a carbonyl carbon at δ_C 206.6 and each of the *meta*-coupled protons in a phloroglucinaldehyde-like structure (Figure 5.2). This behaviour is typical of a C-4 carbonyl of the A-ring of a chalcone. Five signals with δ_C between 60 and 80, which are typically the result of a carbon bound to an electronegative atom like oxygen, suggested that these are five C-Os of glucose. Based on these observations, compound **257** was proposed to belong to the class of chalcone glucosides.

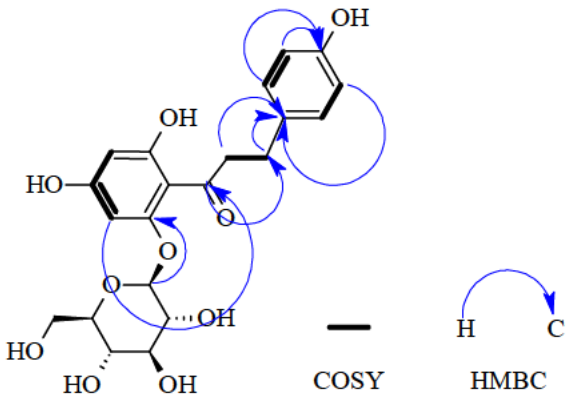

Figure 5.3: COSY and HMBC correlations observed for phlorizin (**259**)

Table 5.1: Experimental (in CD_3OD, referenced to δ_H 3.31 and δ_C 49.03) and literature values (in DMSO-d_6) of phlorizin (**259**) NMR chemical shifts

Position	Type	Experimental values (100 and 400 MHz for δ_C and δ_H, respectively)		Literature values (Shirosaki et al., 2012)	
		δ_C	δ_H	δ_C	δ_H
α	sp^3, CH_2	46.8	3.43 (2H, t, *J* = 7.3 Hz)	47.5	3.43 (2H, m)
β	sp^3, CH_2	31.0	2.88 (2H, t, *J* = 7.3 Hz)	31.4	2.88(2H, t, *J* = 7.4 Hz)
β'	sp^2, C=O	206.6	-	207.1	-
1'	sp^2, C	106.5	-	107.4	-
2'	sp^2, C-OGluc	162.2	-	162.8	-
3'	sp^2, C-H	98.8	5.96 (1H, d, *J* = 2.1 Hz)	98.9	5.96 (1H, d, *J* = 1.9 Hz)
4'	sp^2, C-O	167.5	-	165.9	-
5'	sp^2, C-H	96.1	6.18 (1H, d, *J* = 2.1 Hz)	96.0	6.18 (1H, d, *J* = 1.9 Hz)
6'	sp^2, C-O	167.1	-	164.9	-
1	sp^2, C	134.0	-	132.0	-
2, 6	sp^2, C-H	130.3	7.07 (2H, d, *J* = 8.5 Hz)	130.9	7.06 (2H, d, *J* = 8.4 Hz)
3, 5	sp^2, C-H	116.2	6.71 (2H, d, *J* = 8.5 Hz)	116.6	6.68 (2H, d, *J* = 8.4 Hz)
4	sp^2, C-O	156.1	-	156.9	-
1"	sp^3, OCH-O	101.9	5.06 (1H, d, *J* = 7.5 Hz)	102.6	5.11 (1H, d, *J* = 7.0 Hz)
2"	sp^3, CHO	74.5	3.49 m	75.2	3.45 (1H, m)
3"	sp^3, CH-O	78.4	3.47 m	79.0	3.47 (1H, m)
4"	sp^3, CH-O	70.9	3.41 m	71.7	3.39 (1H, m)
5"	sp^3, CH-O	78.3	3.42 m	79.0	3.41 (1H, m)
6" b	sp^3, CH_2-O	62.4	3.91 (1H, dd, *J* = 12.1, 2.0 Hz)	63.0	3.91 (1H, d, *J* = 11.9 Hz)
6" a			3.73 (1H, dd, *J* = 12.1, 5.3 Hz)		3.72 (1H, dd, *J* = 11.9, 5.1 Hz)

An HMBC correlation between the signals δ_C 162.2 (C-5) and δ_H 5.06 (H-1"), together with the *meta*-coupling of protons of the A-ring, implied that the glycosidic bond occurs at position C-5 of the chalcone. Compound **257** was therefore assigned as phlorizin (Figure 5.1), which is also present in *Malus huphensis* (Lv et al., 2019). The COSY and HMBC correlations are shown in Figure 5.3. The NMR chemical shifts were found to agree with literature values (Shirosaki et al., 2012) as shown in Table 5.1. This is the first report of the isolation of phlorizin from *C. dentata*.

5.3.2 Structural elucidation of (+)-catechin (258) from C. dentata bark

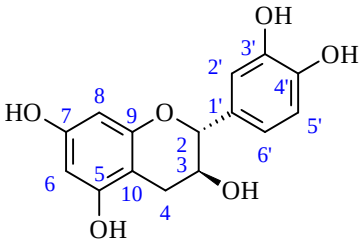

Figure 5.4: Structure of (+)-catechin (**258**)

The compound was obtained as a brown powder. The specific rotation observed was $[\alpha]_D^{25}$-23.2°. The molecular weight was determined by HR-ESI-MS (Figure S7.1), which showed an $[M+H]^+$ ion at an *m/z* of 291.0883 (calculated for $C_{15}H_{15}O_6$ 291.0869), indicating nine degrees of unsaturation. The IR spectrum (Figure S7.3) showed absorption bands at ν_{max} MeOH (cm^{-1}) 3223 (OH), 2938 (CH), 1614 (C=O), 1460 (aromatic ring) indicating the presence of OH, CH, C=O, and aromatic ring bonds, respectively. The UV-Vis spectrum showed absorbance at λ_{max} 279 nm (Figure S7.2), consistent with a flavonol structure (Figure 5.4). The chemical structure of the compound is shown in Figure 5.4.

The ^{1}H NMR spectrum (Figure S7.4) shows two up-field signals at δ_H 5.95 (1H, d, *J* = 1.8 Hz) and δ 5.88 (1H, d, *J* = 1.8 Hz). The coupling constant suggests *meta*-coupling. This description is a feature of a tetrasubstituted benzene ring. This, together with the lack of chemically equivalent sp^2-bound proton signals, led to a tentative suggestion that the tetrasubstituted ring is the A-ring of a flavonoid bound to the C-ring. The signals were assigned as H-8 and H-6 of a flavonoid. Signals at δ_H 6.85 (1H, d, *J* = 1.3 Hz), 6.78 (1H, d, *J* = 8.1 Hz) and 6.72 (1H, dd, *J* = 8.1 Hz, 1.3 Hz) were also observed. The coupling constant of 8.1 Hz points to *ortho*-coupling between two of the protons, while *J* = 1.3 Hz points to *meta*-coupling. This arrangement exists in a 4-alkylcatechol-type moiety (Fig. 5.5), which exists in the B-ring of catechin. The signals were assigned as H-2', H-5', and H-6' of catechin, respectively.

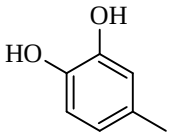

Figure 5.5: 4-methyl catechol

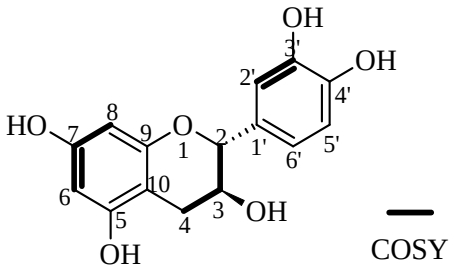

Figure 5.6: COSY correlations observed for (+)-catechin (**258**)

Table 5.2: Experimental (in CD_3OD, referenced to δ_H 3.31 and δ_C 49.03) and literature (in CD_3OD) NMR chemical shift values of (+)-catechin (**258**)

Position	Type	Experimental values (100 and 400 MHz for δ_C and δ_H, respectively)		Literature (Hye et al., 2009)	
		δ_C	δ_H	δ_C	δ_H
2	sp^3, CH	82.5	4.59 (1H, d, *J* = 7.4 Hz)	80.9	4.56 (1H, d, *J* = 7.8 Hz)
3	sp^3, CH-O	68.5	3.99 m	66.3	4.00 (1H, ddd, *J* = 5.9, 8.5, 7.8 Hz)
4a	sp^3, CH_2	28.2	2.85 (1Ha, dd, *J* = 14.9 Hz, 5.2 Hz)	27.7	2.90 (1Ha, dd, *J* = 8.5, 12.1 Hz)
4b			2.52 (1Hb, dd, *J* = 14.9 Hz, 8.0 Hz)		2.54 (1Hb, dd, *J* = 8.5, 16.1 Hz)
5	sp^2, C-O	157.5		157.5	
6	sp^2, CH	95.6	5.88 (1H, d, *J* = 1.8 Hz)	93.9	5.87 (1H, d, *J* = 2.3 Hz)
7	sp^2, C-O	157.7		157.7	
8	sp^2, CH	96.4	5.95 (1H, d, *J* = 1.8 Hz)	95.1	6.01 (1H, d, *J* = 2.3 Hz)
9	sp^2, C-O	156.8		156.8	
10	sp^2, C	100.9		101.0	
1'	sp^2, C	132.2		132.2	
2'	sp^2, CH	115.3	6.85 (1H, d, *J* = 1.8 Hz)	114.5	6.89 (1H, d, *J* = 2.0 Hz)
3'	sp^2, C-O	146.1		146.2	
4'	sp^2, C-O	146.2		146.4	
5'	sp^2, CH	116.1	6.78 (d, *J* = 8.1 Hz)	115.1	6.79 (1H, d, *J* = 8.1 Hz)
6'	sp^2, CH	120.2	6.72 (dd, *J* = 8.1 Hz, 1.4 Hz)	120.2	6.73 (1H, dd, *J* = 8.2, 1.9 Hz)

Four signals were observed at δ_H 2.52, 2.85, 3.99, and 4.59. A COSY correlation between the signals at δ_H 2.52 and 2.85, together with a coupling constant of J = 14.9 Hz, suggests a geminal coupling in a methylene. Both signals show a COSY correlation with the signal at δ_H 3.99 which in turn correlates with the signal at δ_H 4.59. This arrangement is typical of protons in the C-ring of a catechin. The signals at δ_H 2.52 and 2.85 were therefore assigned as the methylene protons on C-4 of a catechin. The signals at δ_H 3.99, and 4.59 were assigned as H-3 and H-2, respectively.

The ^{13}C NMR spectrum (Figure S7.6) showed six signals at δ_C 96.4, 95.6, 115.3, 116.1, 120.2, and 132.2 which are typical of the sp^2 chemical shifts of benzene rings. Signals at δ_C 146.1, 146.2, 157.7, and 157.5 are characteristic of deshielded aromatic carbons bound to electronegative atoms, typically oxygen. The DEPT spectrum (Figure S7.7) showed the presence of one methylene carbon at δ_C 28.2. In the HSQC (Figure S7.8), this carbon corresponds to two signals: δ_H 2.85 and 2.52. The COSY spectrum (Figure S7.5) showed a correlation between these protons. The HSQC showed that the H-3 proton is attached to a carbon with signal δ_C 68.5, which suggests that C-3 is, in turn, attached to an electronegative atom like oxygen. This arrangement is typical of the C-4 and C-3 of a catechin. COSY correlations are shown in Figure 5.6.

The proposed compound is (+)-catechin. The NMR values agreed with the literature (Hye et al., 2009), as shown in Table 5.2. This is the first report of the isolation of (+)-catechin from *C. dentata*.

5.3.3 Structural elucidation of loganic acid (116) isolated from C. dentata bark and leaves

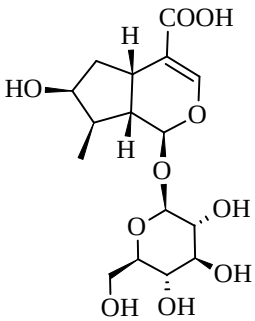

Figure 5.7: Structure of loganic acid (**116**)

The compound was obtained as a yellow amorphous solid. The molecular weight was determined by HR-ESI-MS (Figure S8.1), which showed an $[M+Na]^+$ ion at an *m/z* of 399.1282 (calculated for $C_{16}H_{24}O_{10}Na$ 399.1267), indicating five degrees of unsaturation. The UV-Vis

spectrum (Figure S8.2) showed λ_{max} of 230 nm. The chemical structure of the compound is shown in Figure 5.7.

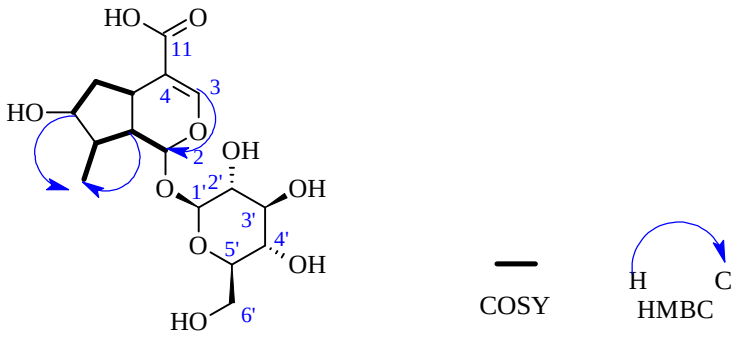

Figure 5.8: COSY AND HMBC correlations observed for loganic acid (**116**)

The ^{1}H NMR (Figure S8.3) showed characteristics of an iridoid glycoside. A chemical shift at δ_H 7.01 typifies the H-3 proton of an iridoid. The downfield shift from the standard vinylic chemical shifts ($7.00 > \delta_H > 4.50$) in the ^{1}H NMR (Figure S8.3) suggests less shielding around the atom, possibly in an enolic moiety, which is typical of iridoids. Two acetal proton chemical shifts at δ_H 4.64 and 5.22 are representative of the H-1'and H-1 protons of the iridoid glycoside, respectively. The COSY spectrum (Figure S8.4) showed a correlation between the H-1 proton and a proton signal at δ_H 2.01. This latter proton was assigned as H-9. A COSY correlation could be observed between H-9 and the signal at δ_H 1.86. This signal was assigned as H-8. A methyl signal at δ_H 1.07 had a COSY correlation with H-8. This arrangement occurs in iridoids in which a methyl group (C-10) is attached to C-8. The methyl protons were, therefore, assigned as H-10. Two signals at δ_H 2.18 and 1.74 were observed. COSY correlation between the two signals together with a coupling constant of J = 14.3 Hz were also observed. This is typical of geminal coupling in a methylene. A COSY correlation between the methylene protons and a signal at δ_H 3.13 (typical of the iridoid H-5 proton) led to the assignment of the methylene protons as H-6.

The signals in the ^{13}C NMR spectrum were not visible due to the low concentration of the compound. In the DEPT-135 (Figure S8.5), 14 resonance signals were observed, one methyl, two methylene and eleven methine carbon atoms. A ^{13}C NMR signal with a chemical shift of δ_C 145.9 and an HSQC (Figure S8.6) correlation with a proton at δ_H 7.01 suggests a sp^2 carbon. The signal at δ_C 145.9 was therefore assigned as C-3. Two resonances at δ_C 99.6 and 96.5 corresponded to protons with chemical shifts of δ_H 4.64 (1H, d, 7.9 Hz) and 5.22 (1H, d, 3.7

Hz). The chemical shifts suggest that the carbons are each bound to two oxygen atoms in an acetal moiety. The presence of two acetal protons is typical of iridoid glycosides. Five methine carbons (δ_C 78.00, 77.69, 75.11, 74.65, 71.40) and one of the methylenes (δ_C 62.52) had chemical shifts that indicated that they are attached to oxygen atoms.

The high number of oxygen-bound carbons points to the presence of a glycoside. Considering that iridoid glycosides have been isolated from members of the Cornales order, of which *C. dentata* is a part, the compound was proposed to be an iridoid glycoside.

An HMBC (Figure S8.7) correlation between a DEPT-135 signal at δ_C 176.1 and H-3 suggests the presence of a carbonyl carbon, which often occurs in iridoids as part of a carboxylic acid or methyl ester group attached to C-4. An HMBC correlation between C-3 and a proton H-1 was observed. This correlation is typical of iridoids.

The HSQC spectrum indicated that H-9 correlates with a signal at δ_C 46.8. This signal was assigned as C-9. An HMBC correlation between C-9 and methyl protons at δ_H 1.07 (3H, d, 6.9 Hz) was observed. The COSY spectrum showed that the signal at δ_H 1.86 (1H, m) correlates to both H-9 and the methyl protons. This suggests that the carbon that carries the proton at δ_H 1.86 (1H, m) is bound to both the methyl carbon and C-9. The signal was assigned as H-8, and the methyl protons were assigned as H-10. The signal at δ_C 75.1 was assigned as C-7 due to an HMBC correlation between that signal and H-10, together with a COSY correlation between H-8 and the proton on δ_C 75.1 (established via HSQC). The chemical shift of C-7 suggests that it is attached to a hydroxy group.

Two methylenes were observed in the DEPT spectrum at δ_C 62.5 and 42.2. The former chemical shift is typical of C- 6' of a glucosyl moiety. The methylene protons on the carbon at δ_C 42.2 were correlated to δ_H 2.18 and 1.74 in the HSQC and had COSY correlations with H-7 and H-5. The methylene carbon was assigned as C-6. A methyl carbon resonating at δ_C 13.1 had HMBC correlations with H-7 and H-9 and was tentatively assigned to C-10. The structure of compound **116** was assigned as loganic acid (Figure 5.7), an iridoid glycoside that is present in *Lonicera periclymenum* and *Gentiana loureirii* (Calis et al., 1984; Wu et al., 2009). The experimental NMR values agree reasonably with those found in the literature, as shown in Table 5.3. The difference in chemical shifts between C3 experimental values and literature values was attributed to possible proton exchange between the compound organic acid group and solvent. The C4 chemical shift was obtained by estimation using HMBC correlations,

which may explain the discrepancy with literature values. The COSY and HMBC correlations are depicted in Figure 5.8. This is the first report on isolating loganic acid from *C. dentata*.

Table 5.3: Experimental (in CD_3OD, referenced to δ_H 3.31 and δ_C 49.03) and literature (in CD_3OD) NMR chemical shift values of loganic acid (**116**)

Position	Type	Experimental values (100 and 400 MHz for δ_C and δ_H, respectively)		Literature (Calis et al., 1984; Wu et al., 2009)	
		δ_C	δ_H	δ_C	δ_H
1	sp^3, OCH-O	96.5	5.22 (1H, d, *J* = 3.7 Hz)	97.6	5.24 (1H, d, *J* = 4.1 Hz)
3	sp^2, CH	145.9	7.01 (1H, d, *J* = 1.0 Hz)	152.0	7.21 (1H, s)
4	sp^2, C	121.6		114.2	
5	sp^3, CH	32.6	3.13	32.7	3.10 (1H, m)
6b	sp^3, CH_2	42.2	2.18 (1H, ddd, *J* = 14.3, 8.1, 2.0 Hz)	42.6	2.01 (1H, dt, *J* = 9.2, 9.2, 4.1 Hz)
6a			1.74 (1H, dt, *J* = 14.3, 5.8 Hz)		1.69 (1H, m)
7	sp^3, CH-O	75.1	4.04 (1H, td, *J* = 5.1, 1.8 Hz)	75.0	4.03 (1H, t, *J* = 4.1 Hz)
8	sp^3, CH	41.5	1.86 (1H, m)	42.0	1.86 (1H, m)
9	sp^3, CH	46.8	2.01 (1H, td, *J* = (3.7, 9.2 Hz)	46.4	2.20 (1H, dd, *J* = 13.8, 7.9 Hz)
10	sp^3, CH_3	13.1	1.07 (3H, d, *J* = 6.9 Hz)	13.5	1.07 (1H, d, *J* = 6.9 Hz)
11	sp^2, C	176.1		171.4	
1'	sp^3, OCH-O	99.6	4.64 (1H, d, *J* = 7.9 Hz)	99.9	4.64 (1H, d, *J* = 8.0 Hz)
2'	sp^3, CH-O	74.6	3.21 (1H, dd, *J* = 8.9, 8.0 Hz)	74.6	3.17–3.40 (4H, m)
3'	sp^3, CH-O	77.6	3.37 (1H, m)	77.9	
4'	sp^3, CH-O	71.3	3.32 (m)	71.4	
5'	sp^3, CH-O	77.9	3.31 (m)	78.1	
6'b	sp^3, CH_2-O	62.5	3.88 (1H, dd, *J* = 11.8, 0.8 Hz)	62.7	3.88 (1H, d, *J* = 11.8, 1.3 Hz)
6'a			3.68 (1H, dd, *J* = 11.8, 5.1 Hz)		3.66 (1H, dd, *J* = 11.8, 5.1 Hz)

*Non-protonated carbon chemical shifts were estimated from HMBC correlations.

5.3.4 Structural elucidation of geniposide (131) isolated from C. dentata leaves

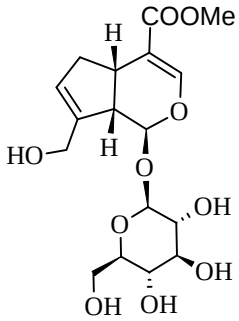

Figure 5.9: Structure of geniposide (**131**)

The compound was obtained as a yellow amorphic solid. The molecular weight was determined by HR-ESI-MS (Figure S9.1), which showed an $[M+Na]^+$ ion at an *m/z* of 411.1279 (calculated for $C_{17}H_{24}O_{10}Na$ 411.1267), indicating six degrees of unsaturation. The UV-Vis spectrum (Figure S9.2) showed λ_{max} of 240 nm. The chemical structure of the compound is shown in Figure 5.9.

The typical iridoid glycoside ^1H NMR (Figure S9.3) signals at δ_H 7.51 (enolic proton at H-3), 5.80 (a vinylic proton at H-6, 7 or 8), 4.17 and 5.17 (the acetal protons at H-1' and H-1) and 4.71 (anomeric β-glucose proton) were observed. The structure was, therefore, proposed to be that of an iridoid glucoside. A COSY (Figure S9.4) correlation between H-1 and a signal at δ_H 2.73 led to establishing the latter as H-9. H-5 (δ_H 3.18) was confirmed with a COSY correlation with H-9. H-5 also has a COSY correlation to a proton at δ_H 2.82. This proton correlates to a signal at δ_H 2.09 and one of the coupling constants of its doublet of doublets is J = 16.3 Hz. This suggests that the proton is part of a methylene that exhibits geminal coupling. The signals at δ_H 2.82 and 2.09 were therefore assigned as H-6b and H-6a methylene protons, respectively.

The DEPT spectrum (Figure S9.5) shows the presence of three methylene carbons with signals at δ_C 39.4, 61.2 and 62.4. The latter two are shifted downfield, suggesting that they are bound to an electronegative atom, likely the oxygen of a hydroxy. The HSQC (Figure S9.6) showed that the carbon at 62.4 is attached to protons at δ_H 3.85 and 3.64. These protons have COSY correlations with δ_H 3.28, whose corresponding carbon is at δ_C 78.1, as confirmed by the HSQC. This is typical of the glucose position C-5'. This led to the proposal that δ_C 62.4 was C-6' of the sugar. The signal at δ_C 39.4 showed a correlation with H-6 protons in the HSQC spectrum. The signal was, therefore, assigned as C-6.

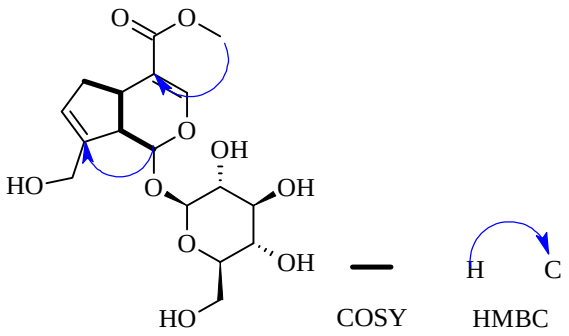

Figure 5.10: COSY and HMBC correlations observed for geniposide (**131**)

Table 5.4: Experimental (in CD_3OD, referenced to δ_H 3.31 and δ_C 49.03) and literature values (in DMSO-*d*$_6$) NMR chemical shifts of geniposide (**131**)

Position	Type	Experimental values (125 and 500 MHz for δ_C, and δ_H, respectively)		Literature values δ_C (Ono et al., 2005)	
		δ_C	δ_H	δ_C	δ_H
1	sp^3, OCH-O	98.0	5.17 (1H, d, *J* = 7.5 Hz)	98.3	5.16 (1H, d, *J* = 7.5 Hz)
3	sp^2, CH	153.1	7.51 (1H, d, *J* = 1.0 Hz)	153.3	7.51 (1H, d, *J* = 1.5 Hz)
4	sp^2, C	112.4		112.6	
5	sp^3, CH	36.3	3.18 (1H, m)	36.6	3.18 (1H, ddd, *J* = 8.0, 8.0, 8.0 Hz)
6b	sp^3, CH_2	39.4	2.82 (1H, dd, *J* = 16.3, 8.3 Hz)	39.7	2.82 (1H, dd, *J* = 8.0, 16.5 Hz)
6a			2.09 (1H, m)		2.09 (1H, dddd (1.5, 1.5, 8.0, 16.5 Hz)
7	sp^2, CH	128.1	5.80 (1H, s)	128.4	5.80 (1H, s)
8	sp^2, C	144.1		144.8	
9	sp^3, CH	46.8	2.73 (1H, dd, *J* = 7.7, 7.8 Hz)	47.1	2.72 (1H, dd, *J* = 7.5, 8.0 Hz)
10b	sp^3, CH_2	61.2	4.31 (1H, d, *J* = 14.6 Hz)	61.4	4.31 (1H, br d, *J* = 14.5 Hz)
10a			4.19 (1H, d, *J* = 14.6 Hz)		4.18 (1H, d, *J* = 1.5, 14.5 Hz)
11	sp^2, C	168.7		169.5	
12	sp^3, CH_3-O	51.5	3.71 (3H, s)	51.7	3.71 (3H, s)
1'	sp^3, CH-O	100.1	4.71 (1H, d, *J* = 7.9 Hz)	100.4	4.71 (1H, d, *J* = 8.0 Hz)
2'	sp^3, CH-O	74.6	3.21 m	74.9	3.22 (1H, dd, *J* = 8.0, 9.0 Hz)
3'	sp^3, CH-O	77.6	3.37 m	77.9	3.39
4'	sp^3, CH-O	71.3	3.28	71.6	3.29
5'	sp^3, CH-O	78.1	3.28	78.3	3.29
6'b	sp^3, CH_2-O	62.4	3.85	62.7	3.86 (1H, d, J = 11.5 Hz)
6'a			3.64		3.64 (1H, dd, *J* = 3.5, 11.5 Hz)

The signal at δ_H 3.71 (3H, s) is typical of a methyl ester. Some iridoids are known to have this moiety attached to C-4. The HMBC (Figure S9.7) correlation between the methyl and a signal at δ_C 168.7 confirms this as the carbonyl carbon chemical shift.

The HMBC correlation was observed between signals at δ_H 5.17 (H-1) and δ_C 144.1. The ^{13}C NMR signal suggests that it is a vinylic carbon. The absence of the ^{13}C signal in the DEPT implied that it is a proton-less carbon. The ^{13}C signal was assigned as C-8. Vinylic C-8 carbons of an iridoid that are not attached to protons typically are bound to a C-10 substituent. It was proposed that the remaining methylene at δ_C 61.2 is C-10. The chemical shift suggests that the carbon is bound to an electronegative atom, which in iridoids is typically an oxygen of a hydroxy group. The HSQC showed that C-10 was correlated to protons at δ_H 4.31 and 4.19, which were assigned as H-10b and H-10a, respectively. The outstanding vinylic chemical shift of δ_H 5.80 was assigned to H-7.

This information, together with the calculated mass of the expected compound of *m/z* 388 deduced from the mass spectrum, led to the proposal that the compound is geniposide. The COSY and HMBC correlations are shown in Figure 5.10. The experimental chemical shifts agreed with literature values (Ono et al., 2005) as shown in Table 5.4. This is the first report of the isolation of geniposide from *C. dentata*.

5.3.5 Structural elucidation of secologanoside (260) from C. dentata leaves

The compound was obtained as a yellowish viscous substance. The molecular weight was determined by HR-ESI-MS (Figure S10.1), which showed an $[M+Na]^+$ ion at an *m/z* of 413.1079 (calculated for $C_{16}H_{22}O_{11}Na$ 413.1060), indicating six degrees of unsaturation. The IR spectrum (Figure S10.3) shows absorption bands at ν_{max} MeOH (cm^{-1}) 3311, 2918, 1636, and 1604, which indicate the presence of OH, CH, C=O and C=C bonds, respectively. The UV-Vis mass spectrum (Figure S10.2) showed λ_{max} at 233 nm. The chemical structure of the compound can be seen in Figure 5.11.

The ^1H NMR (Figure S10.4) showed the typical iridoid enolic proton chemical shift at δ_H 7.23 which is typical of the H-3 proton of an iridoid. Two acetal proton signals were observed at δ_H 5.40 (1H, d, 3.8 Hz) and 4.65 (1H, d, 7.8 Hz). They were assigned as H-1 and H-1'. The compound was tentatively proposed to be an iridoid. The coupling constant of J = 7.8 Hz on the H-1' proton is consistent with that of the β-glucose anomeric proton, suggesting that the compound is an iridoid glucoside.

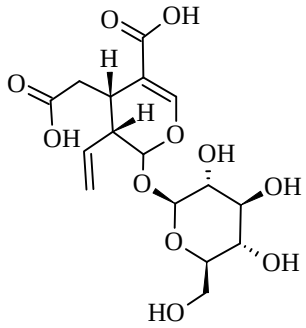

Figure 5.11: Structure of secologanoside (**260**)

In iridoids, multiplet signals between δ_H 5.00 and 6.00 typically occur due to vinylic protons on double bonds of the iridoid pentane ring or those of the secoiridoid group of iridoids discussed in Chapter 3. The presence of vinylic signals at δ_H 5.24 and 5.19 with geminal coupling (J = 1.8 Hz) is typical of the terminal protons of a secoirioid double bond. Additionally, the vinylic chemical shift at δ_H 5.68 shared a trans coupling constant (17.2 Hz) with the vinylic signal at δ_H 5.24, suggesting that a terminal vinylic carbon is attached to a proton-bound non-terminal vinylic carbon.

On the COSY spectrum (Figure S10.5), the H-1 proton (δ_H 5.40) correlates with a signal at δ_H 2.82, which was designated as H-9. H-9 has a COSY correlation with a proton at vinylic signals at δ_H 3.26. This proton was assigned as H-5. H-5 correlates to a signal at δ_H 2.19, which was assigned as H-6. H-6 correlates to a proton with a typical vinylic chemical shift of δ_H 2.96 and the proton signals each have a coupling constant of J = 16.2 Hz in common. This suggests that there is geminal coupling between the protons. The signal at δ_H 2.96 was also assigned as H-6.

H-9 also has a COSY correlation with one of the vinylic protons at δ_H 5.68 (1H, dt, 17.2, 9.8 Hz). This proton was assigned as H-8. H-8 has a COSY correlation with 2 protons at δ_H 5.24 (1H, dd, 17.2, 1.2 Hz) and 5.19 (1H, dd, 11.2, 1.8 Hz). These protons were assigned as H-10b and H-10a, respectively. This coupling pattern is typical of vinylic trans, cis and geminal coupling, as shown in Figure 5.12.

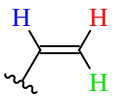

H-H vinylic trans coupling: ^3J = 11-18 Hz
H-H vinylic cis coupling: ^3J = 6-15 Hz
H-H vinylic geminal coupling: ^3J = 0-5 Hz

Figure 5.12: Types of coupling across a double bond

The DEPT spectrum (Figure S10.6) showed the presence of three methylenes at δ_C 36.3, 62.4 and 119.8. Four vinylic chemical shifts were observed at δ_C 114.8, 119.8, 134.9, and 149.7. Two carbonyl carbon chemical shifts were observed at δ_C 173.0 and 178.8. Acetal methine carbon chemical shifts were observed at δ_C 97.0 and 99.4. The HSQC showed that the H-1 and H-1' protons are attached to carbons resonating at δ_C 97.0 and 99.4, respectively. The vinylic methylene chemical shift (δ_C 119.8) was assigned as C-10 based on the HSQC correlations (Figure S10.7). The chemical shift of δ_C 62.4 is typical of the oxygen-bound carbon of glucose. This methylene signal was therefore, assigned as the C-6' position of the glucose. The methylene at δ_C 36.3 showed HSQC correlations with H-6 protons and was therefore assigned as C-6. The H-6 proton at δ_H 2.19 showed an HMBC (Figure S10.8) correlation with one of the carbonyl carbon chemical shifts at δ_C 178.8. The carbonyl carbon at δ_C 173.0 had an HMBC correlation with H-3. This carbonyl carbon was assigned as C-11. The remaining carbonyl carbon was assigned as C-7. A lack of methyl chemical shifts suggested both carbonyl groups were carboxylic acids instead of methyl ester groups.

These data, together with the molecular mass of 390 deduced from HR-ESI MS, led to the supposition that the compound could be secologanoside. The COSY and HMBC correlations are shown in Figure 5.13. The experimental chemical shifts were in reasonable agreement with literature values (Karioti et al., 2006; Liu et al., 2012) as shown in Table 5.5. This is the first report of the isolation of secologanoside from *C. dentata*.

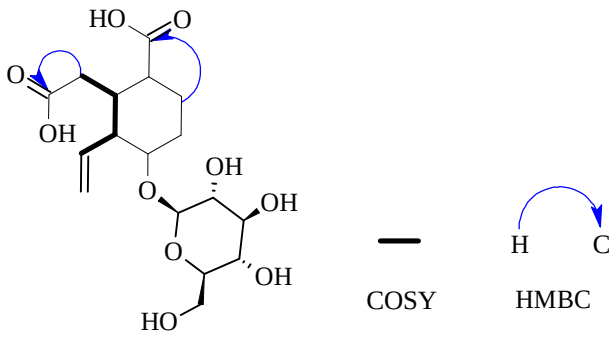

Figure 5.13: COSY and HMBC correlations observed for secologanoside (**260**)

Table 5.5: Experimental (in CD_3OD, referenced to δ_H 3.31 and δ_C 49.03) and literature (in CD_3OD) NMR chemical shift values for secologanoside (**260**)

Position	Type	Experimental values (100 and 400 MHz for δ_C and δ_H, respectively)		Literature values (Karioti et al., 2006)	
		δ_C	δ_H	δ_C	δ_H
1	sp^3, OCHO	97.0	5.40 (1H, d, *J* = 3.8 Hz)	98.2	5.35 (1H, d, *J* = 4.0 Hz)
3	sp^2, CH	149.7	7.23 (1H, d, *J* = 0.9 Hz)	154.0	7.49 (1H, d, *J* = 1.8 Hz)
4	sp^2, C	114.8		110.7	
5	sp^3, CH	29.1	3.26 m	29.0	3.23 (1H, m)
6b	sp^3, CH_2	36.3	2.96 (1H, dd, 16.2, *J* = 3.7 Hz)	35.5	2.98 (1H, dd, *J* = 16.5, 4.8 Hz)
6a			2.19 (1H, dd, 16.2, *J* = 9.6 Hz)		2.21 (1H, dd, *J* = 16.5, 9.5 Hz)
7	sp^2, C=O	178.8		176.7	
8	sp^2, CH	134.9	5.68 (1H, dt, *J* = 17.2, 9.8 Hz)	134.9	5.60 (1H, td, *J* = 16.5, 9.5 Hz)
9	sp^3, CH	45.2	2.82 (1H, dt, *J* = 9.8, 4.6 Hz)	45.7	2.98 (1H, ddd, *J* = 9.5, 5.5, 4.0 Hz)
10b	sp^2, CH_2	119.8	5.24 (1H, dd, *J* = 17.2, 1.8 Hz)	121.0	5.25 (1H, d, *J* = 17.2 Hz)
10a			5.19 (1H, dd, *J* = 11.2, 1.8 Hz)		5.22 (1H, dd, *J* = 10.0, 1.8 Hz)
11	sp^2, C=O	173.0		169.6	
				Glucose NMR (Liu et al., 2012)	
1'	sp^3, CH-O	99.4	4.65 (1H, d, *J* = 7.8 Hz)	99.9	4.64 (d, *J* = 8.3 Hz)
2'	sp^3, CH-O	74.4	3.28 m	74.6	3.20 (t, *J* = 8.3 Hz)
3'	sp^3, CH-O	78.0	3.39 m	78.0	3.34 (t, *J* = 8.3 Hz)
4'	sp^3, CH-O	71.3	3.24 m	71.5	3.28 (overlap)
5'	sp^3, CH-O	77.5	3.31 m	78.4	3.28 (overlap)
6'b	sp^3, CH_2-O	62.4	3.88 (1H, d, *J* = 11.3 Hz)	62.7	3.88 (dd, *J* = 2.0, 11.7 Hz)
6'a			3.68 m		3.65 (dd, *J* = 5.5, 11.7 Hz)

5.3.6 Structural elucidation of juglalin (262) isolated from C. dentata leaves

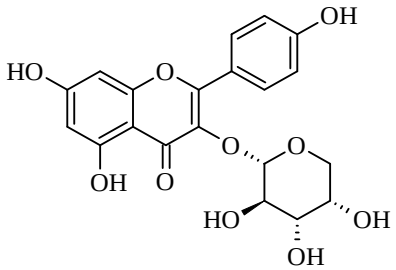

Figure 5.14: Structure of juglalin (**262**)

This compound was obtained as a yellow amorphous solid. The molecular weight was determined by HR-ESI-MS (Figure S11.1), which showed an $[M+Na]^+$ ion at an *m/z* of 441.0819 (calculated for $C_{20}H_{18}O_{10}Na$ 441.0798), indicating six degrees of unsaturation. The UV-Vis spectrum (Figure S11.2) gave absorptions at λ_{max} 266 and 349 nm. The chemical structure of the compound can be seen in Figure 5.14.

On the ^1H NMR spectrum (Figure S11.3) the characteristic signals of a kaempferol aglycon were observed. These are the two sets of doublet pairs at δ_H 8.01 (H-2', 6'), 6.83 (H-3', 5'), 6.12 (H-8) and 5.99 (H-6). Their designation has been described in the previous chapter under the elucidation of kaempferitrin. Signals with chemical shifts in the region between δ_H 3.60 to 3.90 were observed. These chemical shifts are typical of secondary alcohol protons in an ethylene glycol moiety and suggest the presence of a glycoside. A probable glycoside anomeric proton had a signal at δ_H 4.92 with a coupling constant of 6.5 Hz was also observed.

Using the DEPT-135 (Figure S11.5), four signals at δ_C 66.7, 68.8, 72.6, and 74.0, which resonate at the typical range for the alkoxy carbons of a sugar, were observed. The signal at δ_C 66.7 is a methylene. The HSQC (Figure S11.6) correlated the carbons to ^1H NMR signals in the range of δ_H 3.60 to 3.90 which falls within the range for glycoside protons. The HSQC showed that the anomeric proton is attached to a carbon at δ_C 105.1. This signal was assigned as the acetal anomeric carbon of a glycoside. The ^{13}C NMR spectrum signals had low intensity due to the small amount of the sample. These parameters are inconsistent with a glucoside, which we have encountered so far. The observation of five downfield shifted sp^3 carbons suggests that they are the oxygen-bound carbons of a pentose sugar.

The HSQC shows that the signal at δ_C 72.6 is attached to a proton that resonates at δ_H 3.88. This proton has a COSY (Figure S11.4) correlation with the tentative anomeric proton and a proton at δ_H 3.61. The signals at δ_H 3.88 and δ_C 72.6 were therefore assigned as H-2" and C-2", respectively. The proton at δ_H 3.61 has an HSQC correlation to the signal at δ_C 74.0. The proton

and carbon were assigned as H-3" and C-3", respectively. An additional COSY correlation between H-3" and δ_H 3.78 led to the assignment of that signal as H-4". A COSY correlation was observed between H-4" and a signal at δ_H 3.47. This signal is assigned as H-5". The signal is a doublet of doublets which in turn correlates with a signal at δ_H 3.80. The presence of a coupling constant of 13.8 Hz suggests geminal coupling in a methylene. The HSQC shows that signals δ_H 3.47 and 3.80 are both attached to the methylene carbon with signal δ_C 66.7. The presence of the C-5" methylene prompted the proposal of arabinose as the glycoside.

Table 5.6: Experimental (in CD_3OD, referenced to δ_H 3.31 and δ_C 49.03) and literature (in CD_3OD) NMR chemical shift values for juglalin (**262**)

Position	Type	Experimental values (100 and 400 MHz for δ_C, and δ_H, respectively)		Literature values (Pérez-Vásquez et al., 2020)	
		δ_C	δ_H	δ_C	δ_H
2	sp^2, C	157.8		158.4	
3	sp^2, C-O	135.0		135.4	
4	sp^2, C=O	177.2		179.2	
5	sp^2, C-O	162.9		162.9	
6	sp^2, CH	105.1	5.99 (1H, d, *J* = 2.0 Hz)	101.0	6.17 (1H, d, *J* = 2.0 Hz)
7	sp^2, C-O			169.3	
8	sp^2, CH	97.1	6.12 (1H, d, *J* = 2.0 Hz)	95.5	6.35 (1H, d, *J* = 2.0 Hz)
9	sp^2, C-O	159.4		158.7	
10	sp^2, C	102.6		104.7	
1'	sp^2, C	122.7		122.7	
2', 6'	sp^2, CH	131.7	8.01 (1H, d, *J* = 8.9 Hz)	132.2	8.08 (1H, d, *J* = 8.8 Hz)
3', 5'	sp^2, CH	116.5	6.83 (1H, d, *J* = 8.9 Hz)	116.3	6.90 (1H, d, *J* = 8.9 Hz)
4'	sp^2, C-O	159.6		161.7	
1"	sp^3, OCH-O	105.1	4.92 (1H, d, *J* = 6.5 Hz)	104.6	5.11 (1H, d, *J* = 6.4 Hz)
2"	sp^3, CH-O	72.6	3.88 (1H, dd, *J* = 8.3, 6.6 Hz	72.8	3.91 (1H, dd, *J* = 6.4, 8.3 Hz)
3"	sp^3, CH-O	74.0	3.61 (1H, dd, *J* = 8.3, 3.2 Hz)	74.1	3.65 (1H, dd, *J* = 3.2, 8.3 Hz)
4"	sp^3, CH-O	68.8	3.78 (overlap)	69.0	3.8-3.7 (2H, m)
5"b	sp^3, CH_2-O	66.7	3.80 (overlap)	66.8	3.8-3.7 (2H, m)
5"a			3.47 (1H, dd, *J* = 2.9, 13.8 Hz)		3.45 (1H, dd, *J* = 3.2, 13.2 Hz)

An HMBC (Figure S11.7) correlation between δ_C 135.0 and the anomeric proton suggests that the sugar is attached at position C-3 of the flavonoid. The arabinopyranoside moiety of juglalin,

which has a coupling constant of 6.5 Hz, was differentiated from the arabinofuranoside moiety of juglanin, which has a coupling constant of ~2.0 Hz (Chang et al., 2000).

The COSY and HMBC correlations are shown in Figure 5.15. The NMR values of the compound were compared with literature values (Pérez-Vásquez et al., 2020) for kaempferol-3-*O*-α-L-arabinoside [juglalin (**261**)] as shown in Table 5.6. The chemical shifts were in general agreement apart from C-7, which could not be located, probably as a result of the low intensity of the sample. This is the first report of the isolation of juglalin from *C. dentata*.

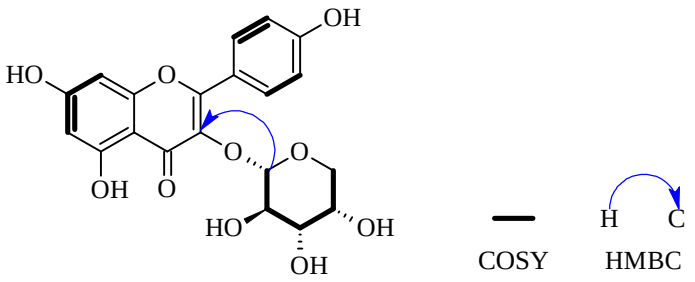

Figure 5.15: COSY and HMBC correlations observed for juglalin (**262**)

5.3.7 Structural elucidation of sweroside (114) isolated from C. dentata leaves

This compound was obtained as a yellow solid. The molecular weight was determined by HR-ESI-MS (Figure S12.1), which showed an $[M+Na]^+$ ion at an *m/z* of 381.1177 (calculated for $C_{16}H_{22}O_9Na$ 381.1162), indicating six degrees of unsaturation. The UV-Vis spectrum (Figure S12.2) shows absorption at λ_{max} 242 nm. Due to spillage after running the MS and ^1H NMR spectroscopic experiments, C13, and other 2D NMR experiments could not be obtained. The chemical structure of the compound is shown in Figure 5.16.

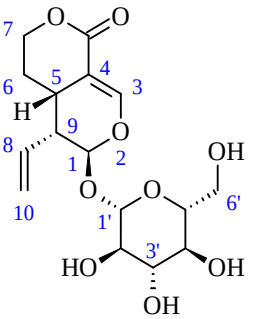

Figure 5.16: Structure of sweroside (**114**)

The ^{1}H NMR spectrum (Figure S12.3) showed the characteristic enolic proton signal of an iridoid at δ_H 7.59. The signal at δ_H 4.68 has a coupling constant of 7.9 Hz. This is typical of the acetal β-glucose anomeric proton. A second acetalic proton chemical shift was observed at δ_H 5.55. There are two signals that overlap at that chemical shift; the multiplicity of one of them is a doublet, and the other is a doublet of triplets. The doublet acetal proton signal is typical of the H-1 proton of an iridoid. This acetal proton showed a correlation in the COSY spectrum (Figure S12.4) with a proton at δ_H 2.70 (1H, ddd). In line with the proposition that the compound is an iridoid glycoside, the doublet of doublets of doublets was assigned as H-9. COSY correlations between H-9 and two protons at δ_H 5.55 (dt) and 3.15 (m) were observed.

The COSY spectrum showed correlations between the doublet of triplets and signals at δ_H 5.28 and 5.31 The presence of signals with typical vinylic proton chemical shifts between δ_H 5.00 and 6.00 suggests that the compound is a secoiridoid. The doublet of triplets had coupling constants of 17.1 and 10.0 Hz and the signal was assigned as H-8. The coupling constants are suggestive of a vinylic proton with trans and cis coupling, as shown in Figure 5.17. H-8 showed COSY correlations with signals at δ_H 5.31 and 5.28 which were assigned as H-10b and H-10a, respectively.

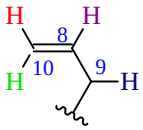

H-H vinylic trans coupling: ^{3}J = 17.1 Hz
H-H vinylic cis coupling: ^{3}J = 10 Hz
H-H vinylic geminal coupling: ^{3}J = 0-5 Hz
H-H ^{3}J = 10 Hz

Figure 5.17: Coupling constants of the vinylic moiety of **114**

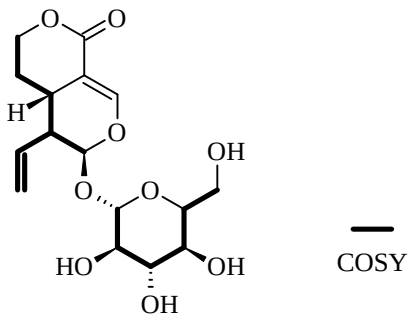

Figure 5.18: COSY correlations observed for sweroside (**114**)

Table 5.7: Experimental (in CD_3OD, referenced to δ_H 3.31) and literature (in CD_3OD) NMR chemical shift values for sweroside (**114**)

Position	Type	Experimental values (400 MHz for δ_H)	Literature values (Cambie et al., 1990)
1	sp^3, OCHO	5.55 (1H, d, *J* = 1.5 Hz) overlap	5.55 (d, *J* = 2 Hz)
3	sp^2, CH	7.59 (1H, d, *J* = 2.4 Hz)	7.59 (1H, d, *J* = 2 Hz)
5	sp^3, CH	3.15 overlap	3.15 (ddt, *J* = 12, 2, 6 Hz)
6a	sp^3, CH_2	1.78 m	1.77 (dq, *J* = 12, 4 Hz)
6b		1.71 m	1.70 (ddt, *J* = 12, 5, 2 Hz)
7	sp^3, CH_2-O	4.46 (1H, ddd, *J* = 11.7, 4.2, 2.1 Hz)	4.45 (1H, dq, *J* = 12, 2 Hz)
7		4.37 (1H, td, *J* = 11.7, 2.1 Hz)	4.36 (1H, dt, *J* = 12, 2 Hz)
8	sp^2, CH	5.55 (dt, overlap, *J* = 17.1, 10.0 Hz)	5.55 (1H, dt, *J* = 17, 10 Hz)
9	sp^3, CH	2.70 (1H, ddd, *J* = 10.0, 6.3, 1.5 Hz)	2.70 (1H, ddd, *J* = 10, 6, 2 Hz)
10b	sp^2, CH_2	5.31 (1H, dd, *J* = 17.1, 1.5 Hz)	5.31 (1H, dd, *J* = 17, 2 Hz)
10a		5.28 (1H, dd, *J* = 11.1, 1.5 Hz)	5.27 (1H, dd, *J* = 10, 2 Hz)
1'	sp^3, OCH-O	4.68 (1H, d, *J* = 7.9 Hz)	4.68 (1H, d, *J* = 8 Hz)
2'	sp^3, CH-O	3.19 (1H, dd, *J* = 8.9, 8.0 Hz)	3.19 (t, *J* = 8 Hz)
3'	sp^3, CH-O	3.38 (1H, t, *J* = 8.7 Hz)	3.37 (1H, t, *J* = 8 Hz)
4'	sp^3, CH-O	3.28, solvent peak overlap	3.27 (t, *J* = 8 Hz)
5'	sp^3, CH-O	3.32, solvent peak overlap	3.31 (1H, ddd,*J* = 8, 6, 2 Hz)
6'b	sp^3, CH_2-O	3.89 (1H, dd, *J* = 11.9, 2.0 Hz)	3.89 (1H, dd, *J* = 12, 2 Hz)
6'a		3.67 (1H, dd, *J* = 11.9, 5.5 Hz)	3.66 (1H, dd, *J* = 12, 6 Hz)

The signal at δ_H 3.15, which had a COSY correlation with H-9, was assigned as H-5. In the COSY spectrum, this H-5 also couples to two signals at δ_H 1.78 and 1.71. The two protons couple with each other on the COSY spectrum. This correlation pattern prompted the suggestion that these signals represent the prochiral methylene of H-6. COSY correlations between the H-6 methylene signals and two signals at δ_H 4.37 and 4.46 were observed. The two later signals also couple to each other and have a coupling constant of 11.7 Hz. The coupling constant is typical of geminal protons of a prochiral methylene. The chemical shifts suggest that the carbon to which the protons are attached is bound to an electronegative atom, most likely an oxygen atom. This arrangement exists in sweroside, a secoiridoid found in some plants, including *Fagraea gracilipes* (Cambie et al., 1990). The ESI-MS spectrum is consistent with sweroside with a sodium ion adduct in the positive mode. The COSY correlations are depicted in Figure 5.18. The ^{1}H NMR spectrum was compared to the literature data on sweroside (Cambie et al., 1990). There was reasonable agreement between the sets of data as shown in Table 5.7. This is the first report of the isolation of sweroside form *C. dentata*.

5.4 Significance of the findings

5.4.1 Phlorizin (259)

Phlorizin has been known as a pharmacoactive compound for over 188 years (Ehrenkranz et al., 2005). When it was first isolated in 1835 from the bark of the apple tree, phlorizin was presumed to be an antipyretic for the treatment of febrile conditions like malaria. By 1887, it had been discovered that at certain dosages, phlorizin causes glucosuria. Glucosuria refers to the presence of glucose in urine. Over the years researchers involved in renal studies conducted investigations that utilized phlorizin. Some of the investigations included the use of phlorizin to ascertain the quality of renal function after the realization that nephrotic kidneys were not susceptible to phlorizin-enhanced glycosuria (Ehrenkranz et al., 2005).

Around the 1930s, phlorizin was being intravenously administered to produce glycosuria in healthy subjects in order to measure glomerular filtrate rate and renal blood flow. Overtime investigations involving the effect of phlorizin on the renal system led to the identification of the glucose transportation mechanisms in kidneys. It was also discovered that phlorizin at the optimal concentration blocks glucose transport in the small intestines and kidneys (Ehrenkranz et al., 2005). As a result, phlorizin can lower blood sugar levels. In vivo studies have shown that phlorizin can reestablish insulin sensitivity in diabetic mammals due to its capacity to

reduce blood glucose levels. In vivo studies showed that phlorizin slows the rise in blood sugar in mice that were fed a glucose solution orally. This led researchers to develop a derivative of phlorizin which they called T-1095. Administration of T-1095 results in a drastic increase in glucose excretion through urine, thereby lowering blood glucose levels (Ehrenkranz et al., 2005).

A study investigated the effect of phlorizin on obesity, inflammation and high-glucose levels in high-fat diet experimental mice (Shin et al., 2016). The C57BL/6J mice were separated into 3 groups. The first group was fed the American Institute of Nutrition (AIN-76) diet, and the normal diet group was fed a 5% fat diet. The high-fat diet group was allocated a diet comprising 20% fat and 1% cholesterol. The phlorizin group were fed a high-fat diet in combination with 0.02% phlorizin. The treatment continued for 16 weeks after which the mice were sacrificed and blood plasma was analysed. Shin et al. (2016) observed that while phlorizin treatment did not significantly impact food efficiency ratios and body weight, adipocyte hypertrophy and visceral and subcutaneous fatty deposition were reduced compared to the high-fat diet mice. Additional phlorizin treatment resulted in the reduction of white adipose tissue which is known to release chronic inflammation and insulin resistance-promoting adipokines. Phlorizin treatment was also shown to increase the activity of carnitine palmitoyl transferase which is responsible for transporting fatty acids in the mitochondria for β oxidation. These results indicate that phlorizin is an effective treatment for type 2 diabetes and has therapeutic potential for the treatment of chronic inflammation and non-alcoholic liver disease associated with obesity**.**

5.4.2 (+)-catechin (258)

The name catechin comes from catechu which is obtained from extracts of the Fabaceae plant *Acacia catechu* L. It has been found in other herbs, teas and some fruit trees. The biological activities of catechin include: antidiabetic activity, antihypertensive effects, bone growth promotion, central nervous system protection and hepatoprotective effects (Garneshpurkar and Saluja, 2020)

A study involving Wistar albino rats assessed the effect of catechin hydrate on gentamicin-induced nephrotoxicity. The study found that the gentamicin control group, which did not receive catechin hydrate treatment, demonstrated high levels of serum creatinine, blood urea nitrogen levels and damage to glomeruli and tubules. The catechin hydrate treated group, however, showed significant reduction in renal degeneration (Sardana et al., 2015).

5.4.3 Loganic acid (116)

Park et al. (2021) examined three parameters to determine the osteoprotective potential of loganic acid. The parameters were the effect of loganic acid on osteoblast differentiation in mouse preosteoblast MC3T3-E1 cells. Secondly, they examined the effect of loganic acid on osteoclast differentiation. Lastly, they conducted an investigation into how administering loganic acid to mice with ovariectomy-induced osteoporosis affected bone mineral density. The results showed that loganic acid increased the activity of alkaline phosphatase which is one of the transcription factors that regulate differentiation of osteoblasts during bone formation. The researchers also noted that treatment with loganic acid reduced the activity of tartrate-resistant acid phosphatase (TRAP). High TRAP levels are associated with bone resorption activity of osteoclasts. Loganic acid also prevented bone mineral density loss in the in vivo investigation in a similar manner to 17β-oestradiol. These results point to the therapeutic potential of loganic acid for the treatment of osteoporosis.

5.4.4 Geniposide (131)

Geniposide is one of the iridoids found in the popular Chinese medicinal plant, *Gardenia jasminoides* Ellis. An in vivo study was conducted by Zhao et al. (2018) that evaluated the anti-depressant activity of geniposide on ICR mice. The study involved investigating the effect of geniposide treatment on repeated restraint stress (RSS) induced depressive symptoms over a 30-day period. One of the behavioural impacts of RSS is disinclination towards sugar solution consumption in test animals. The study found that treatment with geniposide increased sucrose consumption in a statistically significant manner similar to the known anti-depressant, fluoxetine hydrochloride (FLU). The open field test, which measures the interest in freely moving around to explore space, showed that spontaneous movement in mice treated with geniposide and those treated with FLU were markedly increased compared to untreated mice. Further to this, the control group that did not undergo RRS but received geniposide showed no differences from the non-RRS/non-geniposide mice. This indicates that any anti-depressant activity of geniposide is not due to the excitability of the central nervous system. Additional analysis of the brain tissue of test animals revealed that RRS resulted in the increase of caspase-3 activity and BAX protein in the hippocampus. Both parameters are associated with apoptosis of cells. Geniposide and FLU treatment significantly reversed this effect. As can be concluded from this study, geniposide has anti-depressant properties that can be exploited in the development of new therapies for the condition.

5.4.5 Juglalin (262)

Yang et al. (2014) investigated the ability of juglalin to inhibit adriamycin-induced cellular senescence in human dermal fibroblasts (HDFs) and human umbilical vein endothelial cells (HUVECs). One sign of cellular senescence is the increase in the activity of senescence-associated β-galactosidase (SA-β-gal). Another indicator of senescence is the increase in expression of p53 and p21 proteins which are tumour suppressors whose function is activated upon DNA damage (Georgakilas et al., 2017). A third sign of senescence is the increase in reactive oxygen species. Preliminary SA-β-gal activity assay showed a decrease in SA-β-gal in Adriamycin-treated HDFs and no change in HUVECs (Yang et al., 2014). Juglalin was also shown to reduce p53 and p21 proteins in Adriamycin-treated HDFs. ROS, which are upregulated in Adriamycin treated HDFs, also decreased after treatment with juglalin (Yang et al., 2014). These effects of juglalin on HDFs support the use of *C. dentata* in the treatment of skin conditions.

5.4.6 Sweroside (114)

Yang et al. (2020) assessed the effect of sweroside in a methionine–choline-deficient (MCD) diet-induced non-alcoholic steatohepatitis (NASH) mouse model. The mice were administered the diet alongside sweroside over a two-week period. The MCD diet results in NASH due to the absence of methionine and choline, which are essential for mitochondrial fatty acid β-oxidation (Houten et al., 2016). This deficiency leads to liver damage and, consequently, the activation of the NLRP3 inflammasome protein, which mediates the release of pro-inflammatory cytokines (Kelley et al., 2019). The research showed that sweroside resulted in a decrease in IL-1β and caspase 1 production. The decrease is an indicator that NLRP3 activation was inhibited. These results suggest that sweroside could be a potential medication for NASH and other conditions which result from inflammation.

5.5 Conclusion

The isolation of phlorizin from the bark of *C. dentata* supports the traditional application of the bark in the treatment of diabetes. Phlorizin has long been shown to ameliorate diabetes conditions. The ability of juglalin to reduce senescence in HDFs could be part of the reason why *C. dentata* has ethnopharmacological applications in the treatment of skin conditions. The isolation of bioactive secondary metabolites from *C. dentata* supports the use of the plant in ethnomedicine. Further to this, the isolation of iridoids from *C. dentata* confirms our initial

hypothesis that if other plants in the Cornales order have been found to have iridoids, *C. dentata* is likely to produce them as well.

5.6 References

Afolayan, A., Mbaebie, B., 2010. Ethnobotanical study of medicinal plants used as anti-obesity remedies in Nkonkobe Municipality of South Africa. Pharmacognosy Journal 2, 368-373.

Berry, P.E., 2013. Cornales, Encyclopedia Britannica.

Bih, R.A., Monyama, M.C., Lebelo, S.L., 2023. South African medicinal plants used in the treatment of human bacterial infections: An updated review. Biomedical and Pharmacology Journal 16, 1927-1947.

Calis, I., Lahloub, M.F., Sticher, O., 1984. Loganin, loganic acid and periclymenoside, a new biosidic ester iridoid glucoside from *Lonicera periclymenum* L. (Caprifoliaceae). Helvetica Chimica Acta 67, 160-165.

Cambie, R.C., Lal, A.R., Rickard, C.E., Tanaka, N., 1990. Chemistry of Fijian plants. V.: Constituents of *Fagraea gracilipes* A. Gray. Chemical and Pharmaceutical Bulletin 38, 1857-1861.

Chang, Y.C., Chang, F.R., Wu, Y.C., 2000. The constituents of *Lindera glauca*. Journal of the Chinese Chemical Society 47, 373-380.

Craik, D.J., Henriques, S.T., Mylne, J.S., Wang, C.K., 2012. Chapter Three - Cyclotide isolation and characterization, in: Hopwood, D.A. (Ed.) Methods in Enzymology. Academic Press, pp. 37-62.

DeLeon-Pennell, K.Y., Meschiari, C.A., Jung, M., Lindsey, M.L., 2017. Matrix metalloproteinases in myocardial infarction and heart failure. Progress in Molecular Biology and Translational Science 147, 75-100.

Dold, A.P., Cocks, M.L., 2001. Traditional veterinary medicine in the Alice district of the Eastern Cape Province, South Africa: Research in action. South African Journal of Science 97, 375-379.

Doughari, J.H., Ndakidemi, P.A., Human, I.S., Benade, S., 2012. Antioxidant, antimicrobial and antiverotoxic potentials of extracts of *Curtisia dentata*. Journal of Ethnopharmacology 141, 1041-1050.

Ehrenkranz, J.R., Lewis, N.G., Ronald Kahn, C., Roth, J., 2005. Phlorizin: a review. Diabetes/Metabolism Research and Reviews 21, 31-38.

Ganeshpurkar, A. and Saluja, A., 2020. The pharmacological potential of catechin. Indian Journal of Biochemistry and Biophysics, 57(5), 505-511.

Georgakilas, A.G., Martin, O.A., Bonner, W.M., 2017. p21: a two-faced genome guardian. Trends in Molecular Medicine 23, 310-319.

Gousiadou, C., Li, H.-Q., Gotfredsen, C., Jensen, S.R., 2016. Iridoids in Hydrangeaceae. Biochemical Systematics and Ecology 64, 122-130.

Grierson, D.S., Afolayan, A.J., 1999. An ethnobotanical study of plants used for the treatment of wounds in the Eastern Cape, South Africa. Journal of Ethnopharmacology 67, 327-332.

Hao, Z.-Y., Wang, X.-L., Yang, M., Cao, B., Zeng, M.-N., Zhou, S.-Q., Li, M., Cao, Y.-G., Xie, S.-S., Zheng, X.-K., Feng, W.-S., 2023. Minor iridoid glycosides from the fruits of *Cornus officinalis* Sieb. et Zucc. and their anti-diabetic bioactivities. Phytochemistry 205, 113505.

Houten, S.M., Violante, S., Ventura, F.V., Wanders, R.J.A., 2016. The biochemistry and physiology of mitochondrial fatty acid β-oxidation and its genetic disorders. Annual Review of Physiology 78, 23-44.

Hutchings, A., Scott, A.H., Lewis, G., Cunningham, A.B., 1996. Zulu Medicinal Plants: An Inventory. University of Natal Press, Pietermaritzburg.

Hye, M.A., Taher, M.A., Ali, M.Y., Ali, M.U. and Zaman, S., 2009. Isolation of (+)-catechin from Acacia catechu (Cutch Tree) by a convenient method. Journal of Scientific Research, 1(2), 300-305.

Kalemba, M.R.K., Makhuvele, R., Njobeh, P.B., 2024. Phytochemical screening, antioxidant activity of selected methanolic plant extracts and their detoxification capabilities against AFB1 toxicity. Heliyon 10, e24435.

Karioti, A., Chatzopoulou, A., Bilia, A.R., Liakopoulos, G., Stavrianakou, S., Skaltsa, H., 2006. Novel secoiridoid glucosides in *Olea europaea* leaves suffering from boron deficiency. Bioscience, Biotechnology, and Biochemistry 70, 1898-1903.

Kelley, N., Jeltema, D., Duan, Y., He, Y., 2019. The NLRP3 inflammasome: an overview of mechanisms of activation and regulation. International Journal of Molecular Sciences 20, 3328.

Koduru, S., Grierson, D., Afolayan, A., 2007. Ethnobotanical information of medicinal plants used for treatment of cancer in the Eastern Cape Province, South Africa. Current Science, 906-908.

Liu, J., Zhang, J., Wang, F., Chen, X., 2012. New secoiridoid glycosides from the buds of *Lonicera macranthoides*. Natural Product Communications 7, 1934578X1200701202.

Lv, Q., Lin, Y., Tan, Z., Jiang, B., Xu, L., Ren, H., Tai, W.C.-s., Chan, C.-o., Lee, C.-s., Gu, Z., 2019. Dihydrochalcone-derived polyphenols from tea crab apple (*Malus hupehensis*) and their inhibitory effects on α-glucosidase in vitro. Food & Function 10, 2881-2887.

Manchester, S.R., Xiang, Q.-Y., Xiang, Q.-P., 2007. Curtisia (Cornales) from the Eocene of Europe and its phytogeographical significance. Botanical Journal of the Linnean Society 155, 127-134.

Maroyi, A., 2019. *Curtisia dentata*: a review of its botany, medicinal uses, phytochemistry and biological activities. Journal of Pharmaceutical Sciences and Research 11, 3404-3410.

Ono, M., Ueno, M., Masuoka, C., Ikeda, T. and Nohara, T., 2005. Iridoid glucosides from the fruit of *Genipa americana*. Chemical and pharmaceutical bulletin, 53(10), 1342-1344.

Osuntokun, O.T., Idowu, T., Gamberini, M.C., 2018. Bio-guided isolation, purification and chemical characterization of epigallocatechin; epicatechin, stigmasterol, phytosterol from of ethyl acetate stem bark fraction of *Spondias mombin* (Linn.). Biochemistry and Pharmacology 7, 1-9.

Park, E., Lee, C.G., Lim, E., Hwang, S., Yun, S.H., Kim, J., Jeong, H., Yong, Y., Yun, S.-H., Choi, C.W., Jin, H.-S., Jeong, S.-Y., 2021. Osteoprotective effects of loganic acid on osteoblastic and osteoclastic cells and osteoporosis-induced mice. International Journal of Molecular Sciences 22, 233.

Pérez-Vásquez, A., Aguilar-Cruz, R., Bye, R., Linares, E., Rivero-Cruz, I., 2020. UHPLC-MS analysis of polyphenols in the aqueous extract of *Hydrangea seemannii*. Revista Brasileira de Farmacognosia 30, 7-11.

POWO, 2023. Plants of the World Online. Royal Botanic Gardens, Kew, On the Internet.

Raletsena, M.V., Pooe, O.J., Mongalo, N.I., 2023. A systematic review of *Curtisia dentata* endemic to South Africa: Phytochemistry, pharmacology, and toxicology. Life 13, 2159.

Rodríguez, V., Schripsema, J., Jensen, S.R., 2002. An iridoid glucoside from *Gronovia scandens* (Loasaceae). Biochemical Systematics and Ecology 30, 243-247.

Sardana, A., Kalra, S., Khanna, D. and Balakumar, P., 2015. Nephroprotective effect of catechin on gentamicin-induced experimental nephrotoxicity. Clinical and experimental nephrology, 19, 178-184.

Seo, C., Jeong, W., Lee, J.E., Kwon, J.G., Kim, J.K., Hong, S.S., 2019. Flavonoids from the aerial parts of *Astilbe rubra*. Chemistry of Natural Compounds 55, 1153-1155.

Shai, L.J., McGaw, L.J., Aderogba, M.A., Mdee, L.K., Eloff, J.N., 2008. Four pentacyclic triterpenoids with antifungal and antibacterial activity from *Curtisia dentata* (Burm.f) C.A. Sm. leaves. Journal of Ethnopharmacology 119, 238-244.

Shin, S.-K., Cho, S.-J., Jung, U.J., Ryu, R., Choi, M.-S., 2016. Phlorizin supplementation attenuates obesity, inflammation, and hyperglycemia in diet-induced obese mice fed a high-fat diet. Nutrients 8, 92.

Shirosaki, M., Koyama, T. and Yazawa, K., 2012. Apple leaf extract as a potential candidate for suppressing postprandial elevation of the blood glucose level. Journal of nutritional science and vitaminology, 58(1), 63-67.

Van Wyk, A.S., 2020. Phytochemical evaluation of *Curtisia dentata* (Burm. f.) CA Sm. stem bark and seasonal and geographical region variability, Doctor of Philosphy, University of South Africa, Pretoria.

van Wyk, A.S., Prinsloo, G., 2021. NMR-based metabolomic analysis of the seasonal and regional variability of phytochemical compounds in *Curtisia dentata* stem bark. Biochemical Systematics and Ecology 94, 104197.

Wu, M., Wu, P., Liu, M., Xie, H., Jiang, Y., Wei, X., 2009. Iridoids from *Gentiana loureirii*. Phytochemistry 70, 746-750.

Yamazaki, K.G., Romero-Perez, D., Barraza-Hidalgo, M., Cruz, M., Rivas, M., Cortez-Gomez, B., Ceballos, G., Villarreal, F., 2008. Short-and long-term effects of (−)-epicatechin on myocardial ischemia-reperfusion injury. American Journal of Physiology-Heart and Circulatory Physiology 295, H761-H767.

Yang, G., Jang, J.H., Kim, S.W., Han, S.-H., Ma, K.-H., Jang, J.-K., Kang, H.C., Cho, Y.-Y., Lee, H.S., Lee, J.Y., 2020. Sweroside prevents non-alcoholic steatohepatitis by suppressing activation of the NLRP3 inflammasome. International Journal of Molecular Sciences 21, 2790.

Yang, H.H., Hwangbo, K., Zheng, M.S., Son, J.-K., Kim, H.Y., Baek, S.H., Choi, H.C., Park, S.Y., Kim, J.-R., 2014. Inhibitory effects of juglanin on cellular senescence in human dermal fibroblasts. Journal of Natural Medicines 68, 473-480.

Zhao, Y., Li, H., Fang, F., Qin, T., Xiao, W., Wang, Z., Ma, S., 2018. Geniposide improves repeated restraint stress-induced depression-like behavior in mice by ameliorating neuronal apoptosis via regulating GLP-1R/AKT signaling pathway. Neuroscience Letters 676, 19-26.

Chapter 6 Conclusion

The previous five chapters of this thesis have painted a picture of the potential for discovering biologically active compounds from plants in southern Africa. Plants used in traditional medicine are the primary targets because their medicinal use is documented, and there is already some knowledge to build on. While in bygone eras, plant medicines were part of a limited therapeutic arsenal, in contemporary times, plant medicines, in their raw state, are mainly used in countries of low economic status, where medical systems are less developed. However, the contribution of plants to developing advanced medicines is still essential. Plant secondary metabolites form a large segment of drug lead compounds that are derivatised to produce commercial pharmaceuticals.

Southern Africa is a vast region with numerous medicinal plants. To rationally approach phytochemical research, it is essential to determine which taxonomic groups are most exploited for medicinal purposes. Targeting taxonomic groups at the genus level is crucial, where intra-group similarities are pronounced. This approach presumes that selecting traditional medicinal plants is not a random process of trial and error but a systematic selective process.

Chapter two presents the first time that the over-represented medicinal taxa of southern Africa have been analysed independently. It is also the first time that analysis at the genus level has been undertaken for medicinal plant species. It was shown in Chapter 2 that southern Africa has specific over-represented genera and families. The study confirmed that indigenous medicinal plant knowledge is not a random collection of plants but that practitioners gravitated towards certain groups of plants. Furthermore, variations in over-represented medicinal taxa occur among southern African countries and across disease categories. Southern Africa has at least 92 and 42 over-represented medicinal plant genera and families, respectively. The findings of this study may be used to select medicinal plant taxonomic groups for phytochemical and bioactivity investigations. This opens up future lines of enquiry that could help verify the utility of using statistical methods to streamline the selection of plant species for investigation.

The research also acknowledged that countries needed a comparable wealth of data on ethnopharmacological plant use. South Africa stood out with overwhelmingly high numbers of recorded medicinal plants. There is a lack of comparable data in neighbouring countries, and more ethnopharmacological surveys are needed in other southern African countries.

The Loganiaceae and *Albizia* taxonomic groups are over-represented in southern African ethnopharmacology. Future studies may use an over-representation-guided approach to study the phytochemical characteristics of medicinal taxa. This may be a more efficient way of assessing the potential of southern African flora as a source of medicinal products and drug-lead compounds. Furthermore, Ebenaceae and *Albizia*, Canellaceae and *Dicoma*, Combretaceae and *Pterocelastrus*, Ebenaceae and *Bersama*, Francoaceae and *Erythrina*, and Aristolochiaceae and *Strychnos* are over-represented among STIs, febrile and mosquito-vector diseases, microbial infections, pain, skin conditions, and female sexual/reproductive problems, respectively. These findings can form the basis of over-representation-guided selection and investigation of plant bioactivities against the causative agents of these conditions. The Rubiaceae were also found to be one of the over-represented medicinal plant families of southern Africa.

In Chapter 3, the Rubiaceae of southern Africa was reviewed. The family has a broad range of ethnobotanical and ethnopharmacological uses. Reported bioactivities and the phytochemical constituents were also examined. The results show that some preparation modes and the specific plant parts used for therapies still need to be reported. The review of publications that report studies of southern African Rubiaceae showed that 23 of 34 anti-inflammatory and analgesic species, 17 out of 31 anti-viral and anti-bacterial plants, and 13 out of 27 Rubiaceae species used for sexual and reproductive problems have not undergone preparative phytochemical analysis. Additionally, only 52 species were found to have been subjected to assays for bioactivity. There is a need to investigate species for which data has not been reported. This shows that the species of Rubiaceae of southern Africa need further investigation.

Chapter 4 reported the phytochemical investigation of two Rubiaceae species, *C. rudis* and *K. gueinzii*. To our knowledge, this is the first isolation and characterisation of astragalin, gardenoside, and geniposidic acid from *C. rudis*. This is also the first report of the isolation of kaempferitrin from *K. gueinzii*. These are known compounds with reported bioactivities. The pharmacological activities of astragalin, gardenoside, geniposidic acid, and kaempferitrin

support the use of *C. rudis* and *K. gueinzii* for medicinal purposes. Knowledge on the phytochemistry of southern African Rubiaceae is limited, and this investigation adds to that body of knowledge.

Chapter 5 is a report on the phytochemical investigation of *C. dentata*. Phytochemical studies have been performed on this species, and literature reviews on *C. dentata* have been published. However, the compounds described in this study have yet to be reported from *C. dentata*. Previous phytochemical investigations on *C. dentata* focused on the non-polar compounds. However, the results obtained from this study have shown that the bioactive compounds are present in the polar extracts (EtOH-H_2O) of this plant. This investigation constitutes the first published report of the isolation of phlorizin and epicatechin from the bark of *C. dentata*. It is also the first time that loganic acid, sweroside, secologanoside, and geniposide, and, in fact, any iridoid, have been observed in this species. The flavonol glycoside juglalin have also not been isolated from this species previously. The isolation of the anti-diabetic dihydrochalcone phlorizin is interesting as it corroborates the traditional use of bark decoctions for treating diabetes in the Eastern Cape province of South Africa.

Bioassay-guided fractionation was not performed in this investigation, and in future, such experiments will help identify compounds that are effective against particular targets. Bioassays that address the claimed ethnopharmacological properties would be particularly important in understanding southern African medicinal Rubiaceae species.

The study successfully delineated the most prominent southern African medicinal genera and families using statistical methods, reviewed the published knowledge about southern African Rubiaceae and isolated bioactive natural products from southern African medicinal plants: *C. rudis*, *K. gueinzii* and *C. dentata*.

Phytochemistry of some southern African medicinal Rubiaceae and Curtisiaceae species

(Supplemental file)

By

Prince Nqaba Moyo

211543946

Appendix A Supplement to Chapter 2

INDEX

Explanation of headings in all tables:

A(n)	= Total number of species in family/genus
B(x)	= Number of medicinal species in family/genus
Inf	= Lower limit of the 95% probability interval for family/genus
Mean θ	= proportion of medicinal species in the family/genus
Sup.	= Upper limit of the 95% probability interval for family/genus
Margin of over-representation	= Difference between the Sup. of the total medicinal flora and the Inf. of the taxonomic group's medicinal flora
Genera cumulative margin	= Obtained by adding the margins of the over-representative genera in that family.

Table S.1
IDM analysis of over-represented medicinal plant families in southern Africa (Group 1).

Family	A(n)	B(x)	Inf.	Mean θ	Sup.	Margin of over-representation	Genera cumulative margin
Loganiaceae	18	9	0.218	0.500	0.782	0.142	0.142
Sapotaceae	27	11	0.199	0.407	0.657	0.123	0.032
Ebenaceae	55	18	0.195	0.327	0.499	0.119	0.128
Aristolochiaceae	10	6	0.192	0.600	0.909	0.116	0.032
Anacardiaceae	154	38	0.177	0.247	0.337	0.101	0.168
Capparaceae	79	21	0.166	0.266	0.404	0.090	0.130
Francoaceae	16	7	0.163	0.438	0.756	0.087	0.046
Combretaceae	110	26	0.156	0.236	0.347	0.080	0.111
Dioscoreaceae	30	10	0.156	0.333	0.579	0.080	0.061
Pedaliaceae	49	14	0.156	0.286	0.471	0.080	0.135
Ranunculaceae	45	13	0.153	0.289	0.484	0.077	0.071
Icacinaceae	14	6	0.142	0.429	0.770	0.066	0.009
Phyllanthaceae	106	23	0.139	0.217	0.330	0.063	0.135
Sapindaceae	61	15	0.138	0.246	0.408	0.062	0.023
Burseraceae	63	15	0.133	0.238	0.396	0.057	0.058
Meliaceae	42	11	0.129	0.262	0.466	0.053	0.000
Cannabaceae	11	5	0.128	0.455	0.823	0.052	0.000
Moraceae	68	15	0.123	0.221	0.371	0.047	0.039
Polygonaceae	63	14	0.121	0.222	0.380	0.045	0.056
Lamiaceae	419	65	0.121	0.155	0.200	0.045	0.246
Cucurbitaceae	136	25	0.120	0.184	0.278	0.044	0.083
Lauraceae	17	6	0.119	0.353	0.685	0.043	0.042
Oleaceae	29	8	0.115	0.276	0.532	0.039	0.023
Menispermaceae	35	9	0.114	0.257	0.487	0.038	0.000
Rubiaceae	572	81	0.113	0.142	0.178	0.038	0.336
Solanaceae	106	19	0.108	0.179	0.289	0.032	0.056
Convolvulaceae	143	24	0.108	0.168	0.258	0.032	0.057
Malvaceae	552	75	0.108	0.136	0.172	0.032	0.147
Celastraceae	129	22	0.107	0.171	0.267	0.032	0.023
Caprifoliaceae	26	7	0.103	0.269	0.543	0.027	0.000
Bignoniaceae	20	6	0.102	0.300	0.615	0.026	0.000
Salvadoraceae	4	3	0.099	0.750	0.996	0.023	0.000
Ochnaceae	55	11	0.099	0.200	0.372	0.023	0.038
Peraceae	42	9	0.096	0.214	0.419	0.020	0.006
Vitaceae	134	20	0.092	0.149	0.241	0.016	0.000
Clusiaceae	17	5	0.087	0.294	0.639	0.011	0.027
Annonaceae	97	15	0.086	0.155	0.269	0.010	0.000
Primulaceae	24	6	0.086	0.250	0.540	0.010	0.000
Fabaceae	2634	256	0.086	0.097	0.110	0.010	0.743
Euphorbiaceae	670	73	0.086	0.109	0.139	0.010	0.121
Verbenaceae	47	9	0.086	0.191	0.382	0.010	0.023
Boraginaceae	127	18	0.084	0.142	0.236	0.008	0.177
Total species in group	28426[a]	2069[b]	0.070	0.073	0.076		

[a]Total number of plant species (including species in under-represented taxonomic groups) [b]Total number of medicinal plant species (including medicinal plant species in under-represented taxonomic groups).

Table S.2
IDM analysis of over-represented medicinal plant genera in southern Africa (Group 1).

Genus	Family	A(n)	B(x)	Inf.	Mean θ	Sup.	Margin of over-representation
Albizia	Fabaceae	20	10	0.232	0.500	0.768	0.156
Strychnos	Loganiaceae	18	9	0.218	0.500	0.782	0.142
Sesamum	Pedaliaceae	22	10	0.211	0.455	0.722	0.135
Bridelia	Phyllanthaceae	9	6	0.211	0.667	0.945	0.135
Cymbopogon	Poaceae	9	6	0.211	0.667	0.945	0.135
Vachellia	Fabaceae	45	16	0.204	0.356	0.547	0.128
Ehretia	Boraginaceae	10	6	0.192	0.600	0.909	0.116
Gardenia	Rubiaceae	10	6	0.192	0.600	0.909	0.116
Lannea	Anacardiaceae	14	7	0.184	0.500	0.816	0.108
Laggera	Asteraceae	4	4	0.184	1.000	1.000	0.108
Senna	Fabaceae	4	4	0.184	1.000	1.000	0.108
Senegalia	Fabaceae	30	11	0.180	0.367	0.608	0.104
Boscia	Capparaceae	15	7	0.173	0.467	0.785	0.097
Vitex	Lamiaceae	15	7	0.173	0.467	0.785	0.097
Diospyros	Ebenaceae	38	12	0.161	0.316	0.531	0.085
Vangueria	Rubiaceae	25	9	0.159	0.360	0.628	0.083
Grewia	Malvaceae	58	16	0.158	0.276	0.443	0.082
Gymnanthemum	Asteraceae	13	6	0.152	0.462	0.802	0.076
Combretum	Combretaceae	82	20	0.150	0.244	0.378	0.074
Jatropha	Euphorbiaceae	27	9	0.147	0.333	0.594	0.071
Dioscorea	Dioscoreaceae	29	9	0.137	0.310	0.563	0.061
Catunaregam	Rubiaceae	6	4	0.137	0.667	0.972	0.061
Trichodesma	Boraginaceae	6	4	0.137	0.667	0.972	0.061
Ziziphus	Rhamnaceae	6	4	0.137	0.667	0.972	0.061
Commiphora	Burseraceae	57	14	0.134	0.246	0.414	0.058
Zanthoxylum	Rutaceae	15	6	0.133	0.400	0.740	0.057
Ipomoea	Convolvulaceae	63	15	0.133	0.238	0.396	0.057
Brachystegia	Fabaceae	20	7	0.132	0.350	0.655	0.056
Entada	Fabaceae	20	7	0.132	0.350	0.655	0.056
Rumex	Polygonaceae	20	7	0.132	0.350	0.655	0.056
Solanum	Solanaceae	58	14	0.132	0.241	0.408	0.056
Cucumis	Cucurbitaceae	26	8	0.127	0.308	0.577	0.051
Asparagus	Asparagaceae	103	21	0.127	0.204	0.318	0.051
Knowltonia	Ranunculaceae	16	6	0.126	0.375	0.711	0.050
Sida	Malvaceae	16	6	0.126	0.375	0.711	0.050
Searsia	Anacardiaceae	92	19	0.125	0.207	0.329	0.049
Agapanthus	Amaryllidaceae	7	4	0.122	0.571	0.933	0.046
Bersama	Francoaceae	7	4	0.122	0.571	0.933	0.046
Ocimum	Lamiaceae	22	7	0.121	0.318	0.613	0.045
Euclea	Ebenaceae	17	6	0.119	0.353	0.685	0.043
Cassytha	Lauraceae	3	3	0.118	1.000	1.000	0.042
Erythrophleum	Fabaceae	3	3	0.118	1.000	1.000	0.042
Mentha	Lamiaceae	3	3	0.118	1.000	1.000	0.042
Rubia	Rubiaceae	3	3	0.118	1.000	1.000	0.042
Teucrium	Lamiaceae	3	3	0.118	1.000	1.000	0.042
Ficus	Moraceae	47	11	0.115	0.234	0.425	0.039
Lasiosiphon	Thymelaeaceae	29	8	0.115	0.276	0.532	0.039
Ochna	Ochnaceae	35	9	0.114	0.257	0.487	0.038
Hypoxis	Hypoxidaceae	48	11	0.113	0.229	0.417	0.037
Erythrina	Fabaceae	18	6	0.113	0.333	0.660	0.037
Terminalia	Combretaceae	18	6	0.113	0.333	0.660	0.037
Acalypha	Euphorbiaceae	42	10	0.112	0.238	0.443	0.036
Canthium	Rubiaceae	8	4	0.109	0.500	0.891	0.033
Capparis	Capparaceae	8	4	0.109	0.500	0.891	0.033

Secamone	Apocynaceae	8	4	0.109	0.500	0.891	0.033
Momordica	Cucurbitaceae	19	6	0.107	0.316	0.636	0.031
Amaranthus	Amaranthaceae	14	5	0.103	0.357	0.722	0.027
Garcinia	Clusiaceae	14	5	0.103	0.357	0.722	0.027
Strophanthus	Apocynaceae	14	5	0.103	0.357	0.722	0.027
Dracaena	Asparagaceae	26	7	0.103	0.269	0.543	0.027
Athrixia	Asteraceae	9	4	0.099	0.444	0.848	0.023
Brachylaena	Asteraceae	9	4	0.099	0.444	0.848	0.023
Gloriosa	Colchicaceae	9	4	0.099	0.444	0.848	0.023
Lippia	Verbenaceae	9	4	0.099	0.444	0.848	0.023
Aristolochia	Aristolochiaceae	4	3	0.099	0.750	0.996	0.023
Cardiospermum	Sapindaceae	4	3	0.099	0.750	0.996	0.023
Carissa	Apocynaceae	4	3	0.099	0.750	0.996	0.023
Mimusops	Sapotaceae	4	3	0.099	0.750	0.996	0.023
Olea	Oleaceae	4	3	0.099	0.750	0.996	0.023
Pterocelastrus	Celastraceae	4	3	0.099	0.750	0.996	0.023
Clematis	Ranunculaceae	15	5	0.097	0.333	0.692	0.021
Cussonia	Araliaceae	15	5	0.097	0.333	0.692	0.021
Salvia	Lamiaceae	28	7	0.096	0.250	0.514	0.020
Tephrosia	Fabaceae	90	15	0.093	0.167	0.289	0.017
Dicoma	Asteraceae	16	5	0.091	0.313	0.665	0.015
Melhania	Malvaceae	16	5	0.091	0.313	0.665	0.015
Bauhinia	Fabaceae	10	4	0.091	0.400	0.808	0.015
Gomphocarpus	Apocynaceae	10	4	0.091	0.400	0.808	0.015
Mucuna	Fabaceae	10	4	0.091	0.400	0.808	0.015
Croton	Euphorbiaceae	30	7	0.090	0.233	0.487	0.014
Ozoroa	Anacardiaceae	31	7	0.087	0.226	0.475	0.011
Aspilia	Asteraceae	5	3	0.085	0.600	0.968	0.009
Dysphania	Amaranthaceae	5	3	0.085	0.600	0.968	0.009
Hydnora	Aristolochiaceae	5	3	0.085	0.600	0.968	0.009
Manilkara	Sapotaceae	5	3	0.085	0.600	0.968	0.009
Mikania	Asteraceae	5	3	0.085	0.600	0.968	0.009
Pterocarpus	Fabaceae	5	3	0.085	0.600	0.968	0.009
Pyrenacantha	Icacinaceae	5	3	0.085	0.600	0.968	0.009
Nidorella	Asteraceae	18	5	0.082	0.278	0.616	0.006
Clutia	Peraceae	41	8	0.082	0.195	0.403	0.006
Syzygium	Myrtaceae	12	4	0.078	0.333	0.734	0.002
Tulbaghia	Amaryllidaceae	27	6	0.077	0.222	0.494	0.001
Total species in group		28426[a]	2069[b]	0.070	0.073	0.076	

[a]Total number of plant species (including species in under-represented taxonomic groups) [b]Total number of medicinal plant species (including medicinal plant species in under-represented taxonomic groups).

Table S.3
IDM analysis of over-represented medicinal plant families in Botswana and Namibia (Group 2).

Family (J)	A(n)	B(x)	Inf.	Mean θ	Sup.	Margin of over-representation
Combretaceae	31	10	0.151	0.323	0.564	0.060
Phyllanthaceae	10	5	0.139	0.500	0.861	0.048
Celastraceae	17	6	0.119	0.353	0.685	0.028
Anacardiaceae	40	10	0.118	0.250	0.461	0.027
Solanaceae	49	11	0.111	0.224	0.410	0.020
Fabaceae	408	58	0.109	0.142	0.187	0.018
Euphorbiaceae	122	21	0.107	0.172	0.272	0.016
Ebenaceae	14	5	0.103	0.357	0.722	0.012
Capparaceae	22	6	0.094	0.273	0.575	0.003
Total species in group	4483[a]	366[b]	0.074	0.082	0.091	

[a]Total number of plant species (including species in under-represented taxonomic groups) [b]Total number of medicinal plant species (including medicinal plant species in under-represented taxonomic groups).

Table S.4
IDM analysis of over-represented medicinal plant genera in Botswana and Namibia (Group 2).

Genus	Family	A(n)	B(x)	Inf.	Mean θ	Sup.	Margin of over-representation
Vachellia	Fabaceae	19	8	0.172	0.421	0.718	0.081
Solanum	Solanaceae	21	8	0.156	0.381	0.672	0.066
Asparagus	Asparagaceae	26	9	0.153	0.346	0.611	0.062
Albizia	Fabaceae	6	4	0.137	0.667	0.972	0.046
Gymnosporia	Celastraceae	6	4	0.137	0.667	0.972	0.046
Grewia	Malvaceae	20	7	0.132	0.350	0.655	0.041
Dicoma	Asteraceae	7	4	0.122	0.571	0.933	0.031
Combretum	Combretaceae	22	7	0.121	0.318	0.613	0.030
Total species in group		4483[a]	366[b]	0.074	0.082	0.091	

[a]Total number of plant species (including species in under-represented taxonomic groups) [b]Total number of medicinal plant species (including medicinal plant species in under-represented taxonomic groups).

Table S.5
IDM analysis of over-represented medicinal plant families in MW, MO, ZM and ZW (Group 3).

Family (J)	A(n)	B(x)	Inf.	Mean θ	Sup.	Margin of over-representation
Dioscoreaceae	15	8	0.215	0.533	0.827	0.114
Anacardiaceae	60	19	0.192	0.317	0.480	0.091
Pedaliaceae	17	8	0.191	0.471	0.769	0.090
Loganiaceae	14	7	0.184	0.500	0.816	0.083
Aristolochiaceae	4	4	0.184	1.000	1.000	0.082
Combretaceae	68	20	0.181	0.294	0.445	0.080
Meliaceae	24	9	0.165	0.375	0.647	0.064
Olacaceae	6	4	0.137	0.667	0.972	0.035
Ebenaceae	37	10	0.127	0.270	0.491	0.025
Capparaceae	48	11	0.113	0.229	0.417	0.011
Fabaceae	977	127	0.109	0.130	0.156	0.008
Phyllanthaceae	64	13	0.108	0.203	0.359	0.006
Thymelaeaceae	26	7	0.103	0.269	0.543	0.001
Myrtaceae	20	6	0.102	0.300	0.615	0.001
Total species in group	7775[a]	735[b]	0.088	0.095	0.102	

[a]Total number of plant species (including species in under-represented taxonomic groups) [b]Total number of medicinal plant species (including medicinal plant species in under-represented taxonomic groups).

Table S.6
IDM analysis of over-represented medicinal plant genera in MW, MO, ZM and ZW (Group 3).

Genus	Family	A(n)	B(x)	Inf.	Mean θ	Sup.	Margin of over-representation
Senna	Fabaceae	11	7	0.230	0.636	0.916	0.129
Senegalia	Fabaceae	21	9	0.188	0.429	0.709	0.086
Dioscorea	Dioscoreaceae	14	7	0.184	0.500	0.816	0.083
Strychnos	Loganiaceae	14	7	0.184	0.500	0.816	0.083
Combretum	Combretaceae	46	14	0.166	0.304	0.496	0.064
Sesamum	Pedaliaceae	12	6	0.163	0.500	0.837	0.062
Searsia	Anacardiaceae	29	10	0.161	0.345	0.594	0.060
Cucumis	Cucurbitaceae	14	6	0.142	0.429	0.770	0.040
Gardenia	Rubiaceae	6	4	0.137	0.667	0.972	0.035
Entada	Fabaceae	11	5	0.128	0.455	0.823	0.026
Terminalia	Combretaceae	16	6	0.126	0.375	0.711	0.024
Boscia	Capparaceae	7	4	0.122	0.571	0.933	0.020
Euclea	Ebenaceae	7	4	0.122	0.571	0.933	0.020
Mucuna	Fabaceae	7	4	0.122	0.571	0.933	0.020
Aristolochia	Aristolochiaceae	3	3	0.118	1.000	1.000	0.017
Vachellia	Fabaceae	29	8	0.115	0.276	0.532	0.013
Grewia	Malvaceae	37	9	0.108	0.243	0.465	0.007
Albizia	Fabaceae	14	5	0.103	0.357	0.722	0.002
Total species in group		7775[a]	735[b]	0.088	0.095	0.102	

[a]Total number of plant species (including species in under-represented taxonomic groups) [b]Total number of medicinal plant species (including medicinal plant species in under-represented taxonomic groups).

Table S.7
IDM analysis of over-represented medicinal plant families in South Africa (Group 4).

Family	A(n)	B(x)	Inf.	Mean θ	Sup.	Margin of over-representation
Sapotaceae	15	12	0.410	0.800	0.964	0.341
Annonaceae	12	8	0.266	0.667	0.922	0.197
Combretaceae	30	14	0.255	0.467	0.692	0.186
Loganiaceae	10	7	0.251	0.700	0.950	0.182
Icacinaceae	8	6	0.234	0.750	0.977	0.165
Solanaceae	49	16	0.187	0.327	0.510	0.118
Ranunculaceae	26	10	0.179	0.385	0.643	0.110
Francoaceae	12	6	0.163	0.500	0.837	0.094
Anacardiaceae	91	23	0.162	0.253	0.378	0.093
Ebenaceae	34	11	0.159	0.324	0.552	0.090
Cannabaceae	5	4	0.157	0.800	0.997	0.088
Capparaceae	26	9	0.153	0.346	0.611	0.084
Burseraceae	19	7	0.139	0.368	0.678	0.069
Phyllanthaceae	31	9	0.129	0.290	0.535	0.060
Verbenaceae	26	8	0.127	0.308	0.577	0.058
Salicaceae	21	7	0.126	0.333	0.634	0.057
Rubiaceae	206	36	0.124	0.175	0.246	0.054
Menispermaceae	12	5	0.118	0.417	0.787	0.049
Euphorbiaceae	258	41	0.115	0.159	0.220	0.046
Ochnaceae	13	5	0.110	0.385	0.753	0.041
Lauraceae	13	5	0.110	0.385	0.753	0.041
Meliaceae	13	5	0.110	0.385	0.753	0.041
Primulaceae	13	5	0.110	0.385	0.753	0.041
Lamiaceae	261	38	0.104	0.146	0.205	0.035
Polygonaceae	26	7	0.103	0.269	0.543	0.034
Cucurbitaceae	60	12	0.102	0.200	0.362	0.033
Moraceae	28	7	0.096	0.250	0.514	0.027
Caprifoliaceae	23	6	0.090	0.261	0.557	0.021
Celastraceae	87	14	0.088	0.161	0.285	0.019
Urticaceae	17	5	0.087	0.294	0.639	0.017
Sapindaceae	24	6	0.086	0.250	0.540	0.017
Convolvulaceae	87	13	0.079	0.149	0.273	0.010
Pteridaceae	54	9	0.075	0.167	0.339	0.006
Amaranthaceae	133	17	0.075	0.128	0.218	0.005
Vitaceae	46	8	0.073	0.174	0.366	0.004
Malvaceae	318	33	0.072	0.104	0.152	0.003
Oleaceae	21	5	0.071	0.238	0.553	0.002
Total species in group	19365[a]	1268[b]	0.062	0.065	0.069	

[a]Total number of plant species (including species in under-represented taxonomic groups) [b]Total number of medicinal plant species (including medicinal plant species in under-represented taxonomic groups).

Table S.8
IDM analysis of over-represented medicinal plant genera in South Africa (Group 4).

Genus	Family	A(n)	B(x)	Inf.	Mean θ	Sup.	Margin of over-representation
Solanum	Solanaceae	26	14	0.294	0.538	0.765	0.225
Combretum	Combretaceae	24	12	0.255	0.500	0.745	0.186
Strychnos	Loganiaceae	10	7	0.251	0.700	0.950	0.182
Amaranthus	Amaranthaceae	5	5	0.245	1.000	1.000	0.176
Albizia	Fabaceae	11	7	0.230	0.636	0.916	0.161
Zanthoxylum	Rutaceae	6	5	0.212	0.833	0.997	0.143
Croton	Euphorbiaceae	8	5	0.167	0.625	0.940	0.098
Jatropha	Euphorbiaceae	12	6	0.163	0.500	0.837	0.094
Momordica	Cucurbitaceae	5	4	0.157	0.800	0.997	0.088
Knowltonia	Ranunculaceae	13	6	0.152	0.462	0.802	0.083
Acalypha	Euphorbiaceae	18	7	0.146	0.389	0.702	0.077
Commiphora	Burseraceae	19	7	0.139	0.368	0.678	0.069
Cymbopogon	Poaceae	6	4	0.137	0.667	0.972	0.068
Rumex	Polygonaceae	11	5	0.128	0.455	0.823	0.058
Ozoroa	Anacardiaceae	12	5	0.118	0.417	0.787	0.049
Bersama	Francoaceae	3	3	0.118	1.000	1.000	0.049
Bridelia	Phyllanthaceae	3	3	0.118	1.000	1.000	0.049
Gloriosa	Colchicaceae	3	3	0.118	1.000	1.000	0.049
Pyrenacantha	Icacinaceae	3	3	0.118	1.000	1.000	0.049
Teucrium	Lamiaceae	3	3	0.118	1.000	1.000	0.049
Diospyros	Ebenaceae	18	6	0.113	0.333	0.660	0.044
Gymnanthemum	Asteraceae	8	4	0.109	0.500	0.891	0.040
Rubus	Rosaceae	8	4	0.109	0.500	0.891	0.040
Ficus	Moraceae	25	7	0.107	0.280	0.559	0.038
Eulophia	Orchidaceae	27	7	0.099	0.259	0.528	0.030
Athrixia	Asteraceae	9	4	0.099	0.444	0.848	0.030
Dracaena	Asparagaceae	9	4	0.099	0.444	0.848	0.030
Capparis	Capparaceae	4	3	0.099	0.750	0.996	0.030
Carissa	Apocynaceae	4	3	0.099	0.750	0.996	0.030
Cissampelos	Menispermaceae	4	3	0.099	0.750	0.996	0.030
Coleus	Lamiaceae	4	3	0.099	0.750	0.996	0.030
Lannea	Anacardiaceae	4	3	0.099	0.750	0.996	0.030
Manilkara	Sapotaceae	4	3	0.099	0.750	0.996	0.030
Mimusops	Sapotaceae	4	3	0.099	0.750	0.996	0.030
Olea	Oleaceae	4	3	0.099	0.750	0.996	0.030
Pterocelastrus	Celastraceae	4	3	0.099	0.750	0.996	0.030
Lasiosiphon	Thymelaeaceae	28	7	0.096	0.250	0.514	0.027
Tephrosia	Fabaceae	43	9	0.094	0.209	0.411	0.024
Euclea	Ebenaceae	16	5	0.091	0.313	0.665	0.022
Erythrina	Fabaceae	10	4	0.091	0.400	0.808	0.022
Salvia	Lamiaceae	23	6	0.090	0.261	0.557	0.021
Nidorella	Asteraceae	17	5	0.087	0.294	0.639	0.017
Grewia	Malvaceae	24	6	0.086	0.250	0.540	0.017
Hypoxis	Hypoxidaceae	39	8	0.086	0.205	0.420	0.017
Cassipourea	Rhizophoraceae	5	3	0.085	0.600	0.968	0.016
Dalbergia	Fabaceae	5	3	0.085	0.600	0.968	0.016
Gardenia	Rubiaceae	5	3	0.085	0.600	0.968	0.016
Strophanthus	Apocynaceae	5	3	0.085	0.600	0.968	0.016
Thunbergia	Acanthaceae	11	4	0.084	0.364	0.770	0.015
Asparagus	Asparagaceae	83	13	0.083	0.157	0.284	0.014
Hemionitis	Pteridaceae	25	6	0.083	0.240	0.524	0.014
Cucumis	Cucurbitaceae	18	5	0.082	0.278	0.616	0.013
Searsia	Anacardiaceae	67	11	0.081	0.164	0.313	0.012
Convolvulus	Convolvulaceae	12	4	0.078	0.333	0.734	0.009

Ochna	Ochnaceae	12	4	0.078	0.333	0.734	0.009
Dovyalis	Salicaceae	6	3	0.075	0.500	0.925	0.006
Melianthus	Francoaceae	6	3	0.075	0.500	0.925	0.006
Schistostephium	Asteraceae	6	3	0.075	0.500	0.925	0.006
Eucomis	Asparagaceae	13	4	0.073	0.308	0.701	0.003
Helichrysum	Asteraceae	235	26	0.073	0.111	0.170	0.003
Vachellia	Fabaceae	29	6	0.072	0.207	0.467	0.003
Total species in group		19365[a]	1268[b]	0.062	0.065	0.069	

[a]Total number of plant species (including species in under-represented taxonomic groups) [b]Total number of medicinal plant species (including medicinal plant species in under-represented taxonomic groups).

Table S.9
Over-represented families from the IDM analysis of plants used for the treatment of STIs.

Family	A(n)	B(x)	Inf.	Meanθ	Sup.	Margin of over-representation
Ebenaceae	55	10	0.086	0.182	0.353	0.071
Loganiaceae	18	5	0.082	0.278	0.616	0.067
Olacaceae	14	3	0.038	0.214	0.617	0.023
Combretaceae	110	9	0.037	0.082	0.178	0.022
Anacardiaceae	154	11	0.035	0.071	0.145	0.020
Meliaceae	42	4	0.025	0.095	0.295	0.010
Juncaceae	23	3	0.024	0.130	0.436	0.009
Solanaceae	106	6	0.020	0.057	0.151	0.005
Capparaceae	79	5	0.020	0.063	0.183	0.005
Fabaceae	2634	61	0.018	0.023	0.031	0.003
Sapindaceae	61	4	0.017	0.066	0.212	0.002
Polygonaceae	63	4	0.017	0.063	0.206	0.002
Malvaceae	552	16	0.017	0.029	0.053	0.001
Lamiaceae	419	13	0.017	0.031	0.061	0.001
Moraceae	68	4	0.016	0.059	0.193	0.000
Phyllanthaceae	106	5	0.015	0.047	0.140	0.000
Total	28426[a]	388[b]	0.012	0.014	0.015	

[a]Total number of plant species (including species in under-represented taxonomic groups) [b]Total number of medicinal plant species used to treat STIs(including medicinal plant species in under-represented taxonomic groups).

Table S.10
Over-represented genera from the IDM analysis of plants used for the treatment of STIs.

Genus	A(n)	B(x)	Inf.	Mean θ	Sup.	Margin of over-representation
Albizia	20	6	0.102	0.30	0.615	0.087
Senna	4	3	0.099	0.75	0.996	0.084
Strychnos	18	5	0.082	0.28	0.616	0.067
Lannea	14	4	0.068	0.29	0.671	0.053
Euclea	17	4	0.057	0.24	0.592	0.042
Diospyros	38	6	0.056	0.16	0.376	0.040
Erythrina	18	4	0.054	0.22	0.570	0.039
Senegalia	30	5	0.051	0.17	0.423	0.036
Tabernaemontana	3	2	0.043	0.67	0.996	0.028
Ximenia	3	2	0.043	0.67	0.996	0.028
Gymnanthemum	13	3	0.040	0.23	0.646	0.025
Annona	4	2	0.037	0.50	0.963	0.022
Cardiospermum	4	2	0.037	0.50	0.963	0.022
Boscia	15	3	0.036	0.20	0.590	0.021
Vitex	15	3	0.036	0.20	0.590	0.021
Zanthoxylum	15	3	0.036	0.20	0.590	0.021
Asparagus	103	8	0.033	0.08	0.178	0.018
Pterocarpus	5	2	0.032	0.40	0.915	0.017
Terminalia	18	3	0.030	0.17	0.522	0.015
Ziziphus	6	2	0.028	0.33	0.863	0.013
Entada	20	3	0.028	0.15	0.484	0.013
Grewia	58	5	0.027	0.09	0.242	0.012
Solanum	58	5	0.027	0.09	0.242	0.012
Combretum	82	6	0.026	0.07	0.192	0.011
Juncus	22	3	0.025	0.14	0.451	0.010
Cissampelos	7	2	0.025	0.29	0.813	0.010
Vachellia	45	4	0.023	0.09	0.278	0.008
Dracaena	26	3	0.022	0.12	0.397	0.007
Jatropha	27	3	0.021	0.11	0.386	0.006
Brachylaena	9	2	0.021	0.22	0.723	0.006
Gomphocarpus	10	2	0.019	0.20	0.684	0.004
Ozoroa	31	3	0.019	0.10	0.345	0.003
Ipomoea	63	4	0.017	0.06	0.206	0.002
Crinum	35	3	0.017	0.09	0.313	0.001
Aloe	216	8	0.016	0.04	0.088	0.001
Total	28426[a]	388[b]	0.012	0.014	0.015	

[a]Total number of plant species (including species in under-represented taxonomic groups) [b]Total number of medicinal plant species used to treat STIs(including medicinal plant species in under-represented taxonomic groups).

Table S.11
Over-represented families from the IDM analysis of plants used for the treatment of febrile and mosquito-vector diseases.

Family	A(n)	B(x)	Inf.	Mean θ	Sup.	Margin of over-representation
Canellaceae	2	2	0.053	1.00	1.000	0.044
Ebenaceae	55	5	0.029	0.09	0.254	0.020
Lamiaceae	419	16	0.022	0.04	0.069	0.013
Aristolochiaceae	10	2	0.019	0.20	0.684	0.011
Olacaceae	14	2	0.015	0.14	0.560	0.006
Verbenaceae	47	3	0.013	0.06	0.243	0.004
Loganiaceae	18	2	0.012	0.11	0.472	0.003
Rubiaceae	572	11	0.010	0.02	0.041	0.001
Cleomaceae	25	2	0.009	0.08	0.369	0.000
Total	28426[a]	210[b]	0.006	0.01	0.009	

[a]Total number of plant species (including species in under-represented taxonomic groups) [b]Total number of medicinal plant species used for treating febrile and mosquito-vector diseases (including medicinal plant species in under-represented taxonomic groups).

Table S.12
Over-represented genera from the IDM analysis of plants used for the treatment of febrile and mosquito-vector diseases.

Genus	A(n)	B(x)	Inf.	Mean θ	Sup.	Margin of over-representation
Dicoma	16	4	0.061	0.25	0.62	0.052
Warburgia	2	2	0.053	1.00	1.00	0.044
Zanha	2	2	0.053	1.00	1.00	0.044
Teucrium	3	2	0.043	0.67	1.00	0.035
Ximenia	3	2	0.043	0.67	1.00	0.035
Annona	4	2	0.037	0.50	0.96	0.028
Aristolochia	4	2	0.037	0.50	0.96	0.028
Lasiosiphon	29	4	0.035	0.14	0.40	0.027
Nidorella	18	3	0.030	0.17	0.52	0.022
Catunaregam	6	2	0.028	0.33	0.86	0.020
Diospyros	38	4	0.027	0.11	0.32	0.019
Lippia	9	2	0.021	0.22	0.72	0.012
Gardenia	10	2	0.019	0.20	0.68	0.011
Vigna	30	3	0.019	0.10	0.35	0.011
Gymnanthemum	13	2	0.016	0.15	0.59	0.007
Zanthoxylum	15	2	0.014	0.13	0.53	0.005
Strychnos	18	2	0.012	0.11	0.47	0.003
Momordica	19	2	0.011	0.11	0.45	0.003
Albizia	20	2	0.011	0.10	0.44	0.002
Entada	20	2	0.011	0.10	0.44	0.002
Cleome	25	2	0.009	0.08	0.37	0.000
Total	28426[a]	210[b]	0.006	0.01	0.009	

[a]Total number of plant species (including species in under-represented taxonomic groups) [b]Total number of medicinal plant species used for treating febrile and mosquito-vector diseases (including medicinal plant species in under-represented taxonomic groups).

Table S.13
Over-represented families from the IDM analysis of plants used for the treatment of non-STI microbial infections.

Family	A(n)	B(x)	Inf.	Mean θ	Sup.	Margin of over-representation
Combretaceae	110	13	0.063	0.12	0.220	0.042
Anacardiaceae	154	15	0.054	0.10	0.175	0.034
Canellaceae	2	2	0.053	1.00	1.000	0.032
Phyllanthaceae	106	11	0.051	0.10	0.206	0.031
Bignoniaceae	20	4	0.050	0.20	0.529	0.029
Ranunculaceae	45	6	0.047	0.13	0.326	0.027
Pedaliaceae	49	6	0.044	0.12	0.303	0.023
Caprifoliaceae	26	4	0.039	0.15	0.435	0.018
Meliaceae	42	5	0.037	0.12	0.321	0.016
Celastraceae	129	9	0.032	0.07	0.153	0.011
Loganiaceae	18	3	0.030	0.17	0.522	0.010
Lamiaceae	419	20	0.029	0.05	0.081	0.009
Asteraceae	2593	84	0.026	0.03	0.041	0.005
Moraceae	68	5	0.023	0.07	0.210	0.003
Verbenaceae	47	4	0.022	0.09	0.267	0.002
Sapotaceae	27	3	0.021	0.11	0.386	0.001
Total	28426[a]	536[b]	0.017	0.02	0.021	

[a]Total number of plant species (including species in under-represented taxonomic groups) [b]Total number of medicinal plant species used for treating non-STI microbial infections (including medicinal plant species in under-represented taxonomic groups).

Table S.14
Over-represented genera from the IDM analysis of plants used for the treatment of non-STI microbial infections.

Genus	A(n)	B(x)	Inf.	Mean θ	Sup.	Margin of over-representation
Pterocelastrus	4	3	0.099	0.75	0.996	0.078
Vachellia	45	8	0.075	0.18	0.373	0.054
Sesamum	22	5	0.068	0.23	0.535	0.048
Lannea	14	4	0.068	0.29	0.671	0.047
Clematis	15	4	0.064	0.27	0.643	0.043
Capparis	8	3	0.060	0.38	0.833	0.040
Bridelia	9	3	0.055	0.33	0.789	0.034
Lippia	9	3	0.055	0.33	0.789	0.034
Schistostephium	9	3	0.055	0.33	0.789	0.034
Terminalia	18	4	0.054	0.22	0.570	0.034
Asparagus	103	11	0.053	0.11	0.212	0.032
Lasiosiphon	29	5	0.053	0.17	0.434	0.032
Englerophytum	2	2	0.053	1.00	1.000	0.032
Phragmites	2	2	0.053	1.00	1.000	0.032
Warburgia	2	2	0.053	1.00	1.000	0.032
Gardenia	10	3	0.050	0.30	0.749	0.030
Combretum	82	9	0.050	0.11	0.234	0.029
Ekebergia	3	2	0.043	0.67	0.996	0.023
Mentha	3	2	0.043	0.67	0.996	0.023
Teucrium	3	2	0.043	0.67	0.996	0.023
Ximenia	3	2	0.043	0.67	0.996	0.023
Lepidium	24	4	0.042	0.17	0.463	0.021
Alepidea	26	4	0.039	0.15	0.435	0.018
Acalypha	42	5	0.037	0.12	0.321	0.016
Annona	4	2	0.037	0.50	0.963	0.016
Carissa	4	2	0.037	0.50	0.963	0.016
Parinari	4	2	0.037	0.50	0.963	0.016
Senna	4	2	0.037	0.50	0.963	0.016
Zanthoxylum	15	3	0.036	0.20	0.590	0.015
Senegalia	30	4	0.034	0.13	0.389	0.013
Dicoma	16	3	0.034	0.19	0.566	0.013
Ficus	47	5	0.033	0.11	0.291	0.013
Antidesma	5	2	0.032	0.40	0.915	0.011
Mikania	5	2	0.032	0.40	0.915	0.011
Strychnos	18	3	0.030	0.17	0.522	0.010
Searsia	92	7	0.030	0.08	0.185	0.010
Gymnosporia	36	4	0.029	0.11	0.335	0.008
Albizia	20	3	0.028	0.15	0.484	0.007
Grewia	58	5	0.027	0.09	0.242	0.007
Buddleja	7	2	0.025	0.29	0.813	0.005
Carpobrotus	7	2	0.025	0.29	0.813	0.005
Elaeodendron	7	2	0.025	0.29	0.813	0.005
Heteromorpha	7	2	0.025	0.29	0.813	0.005
Leucas	7	2	0.025	0.29	0.813	0.005
Lichtensteinia	7	2	0.025	0.29	0.813	0.005
Tephrosia	90	6	0.024	0.07	0.176	0.003
Hilliardiella	8	2	0.023	0.25	0.766	0.002
Helichrysum	259	11	0.021	0.04	0.088	0.001
Tulbaghia	27	3	0.021	0.11	0.386	0.001
Brachylaena	9	2	0.021	0.22	0.723	0.000
Macledium	9	2	0.021	0.22	0.723	0.000
Senecio	298	12	0.021	0.04	0.081	0.000
Total	28426[a]	536[b]	0.017	0.02	0.021	

[a]Total number of plant species (including species in under-represented taxonomic groups) [b]Total number of medicinal plant species used for treating non-STI microbial infections (including medicinal plant species in under-represented taxonomic groups).

Table S.15
Over-represented families from the IDM analysis of plants used to treat pain.

Family	A(n)	B(x)	Inf.	Mean θ	Sup.	Margin of over-representation
Ebenaceae	55	11	0.099	0.20	0.372	0.077
Francoaceae	16	4	0.061	0.25	0.616	0.039
Loganiaceae	18	4	0.054	0.22	0.570	0.033
Phyllanthaceae	106	11	0.051	0.10	0.206	0.030
Meliaceae	42	6	0.051	0.14	0.346	0.029
Ranunculaceae	45	6	0.047	0.13	0.326	0.025
Solanaceae	106	9	0.038	0.08	0.184	0.017
Olacaceae	14	3	0.038	0.21	0.617	0.016
Sapotaceae	27	4	0.038	0.15	0.423	0.016
Anacardiaceae	154	11	0.035	0.07	0.145	0.014
Capparaceae	79	7	0.035	0.09	0.213	0.013
Clusiaceae	17	3	0.032	0.18	0.543	0.010
Lauraceae	17	3	0.032	0.18	0.543	0.010
Pedaliaceae	49	5	0.032	0.10	0.281	0.010
Celastraceae	129	9	0.032	0.07	0.153	0.010
Combretaceae	110	8	0.031	0.07	0.168	0.009
Cucurbitaceae	136	9	0.030	0.07	0.146	0.008
Menispermaceae	35	4	0.029	0.11	0.343	0.008
Annonaceae	97	7	0.029	0.07	0.176	0.007
Convolvulaceae	143	9	0.029	0.06	0.139	0.007
Lamiaceae	419	19	0.027	0.05	0.078	0.006
Zingiberaceae	21	3	0.027	0.14	0.467	0.005
Euphorbiaceae	670	25	0.024	0.04	0.060	0.002
Moraceae	68	5	0.023	0.07	0.210	0.001
Rubiaceae	572	21	0.023	0.04	0.061	0.001
Caprifoliaceae	26	3	0.022	0.12	0.397	0.000
Total	28426[a]	569[b]	0.018	0.02	0.022	

[a]Total number of plant species (including species in under-represented taxonomic groups) [b]Total number of medicinal plant species used to treat pain (including medicinal plant species in under-represented taxonomic groups).

Table S.16
Over-represented genera from the IDM analysis of plants used to treat pain.

Genus	A(n)	B(x)	Inf.	Mean θ	Sup.	Margin of over-representation
Bersama	7	4	0.122	0.57	0.933	0.100
Euclea	17	6	0.119	0.35	0.685	0.097
Carissa	4	3	0.099	0.75	0.996	0.077
Senna	4	3	0.099	0.75	0.996	0.077
Manilkara	5	3	0.085	0.60	0.968	0.063
Vachellia	45	8	0.075	0.18	0.373	0.053
Cissampelos	7	3	0.067	0.43	0.878	0.045
Clematis	15	4	0.064	0.27	0.643	0.042
Vitex	15	4	0.064	0.27	0.643	0.042
Zanthoxylum	15	4	0.064	0.27	0.643	0.042
Hilliardiella	8	3	0.060	0.38	0.833	0.038
Dracaena	26	5	0.058	0.19	0.472	0.037
Strychnos	18	4	0.054	0.22	0.570	0.033
Phyllogeiton	2	2	0.053	1.00	1.000	0.031
Zanha	2	2	0.053	1.00	1.000	0.031
Ehretia	10	3	0.050	0.30	0.749	0.029
Solanum	58	7	0.047	0.12	0.281	0.026
Sesamum	22	4	0.045	0.18	0.494	0.024
Acokanthera	3	2	0.043	0.67	0.996	0.021
Ekebergia	3	2	0.043	0.67	0.996	0.021
Erythrophleum	3	2	0.043	0.67	0.996	0.021
Helinus	3	2	0.043	0.67	0.996	0.021
Rubia	3	2	0.043	0.67	0.996	0.021
Ximenia	3	2	0.043	0.67	0.996	0.021
Diospyros	38	5	0.041	0.13	0.349	0.019
Gymnanthemum	13	3	0.040	0.23	0.646	0.019
Garcinia	14	3	0.038	0.21	0.617	0.016
Annona	4	2	0.037	0.50	0.963	0.015
Laggera	4	2	0.037	0.50	0.963	0.015
Ormocarpum	4	2	0.037	0.50	0.963	0.015
Schotia	4	2	0.037	0.50	0.963	0.015
Sclerocroton	4	2	0.037	0.50	0.963	0.015
Boscia	15	3	0.036	0.20	0.590	0.014
Croton	30	4	0.034	0.13	0.389	0.012
Ficus	47	5	0.033	0.11	0.291	0.011
Mikania	5	2	0.032	0.40	0.915	0.010
Trichilia	5	2	0.032	0.40	0.915	0.010
Erythrina	18	3	0.030	0.17	0.522	0.009
Terminalia	18	3	0.030	0.17	0.522	0.009
Aptosimum	19	3	0.029	0.16	0.502	0.007
Momordica	19	3	0.029	0.16	0.502	0.007
Aframomum	6	2	0.028	0.33	0.863	0.006
Cadaba	6	2	0.028	0.33	0.863	0.006
Myrsine	6	2	0.028	0.33	0.863	0.006
Ziziphus	6	2	0.028	0.33	0.863	0.006
Albizia	20	3	0.028	0.15	0.484	0.006
Elaeodendron	7	2	0.025	0.29	0.813	0.003
Heteromorpha	7	2	0.025	0.29	0.813	0.003
Plumbago	7	2	0.025	0.29	0.813	0.003
Canthium	8	2	0.023	0.25	0.766	0.001
Crabbea	8	2	0.023	0.25	0.766	0.001
Philenoptera	8	2	0.023	0.25	0.766	0.001
Cucumis	26	3	0.022	0.12	0.397	0.000
Hypoxis	48	4	0.022	0.08	0.263	0.000
Total	28426[a]	569[b]	0.018	0.02	0.022	

[a]Total number of plant species (including species in under-represented taxonomic groups) [b]Total number of medicinal plant species used to treat pain (including medicinal plant species in under-represented taxonomic groups).

Table S.17
Over-represented families from the IDM analysis of plants used to treat skin medical conditions.

Family	A(n)	B(x)	Inf.	Mean θ	Sup.	Margin of over-representation
Francoaceae	16	4	0.061	0.25	0.6164	0.041
Burseraceae	63	7	0.044	0.11	0.2610	0.024
Ebenaceae	55	6	0.039	0.11	0.2742	0.019
Olacaceae	14	3	0.038	0.21	0.6167	0.018
Anacardiaceae	154	11	0.035	0.07	0.1451	0.016
Cucurbitaceae	136	10	0.035	0.07	0.1546	0.015
Hypericaceae	20	3	0.028	0.15	0.4841	0.008
Rhizophoraceae	20	3	0.028	0.15	0.4841	0.008
Capparaceae	79	6	0.027	0.08	0.1982	0.007
Lamiaceae	419	19	0.027	0.05	0.0779	0.007
Phyllanthaceae	106	7	0.026	0.07	0.1623	0.006
Asphodelaceae	555	21	0.023	0.04	0.0633	0.004
Solanaceae	106	6	0.020	0.06	0.1510	0.001
Oleaceae	29	3	0.020	0.10	0.3644	0.000
Total	28426[a]	515[b]	0.017	0.02	0.020	

[a]Total number of plant species (including species in under-represented taxonomic groups) [b]Total number of medicinal plant species used to treat skin medical conditions (including medicinal plant species in under-represented taxonomic groups).

Table S.18
Over-represented genera from the IDM analysis of plants used to treat skin medical conditions.

Genus	A(n)	B(x)	Inf.	Mean θ	Sup.	Margin of over-representation
Erythrina	18	5	0.082	0.28	0.616	0.062
Rothmannia	6	3	0.075	0.50	0.925	0.055
Trichodesma	6	3	0.075	0.50	0.925	0.055
Bersama	7	3	0.067	0.43	0.878	0.047
Zanthoxylum	15	4	0.064	0.27	0.643	0.044
Pentanisia	8	3	0.060	0.38	0.833	0.040
Phyllogeiton	2	2	0.053	1.00	1.000	0.033
Momordica	19	4	0.052	0.21	0.549	0.032
Albizia	20	4	0.050	0.20	0.529	0.030
Commiphora	57	7	0.048	0.12	0.285	0.028
Ocimum	22	4	0.045	0.18	0.494	0.026
Syzygium	12	3	0.043	0.25	0.677	0.023
Psorospermum	3	2	0.043	0.67	0.996	0.023
Ximenia	3	2	0.043	0.67	0.996	0.023
Dalbergia	26	4	0.039	0.15	0.435	0.019
Lannea	14	3	0.038	0.21	0.617	0.018
Annona	4	2	0.037	0.50	0.963	0.017
Mimusops	4	2	0.037	0.50	0.963	0.017
Ormocarpum	4	2	0.037	0.50	0.963	0.017
Senna	4	2	0.037	0.50	0.963	0.017
Senegalia	30	4	0.034	0.13	0.389	0.014
Cassipourea	16	3	0.034	0.19	0.566	0.014
Dysphania	5	2	0.032	0.40	0.915	0.012
Aloe	216	12	0.029	0.06	0.110	0.009
Launaea	6	2	0.028	0.33	0.863	0.008
Ziziphus	6	2	0.028	0.33	0.863	0.008
Diospyros	38	4	0.027	0.11	0.321	0.007
Agapanthus	7	2	0.025	0.29	0.813	0.005
Carpobrotus	7	2	0.025	0.29	0.813	0.005
Hemionitis	44	4	0.024	0.09	0.283	0.004
Vachellia	45	4	0.023	0.09	0.278	0.003
Aloiampelos	8	2	0.023	0.25	0.766	0.003
Capparis	8	2	0.023	0.25	0.766	0.003
Hilliardiella	8	2	0.023	0.25	0.766	0.003
Zantedeschia	8	2	0.023	0.25	0.766	0.003
Ficus	47	4	0.022	0.09	0.267	0.002
Cucumis	26	3	0.022	0.12	0.397	0.002
Salvia	28	3	0.020	0.11	0.375	0.001
Bulbine	78	5	0.020	0.06	0.185	0.001
Total	28426[a]	515[b]	0.017	0.02	0.020	

[a]Total number of plant species (including species in under-represented taxonomic groups) [b]Total number of medicinal plant species used to treat skin medical conditions (including medicinal plant species in under-represented taxonomic groups).

Table S.19
Over-represented family from the IDM analysis of plants used to treat female sexual and reproductive health issues.

Family	A(n)	B(x)	Inf.	Mean θ	Sup.	Margin of over-representation
Aristolochiaceae	10	4	0.091	0.400	0.808	0.072
Loganiaceae	18	5	0.082	0.278	0.616	0.063
Ebenaceae	55	8	0.061	0.145	0.314	0.042
Combretaceae	110	11	0.050	0.100	0.199	0.030
Typhaceae	3	2	0.043	0.667	0.996	0.024
Anacardiaceae	154	12	0.040	0.078	0.153	0.021
Francoaceae	16	3	0.034	0.188	0.566	0.015
Phyllanthaceae	106	8	0.032	0.075	0.173	0.013
Clusiaceae	17	3	0.032	0.176	0.543	0.013
Vitaceae	134	9	0.030	0.067	0.148	0.011
Annonaceae	97	7	0.029	0.072	0.176	0.009
Ochnaceae	55	5	0.029	0.091	0.254	0.009
Meliaceae	42	4	0.025	0.095	0.295	0.006
Rubiaceae	572	21	0.023	0.037	0.061	0.004
Malvaceae	552	20	0.022	0.036	0.062	0.003
Total	28426[a]	495[b]	0.016	0.02	0.019	

[a]Total number of plant species (including species in under-represented taxonomic groups) [b]Total number of medicinal plant species to treat female sexual and reproductive health issues (including medicinal plant species in under-represented taxonomic groups).

Table S.20
Over-represented genera from the IDM analysis of plants used to treat female sexual and reproductive health issues.

Genus	A(n)	B(x)	Inf.	Mean θ	Sup.	Margin of over-representation
Strychnos	18	5	0.082	0.278	0.62	0.063
Albizia	20	5	0.075	0.250	0.57	0.055
Bersama	7	3	0.067	0.429	0.88	0.048
Combretum	82	10	0.058	0.122	0.25	0.039
Euclea	17	4	0.057	0.235	0.59	0.038
Bridelia	9	3	0.055	0.333	0.79	0.036
Typha	3	2	0.043	0.667	1.00	0.024
Ximenia	3	2	0.043	0.667	1.00	0.024
Gymnanthemum	13	3	0.040	0.231	0.65	0.021
Garcinia	14	3	0.038	0.214	0.62	0.019
Lannea	14	3	0.038	0.214	0.62	0.019
Grewia	58	6	0.037	0.103	0.26	0.018
Annona	4	2	0.037	0.500	0.96	0.018
Aristolochia	4	2	0.037	0.500	0.96	0.018
Parinari	4	2	0.037	0.500	0.96	0.018
Senna	4	2	0.037	0.500	0.96	0.018
Sida	16	3	0.034	0.188	0.57	0.015
Hydnora	5	2	0.032	0.400	0.91	0.013
Mikania	5	2	0.032	0.400	0.91	0.013
Trichilia	5	2	0.032	0.400	0.91	0.013
Ochna	35	4	0.029	0.114	0.34	0.010
Trichodesma	6	2	0.028	0.333	0.86	0.009
Ziziphus	6	2	0.028	0.333	0.86	0.009
Entada	20	3	0.028	0.150	0.48	0.009
Diospyros	38	4	0.027	0.105	0.32	0.008
Asparagus	103	7	0.027	0.068	0.17	0.008
Elaeodendron	7	2	0.025	0.286	0.81	0.006
Heteromorpha	7	2	0.025	0.286	0.81	0.006
Ledebouria	65	5	0.024	0.077	0.22	0.005
Commelina	45	4	0.023	0.089	0.28	0.004
Cynodon	8	2	0.023	0.250	0.77	0.004
Hilliardiella	8	2	0.023	0.250	0.77	0.004
Zantedeschia	8	2	0.023	0.250	0.77	0.004
Vangueria	25	3	0.023	0.120	0.41	0.004
Ficus	47	4	0.022	0.085	0.27	0.003
Cucumis	26	3	0.022	0.115	0.40	0.003
Hypoxis	48	4	0.022	0.083	0.26	0.003
Brachylaena	9	2	0.021	0.222	0.72	0.002
Cymbopogon	9	2	0.021	0.222	0.72	0.002
Gloriosa	9	2	0.021	0.222	0.72	0.002
Eulophia	82	5	0.019	0.061	0.18	0.000
Bauhinia	10	2	0.019	0.200	0.68	0.000
Ehretia	10	2	0.019	0.200	0.68	0.000
Gardenia	10	2	0.019	0.200	0.68	0.000
Aloe	216	9	0.019	0.042	0.09	0.000
Total	28426[a]	495[b]	0.016	0.02	0.019	

[a]Total number of plant species (including species in under-represented taxonomic groups) [b]Total number of medicinal plant species to treat female sexual and reproductive health issues (including medicinal plant species in under-represented taxonomic groups).

Table S.21
Niche genera that are over-represented in disease categories but are under-represented in the total pharmacopoeia

STIs	Febrile/ Mosquito vector diseases	Non-STI microbial infections	Pain	Skin conditions	Female sexual/ reproductive health
Aloe	*Annona*	*Alepidea*	*Acokanthera*	*Aloe*	*Aloe*
Annona	*Cleome*	*Annona*	*Aframomum*	*Aloiampelos*	*Annona*
Cissampelos	*Vigna*	*Antidesma*	*Annona*	*Annona*	*Commelina*
Crinum	*Warburgia*	*Buddleja*	*Aptosimum*	*Bulbine*	*Cynodon*
Juncus	*Ximenia*	*Carpobrotus*	*Cadaba*	*Carpobrotus*	*Elaeodendron*
Tabernaemontana	*Zanha*	*Ekebergia*	*Cissampelos*	*Cassipourea*	*Eulophia*
Ximenia		*Elaeodendron*	*Crabbea*	*Dalbergia*	*Heteromorpha*
		Englerophytum	*Ekebergia*	*Hemionitis*	*Hilliardiella*
		Gymnosporia	*Elaeodendron*	*Hilliardiella*	*Ledebouria*
		Helichrysum	*Helinus*	*Launaea*	*Parinari*
		Heteromorpha	*Heteromorpha*	*Ormocarpum*	*Trichilia*
		Hilliardiella	*Hilliardiella*	*Pentanisia*	*Typha*
		Lepidium	*Myrsine*	*Phyllogeiton*	*Ximenia*
		Leucas	*Ormocarpum*	*Psorospermum*	*Zantedeschia*
		Lichtensteinia	*Philenoptera*	*Rothmannia*	
		Macledium	*Phyllogeiton*	*Ximenia*	
		Parinari	*Plumbago*	*Zantedeschia*	
		Phragmites	*Schotia*		
		Schistostephium	*Sclerocroton*		
		Senecio	*Trichilia*		
		Warburgia	*Ximenia*		
		Ximenia	*Zanha*		

Source code for the calculation of Pearson correlation coefficient

```
import pandas as pd
from scipy.stats import pearsonr
from itertools import combinations
# Each country has a dedicated sheet labelled country 1 to country 10
# two columns in each sheet with headings:  Family & Number of Plants_Country1
# Load the data from the single Excel file into a dictionary of DataFrames
excel_file_path = "C:/Users/input your document path.xlsx"  # Replace with the actual path to your
Excel file
xls = pd.ExcelFile(excel_file_path)
sheet_names = xls.sheet_names

data = {}

for sheet_name in sheet_names:
    data[sheet_name] = pd.read_excel(xls, sheet_name)

# Calculate Pearson correlations and p-values for each pair of countries
results = []

for pair in combinations(sheet_names, 2):
    country1, country2 = pair
    df1, df2 = data[country1], data[country2]

    # Merge dataframes based on the "Family" column
    merged_df = df1.merge(df2, on="Family", suffixes=("_" + country1, "_" + country2))

    # Calculate Pearson correlation and p-value for the number of plants in each family
    correlation, p_value = pearsonr(merged_df[f"Number of Plants_{country1}"],
merged_df[f"Number of Plants_{country2}"])

    results.append({
        "Country1": country1,
        "Country2": country2,
        "Pearson_Correlation": correlation,
        "P-Value": p_value
    })

# Create a DataFrame to store the results
results_df = pd.DataFrame(results)

# Print or save the results as needed
print(results_df)
```

Source code for the calculation of Jaccard coefficients in Python

```
import openpyxl
from sklearn.metrics import jaccard_score
from itertools import combinations

# Load the Excel file
workbook = openpyxl.load_workbook('C:/Users/input your document path.xlsx')
#Each country has a dedicated sheet, 1 column of plants with country name as label in each sheet
# Initialise an empty list to store the plant lists
plant_lists = []

# Iterate over each sheet and retrieve the plant data
for sheet_name in workbook.sheetnames:
    sheet = workbook[sheet_name]
    plants = [cell for column in sheet.iter_cols(min_row=2, values_only=True) for cell in column if cell
is not None]
    plant_lists.append(plants)

# Initialise an empty dictionary to store the Jaccard indices
jaccard_indices = {}

# Calculate the Jaccard index for all combinations of lists
for i, j in combinations(range(len(plant_lists)), 2):
    list1 = plant_lists[i]
    list2 = plant_lists[j]

    # Find the common elements between the lists
    common_elements = list(set(list1).intersection(list2))

    # Calculate the Jaccard index
    jaccard_index = len(common_elements) / len(set(list1).union(set(list2)))

    # Store the Jaccard index in the dictionary
    combination_key = f"List {i+1} vs List {j+1}"
    jaccard_indices[combination_key] = jaccard_index

# Print the Jaccard indices
for combination_key, jaccard_index in jaccard_indices.items():
    print(f"{combination_key}: {jaccard_index}
```

Appendix B Supplement to Chapter 3

INDEX

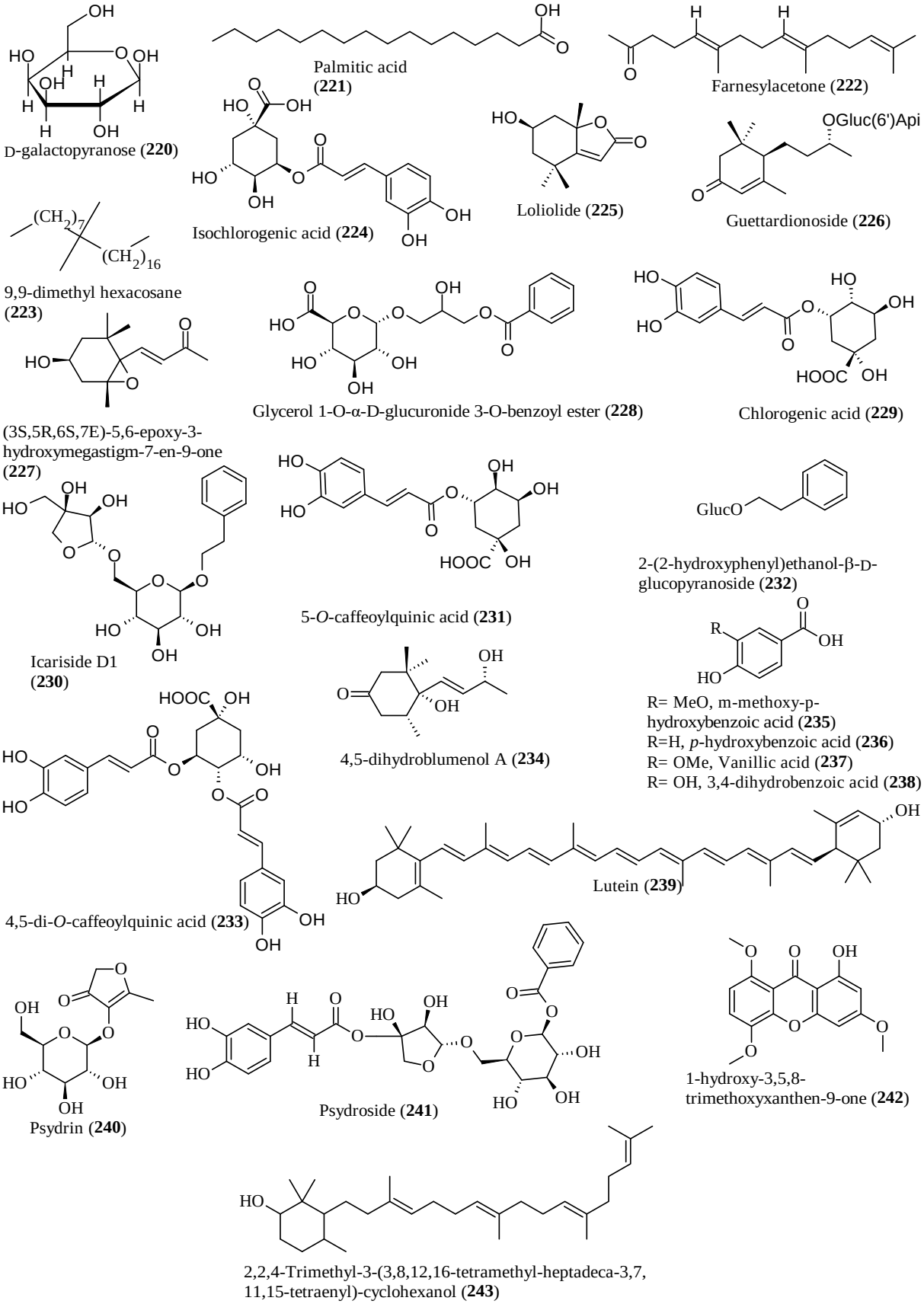

Figure S1.1: Other compounds isolated from southern African Rubiaceae

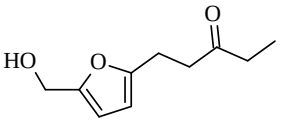

1-(5-(hydroxymethyl)furan-2-yl)pentan-3-one (**244**)

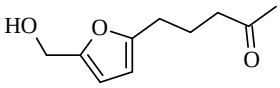

5-(5-(hydroxymethyl)furan-2-yl)pentan-2-one (**245**)

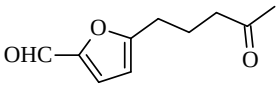

5-(4-oxopentyl)furan-2-carbaldehyde (**246**)

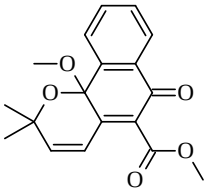

4-methoxy-oxomollugin (**247**)

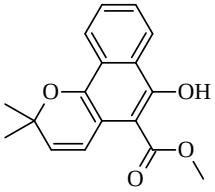

Mollugin (**248**)

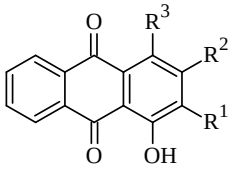

R^1= CH_3, R^2= H, R^3= H, 1-hydroxy-2-methyl-9,10-anthraquinone (**249**)

R^1= CH_3, R^2= H, R^3= OH, 1,4-dihydroxy-2-methylanthraquinone (**250**)

R^1= CH_3, R^2= CH_2OH, R^3= H, ω-hydroxypachybasin (**251**)

R^1= CH_3, R^2= CH_2CH_3, R^3= H, cordifoliol (**252**)

R^1= $CH_2OCH_2CH_3$, R^2= OH, R^3= H, 1,3-dihydroxy-2-ethoxymethyl-9,10-anthraquinone (**253**)

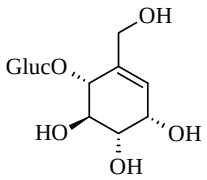

(+)-streptol glucoside (**254**)

Figure S1.2: Other compounds isolated from southern African Rubiaceae

Appendix C Supplement to Chapter 4 and 5

INDEX

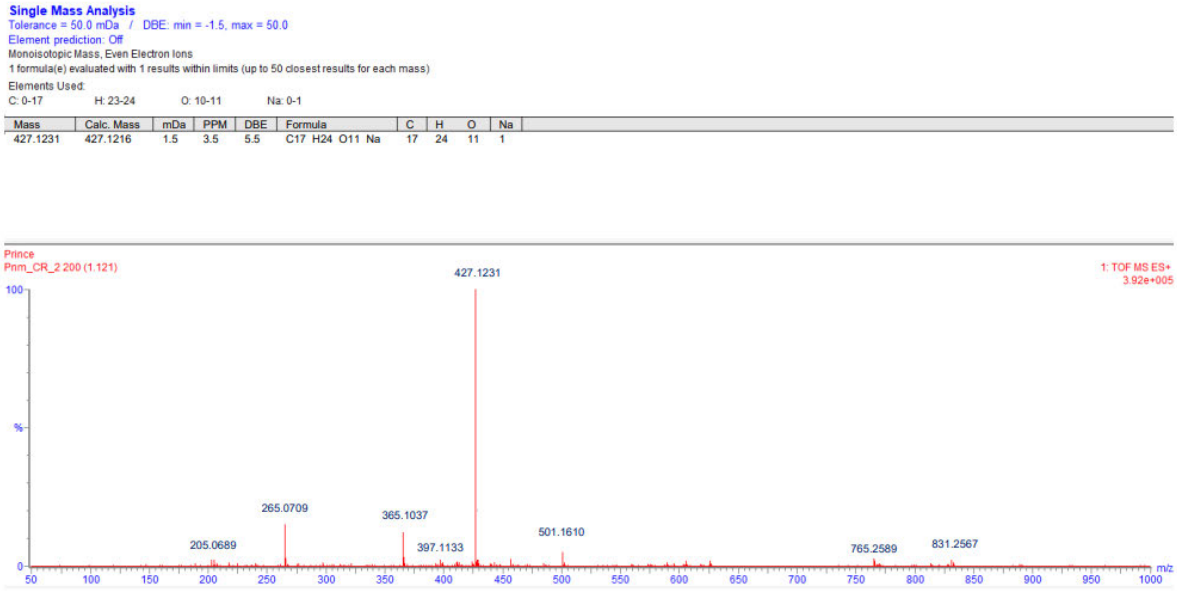

Figure S2.1: HR-(+)-ESI MS of gardenoside (**126**)

Figure S2.2: UV-Vis spectrum of gardenoside (**126**)

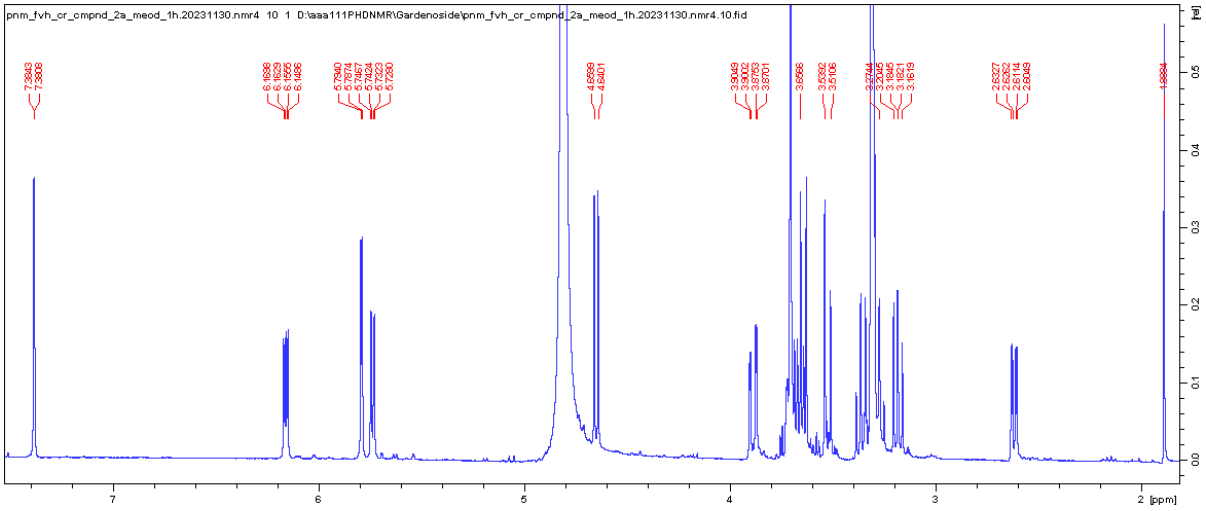

Figure S2.3: ^{1}H NMR spectrum of gardenoside (**126**) in CD_3OD, 400 MHz

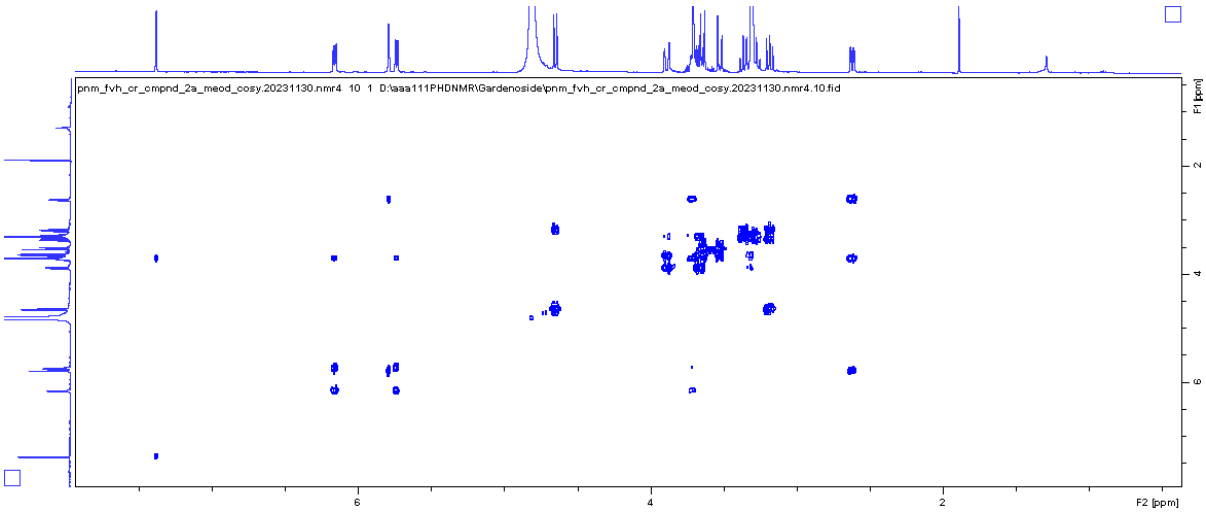

Figure S2.4: COSY spectrum of gardenoside (**128**) in CD_3OD, 400 MHz

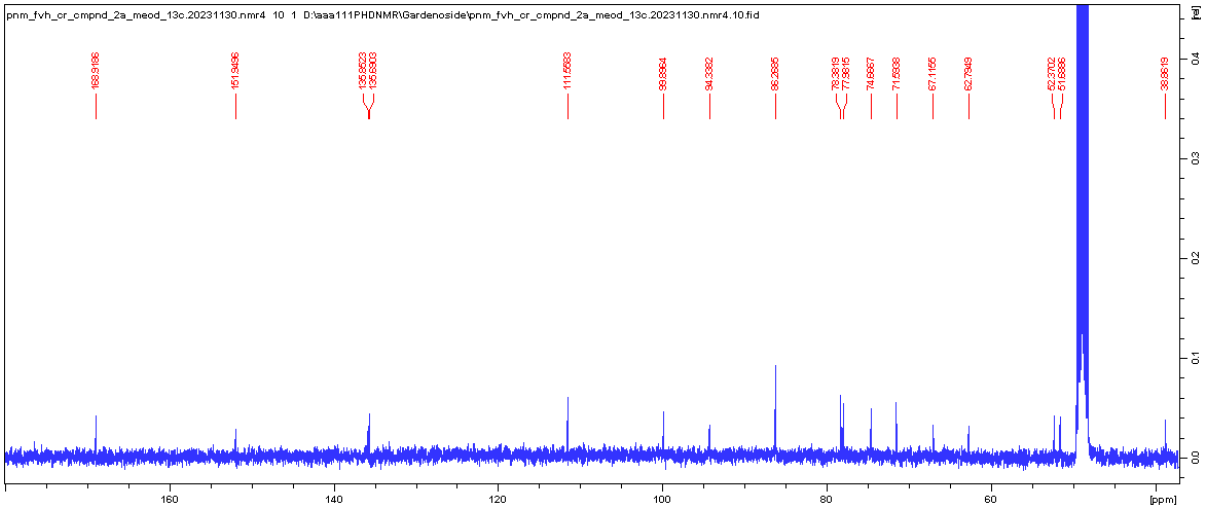

Figure S2.5: ^{13}C NMR spectrum of gardenoside (**126**) in CD_3OD, 100 MHz

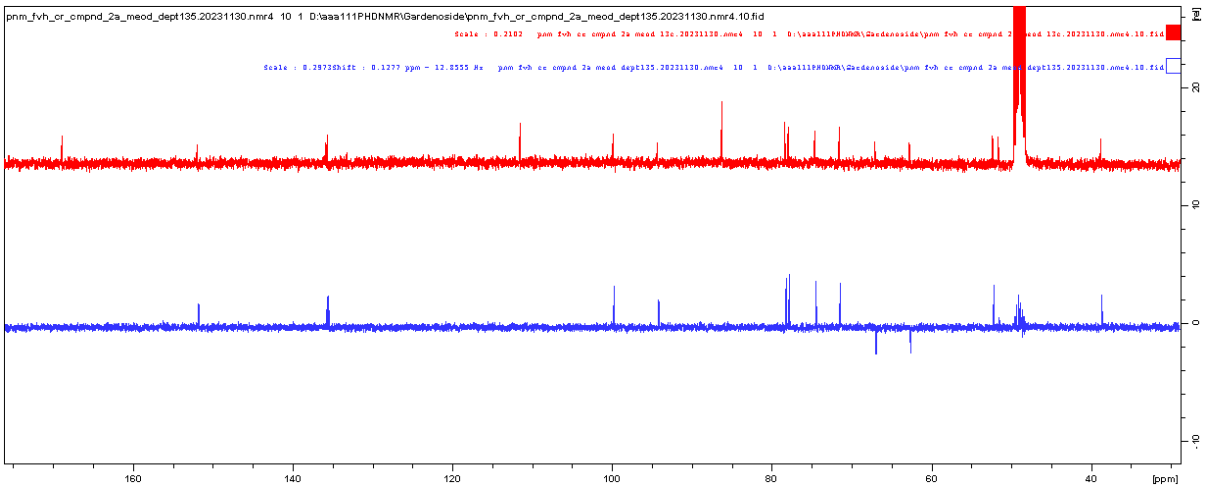

Figure S2.6: DEPT and ^{13}C NMR spectra of gardenoside (**126**) in CD_3OD, 100 MHz

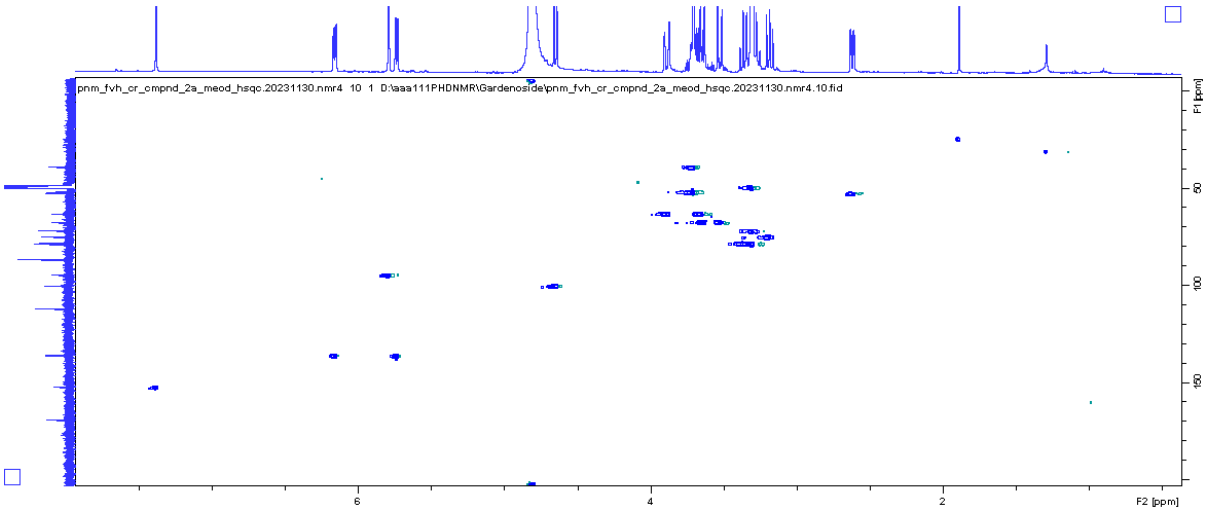

Figure S2.7: HSQC spectrum of gardenoside (**126**) in CD_3OD, 400 MHz

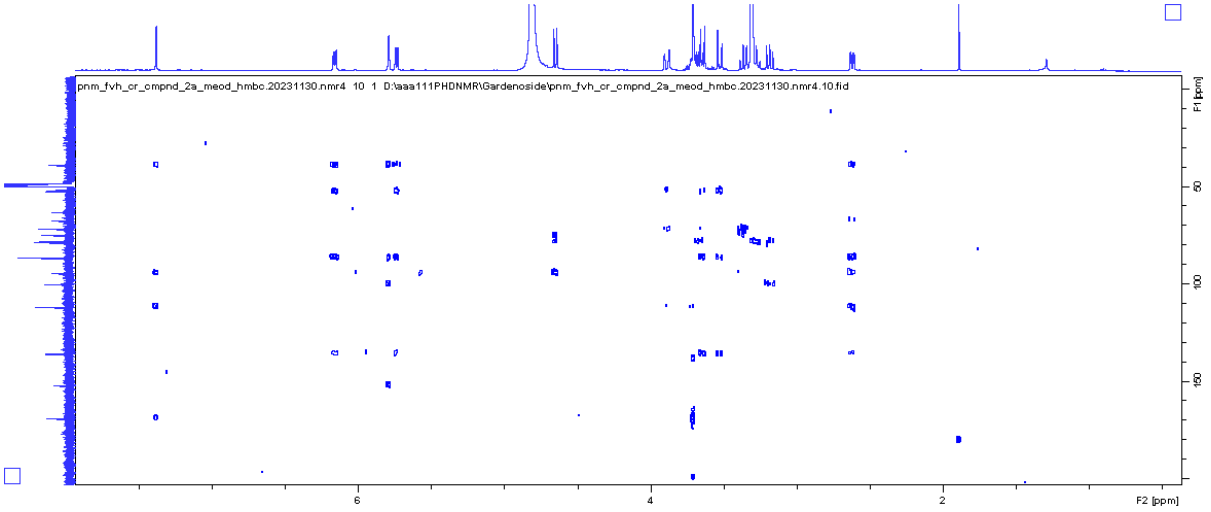

Figure S2.8: HMBC spectrum of gardenoside (**126**) in CD_3OD, 400 MHz

Single Mass Analysis
Tolerance = 50.0 mDa / DBE: min = -1.5, max = 50.0
Element prediction: Off
Number of isotope peaks used for i-FIT = 3
Monoisotopic Mass, Even Electron Ions
1 formula(e) evaluated with 1 results within limits (up to 50 closest results for each mass)
Elements Used:

Mass	Calc. Mass	mDa	PPM	DBE	Formula	i-FIT	i-FIT Norm	Fit Conf %	C	H	O	Na
373.1131	373.1135	-0.4	-1.1	6.5	C16 H21 O10	153.9	n/a	n/a	16	21	10	

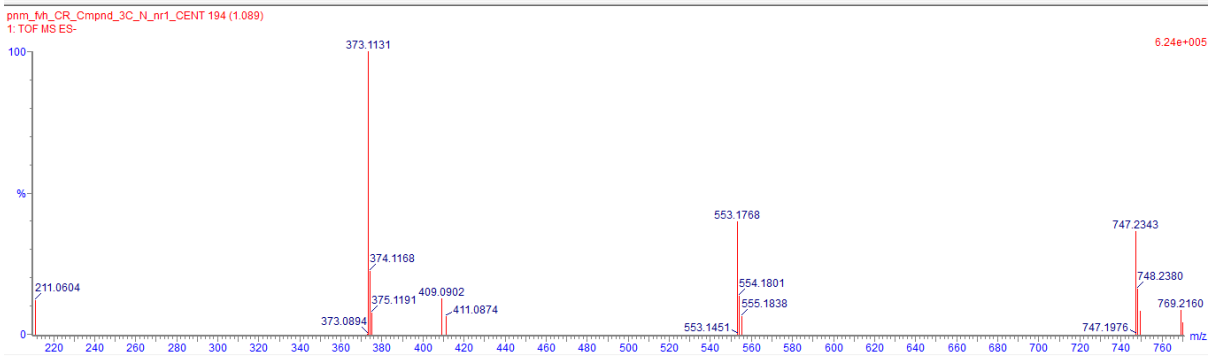

Figure S3.1: HR-(-)-ESI MS of geniposidic acid (**127**)

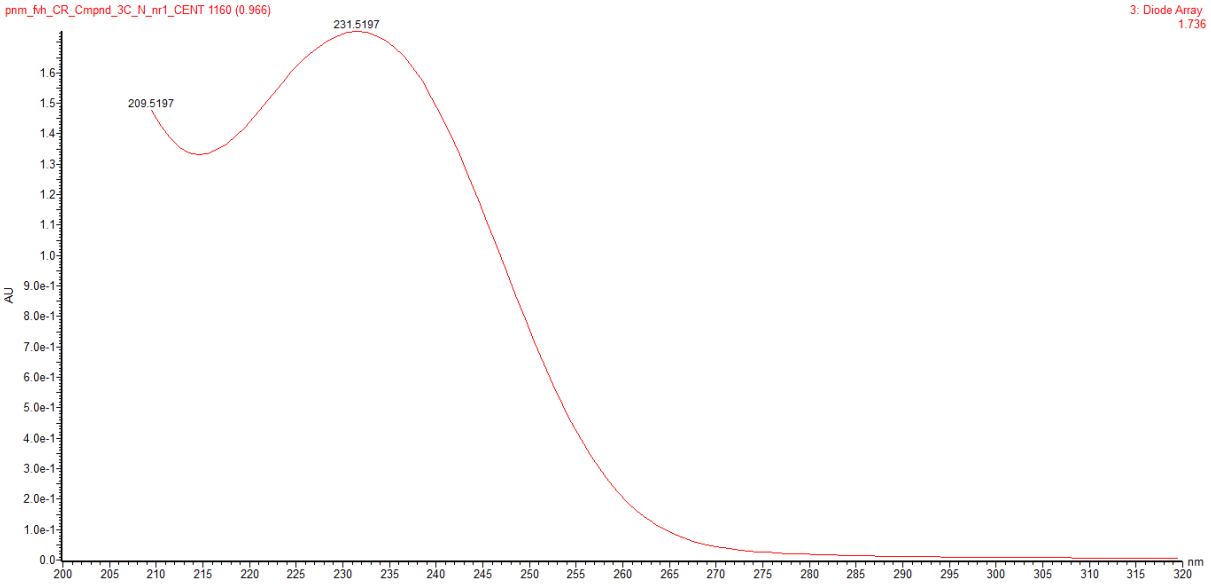

Figure S3.2: UV-Vis spectrum of geniposidic acid (**127**)

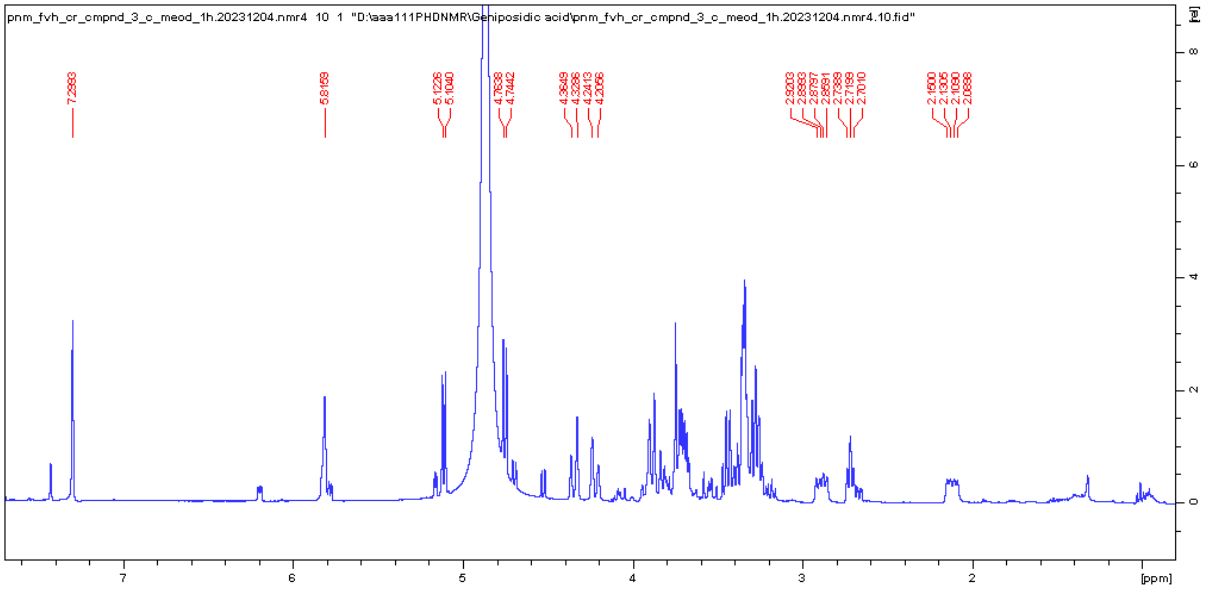

Figure S3.3: ^{1}H NMR spectrum of geniposidic acid (**127**) in CD_3OD, 400 MHz

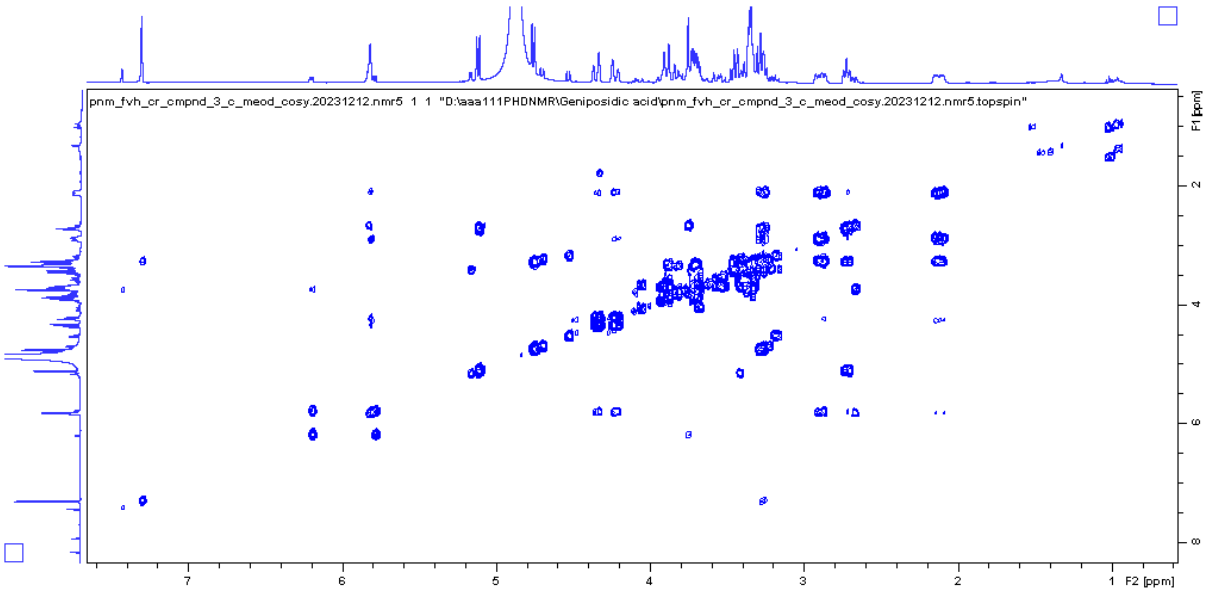

Figure S3.4: COSY spectrum of geniposidic acid (**127**) in CD_3OD, 500 MHz

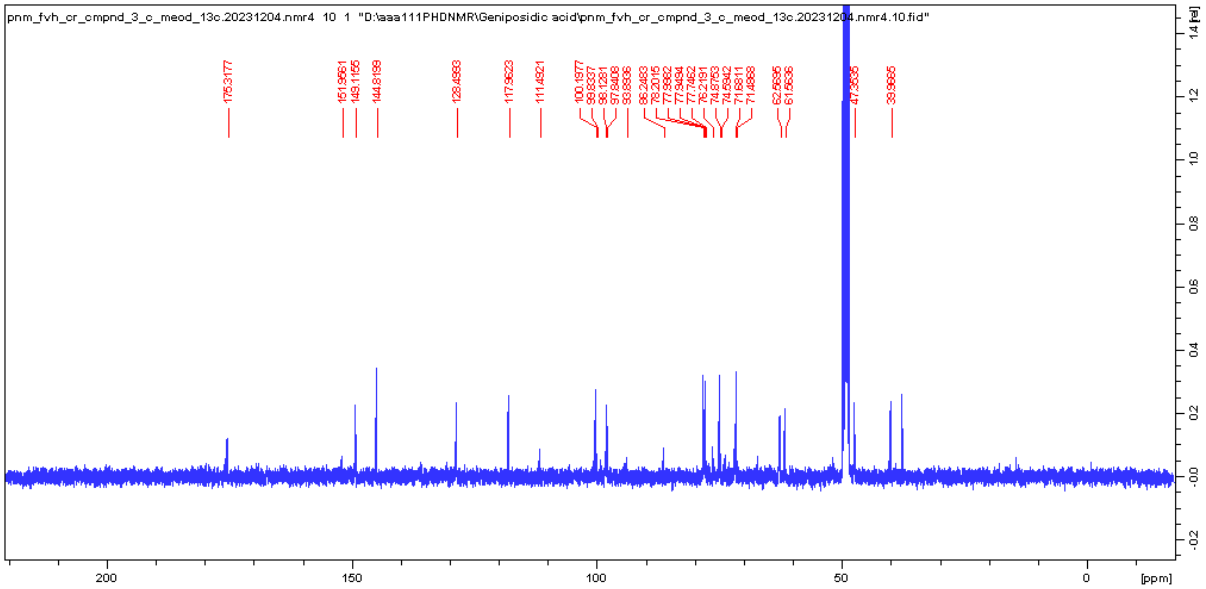

Figure S3.5: ^{13}C NMR spectrum of geniposidic acid (**127**) in CD_3OD, 100 MHz

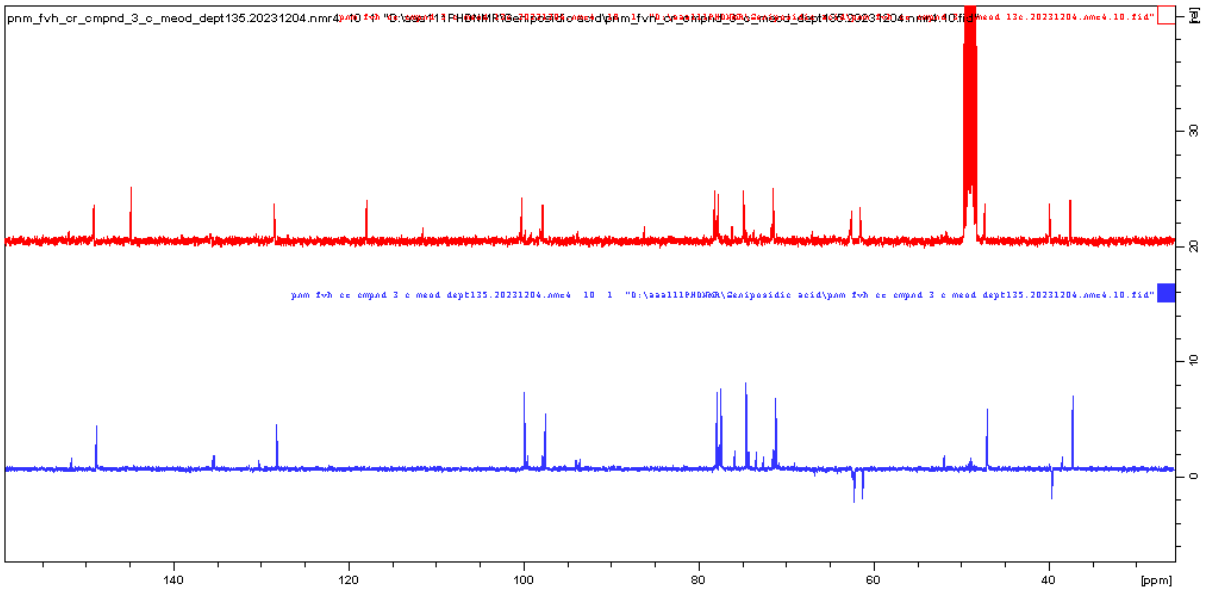

Figure S3.6: ^{13}C NMR and DEPT spectra of geniposidic acid (**127**) in CD_3OD, 100 MHz

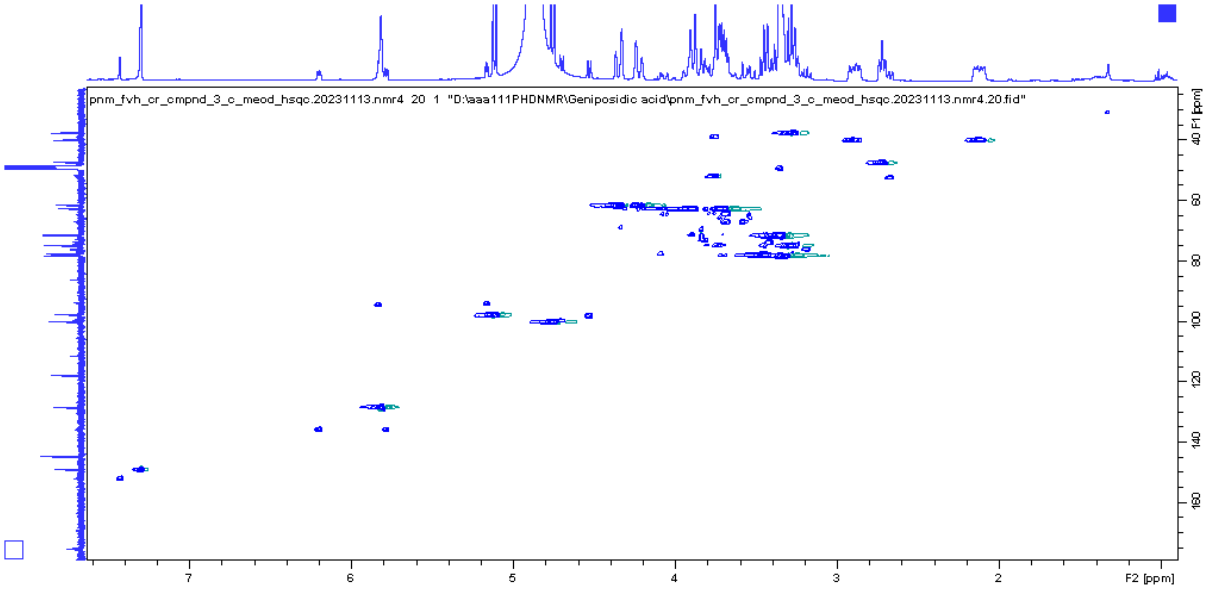

Figure S3.7: HSQC spectrum of geniposidic acid (**127**) in CD_3OD, 400 MHz

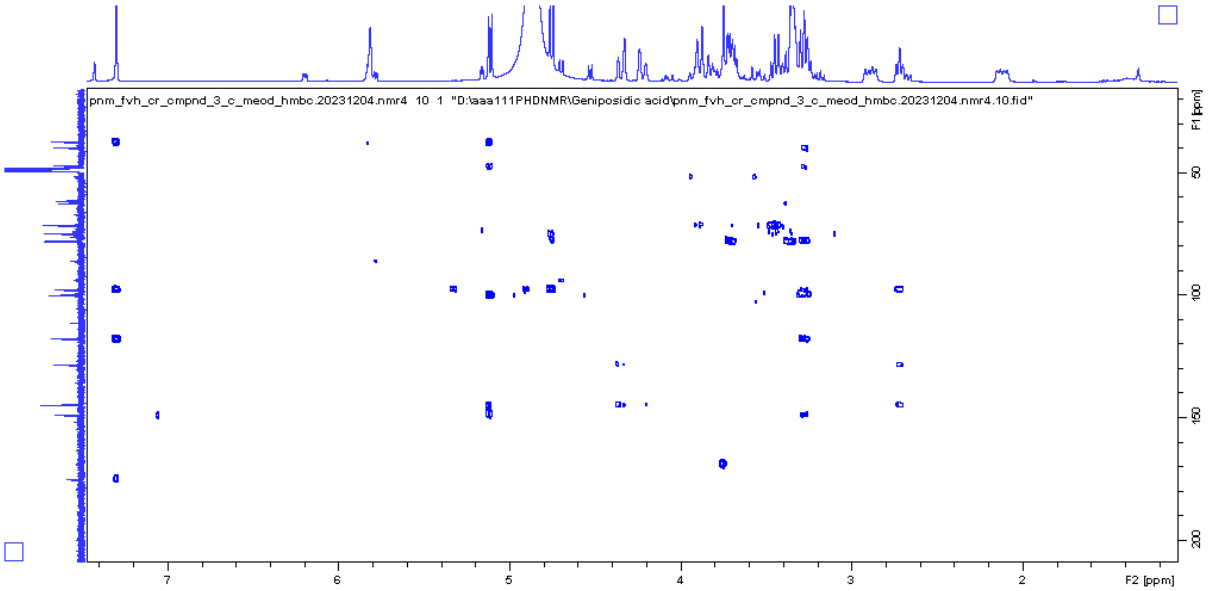

Figure S3.8: HMBC spectrum of geniposidic acid (**127**) in CD_3OD, 400 MHz

Figure S4.1: HR-(-)-ESI MS of astragalin (**89**)

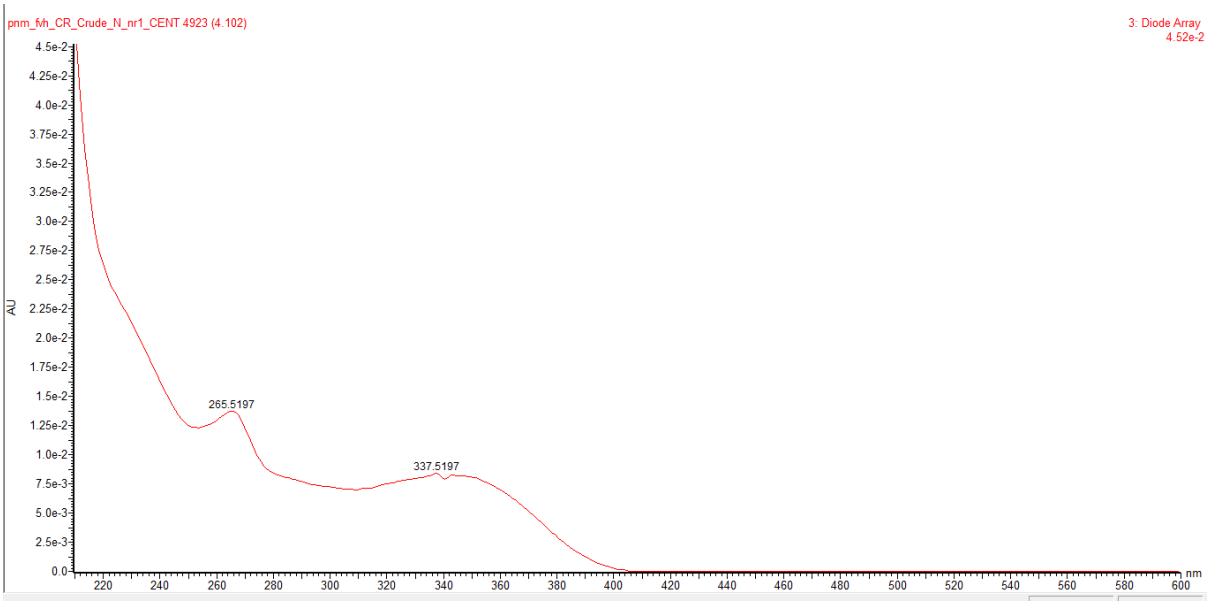

Figure S4.2: UV-Vis spectrum of astragalin (**89**)

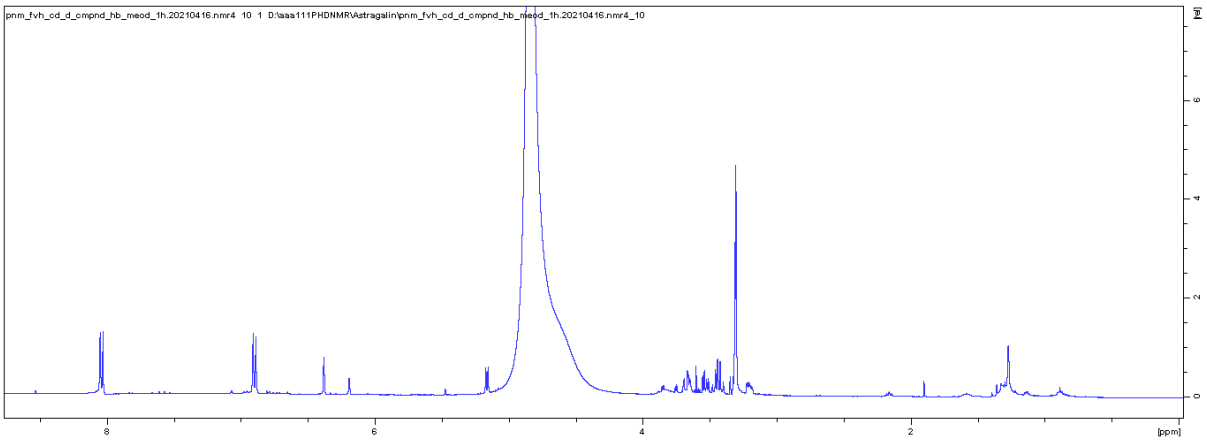

Figure S4.3: ^{1}H NMR spectrum of astragalin (**89**) in CD_3OD, 400 MHz

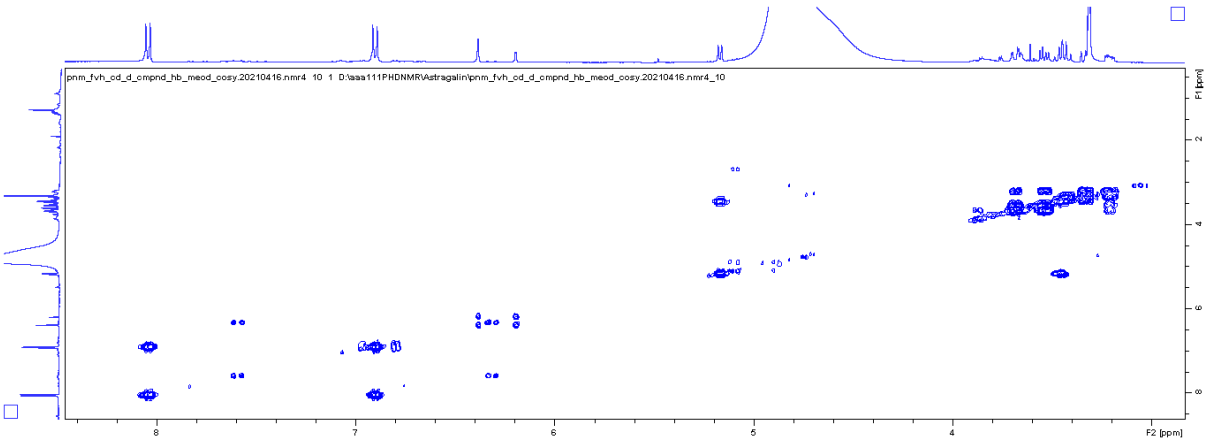

Figure S4.4: COSY spectrum of astragalin (**89**) in CD_3OD, 400 MHz

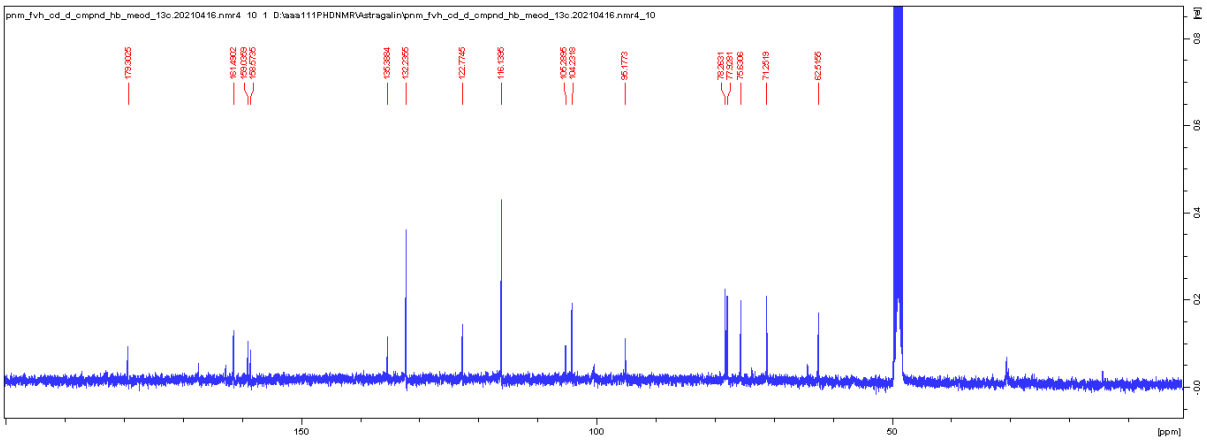

Figure S4.5: ^{13}C NMR spectrum of astragalin (**89**) in CD_3OD, 100 MHz

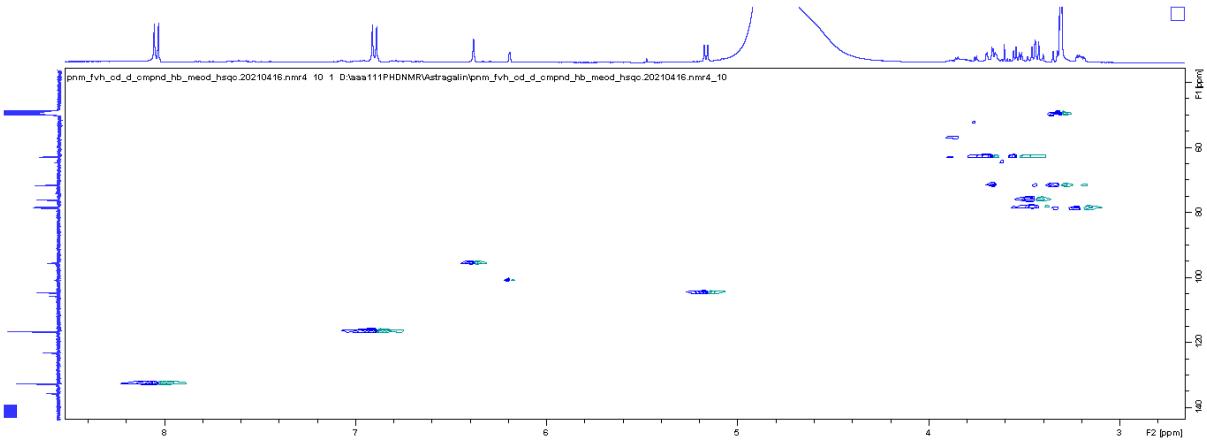

Figure S4.6: HSQC spectrum of astragalin (**89**) in CD_3OD, 400 MHz

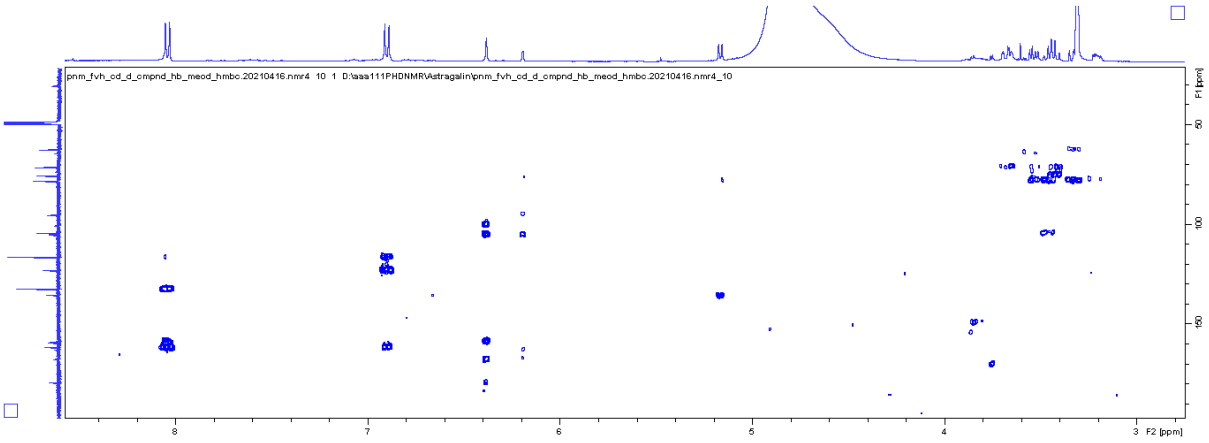

Figure S4.7: HMBC spectrum of astragalin (**89**) in CD_3OD, 400 MHz

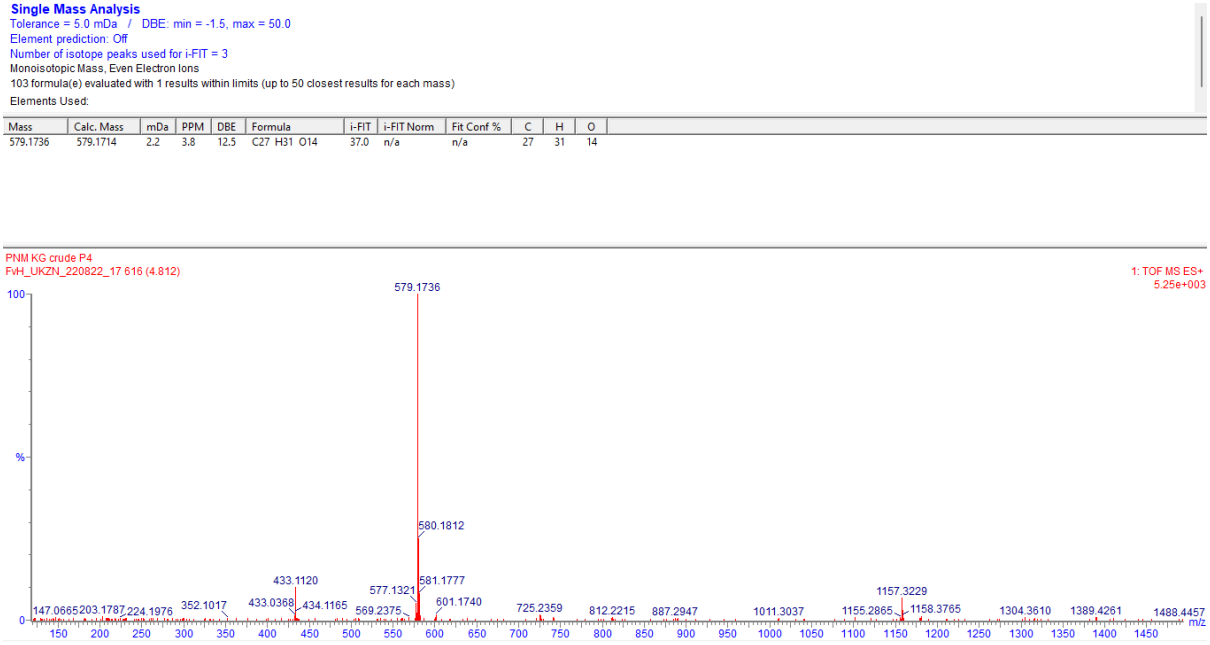

Figure S5.1: HR-(+)-ESI MS of kaempferitrin (**255**)

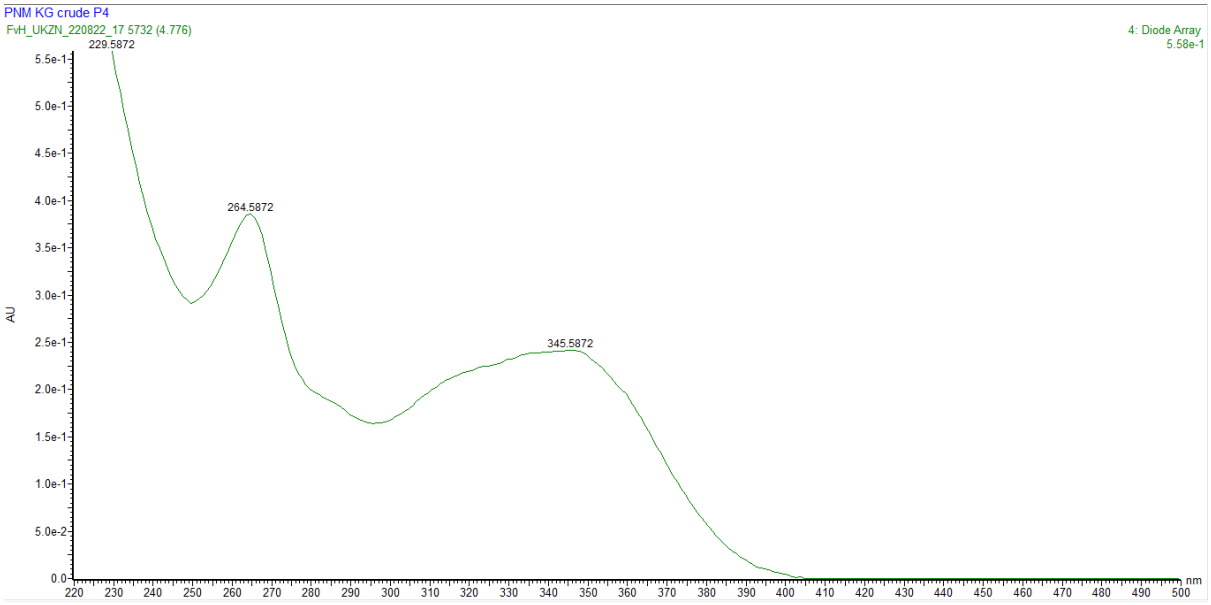

Figure S5.2: UV-Vis spectrum of kaempferitrin (**255**)

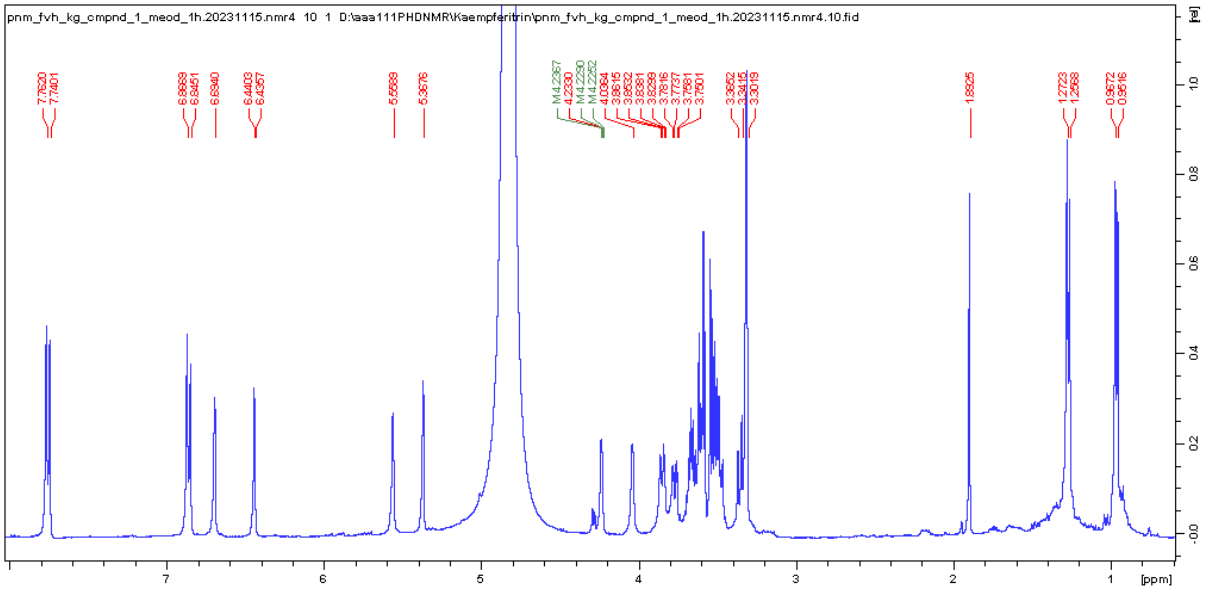

Figure S5.3: ^{1}H NMR spectrum of kaempferitrin (**255)** in CD_3OD, 400 MHz

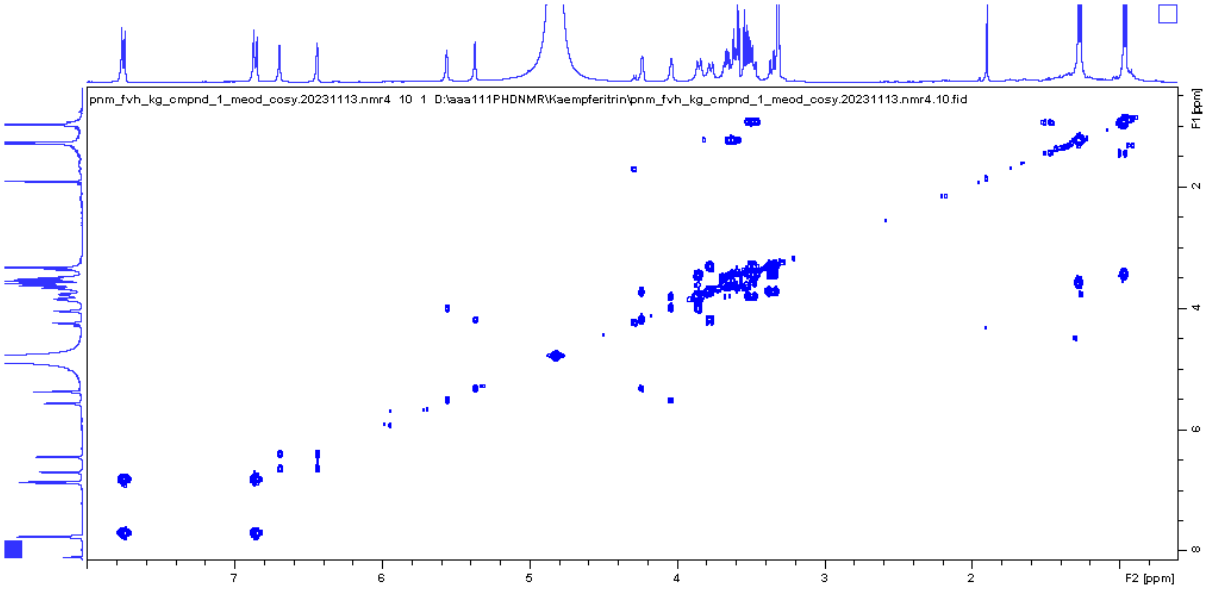

Figure S5.4: COSY spectrum of kaempferitrin (**255)** in CD_3OD, 400 MHz

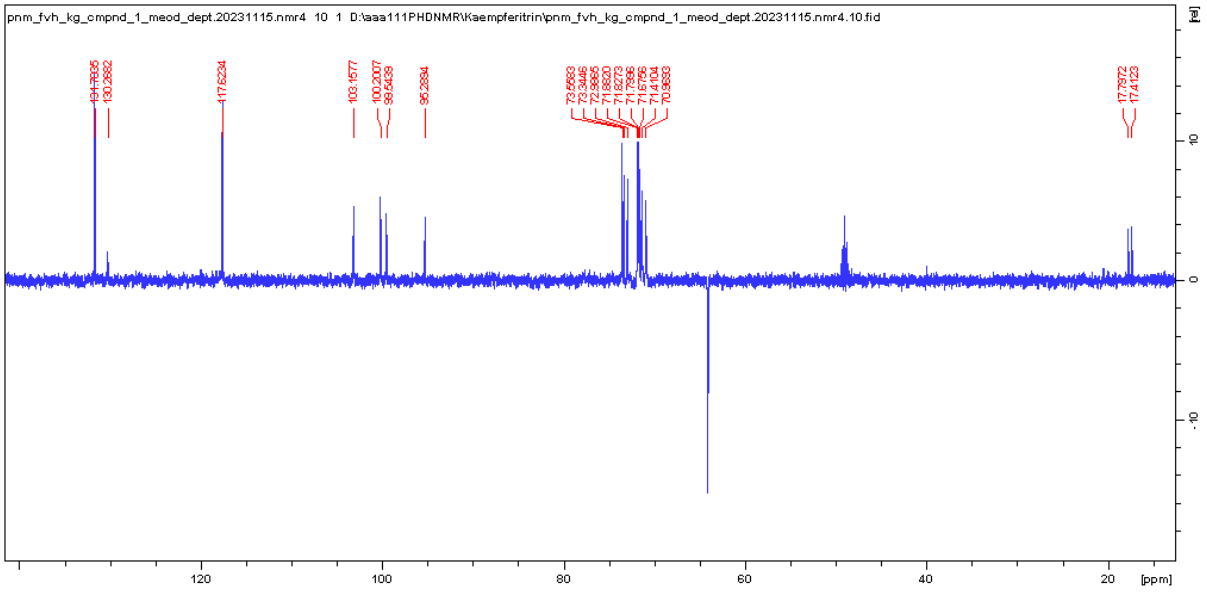

Figure S5.5: DEPT spectrum of kaempferitrin (**255)** in CD_3OD, 100 MHz

Note: The signal at 63.4371 is due to ethyl amine contamination.

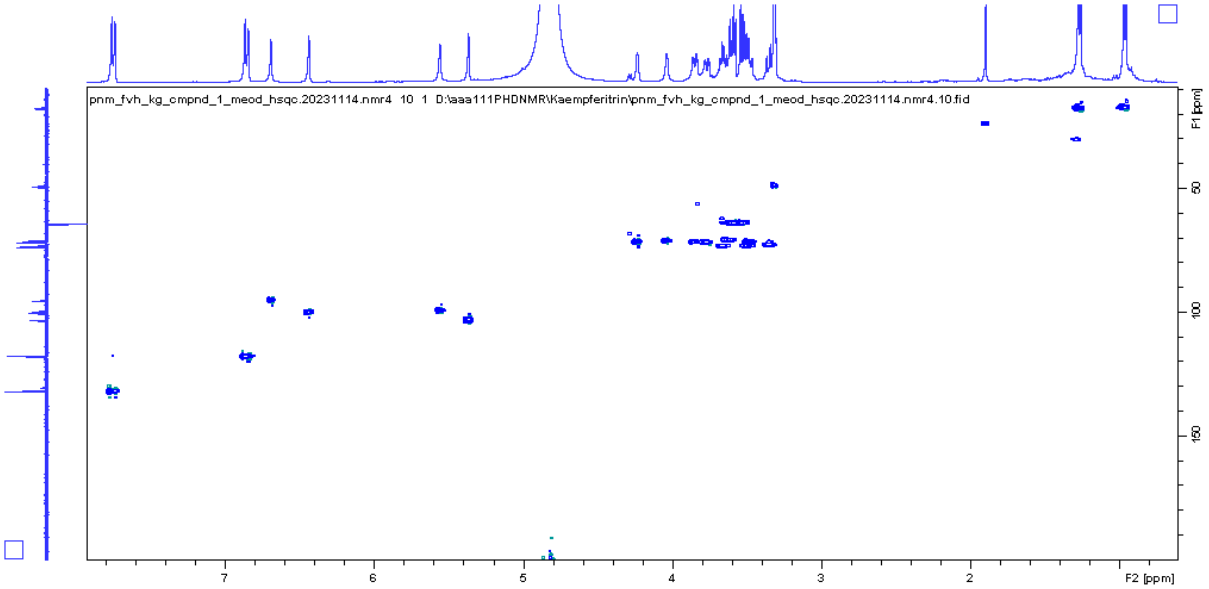

Figure S5.6: HSQC spectrum of kaempferitrin (**255)** in CD_3OD, 400 MHz

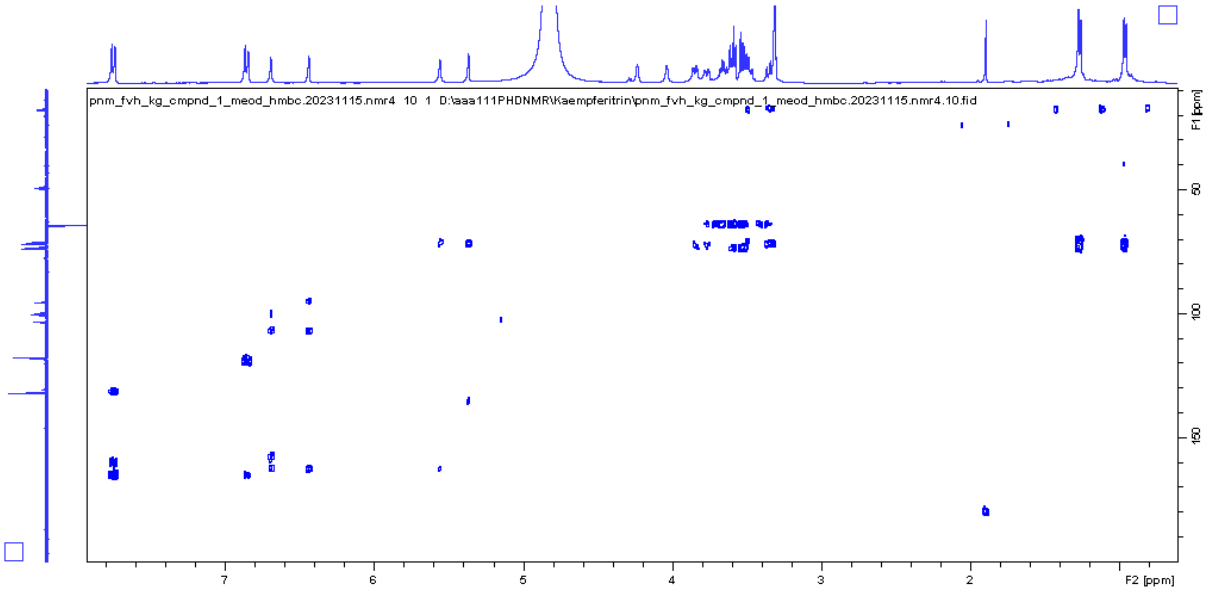

Figure S5.7: HMBC spectrum of kaempferitrin (**255)** in CD_3OD, 400 MHz

Single Mass Analysis
Tolerance = 1000.0 mDa / DBE: min = -1.5, max = 50.0
Element prediction: Off
Number of isotope peaks used for i-FIT = 3
Monoisotopic Mass, Even Electron Ions
13 formula(e) evaluated with 1 results within limits (up to 50 closest results for each mass)
Elements Used:

Mass	Calc. Mass	mDa	PPM	DBE	Formula	C	H	O	Na
459.1288	459.1267	2.1	4.6	9.5	C21 H24 O10 Na	21	24	10	1

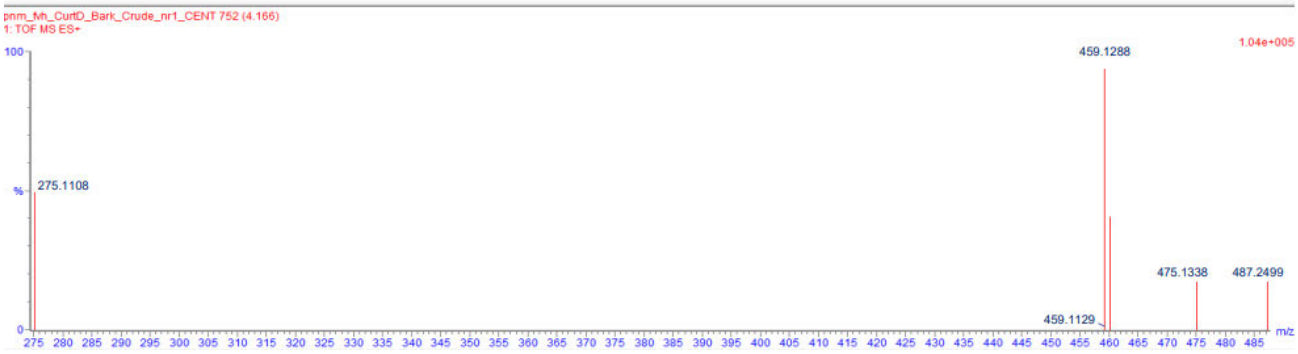

Figure S6.1: HR-(+)-ESI-MS of phlorizin (**259**)

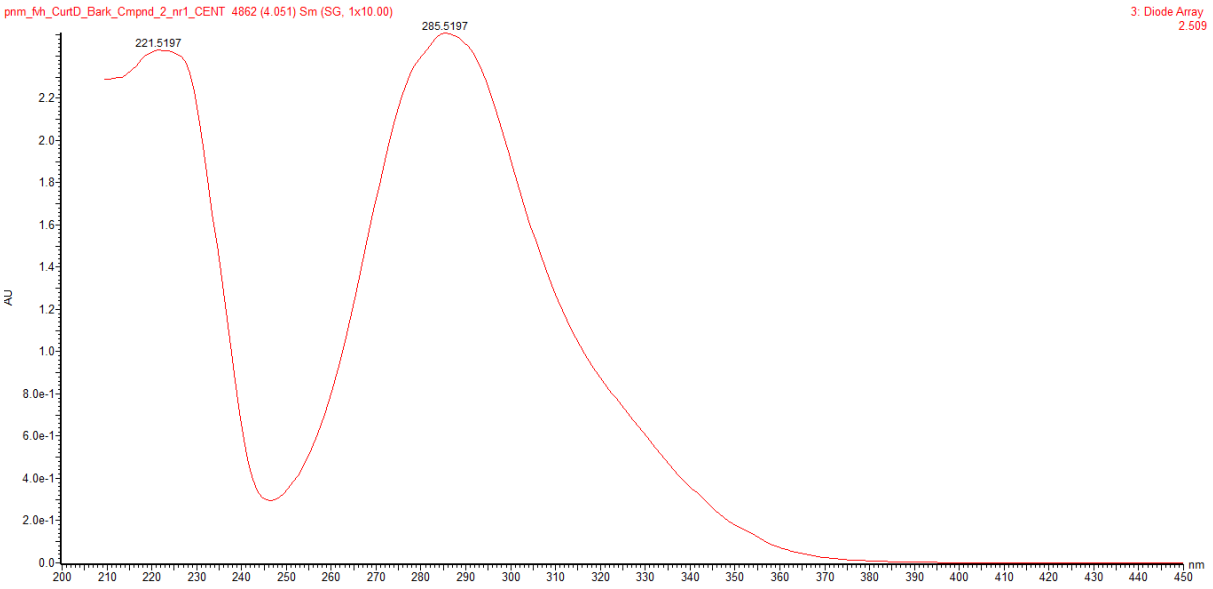

Figure S6.2: UV-Vis spectrum of phlorizin (**259**)

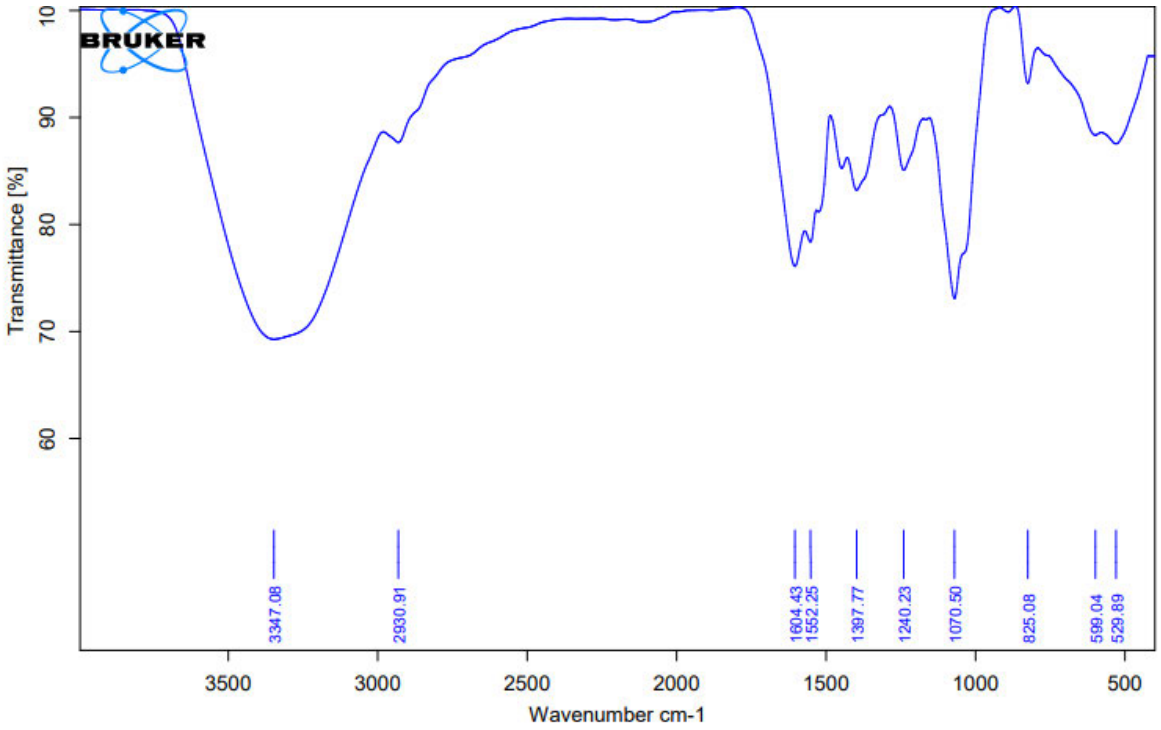

Figure S6.3: IR spectrum of phlorizin (**259**)

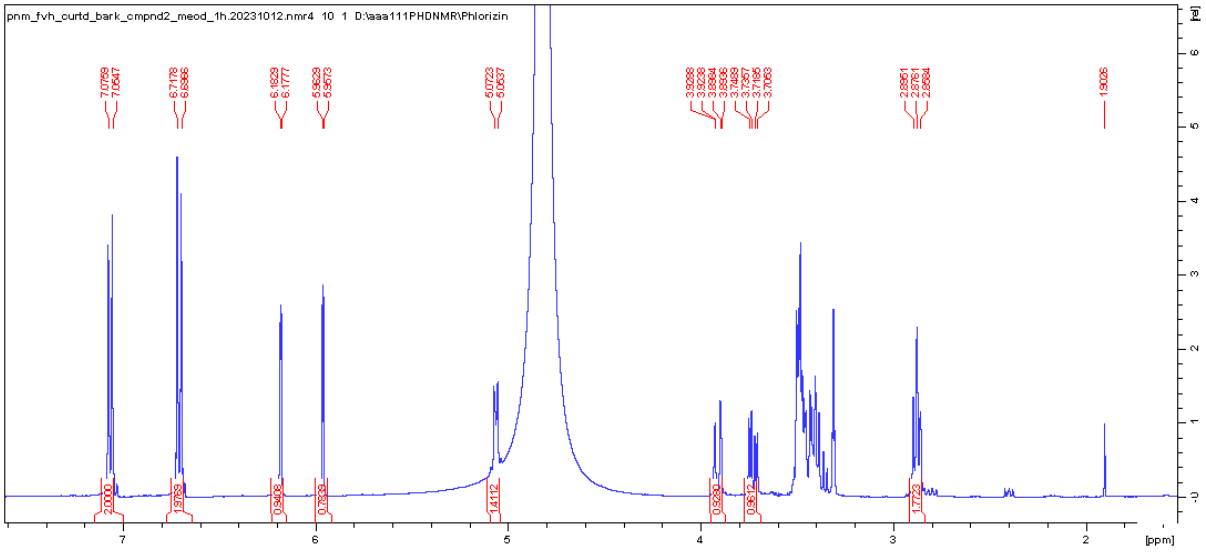

Figure S6.4: ^{1}H NMR spectrum of phlorizin (**259**) in CD_3OD, 400 MHz

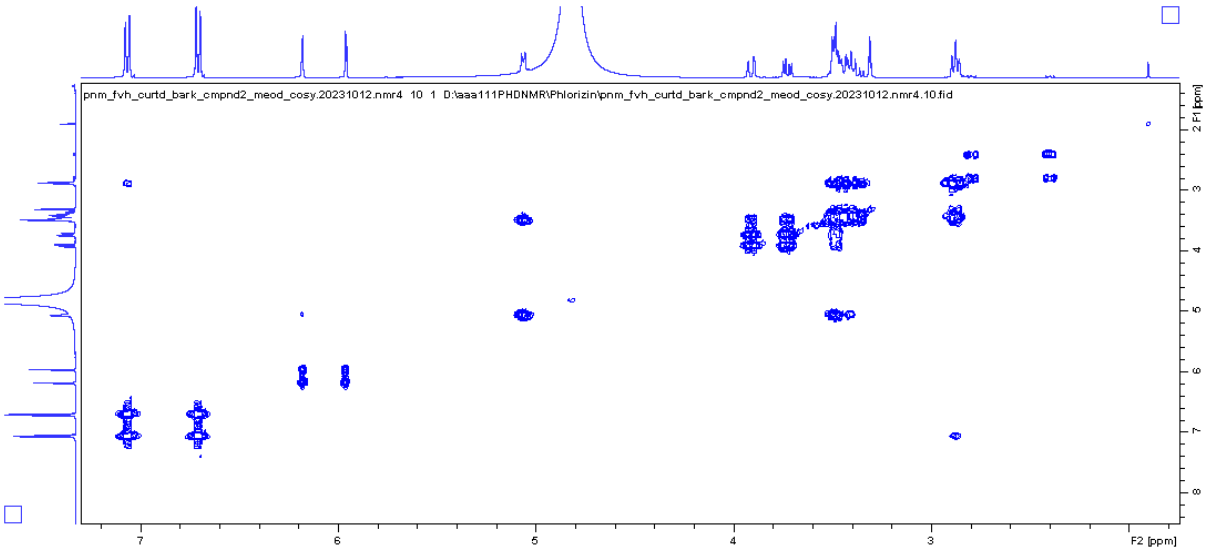

Figure S6.5: COSY spectrum of phlorizin (**259**) in CD_3OD, 400 MHz

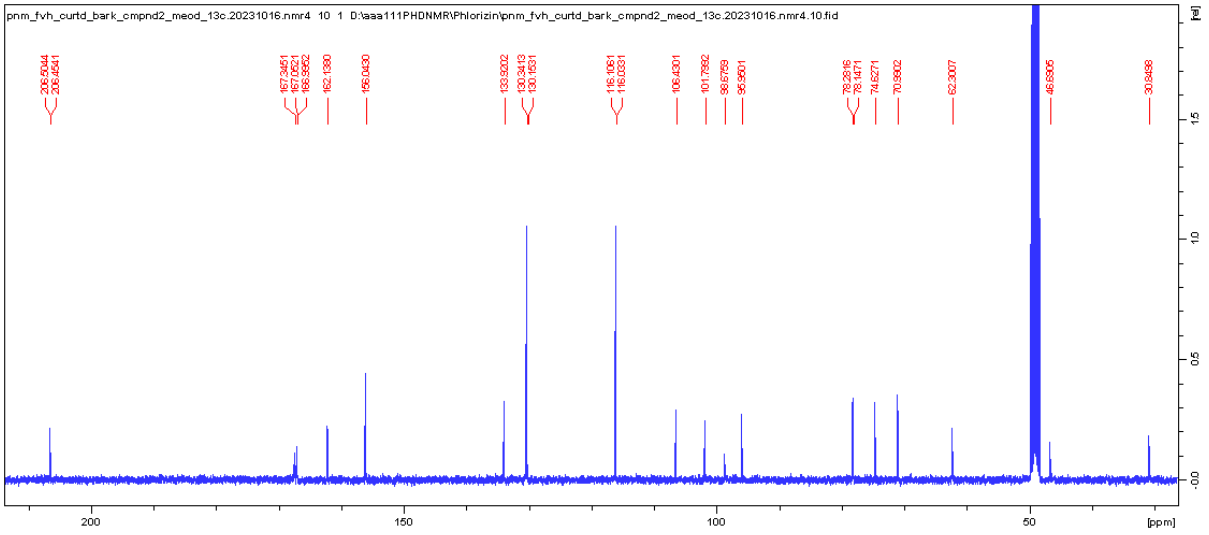

Figure S6.6: ^{13}C NMR spectrum of phlorizin (**259**) in CD_3OD, 100 MHz

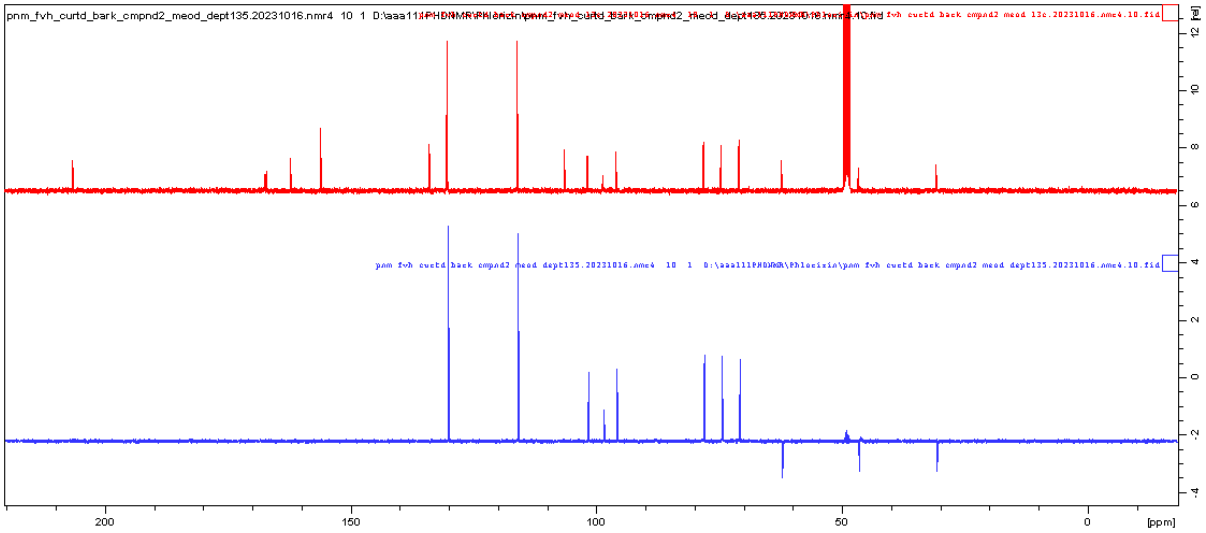

Figure S6.7: ^{13}C NMR and DEPT spectra of phlorizin (**259**) in CD_3OD, 100 MHz

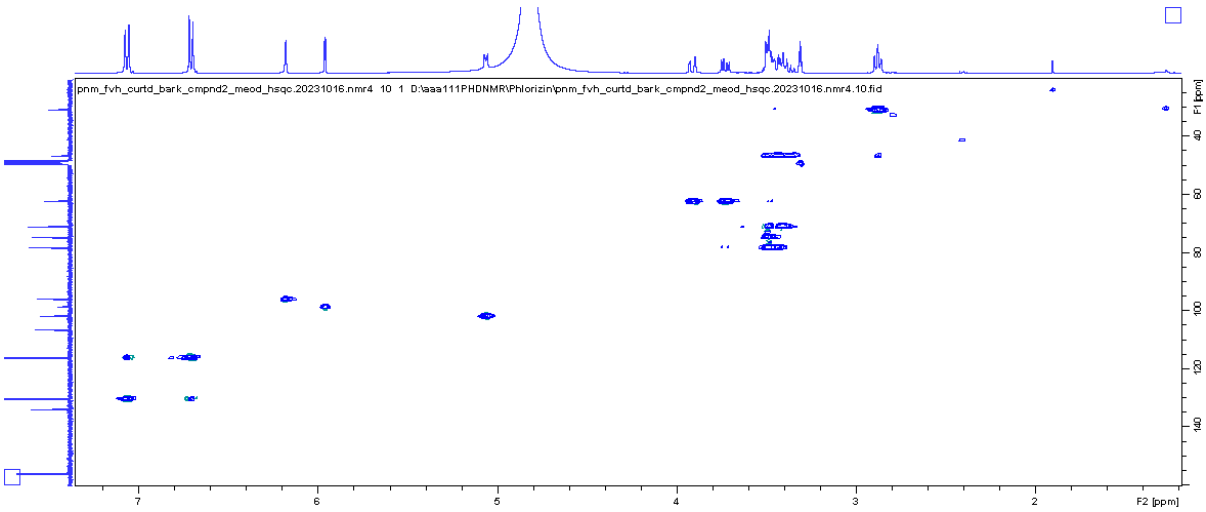

Figure S6.8: HSQC of spectrum of phlorizin (**259**) in CD_3OD, 400 MHz

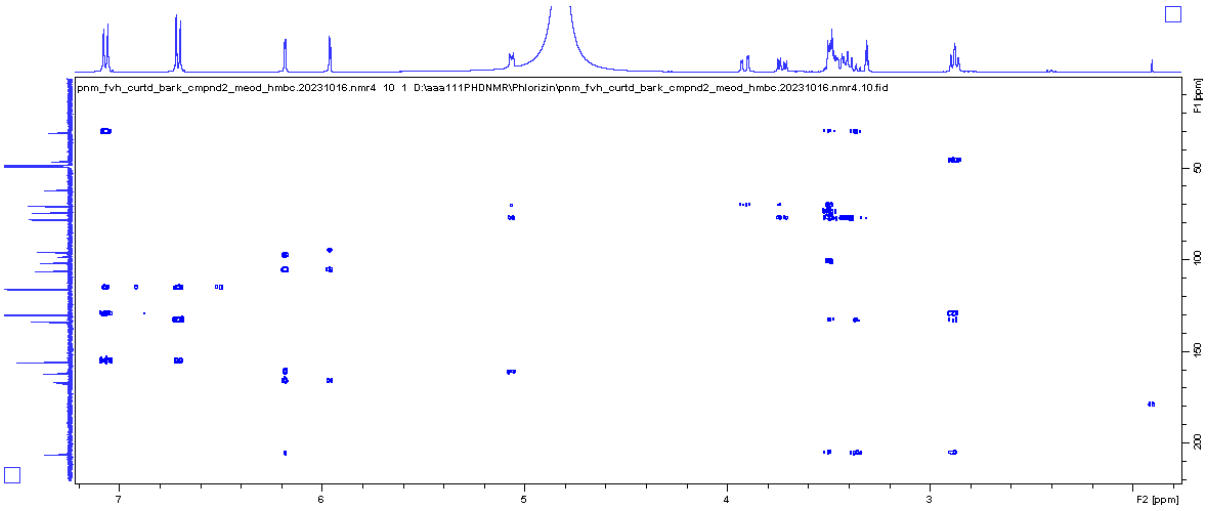

Figure S6.9: HMBC of spectrum of phlorizin (**259**) in CD_3OD, 400 MHz

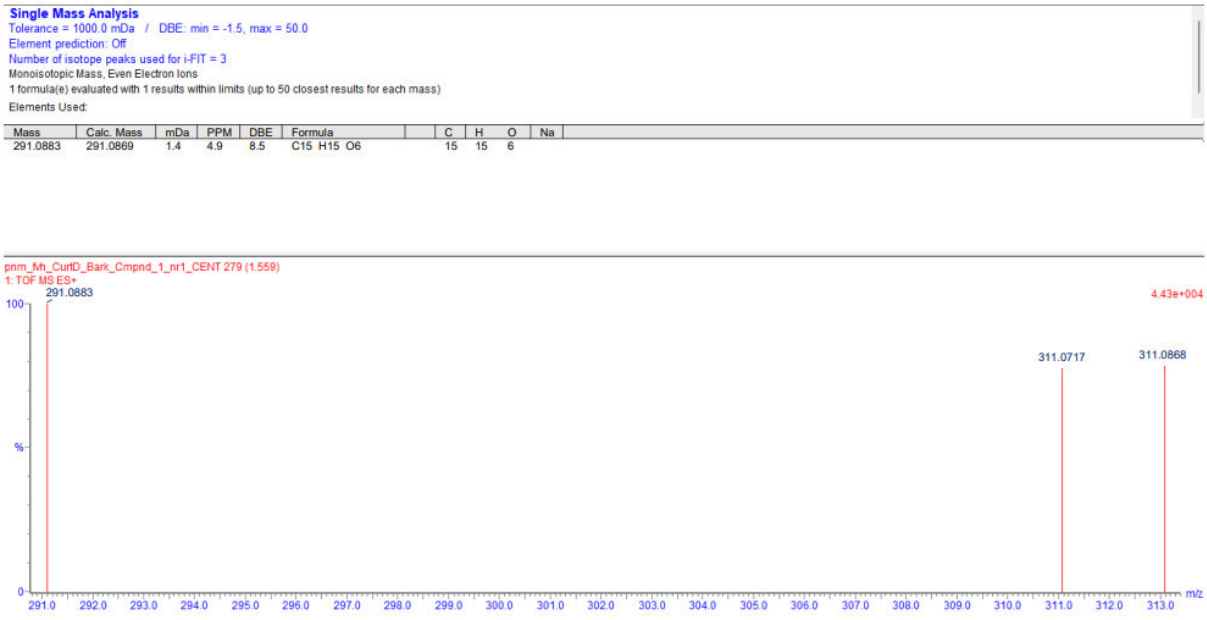

Figure S7.1: HR-(+)-ESI MS of (+)-catechin (**258**)

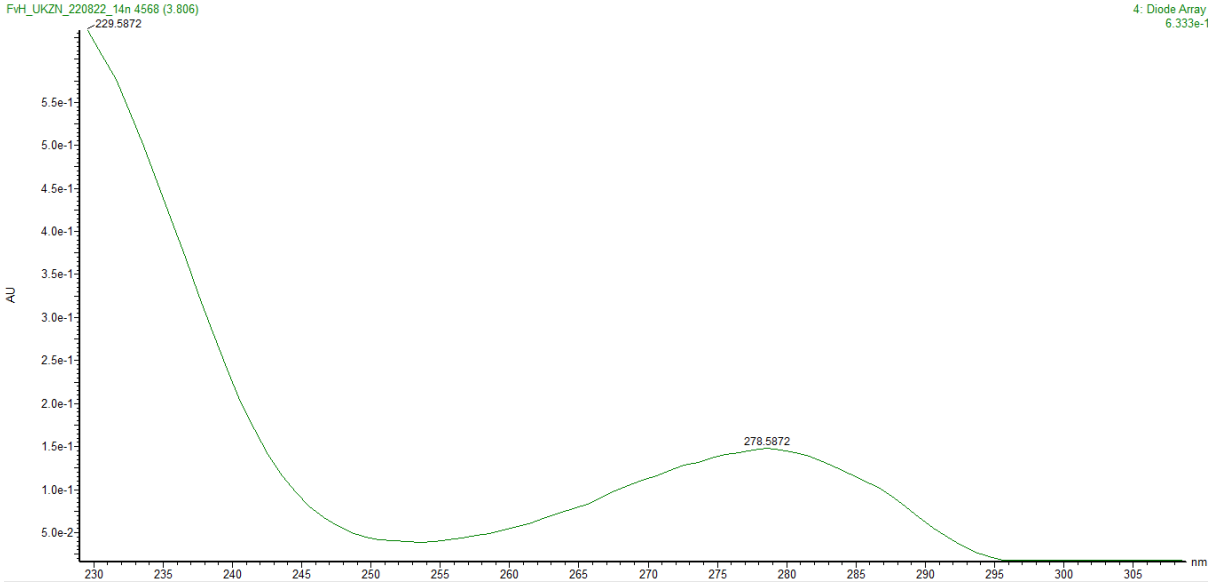

Figure S7.2: UV-Vis spectrum of (+)-catechin (**258**)

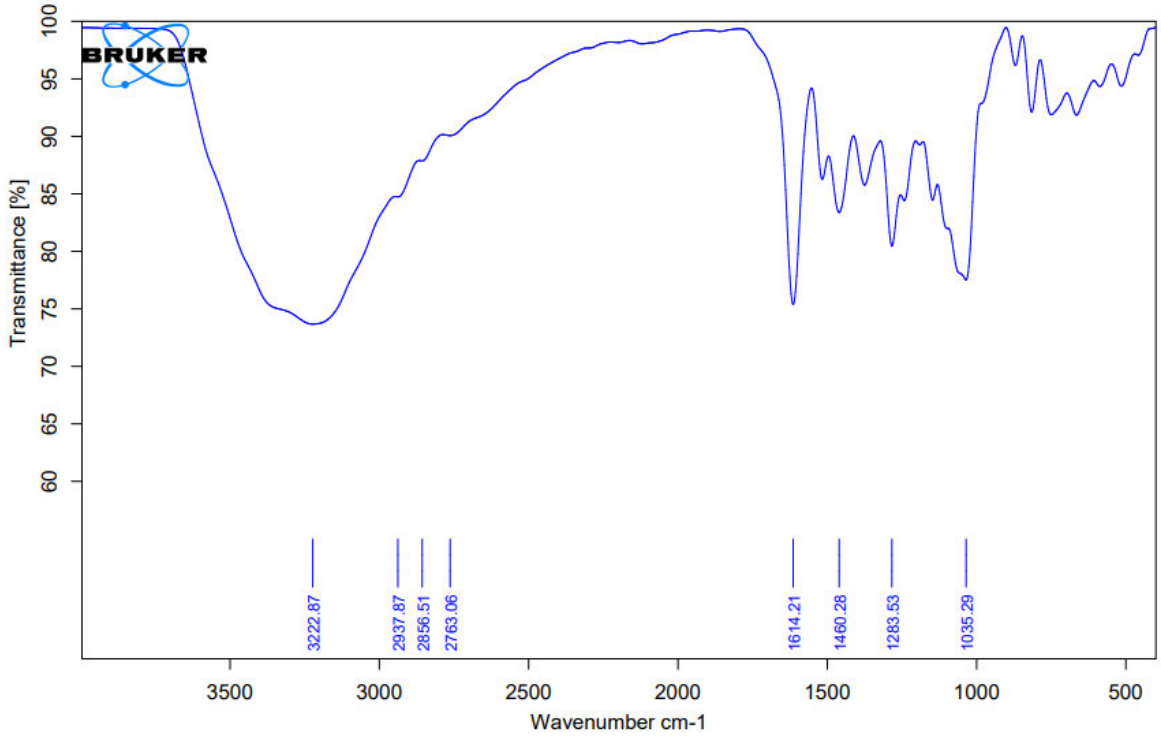

Figure S7.3: IR spectrum of (+)-catechin (**258**)

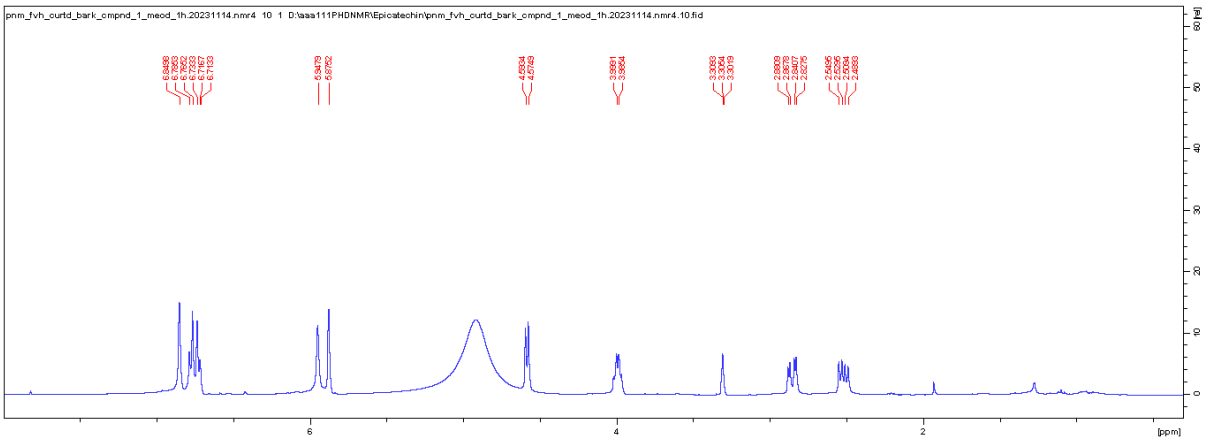

Figure S7.4: ^{1}H NMR spectrum of (+)-catechin (**258**) in CD_3OD, 400 MHz

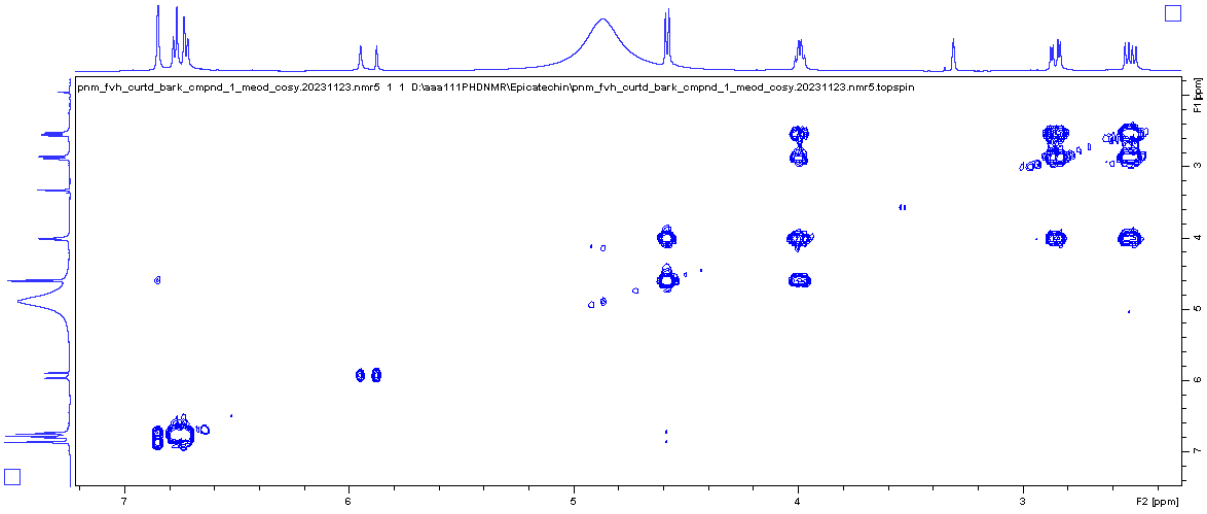

Figure S7.5: COSY spectrum of (+)-catechin (**258**) in CD_3OD, 500 MHz

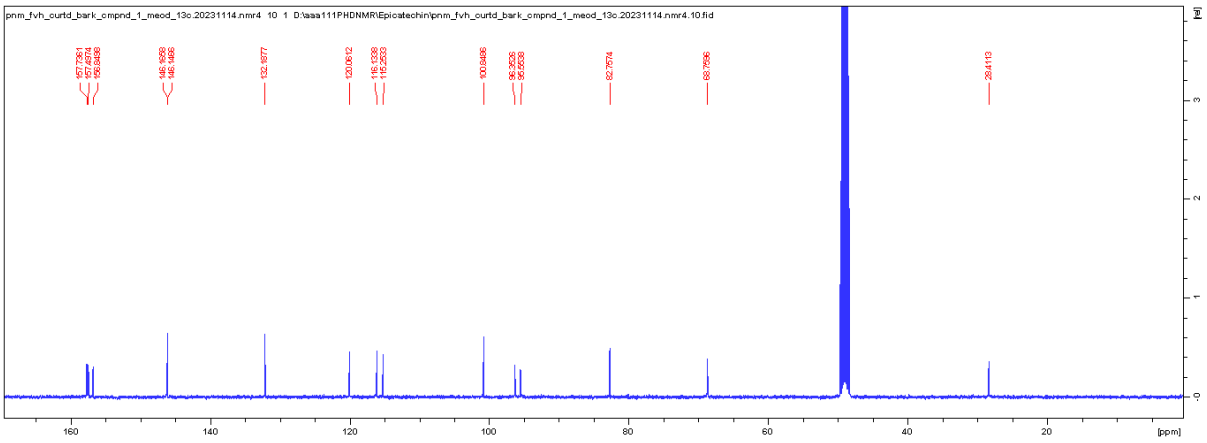

Figure S7.6: ^{13}C NMR spectrum of (+)-catechin (**258**) in CD_3OD, 100 MHz

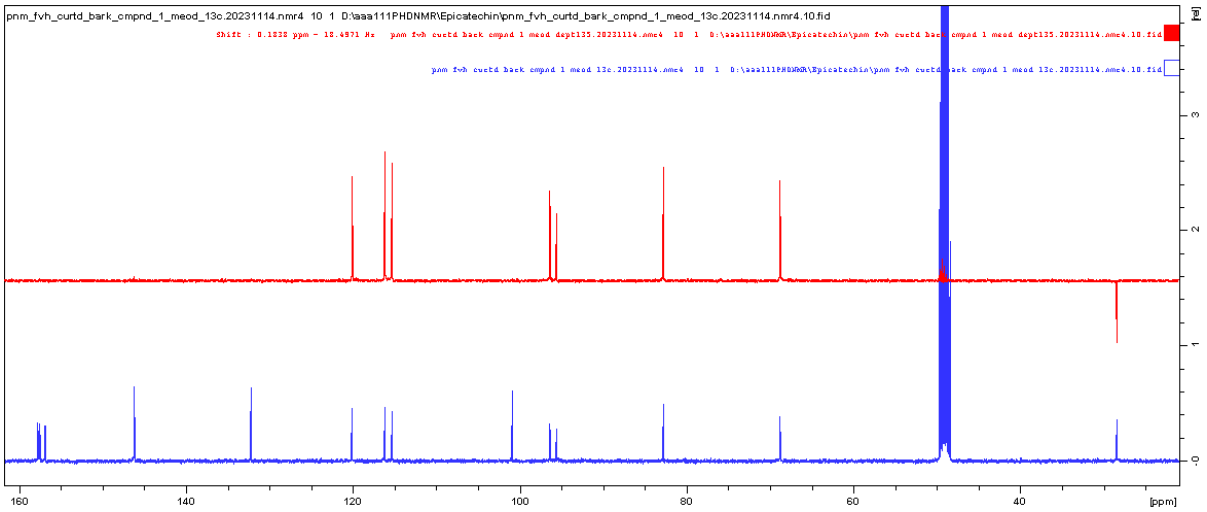

Figure S7.7: ^{13}C NMR and DEPT spectra of (+)-catechin (**258**) in CD_3OD, 100 MHz

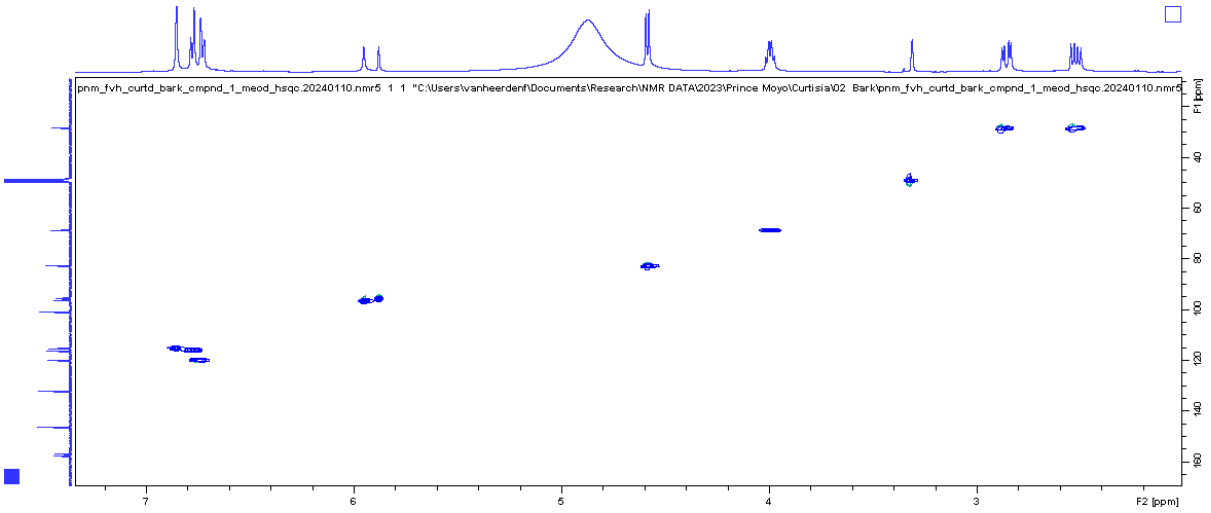

Figure S7.8: HSQC spectrum of (+)-catechin (**258**) in CD_3OD, 500 MHz

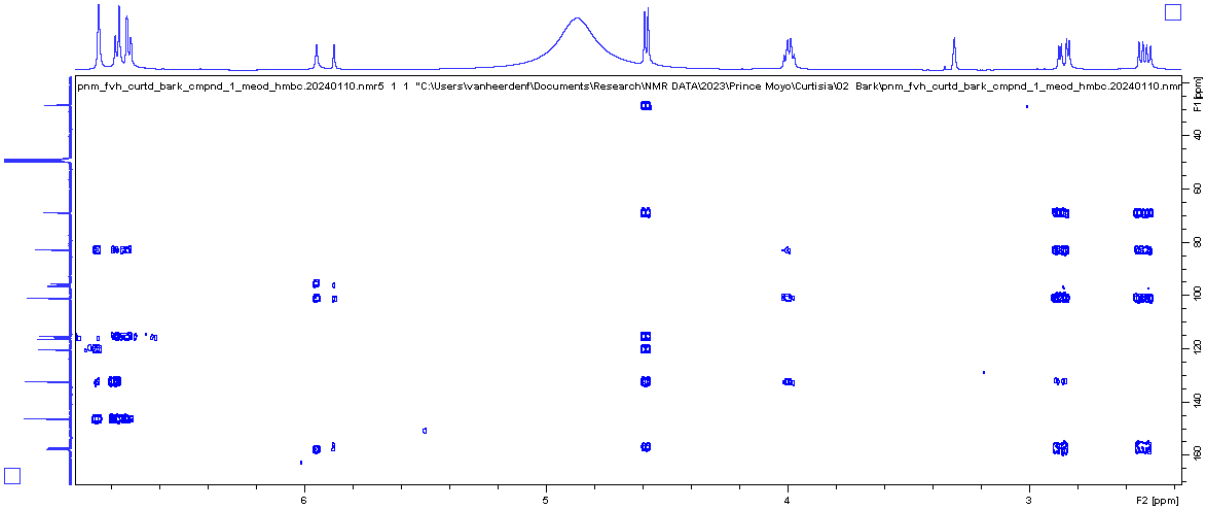

Figure S7.9: HMBC spectrum of (+)-catechin (**258**) in CD_3OD, 500 MHz

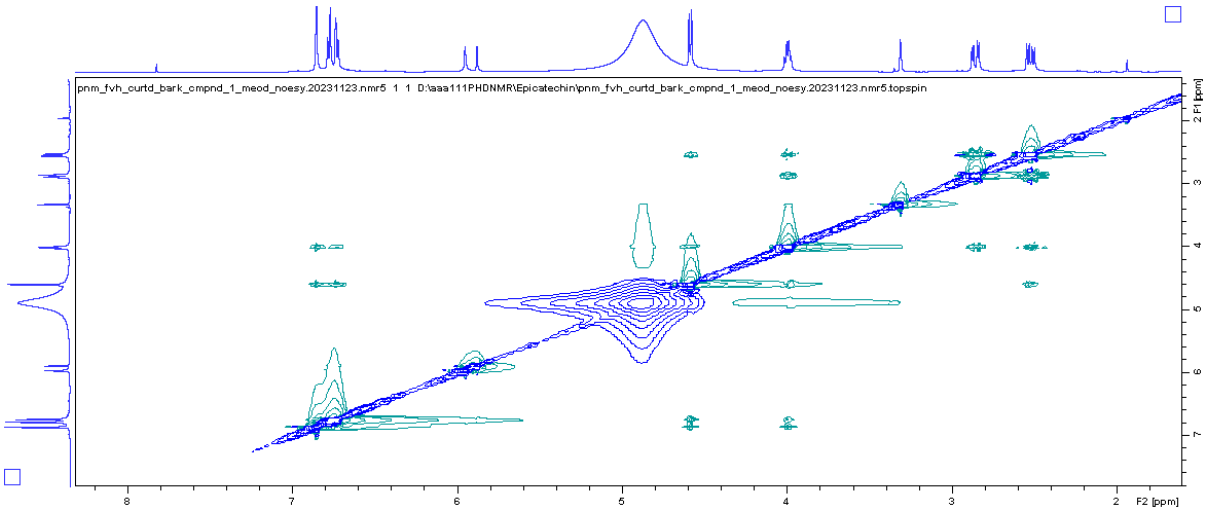

Figure S7.10: NOESY spectrum of (+)-catechin (**258**) in CD_3OD, 500 MHz

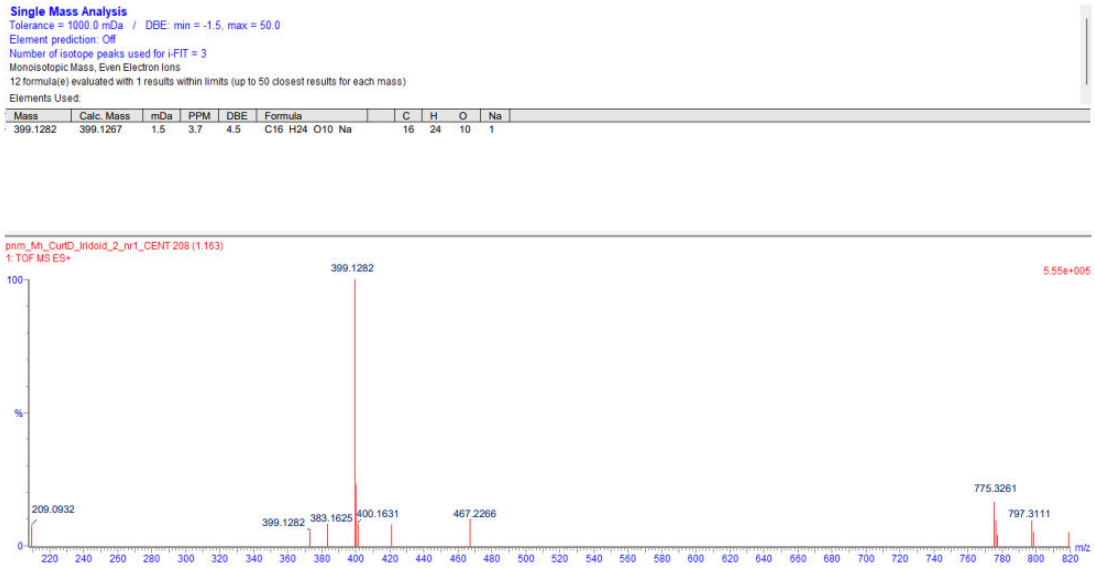

Figure S8.1: HR-(+)-ESI MS of loganic acid (**116**)

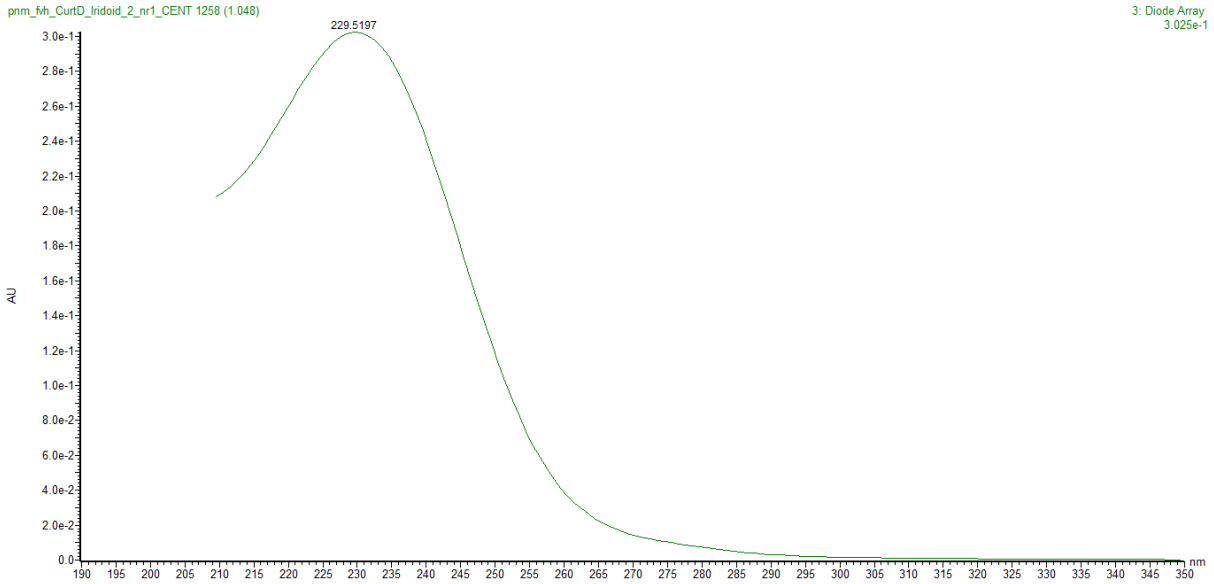

Figure S8.2: UV-vis spectrum of loganic acid (**116**)

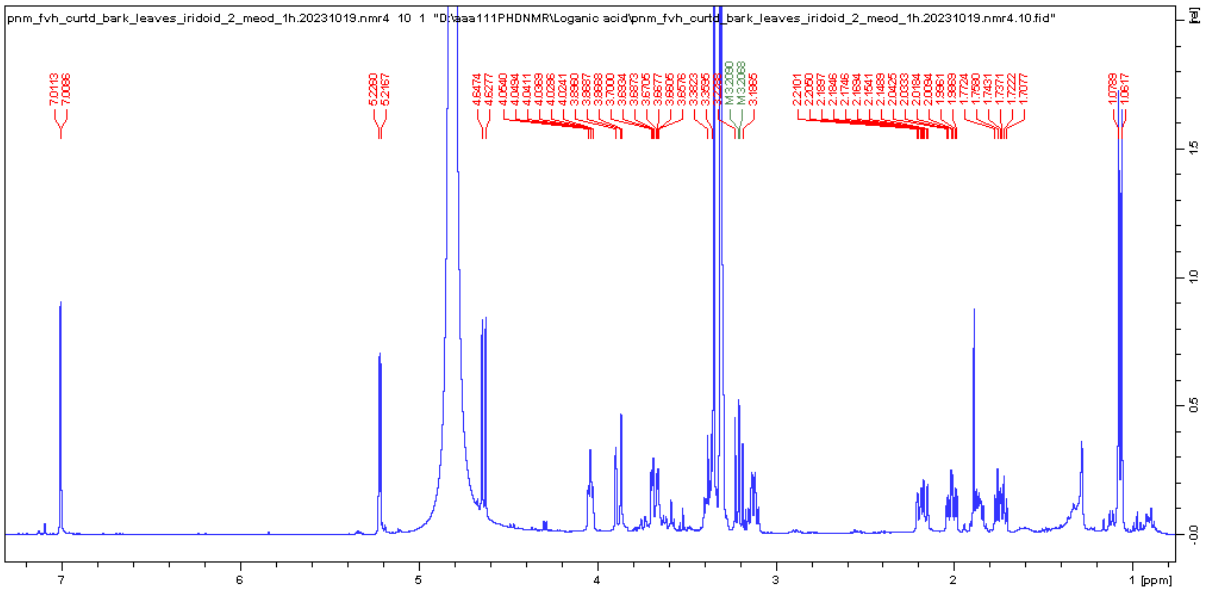

Figure S8.3: ^{1}H NMR spectrum of loganic acid (**116**) in CD_3OD, 400 MHz

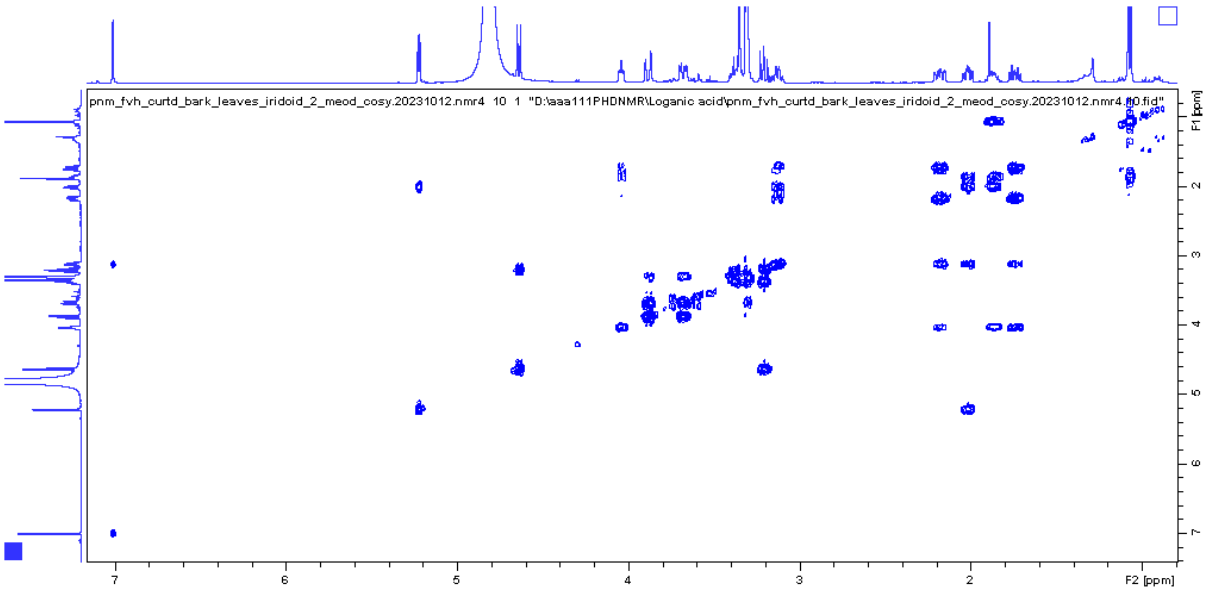

Figure S8.4: COSY spectrum of loganic acid (**116**) in CD_3OD, 400 MHz

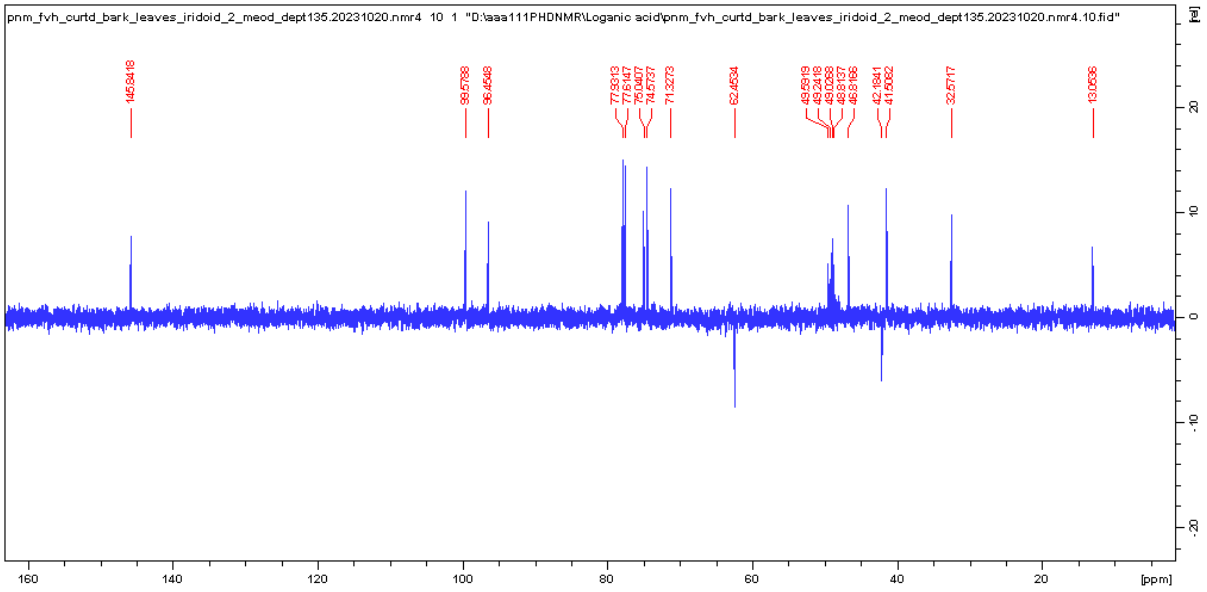

Figure S8.5: DEPT spectrum of loganic acid (**116**) in CD_3OD, 100 MHz

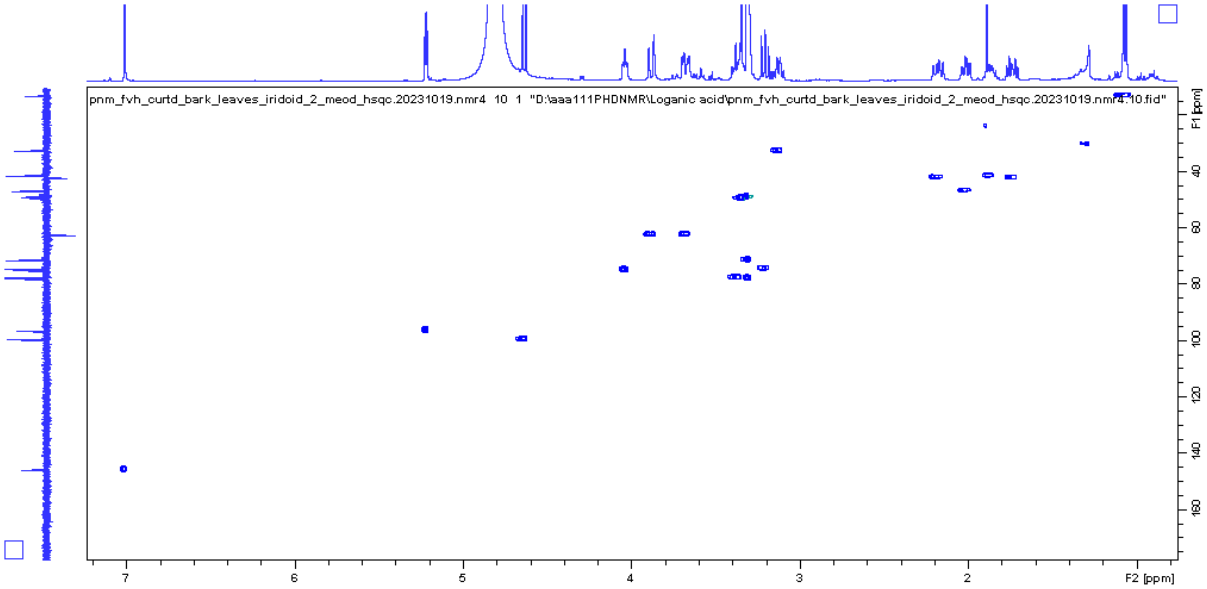

Figure S8.6: HSQC spectrum of loganic acid (**116**) in CD_3OD, 400 MHz

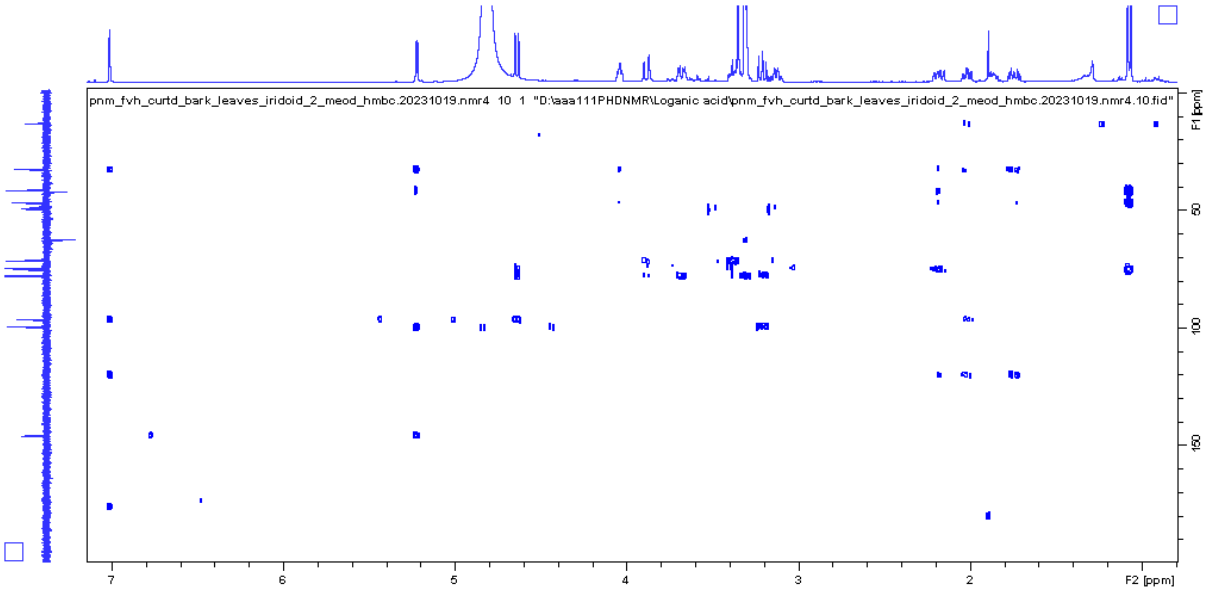

Figure S8.7: HMBC spectrum of loganic acid (**116**) in CD_3OD, 400 MHz

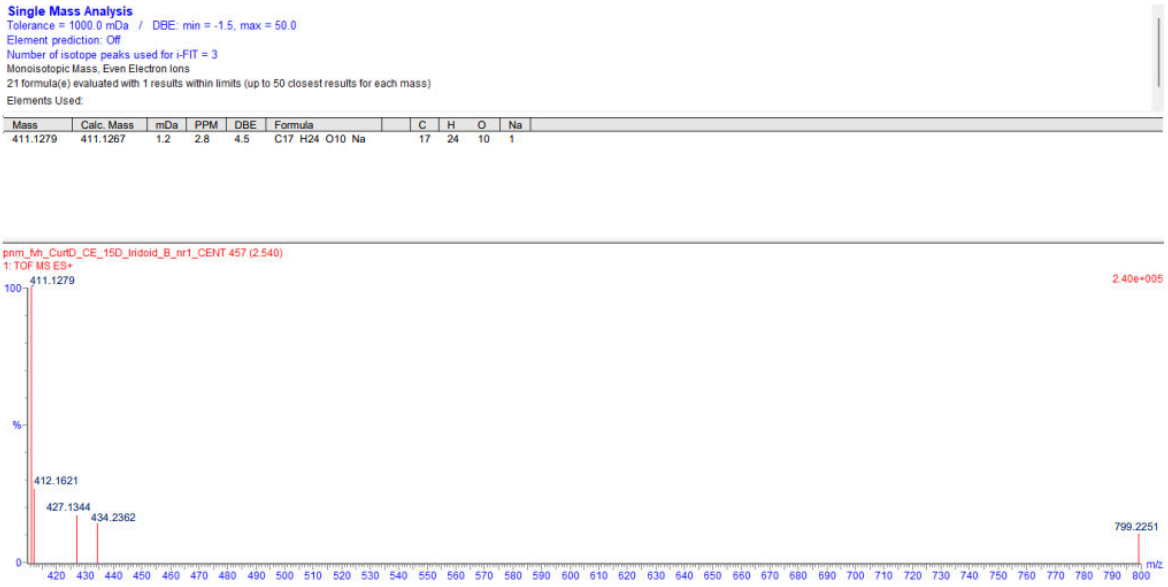

Figure S9.1: HR-(+)-ESI MS of geniposide (**131**)

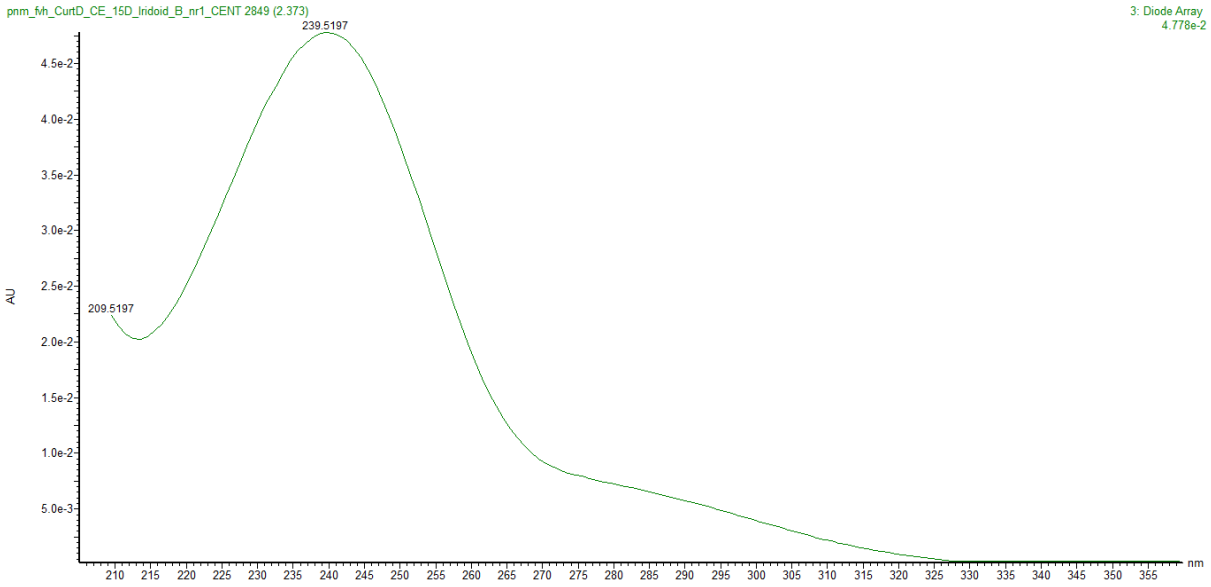

Figure S9.2: UV-Vis spectrum of geniposide (**131**)

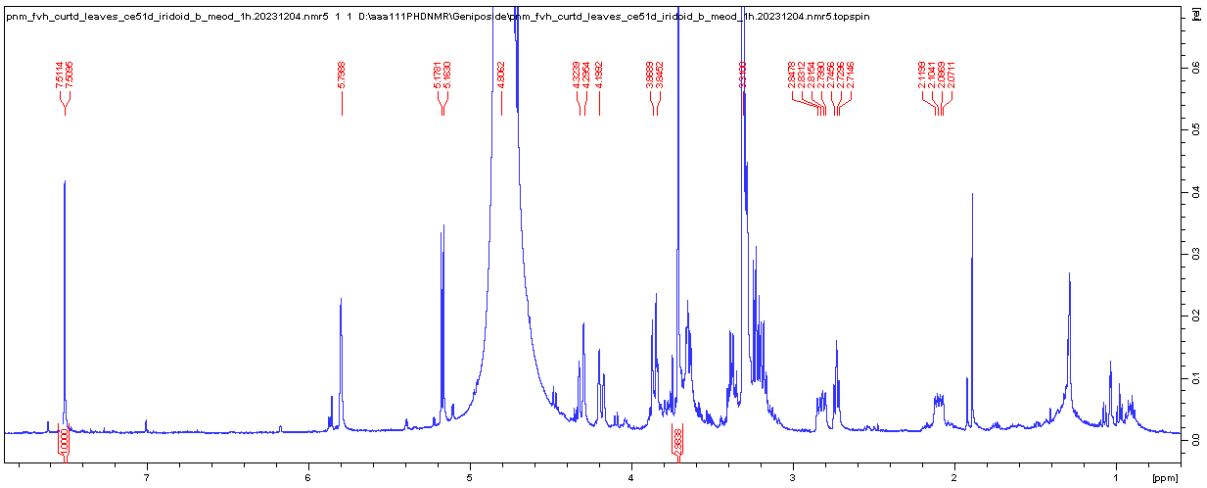

Figure S9.3: ^{1}H NMR spectrum of geniposide (**131**) in CD_3OD, 500 MHz

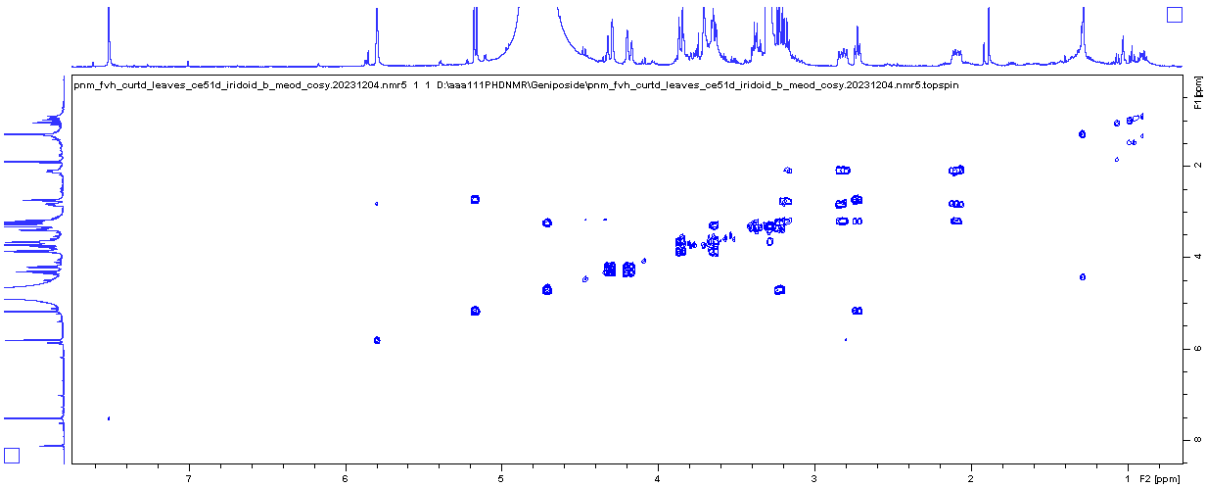

Figure S9.4: COSY spectrum of geniposide (**131**) in CD_3OD, 500 MHz

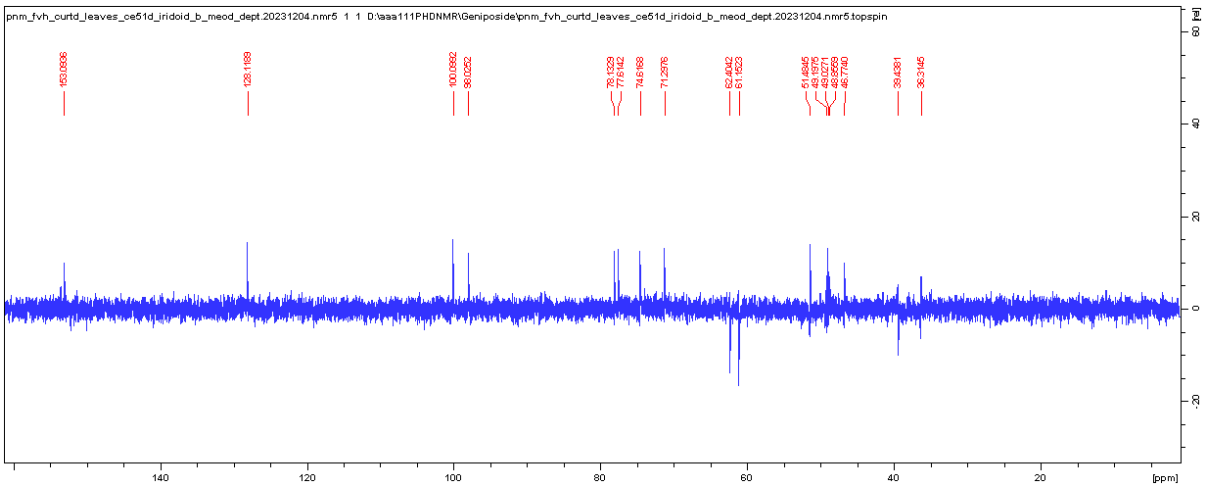

Figure S9.5: DEPT spectrum of geniposide (**131**) in CD_3OD, 125 MHz

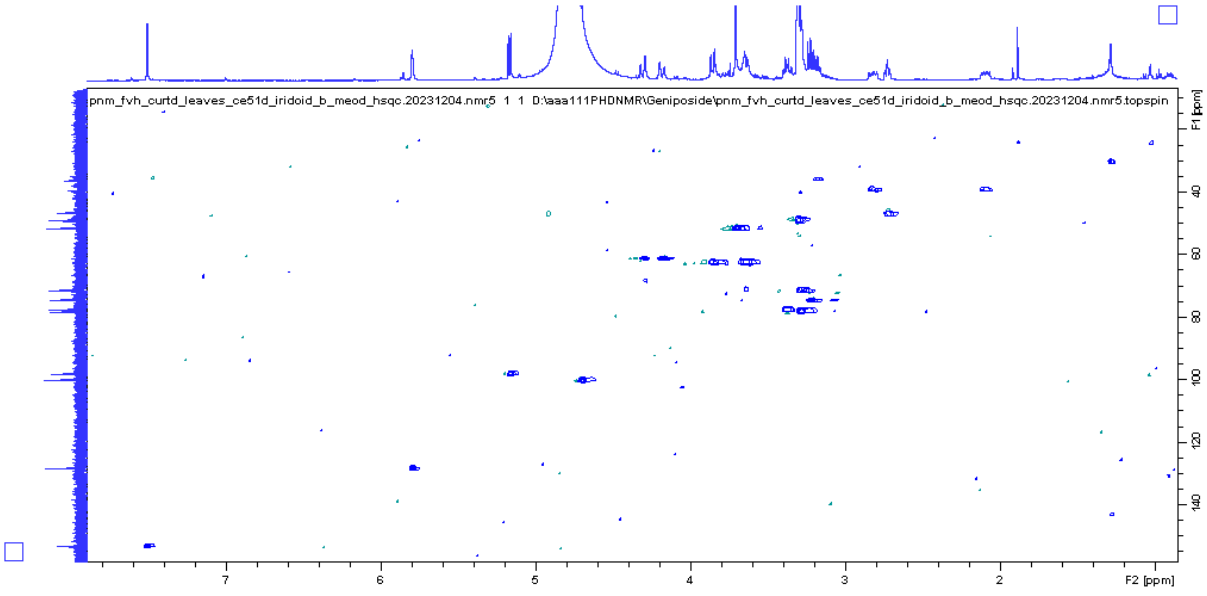

Figure S9.6: HSQC spectrum of geniposide (**131**) in CD_3OD, 500 MHz

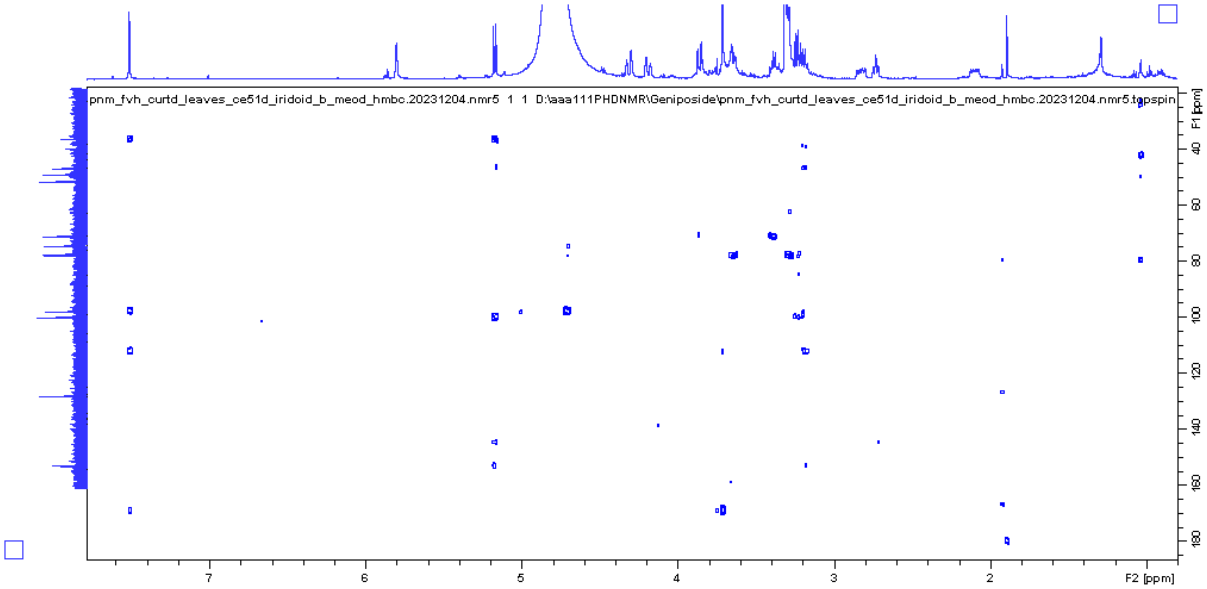

Figure S9.7: HMBC spectrum of geniposide (**131**) in CD_3OD, 500 MHz

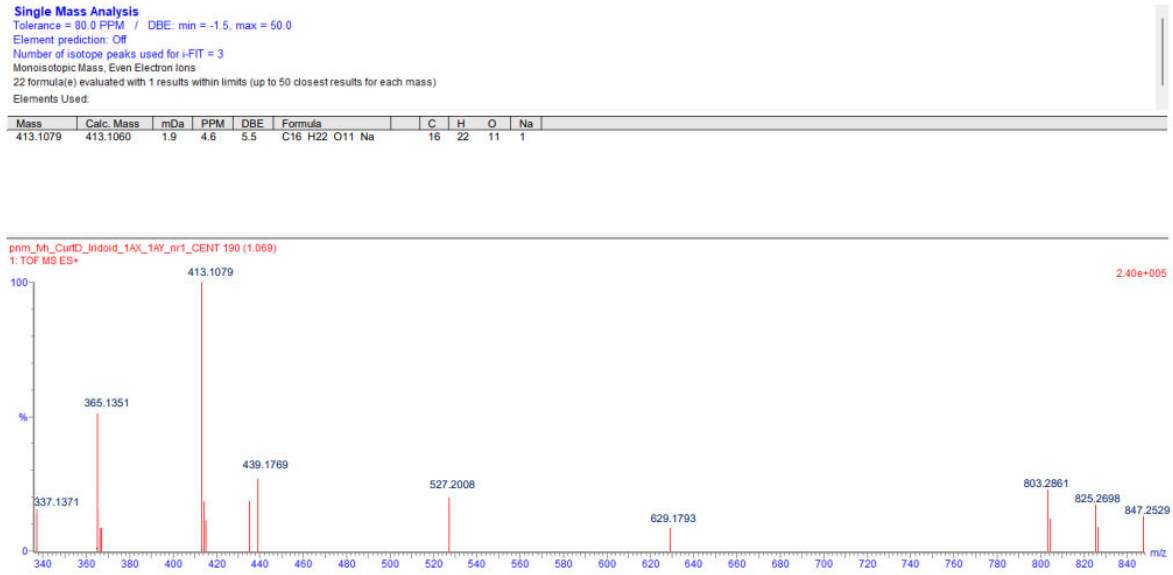

Figure S10.1: HR-(+)-ESI MS of secologanoside (**260**)

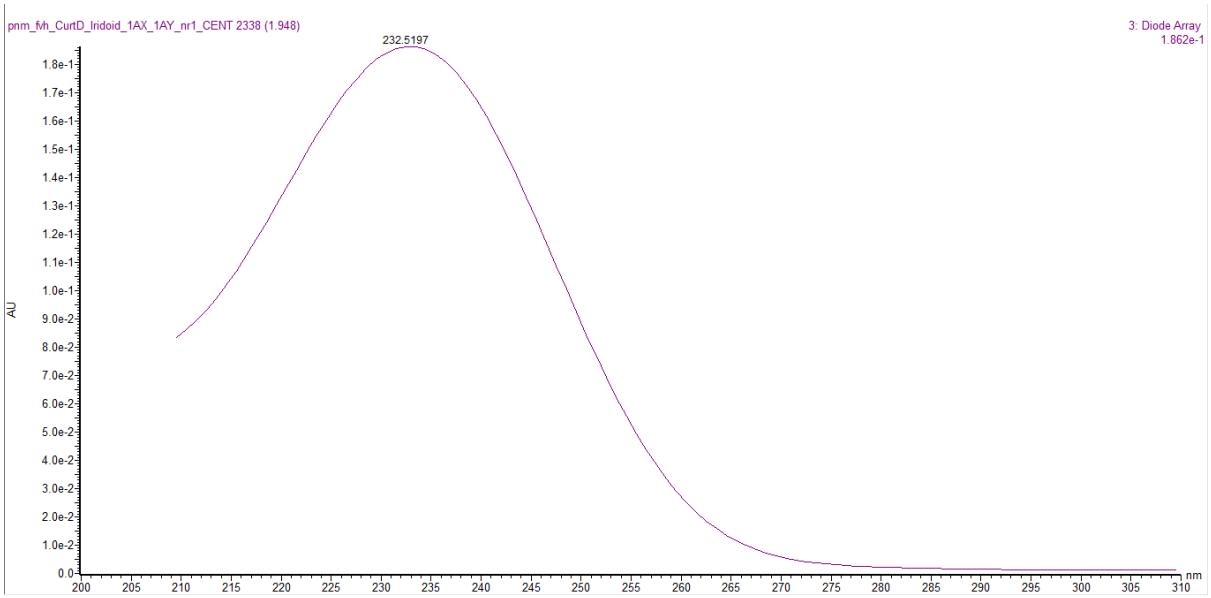

Figure S10.2: UV-Vis spectrum of secologanoside (**260**)

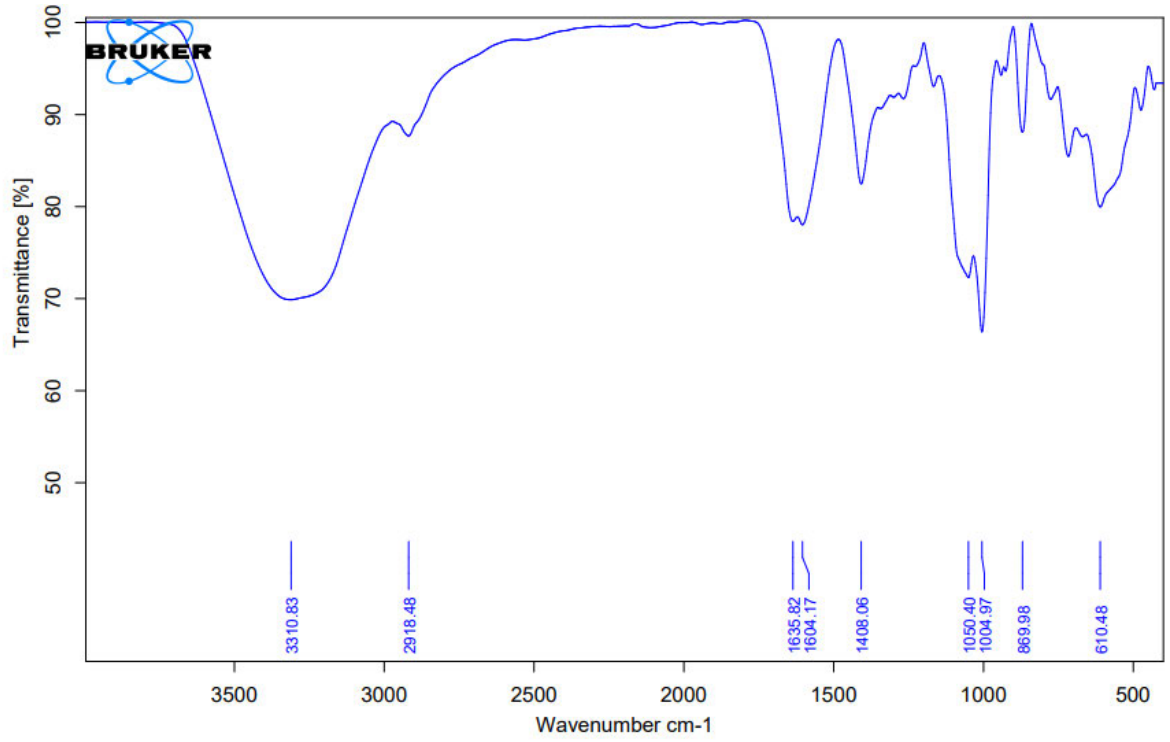

Figure S10.3: IR spectrum of secologanoside (**260**)

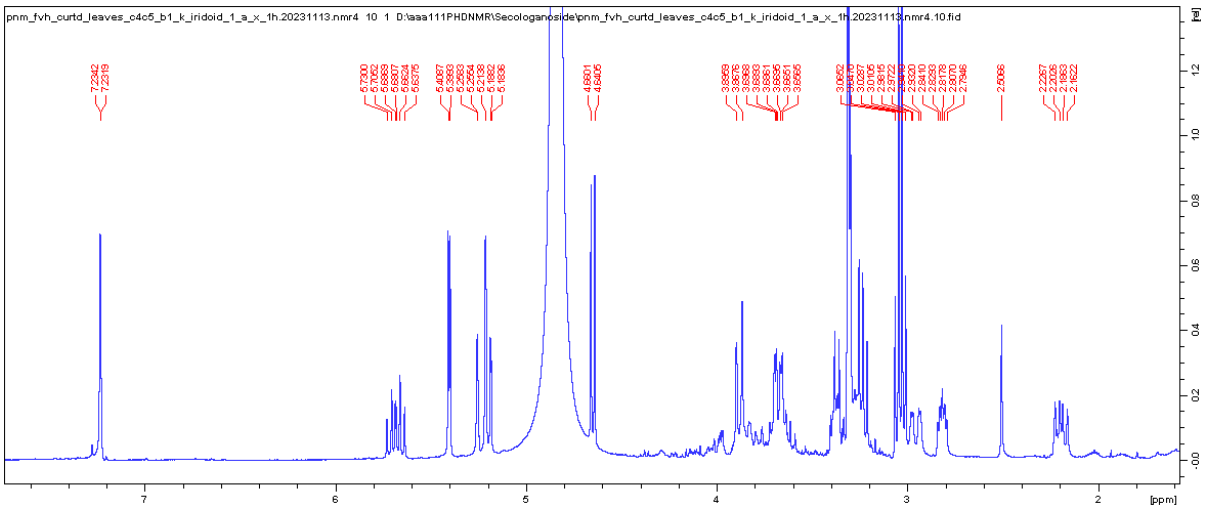

Figure S10.4: ^{1}H NMR spectrum of secologanoside (**260**) in CD_3OD, 400 MHz

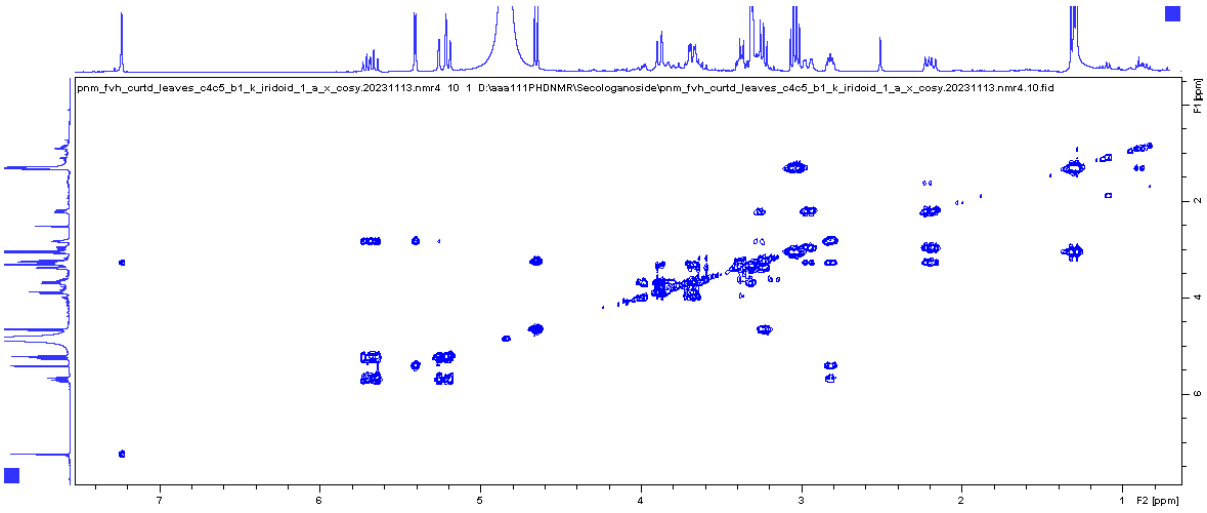

Figure S10.5: COSY spectrum of secologanoside (**260**) in CD_3OD, 400 MHz

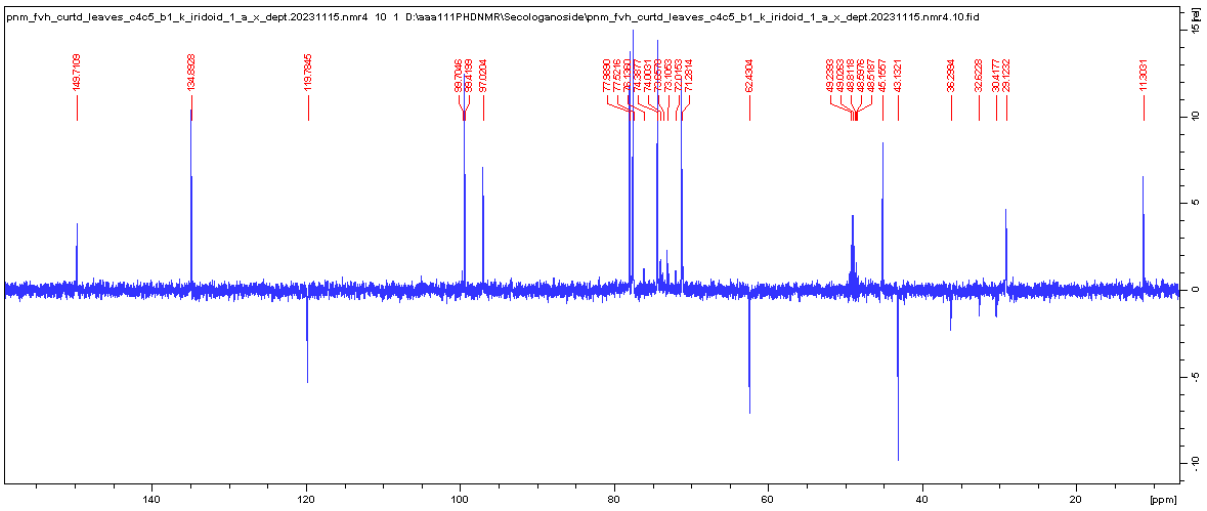

Figure S10.6: DEPT spectrum of secologanoside (**260**) in CD_3OD, 100 MHz

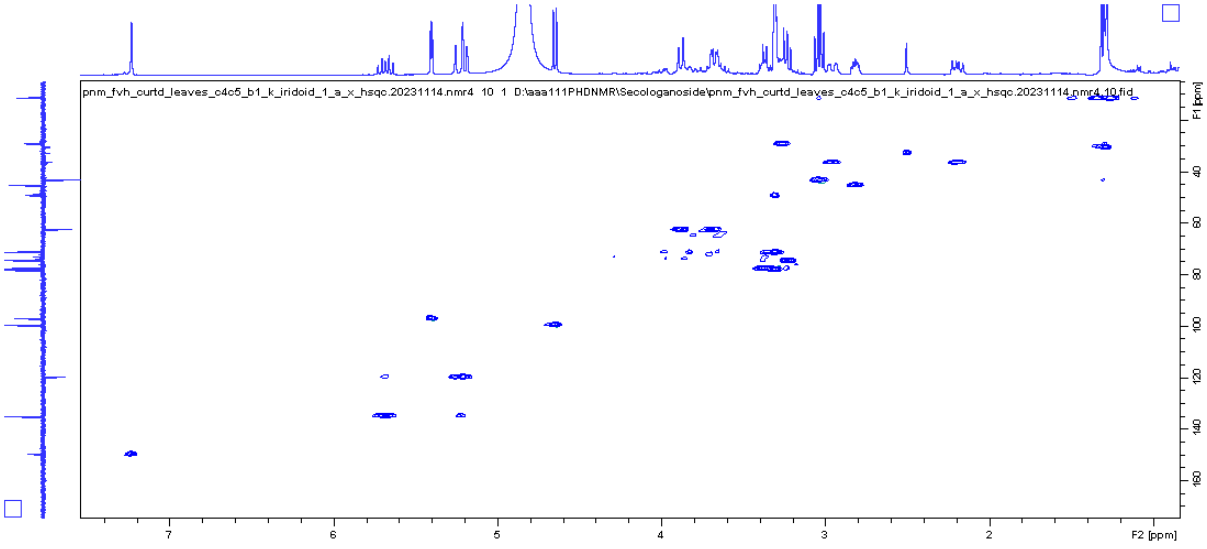

Figure S10.7: HSQC spectrum of secologanoside (**260**) in CD_3OD, 400 MHz

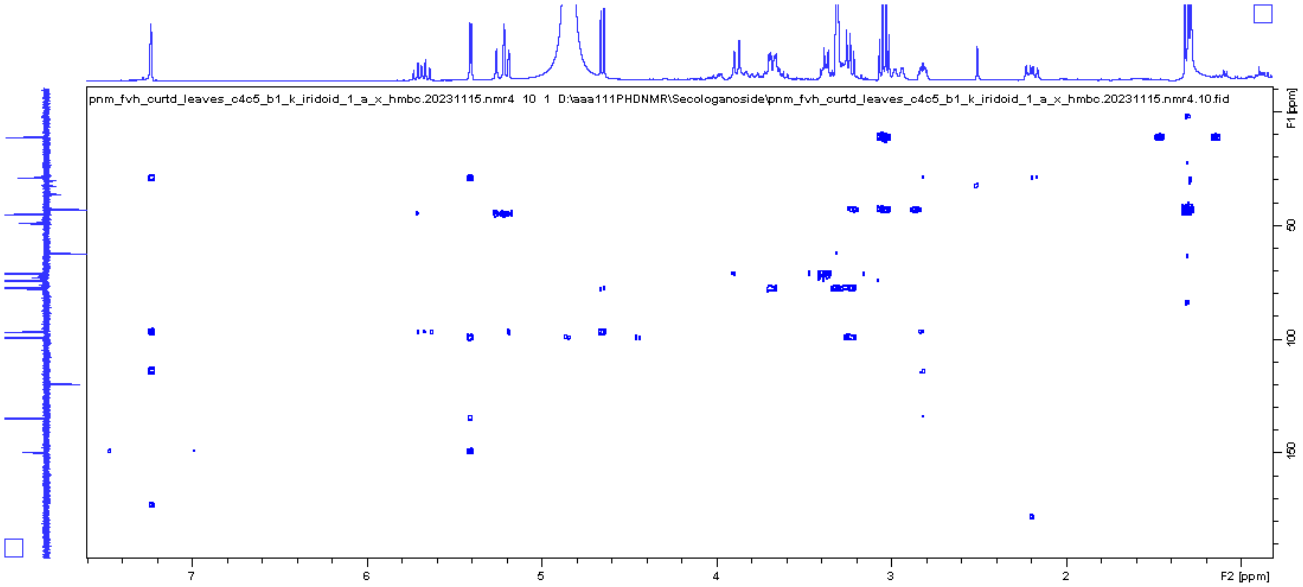

Figure S10.8: HMBC spectrum of secologanoside (**260**) in CD_3OD, 400 MHz

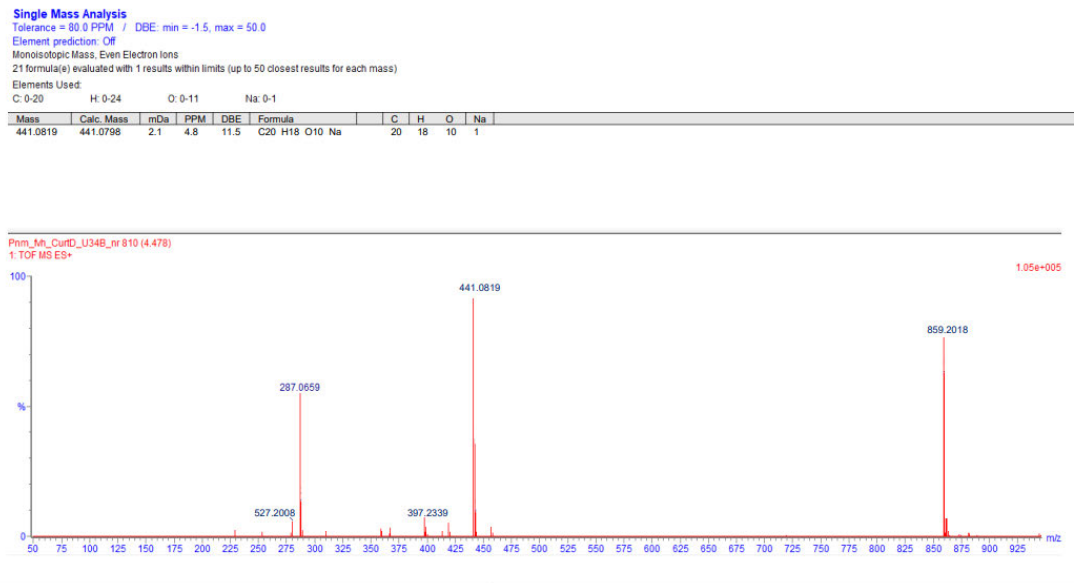

Figure S11.1: HR-(+)-ESI MS of juglalin (**262**)

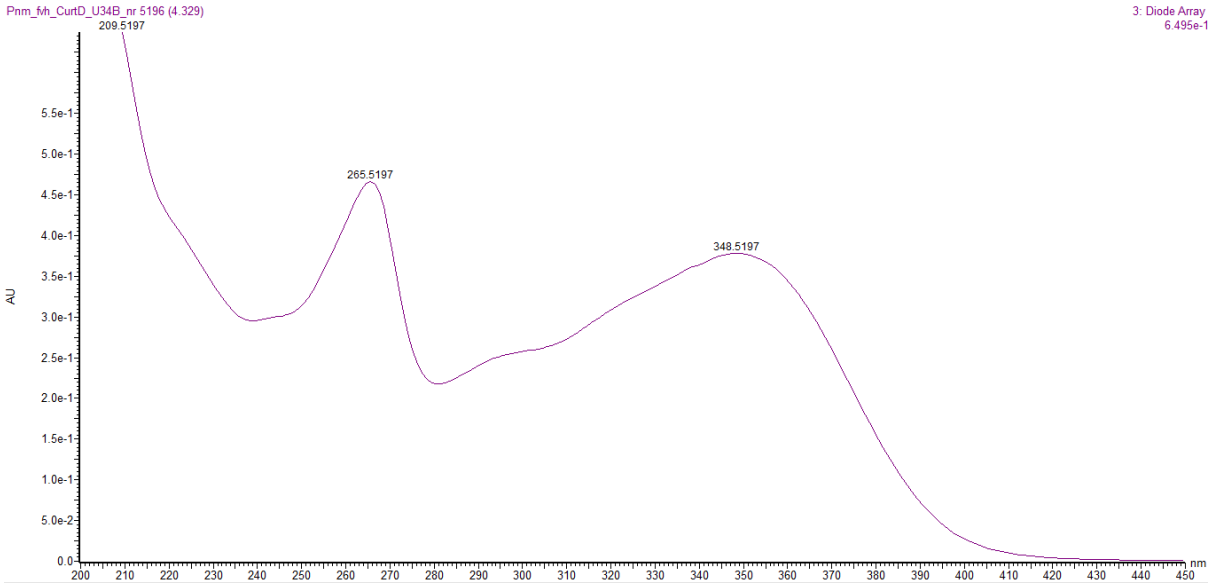

Figure S11.2: UV-Vis spectrum of juglalin (**262**)

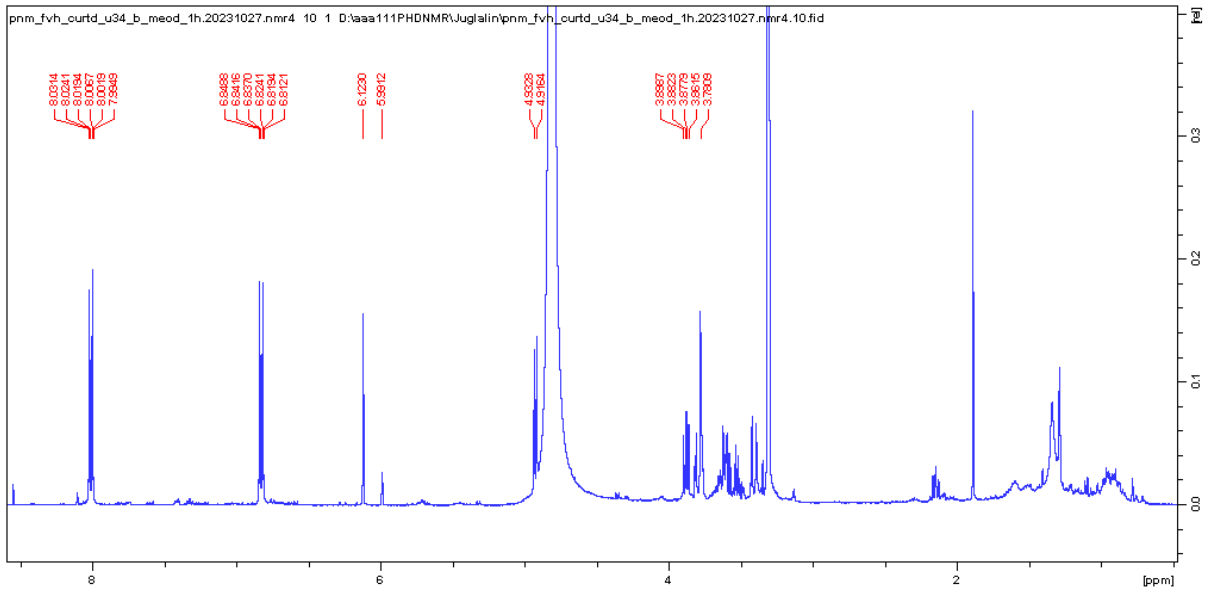

Figure S11.3: ^{1}H NMR spectrum of juglalin (**262**) in CD_3OD, 400 MHz

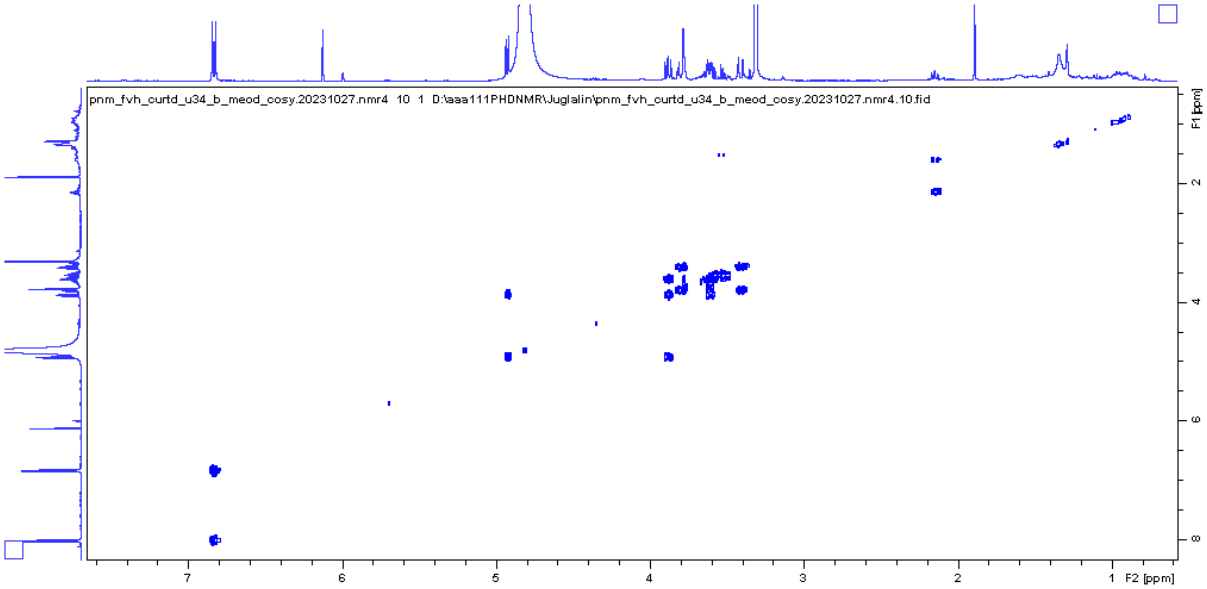

Figure S11.4: COSY spectrum of juglalin (**262)** in CD_3OD, 400 MHz

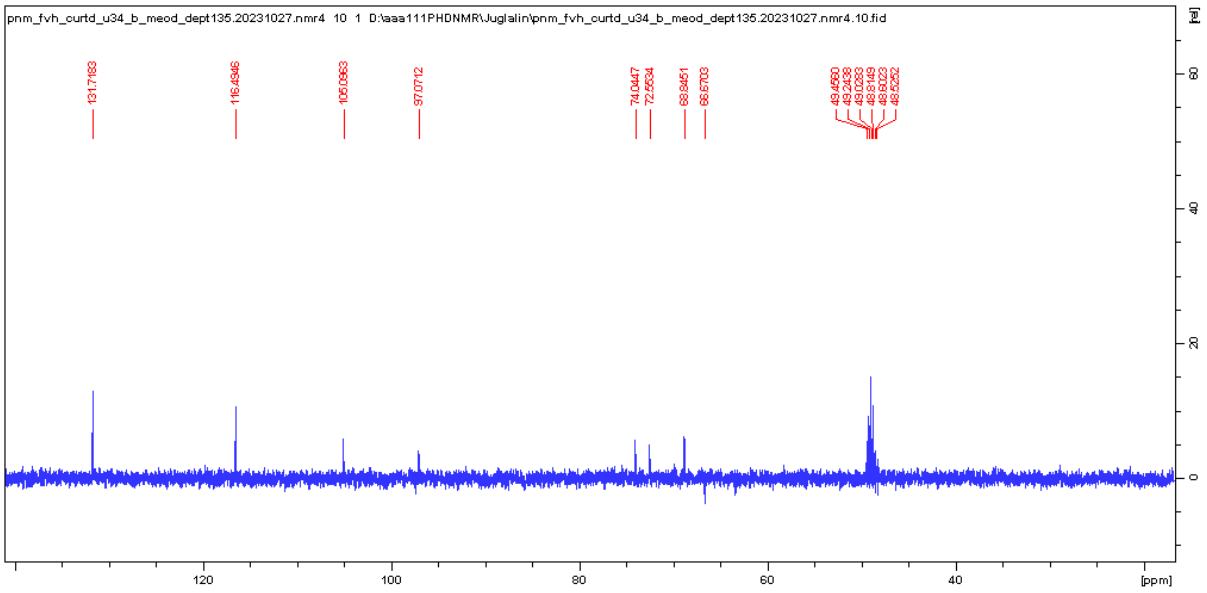

Figure S11.5: DEPT spectrum of juglalin (**262**) in CD_3OD, 100 MHz

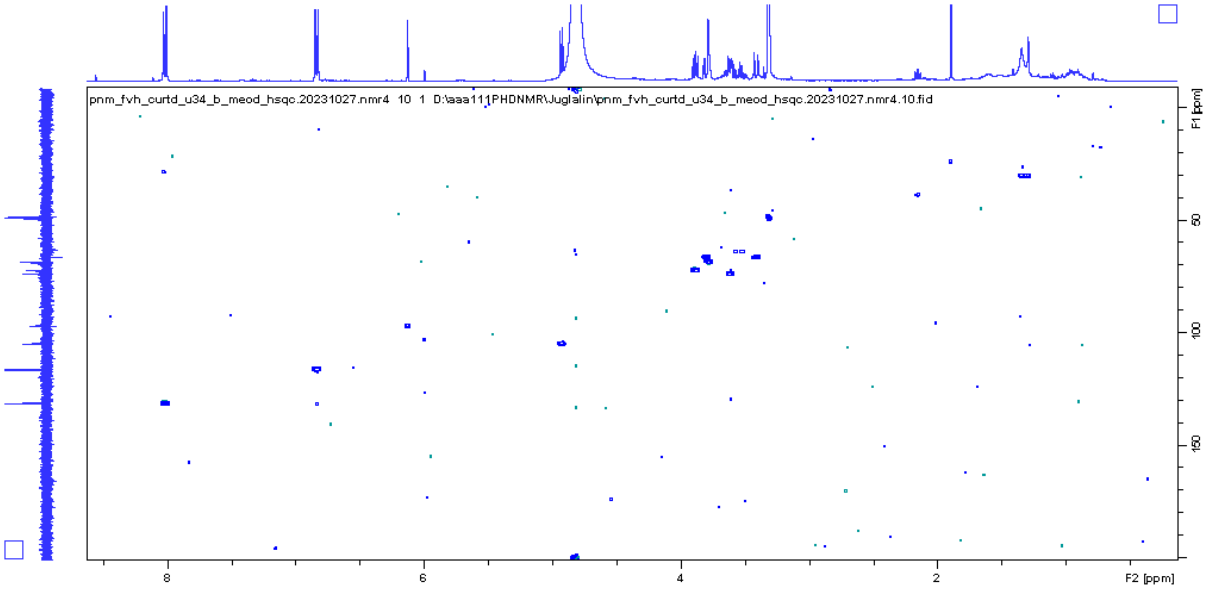

Figure S11.6: HSQC spectrum of juglalin (**262**) in CD_3OD, 400 MHz

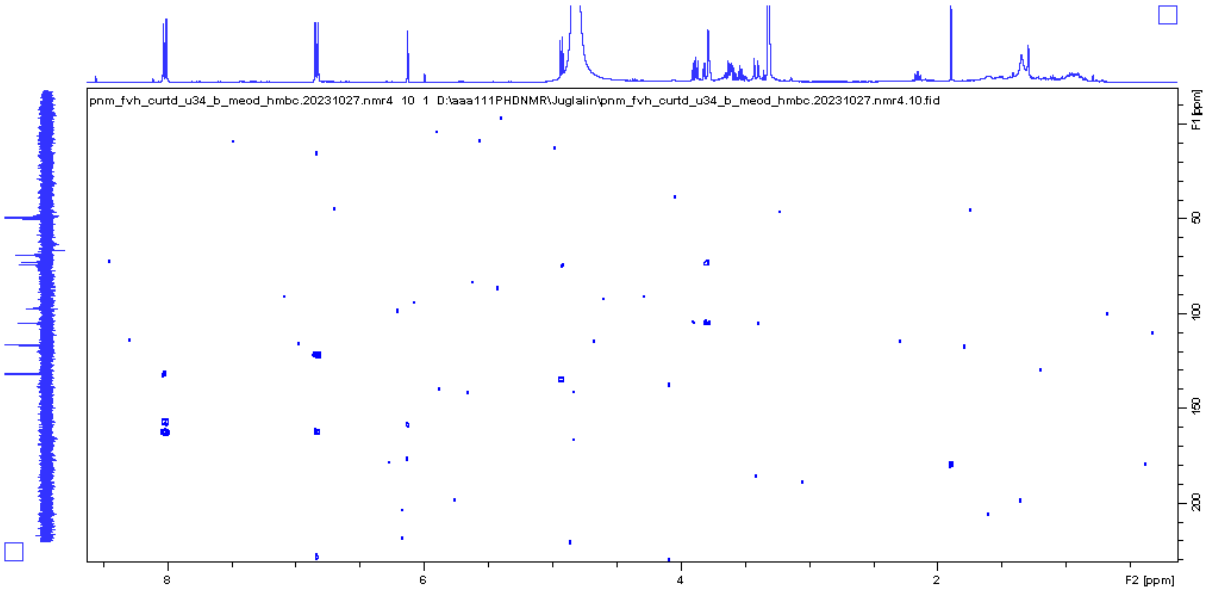

Figure S11.7: HMBC spectrum of juglalin (**262**) in CD_3OD, 400 MHz

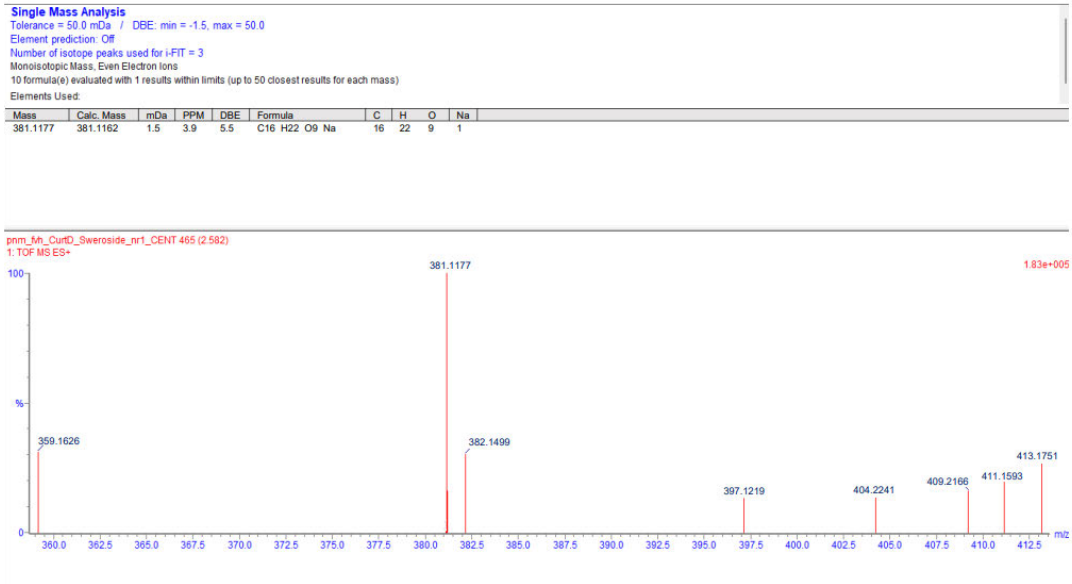

Figure S12.1: HR-(+)-ESI MS of sweroside (**114**)

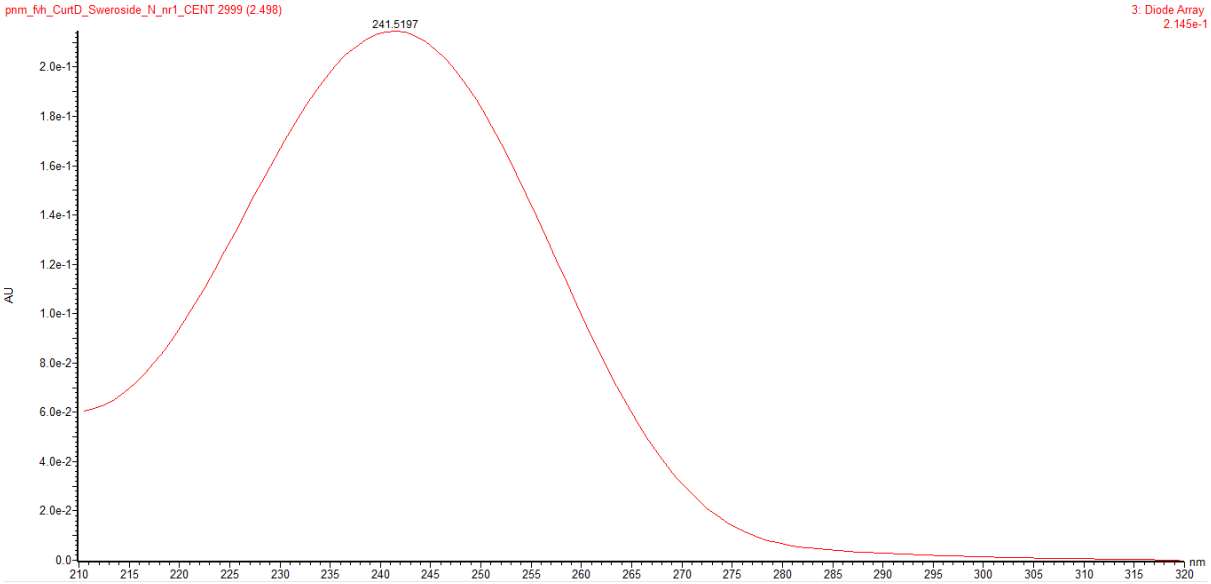

Figure S12.2: UV-Vis spectrum of sweroside (**114**)

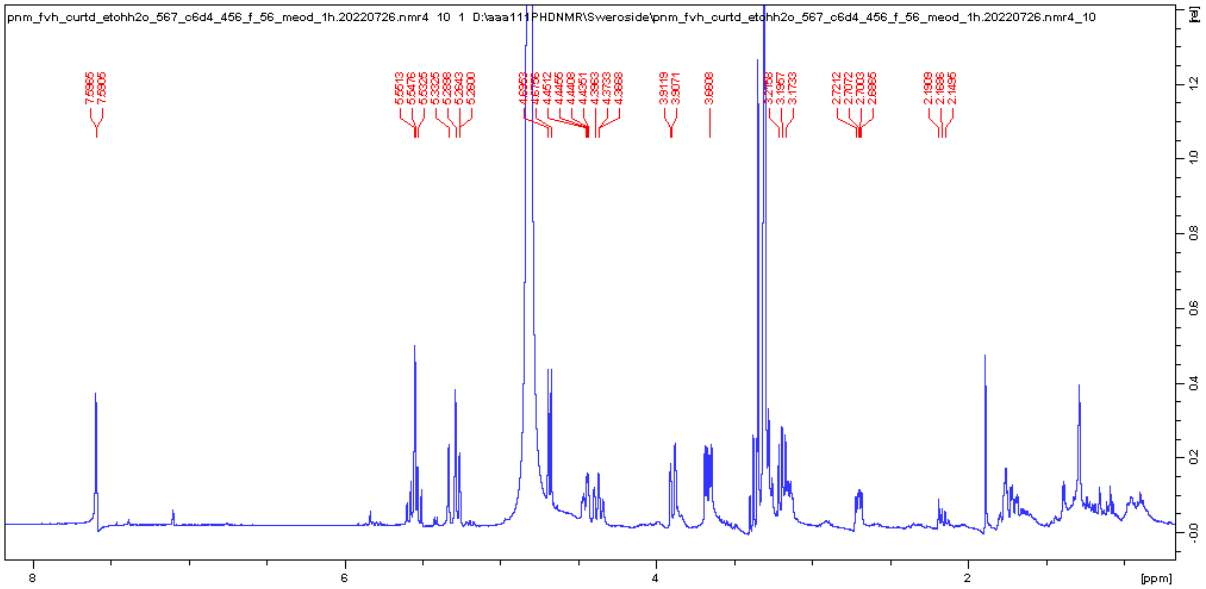

Figure S12.3: ^{1}H NMR spectrum of sweroside (**114**) in CD_3OD, 400 MHz

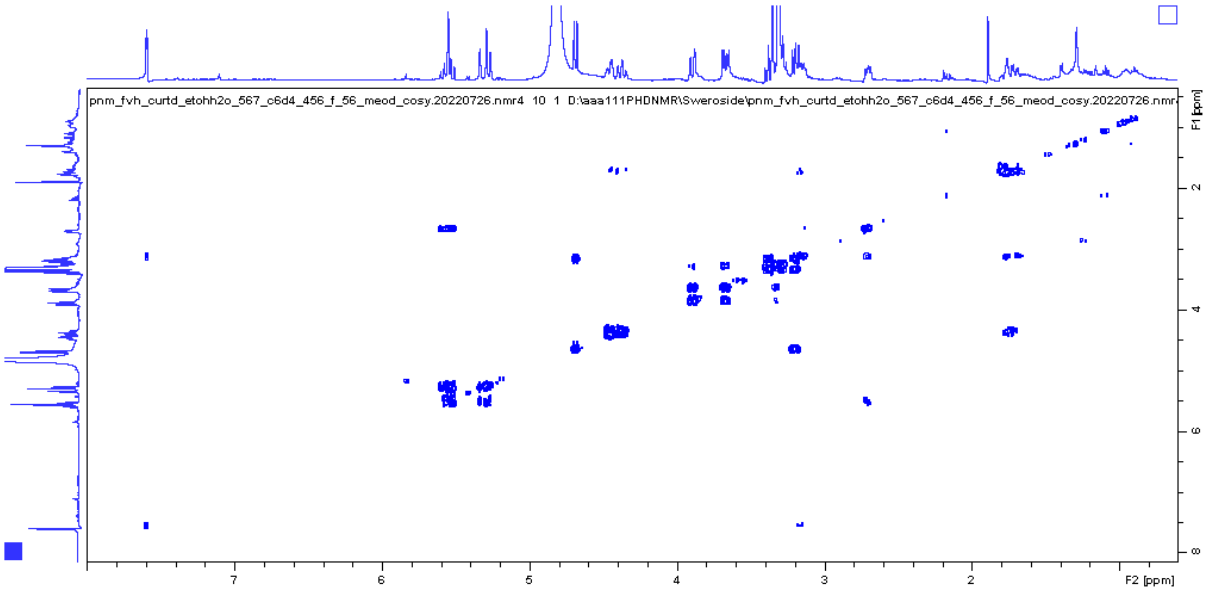

Figure S12.4: COSYspectrum of sweroside (**114**) in CD_3OD, 400 MHz